Molecular and functional analyses of the plant specific 3xHMG-box proteins expressed during mitosis/meiosis

DISSERTATION ZUR ERLANGUNG DES
DOKTORGRADES DER NATURWISSENSCHAFTEN (DR. RER. NAT.)
DER FAKULTÄT FÜR BIOLOGIE UND VORKLINISCHE MEDIZIN
DER UNIVERSITÄT REGENSBURG

vorgelegt von

Martin Antosch

aus Berlin

im Dezember 2014

Das Promotionsgesuch wurde eingereicht am: 19.12.2014

Die Arbeit wurde angeleitet von: Prof. Dr. Klaus D. Grasser

Unterschrift:

Martin Antosch

Molecular and functional analyses of the plant specific 3xHMG-box proteins expressed during mitosis/meiosis

DISSERTATION ZUR ERLANGUNG DES
DOKTORGRADES DER NATURWISSENSCHAFTEN (DR. RER. NAT.)
DER FAKULTÄT FÜR BIOLOGIE UND VORKLINISCHE MEDIZIN
DER UNIVERSITÄT REGENSBURG

vorgelegt von

Martin Antosch

aus Berlin

im Dezember 2014

Table of contents

List of figures VI
List of tables VIII
Abbreviations IX
Preface XI
1. Introduction 1
1.1 Organization of genetic material 1
1.1.1 DNA 1
1.1.2 Chromatin 2
1.1.3 Chromosomes 3
1.2 Cell cycle 4
1.2.1 Cell phases and regulation of the plant cell cycle 5
1.2.2 Mitosis and cytokinesis in plants 7
1.3 Organization, transcription and regulation of rRNA genes in *Arabidopsis* 10
1.3.1 Organization of rDNA 10
1.3.2 The nucleolus 11
1.3.3 Regulation of rDNA transcription and nucleolar dominance 14
1.4 HMG-box containing proteins 16
1.4.1 The HMG-box DNA binding domain 16
1.4.2 High mobility group (HMG)-box proteins 17
1.4.3 Plant HMG-box proteins 19
1.4.4 3xHMG-box proteins 22
1.5 Aim of the thesis 24
2. Material and Methods 25
2.1 Materials 25
2.1.1 Instruments 25
2.1.2 Chemicals, Antibodies and Enzymes 26
2.1.3 Antibiotics 26

2.1.4 Oligonucleotides....26
2.1.5 Plasmids....28
2.1.6 Seed stocks and plant cell culture....29
2.1.7 Bacterial and yeast strains....29
2.1.8 Software....29
2.2 Plant work and cell biological methods....30
2.2.1 Plant growth conditions....30
2.2.2 Soil-based phenotypic analyzes....30
2.2.3 Phenotypic analyzes of roots....31
2.2.4 Crossing of *Arabidopsis thaliana*....31
2.2.5 Preparation of semi-thin sections from leaf tissue....31
2.2.6 Alexander stain of pollen....32
2.2.7 Stable transformation of *Arabidopsis thaliana*....32
2.2.8 Growth and *Agrobacterium*-mediated transformation of *Arabidospsis* cell suspension cultures....33
2.2.9 Immunocytochemistry (ICC)....34
2.2.10 Flourescence *in situ* hybridization (FISH)....34
2.2.11 Microscopy....35
2.3. Microbiological work....35
2.3.1 Growth of bacteria....35
2.3.2 Growth of yeast....35
2.3.3 Production of chemically competent *E.coli* and *A. tumefaciens*....36
2.3.4 Production of chemically competent yeast cells....36
2.3.5 Transformation of *E.coli*....37
2.3.6 Transformation of *Agrobacterium tumefaciens*....37
2.3.7 Transformation of yeast....37
2.4. Molecular biological methods....37
2.4.1 Extraction of genomic DNA from *Arabidopsis*....37

2.4.2 Extraction of total RNA from *Arabidopsis* 38
2.4.3 First strand cDNA synthesis 38
2.4.4 Polymerase chain reaction (PCR) 38
2.4.5 Agarose gel electrophoresis 39
2.4.6 Construction of plasmids 39
2.4.7 Small scale purification of plasmids 40
2.4.8 Medium scale preparation of plasmids 40
2.4.9 Sequencing 40
2.4.10 Bradford assay 41
2.4.11 Sodium dodecyl sulphate polyacrylamide gel electrophoresis 41
2.4.12 Silver staining 41
2.4.13 Expression and purification of His-tagged proteins 42
2.4.14 Desalting of proteins 43
2.4.15 Purification of plant nuclei and micrococcal nuclease (MNase) digestion 43
2.4.16 Western blot (Immunoblot) 44
2.4.17 Northern Blot 44
2.4.18 Southern blot 45
2.4.19 Preparation of radioactive probes for Northern blot and Southern blot 45
2.4.20 Hybridization and detection of radioactively labelled probes 46
2.4.21 Coupling of rabbit-IgG to Epoxy-activated BcMag-beads 46
2.4.22 Immunoprecipitation of GS-tagged proteins 47
3. Results 48
3.1 Analyzes of the spatiotemporal distribution of 3xHMG-box proteins in roots of *A. thaliana* 48
3.1.1 Life cell imaging of 3xHMG-box-GFP fusion proteins in *Arabidopsis* roots 48
3.1.2 Investigation of a putative D-box like degradation domain in the N- terminal region of 3xHMG-box1 51
3.2 Reverse genetic approach 54

3.2.1 Verification of the T-DNA insertion line GK-171F06-013466 54

3.2.2 Knock-down approach using long hairpin RNA (lhRNA) 56

3.2.3 Knock-down approach using artificial micro RNA (amiRNA) 58

3.3 Immunoprecipitation with GS tagged 3xHMG-box proteins..... 60

3.4 Artificial targeting of 3xHMG-box proteins to the nucleus during interphase 62

3.4.1 35S promoter driven expression of 3xHMG-box-GFP in *Arabidopsis thaliana*.....62

3.4.2 35S promoter driven expression of 3xHMG-box-GFP-NLS in *Arabidopsis thaliana*.....64

3.4.3 Phenotypical consequences of 3xHMG-box-GFP-NLS expression during interphase 66

3.4.4 Analysis of nucleoli, 45S rDNA regions and 45S rDNA transcript level in overexpression lines.....70

3.4.5 Investigation of the 45S rDNA compaction state in 3xHMG-box-GFP-NLS overexpression lines.....73

3.5 Contribution of different domains of 3xHMG-box1 to rDNA specificity 75

3.5.1 Construction of reporter constructs for different truncated versions of 3xHMG-box1-GFP-NLS 75

3.5.2 Expression of 3xHMG-box chimera with exchanged N-terminal domains ..77

3.5.3 Affinity of N-terminal domains to 45S rDNA gene fragments.....79

3.6 Association of 3xHMG-box1 with silenced NORs in allotetraploid *Arabidopsis suecica* 80

3.7 Subcellular localisation of 3xHMG-box proteins in yeast..... 83

3.8 Effects of overexpression of linker histones with respect to the distribution of 3xHMG-box proteins on mitotic and interphase chromosomes and vice versa. 85

4. Discussion 91

4.1 Reverse genetic approach to study effects of down regulation of *3xHMG-box* gene expression 91

4.2 Constitutive expression of 3xHMG-box proteins that are fused to GFP or GFP-NLS 92

4.3 Effects of nuclear targeting of 3xHMG-box proteins during interphase 95

4.4 Spatiotemporal distribution of 3xHMG-box proteins and possible functions in mitotic processes 97

4.5 Identification of putative 3xHMG-box interaction partners 100

4.6 Investigation of possible roles of the 3xHMG-box N-terminal domain in 45S rDNA specificity and identification of a D-box motif 101

4.7 Analogies of 3xHMG-box proteins with UBF or HMO1 respectively 106

4.8 Association of 3xHMG-box1 with NORs during mitosis 108

4.9 Investigation of possible competitive DNA binding of 3xHMG-box proteins and linker histones 109

4.10 Perspective 111

5. Summary 113

6. References 114

7. Appendix 128

Danksagung 132

List of figures

Figure 1. The double-helical structure of DNA and chromatin structure. 1
Figure 2. Idiogram of pachytene chromosomes of *A. thaliana*. 4
Figure 3. Eucaryotic cell cycle and cell cycle in plants. 5
Figure 4. Mitosis and cytokinesis in plants. 9
Figure 5. Relationships between the nucleolus, secondary constriction, NOR and ribosomal genes. 11
Figure 6. Main structures of nucleoli and assembly at the end of mitosis. 12
Figure 7. Nucleolar disassembly during mitosis. 13
Figure 8. Organization of NORs during interphase and methaphase and epigenetic markers on ribosomal chromatin. 15
Figure 9. Structur of high mobility group (HMG) box-DNA complexes. 17
Figure 10. Sequence alignment of HMG-box containing plant proteins. 20
Figure 11. 3xHMG-box proteins in *A.thaliana*. 23
Figure 12. Capillary blot. 45
Figure 13. Live cell imaging of 3xHMG-box-GFP fusion proteins in root tips. 50
Figure 14. Identification and site directed mutagenesis of a putative D-box degradation domain in 3xHMG-box2. 52
Figure 15. Contribution of N-terminal D-box motif to degradation of 3xHMG-box2 after mitosis. (A) Schematic representation of pM3 with indication of primers used to generate the construct and introduce a mutation in the putative D-box. 54
Figure 16. Molecular characterization of T-DNA insertion line GK-171F06-013466. 55
Figure 17. Phenotype of *3xhmg-box1* compared to Col-0. 56
Figure 18. Construction of shRNA vector pM4 and introduction in *3xhmg-box1* lines. 58
Figure 19. Construction of amiRNA construct pM5 and introduction in *3xhmg-box1* lines. 59
Figure 20. Co-IP with GS-tagged 3xHMG-box proteins using *Arabidopsis* cell suspension cultures and seedlings. 61
Figure 21. Phenotypcial analyzes of stably transformed *Arabidopsis* plants which express 3xHMG-box-GFP under the control of the 35S promoter. (A) 63
Figure 22. CLSM and Immunostaining analyses of stably transformed *Arabidopsis thaliana* plant lines, which express GFP-NLS and 3xHMG-box-GFP-NLS fusion proteins. 65
Figure 23. Phenotype of *Arabidopsis thaliana* plant lines overexpressing 3xHMG-box1-GFP-NLS, 3xHMG-box2-GFP-NLS and GFP-NLS compared to wild type (Col-0). 67
Figure 24. Pollen viability in *Arabidopsis thaliana* plant lines homozygous for pL8, pM9 and pM10 and self pollination of plants that overexpress 3xHMG-box1-GFP-NLS. 68
Figure 25. Cell number in the division zone of roots and palisade parenchyma of leaves from *Arabidopsis thaliana* plants lines homozygous for pL8, pM9 and pM10 and Col-0. 69
Figure 26. Immunostaining and FISH with root tip cells of overexpression lines. 71

Figure 27. Transcript level and processing of 45S rDNA in knock-out and overexpression lines.....72

Figure 28. MNase accessibility of leaf nuclei chromatin combined with southern blot in order to test compaction state of rDNA in different overexpression mutants. 74

Figure 29. Subnuclear localisation of 3xHMG-box1-GFP-NLS truncated version.....76

Figure 30. Subnuclear localisation of chimeric 3xHMG-box proteins. 78

Figure 31. Affinity of the N-terminal regions of 3xHMG-box proteins for 45S rDNA.....79

Figure 32. Immunostaining of mitotic chromosomes with chromocenter specific anti H3S10ph antibody and anti 3xHMG-box antibody. 81

Figure 33. Association of 3xHMG-box proteins with 45S rDNA regions in allotetraploid A. suecica.....82

Figure 34. Subcellular localization of 3xHMG-box proteins with 45S in yeast. 84

Figure 35. CLSM analysis of mitotic chromosomes in root tips of plants that express 3xHMG-box1-GFP fusion proteins together with either H1.1-RFP or H1.2-RFP fusion proteins. 87

Figure 36. CLSM analysis of mitotic chromosomes in root tips of plants that express either 3xHMG-box1-GFP.....88

Figure 37. Distribution of 3xHMG-box-GFP-NLS and linker histone-RFP fusion proteins during interphase and mitosis.....90

Figure 38. Distinct localization pattern of plant histone H3.3/HTR4.....94

Figure 39. Sequence alignment of 3xHMG-box plant proteins and their N-terminal domains.....105

Supplemental Figure 1. Confirmation of 3xHMG-box reporter lines. 128

Supplemental Figure 2. Site directed mutagenesis of a putative D-box degradation domain in 3xHMG-box2. 128

Supplemental Figure 3. Verification of stably transformed Arabidopsis cell suspension cultures and plants that contain plasmids which mediate expression of GS-tagged 3xHMG-box proteins or the sole GS tag. 129

Supplemental Figure 4. Verification of stably transformed plant lines that contain plasmids which mediate overexpression of 3xHMG-box-GFP-NLS fusion proteins during interphase.129

Supplemental figure 5. Number of palisade parenchyma cells of leaves from Arabidopsis thaliana plants lines homozygous for pL8, pM9 and pM10. 130

Supplemental figure 6. Confirmation of stably transformed *A.thaliana* plant lines that contain plasmids which facilitate expression of 3xHMG-box1-GFP-NLS truncated versions.....130

Supplemental figure 7. Confirmation of stably transformed *A.thaliana* plant lines that contain plasmids which facilitate expression of chimeric 3xHMG-box proteins. 131

Supplemental Figure 8. Verification of crossed plant lines that harbor constructs which allow simultaneous expression of fluorescently labeled 3xHMG-box proteins and linker histones.....131

List of tables

Table 1. List of antibiotics. 26
Table 2. List of oligonucleotides. 26
Table 3. List of plasmids used in this study. 28
Table 4. List of plasmids constructed in this study. 28
Table 5. List of bacterial and yeast strains. 29
Table 6. Wavelengths for excitation and filters. 35

Abbreviations

AcOH	acetic acid
A. tumefaciens	*Agrobacterium tumefaciens*
amp	ampicillin
aa	amino acid
bar	bialaphos resistance
bp	base pairs
BSA	bovine serum albumin
Care	*cardaminopsis arenosa*
CMV	cauliflower mosaic virus
Co	company
Col-0	*Arabidopsis thaliana* wildtype from the University of Missouri-Columbia
Cvi	Cape Verde Islands
DAPI	4‘,6-diamidino-2-phenylindole
DAS	days after stratification
DNA	deoxyribonucleic acid
DSMZ	Deutsche Stammsammlung von Mikroorganismen und Zellkulturen
DTT	dithiothreitol
E.coli	*Escherichia coli*
e.g.	exempli gratia (example given)
EtBr	ethidium bromide
etc.	et cetera (and other things)
EtOH	ethanol
FISH	fluorescence *in situ* hybridization
g	gravity acceleration
GABI KAT	german plant genomics research program - Köllner Arabidopsis T-DNA lines
gent	gentamycine
GFP	green fluorescent protein
h	hours
HAc	acetic acid
HMG	high mobility group
H_2O_{deo}	deionized water

hyg	hygromycin
IgG	immunoglobuline G
ICC	immunocytochemistry
kan	kanamycin
Kas	Kashmir1
kb	kilo base pairs
KOH	kaliumhydroxite
l	liter
LB	luria-bertani broth
Ler	Landsberg erecta
mg	milligram
min	minutes
MQ	Milli-Q
NAA	naphtaleneacetic acid
NEBD	nuclear envelope breakdown
nos	nopalin synthase
Ler	landsberg erecta
NLS	nuclear localization signal
OD	optical density
PCR	polymerase chain reaction
PMSF	phenylmethylsulphonyl fluoride
PPFD	photosynthetic photon flux density
ppi	pixel per inch
tet	tetracycline
RFP	red fluorescent protein
RNA	ribonucleic acid
rif	rifampicine
rpm	rotations per minute
RT	room temperature
T-DNA	transfer DNA
TM	trademark
UV	ultra violet
WS	Wassileskija

Preface

Is it possible, I wonder, to study a bird so closely, to observe and catalogue its peculiarities in such minute detail that it becomes invisible?
Is it possible that while fastidiously calibrating the span of its wings or the length of its tarsus, we somehow lose sight of its poetry?
That in our pedestrian descriptions of a marbled or vermiculated plumage we forfeit a glimpse of living canvases, cascades of carefully toned browns and golds that would shame Kandinsky, misty explosions of color to rival Monet? I believe that we do. I believe that in approaching our subject with the sensibilities of statisticians and dissectionists, we distance ourselves increasingly from the marvellous and spell-binding planet of imagination whose gravity drew us to our studies in the first place.
This is not to say that we should cease to establish facts and to verify our information, but merely to suggest that unless those facts can be imbued with the flash of poetic insight then they remain dull gems; semi-precious stones scarcely worth the collecting.

Daniel Dreiberg

1. Introduction

1.1 Organization of genetic material

1.1.1 DNA

Genetic information in living organisms is basically encoded in form of DNA that consists of nucleotides, which contain either the purine bases adenine (A) and guanine (G) or the pyrimidine bases cytosine (C), and thymine (T) (Khorana et al. 1968). DNA appears mostly in form of two anti parallel polynucleotide strands that are coiled around each other to form a double helix (Watson and Crick 1953), in which purin bases are paired via hydrogen bonds with pyrimidin bases (Figure 1A). The most common and *in vitro* abundant conformational state of double stranded DNA is called B-DNA (Franklin and Gosling 1953) It has a diameter of approximately 2nm, a distance of 0,34nm between the base pairs and 10 base pairs within one 360°-turn. The winding of the DNA strands in this form results in the formation of a

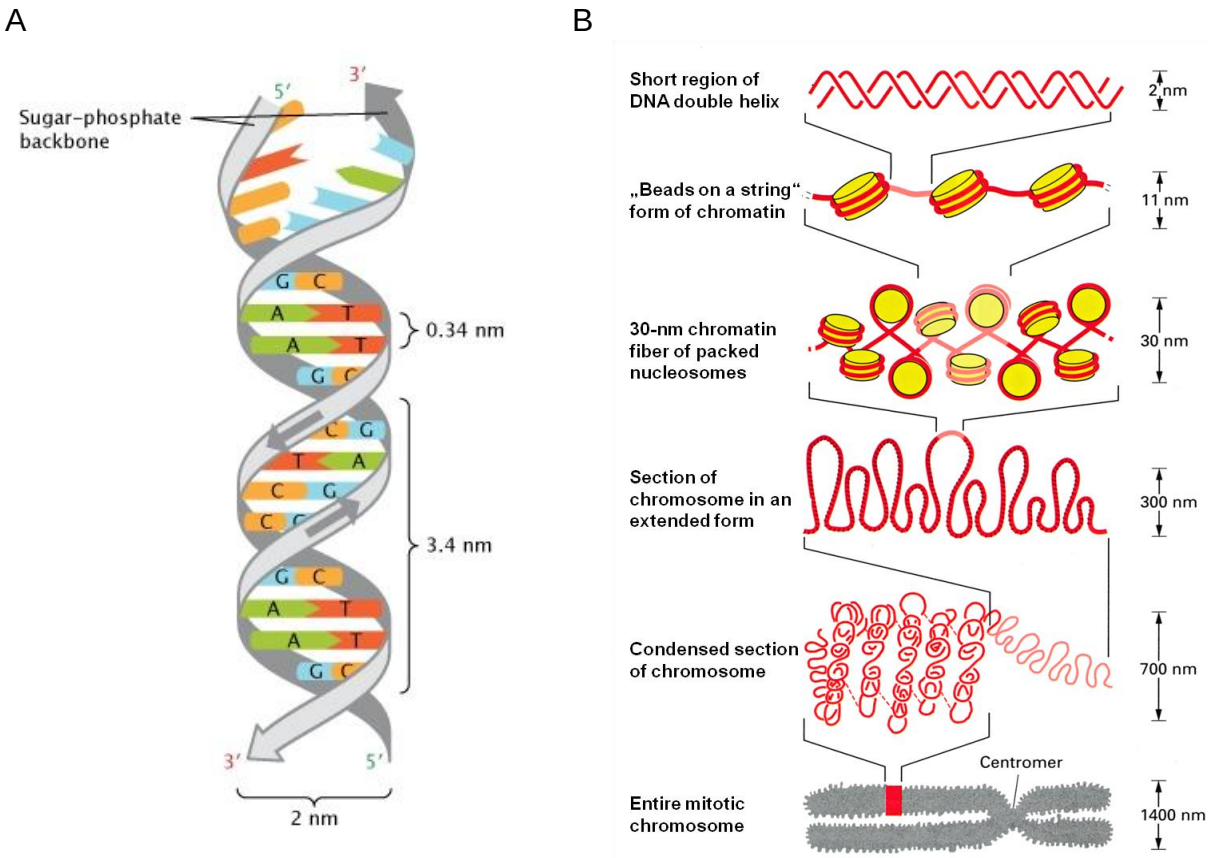

Figure 1. The double-helical structure of DNA and chromatin structure. (A) The 3-dimensional double helix structure of DNA, correctly elucidated by James Watson and Francis Crick. Complementary bases are held together as a pair by hydrogen bonds (2013, Nature Education). **(B)** Step-wise packaging of chromatin (2004, Molecular Biology of the cell)

minor grove with a distance of 1,2 nm and a major groove with a distance of 2,2 nm, which has important consequences for the accessibility of DNA binding proteins. Depending on the species, a haploid genome can contain from 1667867 base pairs in case of *Helicobacter pylori (Tomb et al. 1997)* to ~7,84x10^{10} base pairs in case of *Lepidosiren paradoxa (Vinogradov 2005)*. *A. thaliana* contains ~1,34x10^{8} base pairs *(2000)* and *homo sapiens* ~3,27x10^{9} base pairs (Venter et al. 2001) per haploid genome to give some more prominent examples. That means for example for a human cell, that more than two meters of DNA have to fit into a nucleus of an average diameter of 6 nm (Alberts et al. 2002). Besides supercoiling of the DNA helix (Benham and Mielke 2005) this can only be realized by an extreme form of organization and packaging in which DNA binding proteins play an important role.

1.1.2 Chromatin

Chromatin is a complex of macromolecules, consisting of DNA, RNA, histone proteins and non histone proteins found in eukaryotic cells. Histones are the primary protein compounds of chromatin and are basic proteins that facilitate the formation of compact DNA structures. One distinguishes five major families of histones called H1/H5, H2A, H2B, H3 and H4 (Bhasin et al. 2006). H1 and H5 are known as linker histones and the latter are known as core histones. Two proteins of each H2A, H2B, H3 and H4 form an histone octamer (Luger et al. 1997). 147bp of DNA is wrapped approximately 1.65 times around the the nucleosome core particle in a left-handed-super-helical manner and give rise to the nucleosome. The linker histone binds the nucleosomes at the entry and exit sites of the DNA, thus locking the DNA into place. Modifications of histones or incorporation of different subspecies of histones lead to altered interaction with the DNA double helix and other proteins and thus change their mode of function. Several nucleosomes in a row form the so called “beads on a string” structure named after its appearance observed under the electron microscope (Oudet et al. 1975). This 11 nm fibre is considered to be the primary level of chromatin organization and forms upon binding of linker histones a more condensed fibre with a diameter of 30 nm that is considered to be the secondary level of chromatin organization. Beyond the secondary level, concrete information about the structure is limited but there is some evidence that 30 nm fibres are arranged in loops that constitute the tertiary structure. Besides histones, also non histone proteins like

the high mobility group (HMG) proteins and components of the transcription-, replication- and repair machinery (just to mention some of the components) are essential for the constitution of the tertiary structure. Finally, these chromatin loops are organized in more loosely packed, transcriptional active euchromatin and more tightly packed transcriptional inactive heterochromatin that form together the chromosomes. The different stages of chromatin organization are shown in Figure 1B. The three-dimensional organization of the chromosomes, with respect to each other in the nucleus and to the inner nuclear membrane is also referred to as the quaternary structure of chromatin (Sajan and Hawkins 2012). Thereby, it is assumed that transcriptionally active genomic regions are more distant to the nuclear periphery than those that are silent (Towbin et al. 2009). Nonetheless, during the last years experimental evidences suggest a role of the nuclear pore complex (NPC) in recruitment of active genes to the nuclear periphery and regulation of gene expression (Strambio-De-Castillia et al. 2010).

In general, it can be said that the different levels of chromatin organization are important for its regulatory function. Furthermore, modifications of histones and incorporation of different histone subtypes as well as the activity of chromatin remodeling complexes and association of architectural proteins like HMG proteins with DNA have a major impact on this organization.

1.1.3 Chromosomes

In the three domains of life (Woese and Fox 1977) DNA is constituted as circular or linear chromosomes, which represents the most complex and compacted organisation form of DNA. Eukaryotes contain a special compartment within the cell, called the nucleus, in which the chromosomes are stored, whereas in Prokaryotes the chromosomes, also referred to as “circular chromosomes” in case of archea (Hartman et al. 2010) or “bacterial chromosomes” in case of bacteria (Cairns 1963), are not surrounded by a special membrane system. In Eukaryotes, organelles exist that possess their own genomes, which are organized as circular or linear structures (Nosek et al. 1998). These organelles are termed mitochondria and plastids. The latter are unique for plants and both probably became part of eukaryotic cells due to endophagocytosis (Sagan 1967, Cavalier-Smith 2000). In Eukaryotes the number and constitution of chromosomes and karyotype is a typical attribute for each species. An example for *Arabidopsis thaliana* is shown in Figure 2. Depending on

developmental stage, tissue, species and gender the chromosomes exist in a different copy number and can vary from haploid/monoploid karyotypes e.g. in gametes, mosses and male *Apis mellifera* to diploid karyotypes, like in most somatic cells from e.g. *Homo sapiens* or *A. thaliana* to polyploid karyotypes like in somatic cells of *Triticum aestivum* or muscle cells of *Homo sapiens* (Parmacek and Epstein 2009). During the division of homologous chromosomes in the process of mitosis and meiosis, the chromosomes reach their highest grade of compaction and are largely transcriptional inactive. The process of compaction during early stages of mitosis and meiosis is called condensation. Mitotic chromosomes were also one of the first cytological structures discovered, which leaded to the unveiling of the physiological basis for heredity. They exhibit some prominent structures like the centromers and secondary constrictions that consist of rDNA or nucleolar organizing regions (NORs) respectively (Figure 2, Figure 5).

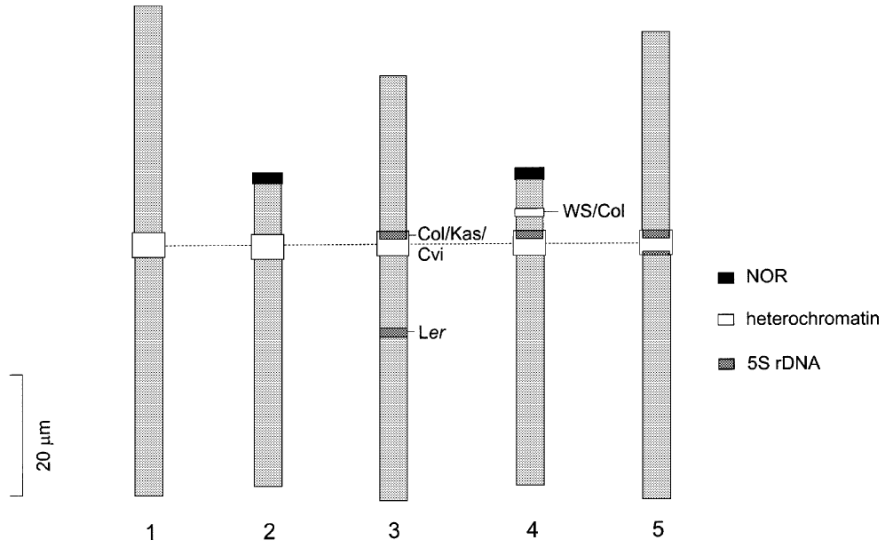

Figure 2. Idiogram of pachytene chromosomes of *A. thaliana*. Polymorphic cytological markers are indicated by the names of the ecotypes (Fransz et al. 1998).

1.2 Cell cycle

A german pathologist named Rudolf Virchow came up in 1858 with a central cell doctrine called “Omnis cellula e cellula” which means that cells emerge from cells. Nowadays this appears to be self-evident but describes the basis for a fundamental and very complex mechanism that is shared by all living organisms, called the cell cycle. The cell cycle is a series of events that leads to the generation of two daughter cells out of one progenitor cell and is highly regulated by hormonal, environmental and developmental signals (Wolters and Jurgens 2009). For this process it is

essential to duplicate the chromosomes and distribute them equally among the daughter cells, except in a special case named endocycle, in which no mitosis occurs and thus ploidy level is exponentially increased (Edgar and Orr-Weaver 2001).
Additionally, in most of the dividing cells also organelles and macro molecules have to be duplicated prior cell division. The cell cycle is characterized by unidirectional progress that is directed by a cell-cycle control system. The duration of a complete cell cycle varies enormously depending on the cell type. A yeast cell for example can divide within 90-120min, while a mammalian liver cell divides one time per year in average (Alberts et al. 2002).

1.2.1 Cell phases and regulation of the plant cell cycle

The eukaryotic cell cycle is traditionally divided in four phases that are shown in Figure 3A. The first phase is the G_1 phase, in which cells commit for a new cell cycle and prepare for the duplication of their genome. Non-proliferative quiescent or senescent cells respectively, may enter from G_1 phase the G_0 phase. During S phase nuclear chromosomes become replicated. In the G_2 phase the genome integrity is checked and cells prepare for cell division. In the M phase, consisting of mitosis and cytokinesis, the duplicated genome and cytoplasmatic components are distributed among the two new forming daughter cells. Besides mitosis, cell cycle may also result in meiosis, a special type of cell division that is necessary for sexual

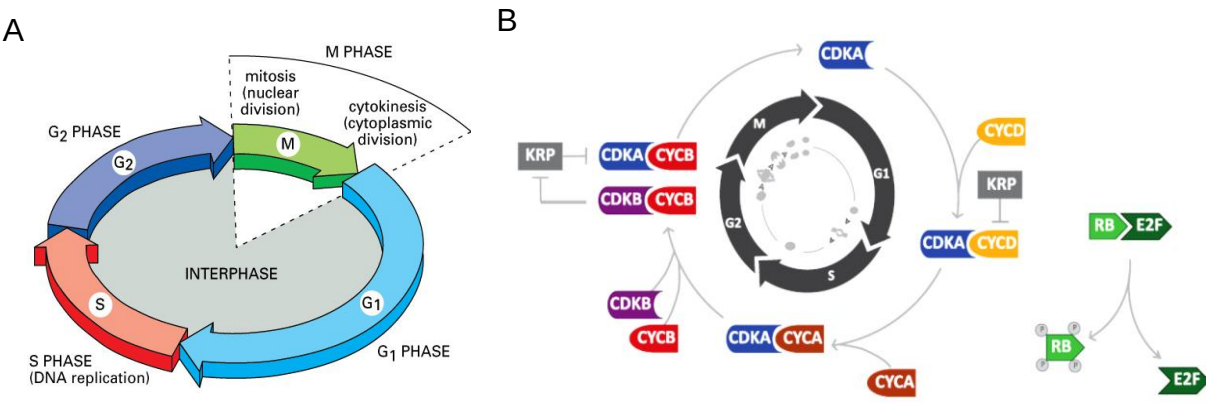

Figure 3. Eucaryotic cell cycle and cell cycle in plants. (A) Cell cycle is traditionally divided in M phase including mitosis and cytokinesis, G_1 phase, S phase in which nuclear DNA is replicated and G_2 phase (Alberts et al. 2002). **(B)** Simplified view of the plant cell cycle. Progression through the different cell phases is controlled by concerted activation/inactivation of CDKs by cyclins and KRP proteins. G_1 phase to S-phase transition is regulated by phophorylation of retinoblastoma protein (RBR) by CYCD activated CDKA, which than releases the transcription factor E2F and thus alter its activity (Scofield et al. 2014).

reproduction in eukaryotes. In this process, homologous chromosomes are distributed among gametes, while the ploidy level is reduced by half relative to the progenitor cell. This includes two meiotic phases in which first homologous chromosomes and after that, sister chromatides become separated. Cell cycle progression is controlled by two key classes of regulatory proteins, namely cyclins (CYCs) and cyclin-dependent kinases (CDKs) (Nigg 1995). Besides, ubiquitin ligase mediated degradation processes, control at the transcriptional level as well as chromatin modifications are crucial for cell cycle regulation. In plants, CDKA plays an essential role during the whole cell cycle, being especially important for the transition from G_1 phase to S phase and, together with CDKB, for the transition from G_2 phase to M phase (Veylder et al. 2003). In order to become functional, CDKs need to be activated by complex formation with cyclins, which are characterized by its transient and cyclical appearance during cell cycle. For example CYCA is important for S phase progression and together with CYCB and CYCD for G_2 phase to M phase transition. Additionally, CYCD is crucial for G_1 phase to S transition (Menges et al. 2005). Furthermore, without going into detail, CDKs that are complexed with CYCs are activated through phosphorylation by CDK-Actvating Kinases (CAKs) and can act as CAKs themselves. In plants also Cyclin-Dependent Kinase inhibitors (CKIs) can be found, that are often designated as Kip-Related Proteins. They can inactivate both CYCs and CDKs by direct interaction (De Veylder et al. 2001). One of the most prominent CDK/CYC target is the Retinoblastoma (Rb) protein, whose homologue in plants is termed RB-related (RBR) protein (Grafi et al. 1996) (Xie et al. 1996). Phosphorylation of RBR leads to the release of E2F/DP transcription factor complexes, thus turning them into their active form. E2F/DP themselves regulate the expression of many genes involving genes required for cell cycle progression (Mariconti et al. 2002). A model for the function of the above mentioned factors for cell cycle progression is shown in Figure 3B. It is important to mention that this model only gives a very simplistic view of the plant cell cycle as hormonal and environmental control as well as the influence of the circadian clock and growth factors in cell cycle regulation is not implemented.

Besides, the above mentioned regulatory circuits of the ubiquitin proteasome system (UPS) appears as a major player for cell cycle control by promoting irreversible proteolysis of regulatory proteins required for cell cycle phase transitions. Ubiquitin ligases (E3s) facilitate the transfer of poly ubiquitin chains to substrate proteins and

thus mark them as targets for the 26S proteasome mediated degradation (Ciechanover et al. 2000). The two main groups of E3 ligases involved in cell cycle regulation are represented by the anaphase promoting complex/cyclosome (APC/C) and the SCF (Skp1, Cdc53 (cullin) and F-box) multimer. The first group is especially important for M-phase progression and exit (Thornton and Toczyski 2006, van Leuken et al. 2008) while the second group mediates transition from G_1 phase to S phase through degradation of cyclin-dependent inhibitors CKIs (Genschik et al. 2014). E3s recognize their substrates by certain domains, in case of APC/C predominantly the KEN-box and Destruction box (D-box) with its RxxL minimal consensus sequence (King et al. 1996, Choi et al. 2008).

During cell cycle, the chromatin structure is highly variable due to nucleosome remodelling, histone modifications and deposition and exchange of histones. These structural changes in chromatin architecture can be correlated with specific cell cycle processes like the licensing of DNA replication origins, the E2F-dependent transcriptional wave during G_1 phase, replication during S phase and preparation for chromatin packaging in the G_2 phase (Desvoyes et al. 2014). The most striking structural change occurs in the end of the G_2 phase when the chromosomes start to condense and M phase, when the chromosomes are distributed among the daughter cells.

1.2.2 Mitosis and cytokinesis in plants

The transition from G_2 into mitosis can be related with a peak of transcription of CDKA and CDKB, which are probably activated by B type cyclins (Weingartner et al. 2003) (Figure 3B). Key substrates of these CDK/CYC complexes are three MYB repeat MYB3R transcription factors (Ito et al. 2001) that trigger upon phosphorylation the expression of M phase specific genes e.g. *KNOLLE*, *CDC20*, *CYCA*, *CYCB* and *NACK1* (Menges et al. 2005). Mitotic progression and exit is further navigated by delicate actions of the APC/C complex that is regulated by itself through interaction with cofactors, inhibitors or reversible phosphorylation (Pesin and Orr-Weaver 2008).

Mitosis itself can be roughly divided into 4 different stages termed prophase, metaphase, anaphase and telophase (Figure 4A). In the following section regulatory and cellular processes like chromosome condensation, alignment and separation as well as formation of the spindle apparatus and cell division will be described according their temporal order based on the mitotic phases

Prophase

In plant cells, the prophase is preceded by a preprophase in which the nucleus is pulled to the middle of the cell and a transverse sheet of cytoplasm, called phragmosome, is formed across the division plane. Additionally, actin filaments and microtubules collect to form the preprophase band around the equatorial plane of the future mitotic spindle.

During the prophase, chromosomes condense in order to facilitate accurate chromosome segregation and the nucleolus disappears. Phosphorylation of H3S10, a histone modification that is conserved across eukaryotes is linked to this condensation process (Houben et al. 1999). Besides histone modifications, the effect of the structural maintenance of chromosome (SMC) compex is central for the formation of mitotic chromosomes (Hudson et al. 2009). Furthermore, the nuclear envelope generates the mitotic spindle, which is organized into two poles by the pre prophase band (PPB) (Figure 4B). Interestingly, as plant cells do not contain centrioles, it is assumed that H1 together with the GTP-binding nuclear protein Ran might facilitate microtubule nucleation at the nuclear envelope in order to form the plant mitotic spindle (Zhang and Dawe 2011).

Metaphase

At promethaphase, the chromosomes are fully condensed and the nuclear envelope breaks down. The PPB disassembles, leaving behind an actin depleted zone that persists and marks the division zone throughout mitosis (Smith 2001). Specialized protein structures, called kinetochores, that are important for the distribution of the sister chromatids to the opposite cell poles are formed at centromeric regions, allowing microtubules to attach. In plants, kinetochore assembly is already initiated in G_2 phase through incorporation of the centromeric histone H3 variant (CENH3) (Lermontova et al. 2007). After the nuclear envelope breakdown, the condensed chromosomes relocate to the center of the cell and their centromeric regions gradually rotate to become orientated vertical to the metaphase plate (Fang and Spector 2005).

At metaphase, the chromosomes are aligned along the metaphase plate, mitotic spindle formation is completed and spindle microtubules are attached to the kinetochores. APC/C mediated polyubiquitylation of a protease inhibitor (PDS1/SECURIN) leads to activation of the Separase protease, which by itself cleaves the cohesion complex that physically attaches sister chromatids (Peters

2006). This degradation step is part of an important control mechanism named spindle assembly checkpoint (SAC) (Musacchio and Ciliberto 2012).

Anaphase

After cleavage of the cohesion complex, sister chromatids are pulled at the kinetochores and move along the spindle microtubules to opposite ends of the cell. Meanwhile the phragmoplast, a structure made out of actin and microtubules, is formed between the separated sister chromatids. The phragmoplast itself guides the movement of cell wall material containing Golgi-derived vesicles to the cell plate (Gunning and Wick 1985). At the end of anaphase, microtubules of the spindle apparatus start to degrade.

Telophase

Chromosomes start to decondense, nuclear membranes are reformed at the opposite ends of the cell. The phragmoplast expands centrifugally until it fuses with the parental plasma membrane and cell wall at the cortical division site that was previously occupied by the PPB (Wick 1991). After telophase, cytokinesis comes into its last stage in which the cell wall is completed and the daughter cells are finally divided.

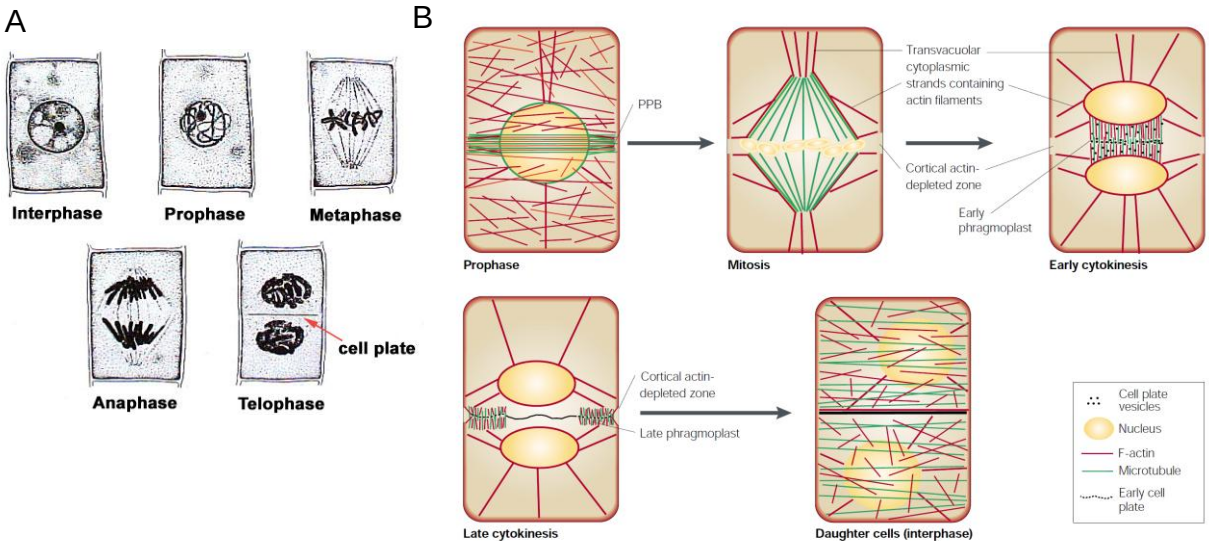

Figure 4. Mitosis and cytokinesis in plants. (A) Illustration of plants cells during Interphase and the different mitotic phases (Armstrong 1988). **(B)** cytoskeletal organization in dividing plant cells. During prophase, a cortical preprophase band (PPB) of microtubules circumscribes the future plane of cell division. When the PPB is disassembled on entry into mitosis, the actin component of the PPB also disappears, leving behind an actin depleted zone in the cell cortex that marks the division site throughout mitosis. After completion of mitosis a phragmoplast is initiated between the daughter cells, which guides movement of Golgi-derived vesicles containing cell wall materials to the cell plate (Smith 2001).

In Figure 4B the main steps of cytokinesis are shown. Here cytokinesis is regarded as a separate process that follows mitosis. Still many processes like the formation of the PPB, which defines the position of the metaphase plate and future cell wall or the formation of the phragmoplast can be related to a specific mitotic phase.

1.3 Organization, transcription and regulation of rRNA genes in *Arabidopsis*

1.3.1 Organization of rDNA

Ribosomal RNA (rRNA) gene transcription accounts for most of RNA in prokaryotic and eukaryotic cells. In eukaryotes, rRNA genes can be found in mitochondria, chloroplasts and nuclei. In case of the organelles, the transcribed rRNA is only used within these compartments. In a nucleus, there are hundreds to thousand rRNA genes which are organized as head-to-tail orientated tandem arrays that span millions of basepairs and form the nucleolus organizer regions. During interphase, the nucleolus that appears as the darkest and most dense feature of the nucleus, is the place where the ribosomes are assembled from ribosomal proteins and four rRNA-types transcribed by RNA Polymerase I (Pol I) (18S, 5,8S, 28S/25S rRNAs) and RNA Polymerase III (Pol III) (5S RNA) (Scheer and Weisenberger 1994). Transcription of rRNA genes by RNA-Polymerase I leads to generation of the primary 45S pre-rRNA, that is subsequently processed to the structural rRNAs (Gerbi SA and AV 2000). The procession of the 45S rRNA, assembly processes as well as modifications of rRNA is mediated by small nucleolar RNAs (snoRNAs) (Brown and Shaw 1998). The basic organization of ribosomal genes in eukaryotes is illustrated in Figure 5. The number of NOR-bearing chromosomes varies depending on the species and ranges from 1 in haploid yeast cells to 10 in human somatic cells. In *A. thaliana* the 45S rDNA genes are located on the short arms of the acrocentric chromosomes 2 and 4 (Figure 2) and the 5S rRNA genes are located on chromosomes 3, 4 and 5 in close proximity to centromer regions (Campell et al. 1992). Also the constitution of rRNA genes shows a high diversity with respect to copy number and intergenic spacer (IGS) length even within the clade of green plants (Rogers and Bendich 1987). For *Arabidopsis thaliana* approximately 570 copies of the 45S rDNA locus and 1000 copies for the 5S rDNA locus were determined (Pruitt and Meyerowitz 1986).

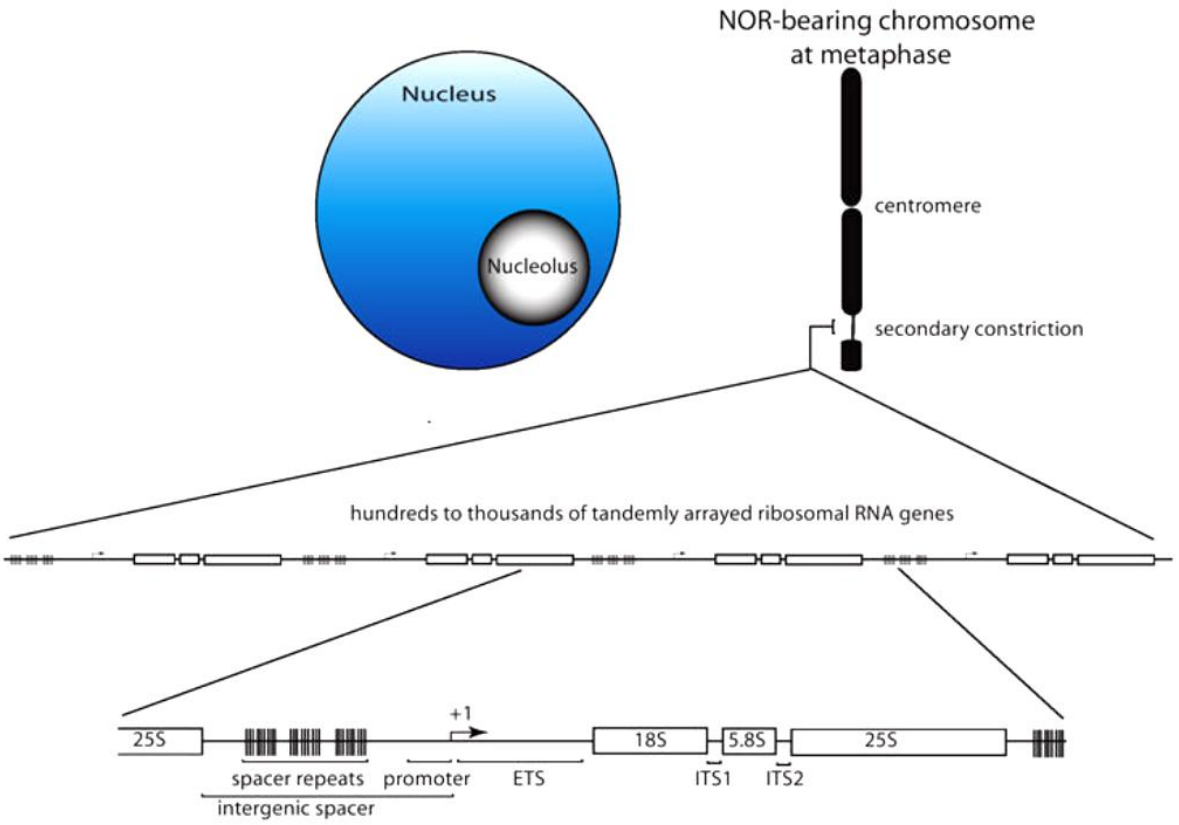

Figure 5. Relationships between the nucleolus, secondary constriction, NOR and ribosomal genes. rRNA genes are arranged as tandem arrays and form the secondary constriction in NOR-bearing methaphase chromosomes, from which the nucleus emanates (Preuss and Pikaard 2007).

1.3.2 The nucleolus

Nucleoli are membraneless organelles located in the nucleus, which are present in all eukaryotic cells and are the sites where different steps of ribosome biogenesis are grouped together. The organization as well as the size of nucleoli are directly related to ribosome production (Smetana K and H 1974). Nowadays the nucleolus is considered a multifunctional domain with extra ribosomal functions assigned to cell cycle, stress sensing, telomere formation, transfer RNA modifications, etc. (Boisvert et al. 2007). In plants it was also shown that important steps of silencing pathways take place within nucleoli (Pontes et al. 2006).

When observed by electron microscopy (EM), nucleoli appear to be composed of fibrils and granules with a high variability of the nucleolar morphology, based on the types or functions in animal and plant cells (Shaw and Jordan 1995). The three main structures, shown in Figure 6A, are designated as fibrillar centers (FCs), dense fibrillar component (DFC) and the granular component (GC). At the border of the FC

and DFC the initiation of rDNA transcription occurs. In the DFC the early processing and in the GC the late processing of the rRNAs happens. In most animal and plant cells a layer of heterochromatin surrounds the nucleoli.

During the cell cycle nucleoli assemble at the exit from mitosis, are functionally active throughout interphase and disassemble at the beginning of mitosis. They emanate from NORs (McClintock 1934), which represent rDNA gene regions that fail to condense during mitosis to the same extend as surrounding chromosomal regions and thus give rise to the secondary constrictions (chapter 1.1.3). During telophase and early G1 phase, when nuclear functions are reactivated, processing complexes that persist throughout mitosis in the cytoplasm or at the chromosome periphery, are regrouped in pre-nucleolar bodies (PNBs) (Jimenez-Garcia et al. 1994). Later on during G1 phase, yet not fully understood processes including the release of proteins involved in pre-rRNA-processing machinery from PNBs and reassembly with the rRNA-transcription machinery on the rDNA lead to the formation of new nucleoli. Finally the NORs move together in the nucleoplasm and fusion of the new nucleoli results in the typical functional nucleoli that are seen during interphase (Boisvert et al. 2007). The assembly of nucleoli at the end of mitosis is shown in Figure 6B.

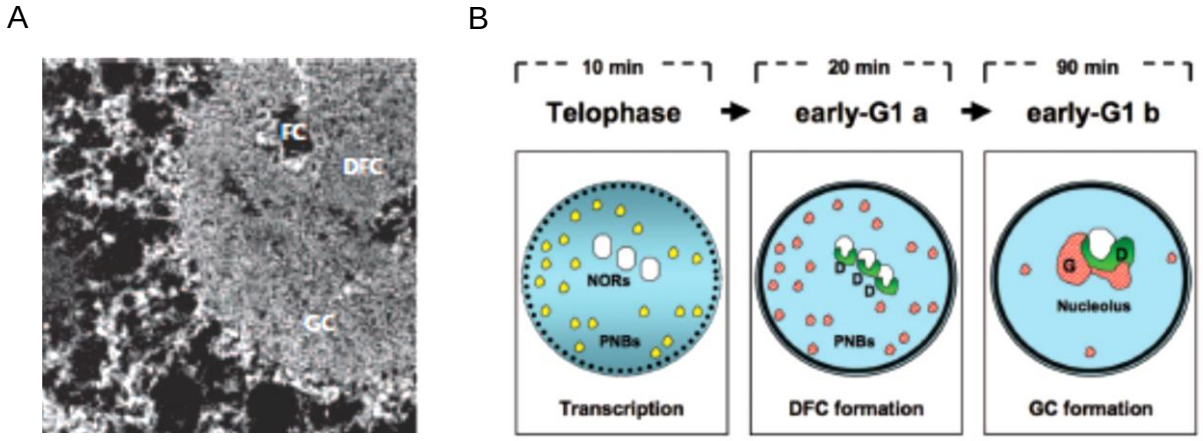

Figure 6. Main structures of nucleoli and assembly at the end of mitosis. (A) Ultrastructural analysis of HeLa cell nucleoli by electron spectroscopic imaging (ESI) showing the three main structures: fibrillar center (FC), dense fibrillar component (DFC) and granular component (GC) (Boisvert et al. 2007). **(B)** Schematic illustration of nucleolar assembly at the end of mitosis. In telophase transcription of the rDNA is activated (white octagons) in several NORs whereas early and late processing complexes are located in PNBs. Release of processing complexes from PNBs and fusion of NORs lead to the formation of nucleoli (Hernandez-Verdun 2011).

The nucleolar disassembly starts at the beginning of mitosis with the ordered release of processing components followed by the repression of Pol I transcription. During early prophase, Pol I transcription is approximately decreased by 30% and stops in late prophase (Gebrane-Younes et al. 1997). It is assumed that the majority of the RNA Pol I transcription machinery remains associated with rDNA repeats of active NORs during mitosis (Roussel et al. 1996). When the nuclear envelope breakdown is achieved at the end of prophase, the nucleolus is no longer visible (Gavet and Pines 2010). As mentioned before, during mitosis a part of the processing components are stored in the cytoplasm packed in nucleolar-derived foci (NDF) while others become attached to the surface of condensed chromosomes also called the perichromosomal region (PR) (Gautier et al. 1992). The PR layer is of irregular thickness and decorates the condensed chromosomes with exception of the centromeres. Besides processing components like ribonucleoproteins RNPs, small nucleolar RNA U3, fibrillarin and pre-rRNA the PR also contains non-nucleolar proteins, such as phosphorylated nucleoplasmin (Dundr et al. 2000). The role of the PR is not clear yet, but it has been proposed that it might function in the protection of chromosome integrity during mitosis and/or serve as a binding site for chromosomal passenger proteins. Another function might be to ensure that processing components are equally distributed between the daughter cells, as the PR-associated components will be moved

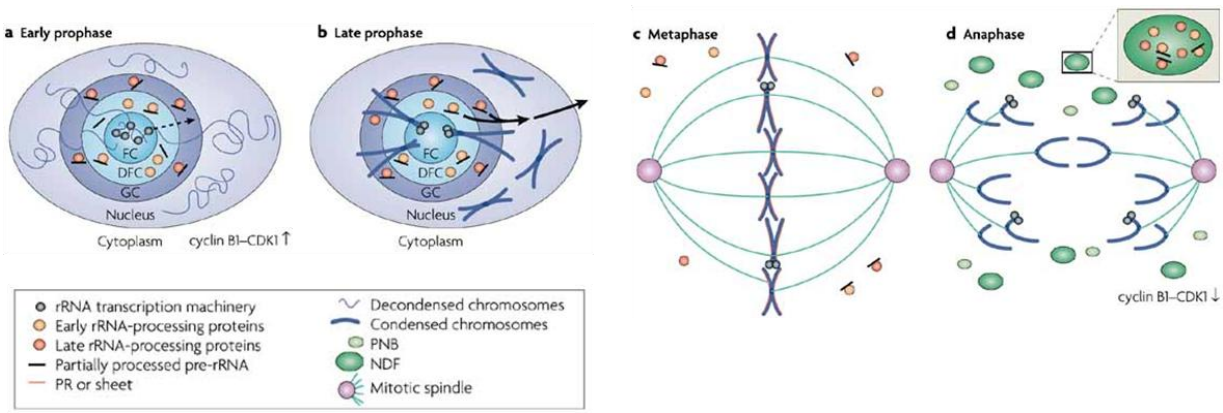

Figure 7. Nucleolar disassembly during mitosis. (a) During early prophase, cyclin-CDK1 levels increase and chromosomes start to decondense. Althought the transcription machinery usually remains attached to active NORs during mitosis, some RNA-Pol I subunits leave the FC. **(b)** In late prophase, early and late processing factors and partially processed pre-RNAs leave the nucleolus at the same time. **(c)** In methaphase, the processing components are distributed in the cytoplasm or associated with the surface of chromosomes as a PR. **(d)** During anaphase, cytoplasmatic processing components become packaged in NDF and cyclinB1-CDK levels decrease (Boisvert et al. 2007).

together with the chromosomes to the respective daughter nuclei. An illustration of the disassembly of a nucleolus is shown in Figure 7.

1.3.3 Regulation of rDNA transcription and nucleolar dominance

For the production of rRNA (except 5S rRNA), higher Eukaryotes possess a specialized transcription machinery with the Pol I. In actively growing cells it was shown that Pol I accounts for up to 80% of the total transcription activity in the nucleus, whereas in non-growing cells Pol I transcription falls to undetectable levels (Pikaard 2002). Pol I consists of 14 subunits and 12 of them have related counterparts in RNA Polymerase II (Pol II) and Pol III (Engel et al. 2013). Interestingly, transcription factor composition and function varies greatly between the phyla. In vertebrates, Pol I specific transcription factors like the upstream binding factor (UBF), the selectivity factor1 (SL1) and Rrn3 are well described. In yeast there are two major activities called Upstream Activation Factor (UAF) and Core Factor (CF) that is regarded to be analogous to SL1 (Keys et al. 1996, Lin et al. 1996). For UBF, no obvious homolog has been found in the genomes of non-vertebrates, including *Arabidopsis thaliana* (Pikaard 2002) but for HMO1, a HMG-box-containing yeast protein it was shown that it may be functionally equivalent to UBF (Gadal et al. 2002). In plants, besides the TATA Binding Protein (TBP) that is also used by Pol II and Pol III, there are no known homologues of Pol I transcription factors like UBF, UAF, SL1 or Pol I TBP Associated Factors (TAFs).

The number of active rDNA genes varies between cell types and level of differentiation and thus are regulated in a complex manner. Interestingly, the number of rRNA genes far exceeds the number expected to be required for supply of cytoplasmatic rRNA and thus excess copies have to be transcriptionally repressed (Rogers and Bendich 1987). In pea for example, it was shown that only about 5% of the 45S rDNA units are transcribed (Gonzalez-Melendi et al. 2001), suggesting that the majority of the 45S rDNA units remain transcriptionally inactive. In many species it seems that this inactivation involves a high level of rDNA chromatin condensation. Spatial organization of this condensed rDNA regions during interphase appears to be quite diverse. In plants, for example, in situ hybridization studies using interphase nuclei of cereals, pea and *Arabidopsis* suggested, that condensed rDNA is seen as chromatin blocks at the nucleolar periphery (Delgado et al. 1995, Pontes et al. 2003) but condensed rDNA chromatin might also appear inside the nucleolus depending on

the species. Whereas in wheat condensed DNA foci are found inside the nucleoli, such spots are not detected in rye (Leitch et al. 1992). The organization of ribosomal chromatin as described in wheat is shown in Figure 8A. In *Arabidopsis thaliana* it was shown that condensed 45S rDNA units are located in the nucleoplasm whereas decondensed 45S rDNA units are located in the nucleolus and hence the subnuclear partitioning of rRNA genes reflect the activity state of rRNA genes (Pontvianne et al. 2013). Traditionally, the silver impregnation technique, designated as AG-NOR staining, has been used to mark active rDNA regions during mitosis, reflecting their continuous association with argyrophilic proteins belonging to the transcription machinery (Miller et al. 1976). It was shown that there exist active and inactive NORs but importantly silver-stained regions have not necessarily to encompass an entire NOR. Instead condensed portions of a NOR can be adjacent to a decondensed silver-stained portion of the same NOR (Caperta et al. 2002). Furthermore by using sequential silver staining and in situ hybridization on mitotic rye chromosomes, it could be observed that the untranscribed rDNA units reside at the centromer proximal NOR domain (Figure 8B) (Caperta et al. 2002) as described also for *Saccharomyces cerevisiae* (Buck et al. 2002).

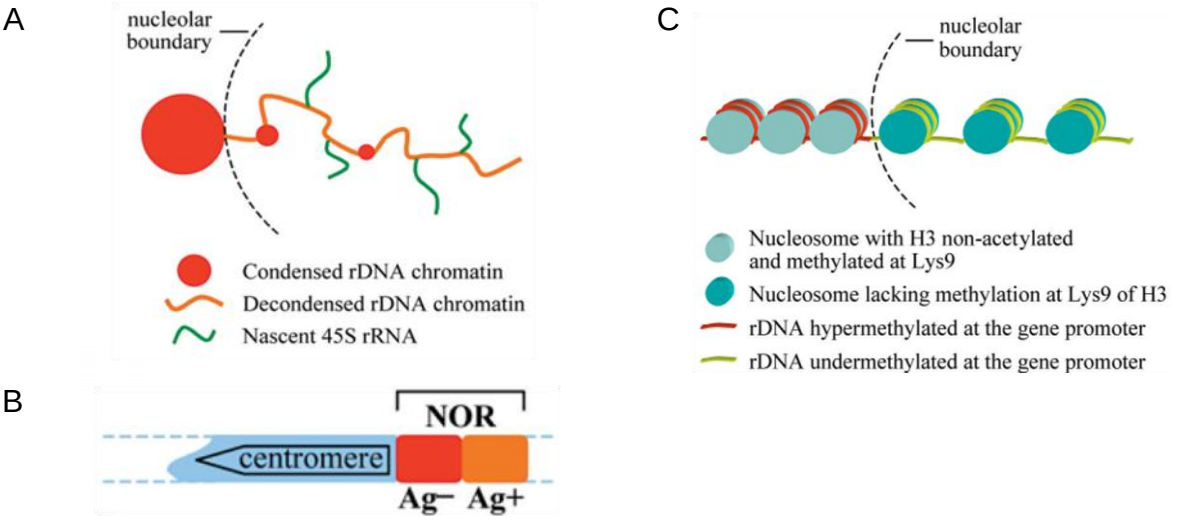

Figure 8. Organization of NORs during interphase and methaphase and epigenetic markers on ribosomal chromatin. (A) During interphase most rDNA units remain condensed at the periphery of the nucleolus. The occurrence of intranucleolar condensed rDNA knobs is a species-specific feature. **(B)** At metaphase, only the centromere-distal NOR domain is revealed by silver staining, indicating previous expression of its rDNA units. **(C)** Condensed perinucleolar blocks are enriched in histone H3 methylated at lysine 9 and are densely methylated at their rDNA gene promoters. Active intranucleolar rDNA units have a low density of cytosine methylation at gene promoters and H3 is barely methylated at lysine 9 (Neves et al. 2005).

Chromatin modifications that usually mark heterochromatin e.g. lysine methylation and post-translational changes on histones can also be found in silenced rRNA gene arrays as shown in Figure 8C and concerted changes in these modifications comprise an epigenetic switch that turns rRNA genes on and off (Lawrence et al. 2004). Intriguingly, one of the earliest recognized epigenetic phenomena, nucleolar dominance, describes the transcription of 45S rDNA genes from only one parent in genetic hybrids and occurs in species of diverse phyla (McStay 2006). Therefore, the nucleolus forms around rRNA genes inherited from only one progenitor, while the rRNA genes of the other progenitor are silenced (Chen and Pikaard 1997). One of the best studied models for nucleolar dominance is the allotetraploid hybrid of *A. thaliana* and *A. arenosa* (Chen and Pikaard 1997), in which the *A. thaliana* NORs are silenced and enriched for the heterochromatic mark H3K9me2 and depleted for the euchromatic mark H3K4me3. However, only a subset of the *A. arenosa* 45S genes is active, decondensed and enriched for the H3K4me3, while the rest is also heterochromatic (Lawrence et al. 2004).

An analogous phenomenom was explored in nonhybrid *A. thaliana,* in which specific classes of rRNA gene variants are inactivated (Pontvianne et al. 2012). *A. thaliana* contains three major 45S gene variants designated *VAR1*, *VAR2* and *VAR3* corresponding to approximately 48, 30 and 22% of total 45S genes and *VAR4* that has only a very low copynumber (Pontvianne et al. 2010).Thereby *VAR1* is only active in germinating seeds, whereas the other variants are preferentially expressed during the later stages of plant development.

1.4 HMG-box containing proteins

1.4.1 The HMG-box DNA binding domain

The HMG-box is defined by a conserved sequence of about 75 amino acids, that forms a characteristic, twisted, L-shaped fold consisting of three α- helices with an angle of approximately ~80° between the arms (Hardman et al. 1995). It is suggested, that the overall structure is conserved to a greater extent than it can be deduced from the amino acid sequence (Baxevanis et al. 1995). HMG boxes preferentially bind to the minor groove of DNA and induce a bend towards the major groove by unwinding and widening the minor groove through electrostatic and hydrophobic interactions. Thereby intercalating residues aid in stabilization of the

distorted DNA structure (Churchill et al. 2010). The extent of DNA bending varies between HMG-boxes. To give an impression, angles of about 54° for the HMG-box of the male sex-determining factor (SRY) (Murphy et al. 2001) to 110° for the HMG-box of LEF-1 (Love et al. 1995) were measured. HMG-boxes typically contain a non-polar amino acid at the N-terminus of α helix 1 that intercalates in the 1° site. Whereas non-sequence specific HMG-boxes contain at the N-terminus of α helix 2 an additional non-polar intercalating residue in the 2° site, a residue at the same position of sequence specific HMG-boxes appear to form base-specific hydrogen bonds (Murphy et al. 1999, Jauch et al. 2012). In Figure 9, an example for a sequence specific and a nonsequence specific HMG-box with their DNA intercalating residues are shown.

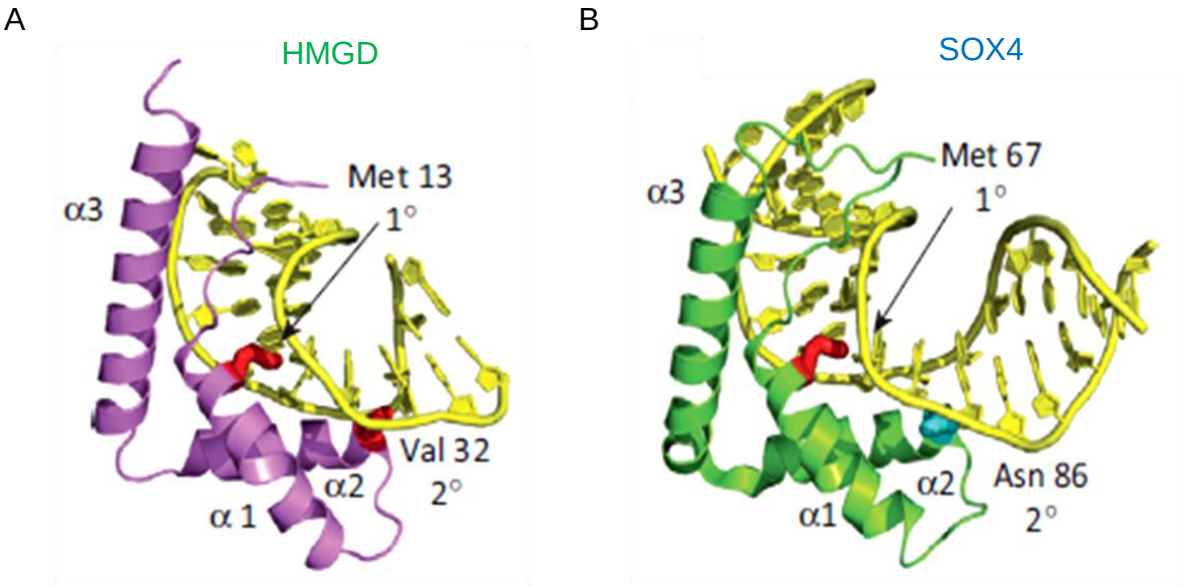

Figure 9. Structur of high mobility group (HMG) box-DNA complexes. (A) Nonsequence-specific HMGD bound to unmodified DNA decamer. **(B)** Sequence-specific Sox4 bound to a 16-base pair DNA oligomer (Malarkey and Churchill 2012).

1.4.2 High mobility group (HMG)-box proteins

The HMG-box is a protein domain that can interact with DNA but also with other proteins and was named after the first discovered protein family in 1973, termed high mobility group (HMG) proteins (Goodwin et al. 1973), containing such a domain. The term “high mobility group” originates from their discovery as proteins in calf thymus extracts, that migrate relatively fast in electrophoresis. After histones, the superfamily of HMG proteins is the second most abundant group of chromatin associated proteins and comprises three families namely HMGA, HMG-N and HMG box (HMGB) (Bustin 2001). HMG proteins serve diverse functions as architectural DNA binding

proteins in the nucleus and mitochondria, as signaling regulators in the cytoplasm and as inflammatory cytokines in the extracellular milieu. Besides proteins that are assigned to the HMG protein super family, also many other proteins involved in manifold cellular processes, e.g. chromatin-remodeling, DNA-recombination/repair etc., possess one or more HMG-box domains (Stros et al. 2007). HMG-box containing proteins have single or multiple HMG-boxes and can be classified as either DNA sequence-specific or non-sequence-specific (Landsman and Bustin 1993). One known exception is the human mitochondrial transcription factor 1 (TFAM), a tandem HMG-box protein that contains both a sequence-specific and non-sequence specific HMG-box domain (Alam et al. 2003). Most HMG-box containing transcription factors are sequence specific and contain a single HMG box (Murphy and Churchill 2000) e.g. Lymphoid Enhancer Factor1 (LEF-1) (Arce et al. 2006) and Sox4 (Badis et al. 2009) (Figure 9B). Often HMG-box domain(s) containing proteins also possess protein domains with different functions, e.g. Structure-Specific Recognition Protein1 (SSRP1) (Bruhn et al. 1992). The ability of HMG-box containing proteins to bend DNA and thereby altering local chromatin structures is one of the main requisites for their function in diverse nuclear processes.

An interesting and one of the best investigated example for a HMG-box containing protein that is considered to have chromatin architectural functions is the vertebrate Pol I transcription factor UBF, mentioned in chapter 1.3.3, which possesses 6 HMG-box domains. It interacts, like other HMG proteins, with the minor groove of duplex DNA (Copenhaver et al. 1994) and is able to bend and wrap linear DNA fragments (Bazett-Jones et al. 1994). It binds DNA as a dimer (McStay et al. 1991) and like many other HMG-box containing proteins displays a higher affinity to certain DNA structures such as DNA kinked by cisplatin, DNA cruciforms or four-way junctions (Copenhaver et al. 1994, Treiber et al. 1994). Beside its function as a central component of the Pre Initiation Complex (PIC) for Pol I mediated transcription it is a prime candidate for “maintaining” the open chromatin state of secondary constrictions during mitosis and may also prevent or reverse the assembly of transcriptionally inactive chromatin structures mediated by linker histone H1 binding (Kermekchiev et al. 1997, Russell and Zomerdijk 2006). Besides UBF, also many other HMG-box containing proteins were shown to affect DNA binding of linker histone H1, by sharing the same binding sites or direct interaction, which suggests a functional interplay

between these two groups of proteins, often in an antagonistic manner (Zhao et al. 1993, Catez et al. 2004, Cato et al. 2008).

1.4.3 Plant HMG-box proteins

As mentioned in chapter 1.4.2, the HMG-box can be found in proteins with various functions and often occurs in combination with other functional protein domains. Compared to mammals, plant genomes appear to encode a smaller number of HMG-box proteins that are less diversified (Riechmann et al. 2000). The human genome for example encodes for 47 HMG-box proteins that range from approximately 15 to 193 kDa, while genomes of higher plants encode for 10-15 different HMG-box proteins that range from approximately 15 to 72 kDa (Stros et al. 2007). Unlike in mitochondria of animal and yeast, mitochondria in plants do not seem to possess any HMG-box proteins (Bonawitz et al. 2006, Kucej and Butow 2007). Also no HMG-box protein in plastids of higher plants has been reported, yet. Furthermore, it is unclear if any plant HMG-box protein can act as a transcription factor and no sequence-specific DNA interaction for a plant HMG-box protein has been proven. Based on their amino acid sequence similarity and overall structure, plant HMG-box proteins can be subdivided in four families: chromosomal HMGB proteins, AT-rich interaction domain (ARID)-HMG proteins, 3xHMG-box proteins, and SSRP1. A multible sequence alignment of poteins from various plant species that contain one or more HMG boxes allowed the construction of a neighbor joining tree that illustrates the four distinct families of plant HMG-box proteins (Figure 10).

The largest subgroup of HMG-box proteins in plants is representsed by the small chromosomal HMG-proteins that range from 13-27 kDa. They possess a single HMG-box domain that is flanked by a basic N-terminal and an acidic C-terminal region (Pedersen and Grasser 2010). They display typical properties of HMGB proteins such as DNA bending activity, low affinity, sequence independent binding to linear DNA and high-affinity interaction with certain DNA structures like hemicatenated DNA loops, four-way junctions, DNA minicircles and supercoiled DNA (Stemmer et al. 1997, Wu et al. 2003, Zhang et al. 2003). Thereby, interactions of the basic N-terminal and acidic C-terminal domain with each other and DNA seem to modulate their binding properties (Ritt et al. 1998, Launholt et al. 2006). Members of the HMGB proteins in plants are mainly found in the nucleus but some of them were

also shown to be able to shuttle between nucleus and cytoplasm (Grasser et al. 2006, Pedersen et al. 2010).

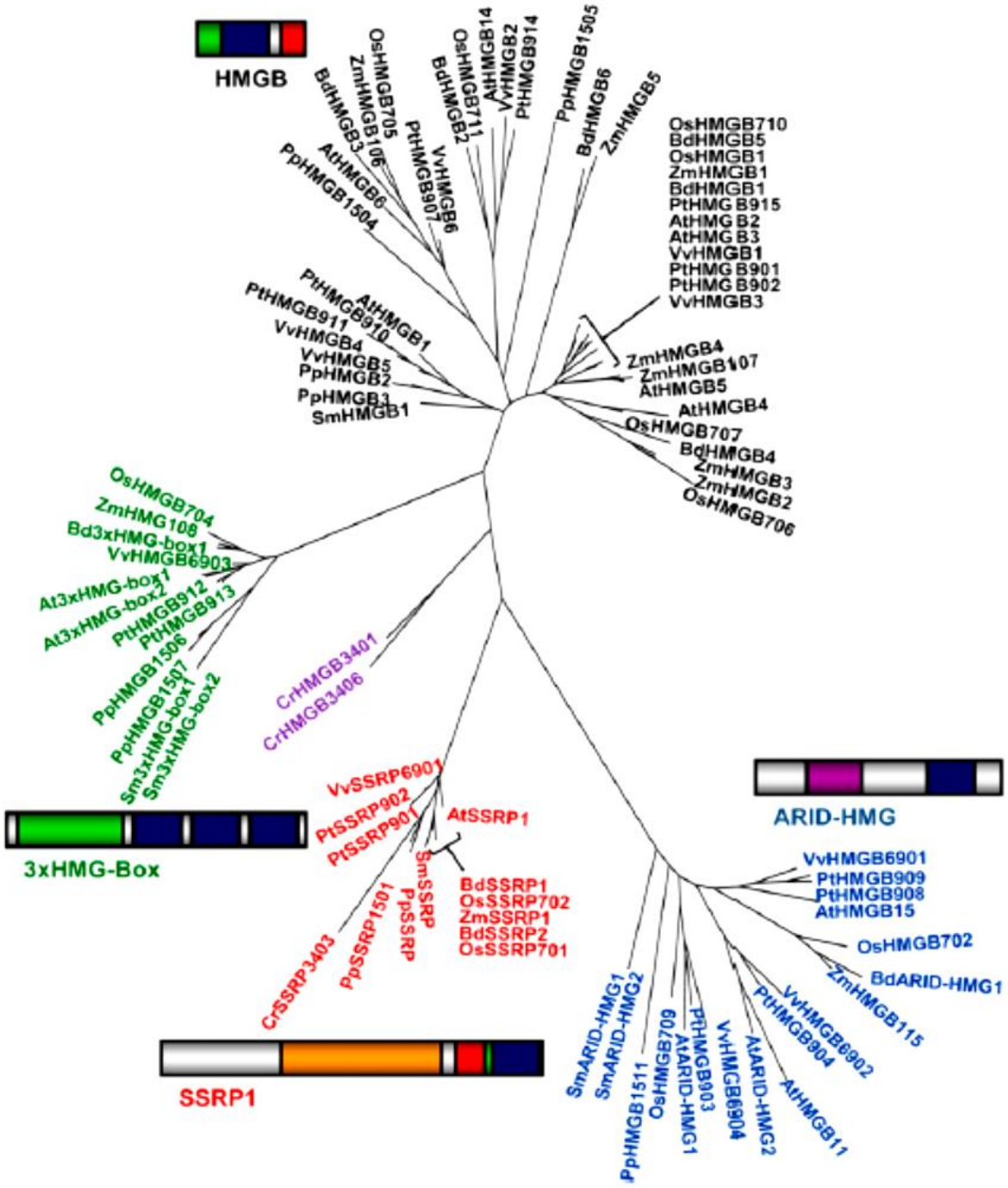

Figure 10. Sequence alignment of HMG-box containing plant proteins. Amino acid sequences of plant HMG-box containing proteins were aligned to create a neighbor-joining tree using SeaView software. Sequences are derived from *Brachipodium distachyon* (Bd), *Oriza sativa* (Os), *Zea mais* (Zm), *Arabidopsis thaliana* (At), *Populus trichocarpa* (Pt), *Vitis vinifera* (Vv), *Selaginella moellendorffii* (Sm), *Physcomitrella patens (*Pp), *Chlamydomonas reinhardtii* (Cr). Overall structure of the four families of HMG-box containing proteins that were identified in plants are represented schematically: HMG-box domain (blue), basic region (green), acidic region (red), SSR domain of SSRP1 (orange) and ARID (violet) (Antosch et al. 2012).

Within the nucleus they were shown to be highly dynamic and associate with chromatin only transiently (Bianchi and Agresti 2005). HMGB proteins mainly function as chromatin architectural factors and besides the well studied interactions with DNA, they were shown to interact with manifold proteins including DNA repair proteins, transcription factors, silencing complexes, site-specific recombination proteins, viral proteins etc. (Stemmer et al. 2002, Agresti and Bianchi 2003). In line with that, interplay with linker histone H1, as already been mentioned in chapter 1.4.2, has been postulated (Bustin et al. 2005, Thomas and Stott 2012). Additionally, in plants it has been demonstrated that HMGB proteins can act as chaperones for the assembly of specific nucleoprotein complexes (Grasser et al. 2007) and that they are involved in stress responses (Kwak et al. 2007, Lildballe et al. 2008) as well as in differentiation and proliferation processes (Hu et al. 2011).

SSRP1 together with SPT16 forms the dimeric facilitates chromatin transcription (FACT) complex (Orphanides et al. 1999) and was first discovered in yeast and mammals. It is able to assemble/disassemble nucleosomes and thus modulate the Pol II catalyzed transcription elongation. Genes for SSRP1 were found in flowering plants as well as in *Selaginella, Physcomitrella* and *Chlamydomonas* (Figure 10). In *Arabidopsis*, FACT was found to be associated with euchromatin and transcribed regions of active genes, underpinning its function in active transcription in plants (Duroux et al. 2004). An *Arabidopsis,* knock out of *SSRP1* is lethal and decreased levels of SSRP1 cause various defects in vegetative and generative development (Lolas et al. 2010). Not too long ago, a novel function of SSRP1 in parent-of origin-specific gene expression was discovered in *Arabidopsis*. It is proposed that SSRP1 is necessary for DNA demethylation and for activation/repression of parentally imprinted genes in the central cell of the female gametophyte (Ikeda et al. 2011).

The ARID-HMG proteins are unique for plants and characterized by a C-terminal HMG-box domain that occurs in combination with an N-terminal AT-Rich Interaction Domain (ARID) DNA binding module that preferentially binds to AT-rich DNA stretches. Coding sequences for ARID-HMG proteins were found in all analyzed flowering plants as well as in *Selaginella* and *Physcomitrella* (Figure 10). In *Arabidopsis,* four genes that encode for this class of proteins are annotated and *ARID-HMG1/2* was shown to be expressed ubiquitously. In tobacco BY-2 suspension cell cultures ARID-HMG1 and ARID-HMG2 are localized in the nucleus. ARID-HMG1 has slightly higher affinity to AT-rich DNA compared to GC-rich DNA and binds DNA

structure specific due to its HMG-box domain (Hansen et al. 2008). The function of ARID-HMG box proteins is not known, yet.

1.4.4 3xHMG-box proteins

This subgroup of HMG-box proteins are only found in plants and appear to be relatively conserved. In flowering plants, one to two 3xHMG-box proteins are encoded per genome, depending on the species. The moss *Physcomitrella patens* has two versions of 3xHMG-box sequences, while no 3xHMG-box sequence could be found in the algae *Chlamydomonas reinhardtii* (Figure 10).

3xHMG-box proteins possess an N-terminal basic region followed by 3 HMG-box domains (Figure 10) and range from 43kDa to 60kDa. Until now only the two *A. thaliana* 3xHMG-box proteins, which share 77% amino acid sequence identity and are termed 3xHMG-box1 and 3xHMG-box2, were experimentally analyzed (Pedersen et al. 2011). Expression was detected in various tissues but in a cell cycle dependent manner, with highest expression level during mitosis.

Surprisingly, 3xHMG-box proteins that were fused to GFP and expressed under the control of the strong constitutive cauliflower mosaic virus promoter in BY-2 protoplasts and in *A. thaliana* plants were mainly localized in the cytoplasm. Only in individual cells of *A. thaliana* roots, 3xHMG-box proteins seemed to be associated with chromatin, likely representing cells in mitotic stage. By immunostaining experiments using root cells, it could be demonstrated that 3xHMG-box proteins are only associated with DNA during mitosis and that 3xHMG-box2 decorates all chromosomes, while 3xHMG-box1 is specifically associated with NOR regions (Figure 11A/B). Furthermore 3xHMG-box proteins were also shown to be associated with condensed chromosomes during meiosis of pollen mother cells. It could be proved that 3xHMG-box1 and 3xHMG-box2 bind structure specifically to DNA and display DNA bending activity. All three HMG-box domains as well as the N-terminal domain were shown to contribute synergistically to DNA binding.

A function for 3xHMG-box proteins could not be identified. Association with mitotic and meiotic chromosomes suggest a function in general division processes that can be linked to chromatin e.g. condensation and segregation but besides many other roles during cell division are thinkable.

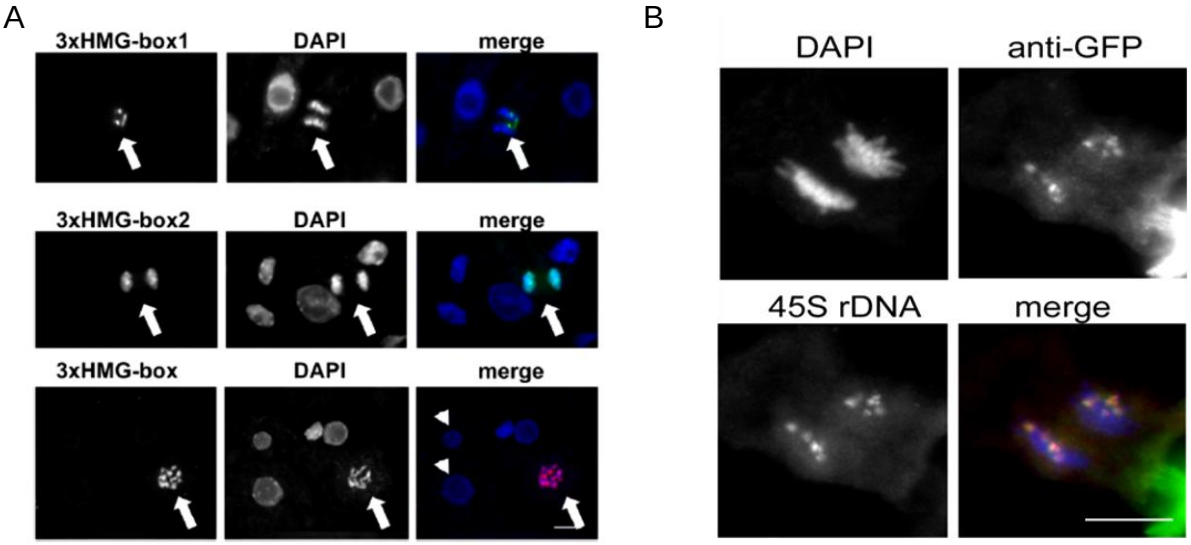

Figure 11. 3xHMG-box proteins in *A.thaliana*. (A) Root cells of *A. thaliana* plants expressing either 3xHMG-box1 or 3xHMG-box2 fused to GFP under the control of the cauliflower mosaic virus 35S promoter were used for immunostaining with antibodies directed against GFP and DAPI as counterstain. 3xHMG-box2 seems to generally associate with condensed chromosomes, while 3xHMG-box1 is detected at specific foci. In the lower panel, root cells of Col-0 plants were used for immunostaining with an antibody that binds to the N-terminal regions of both 3xHMG-box proteins. 3xHMG-box proteins are detected in mitotic prophase cells, but not in interphase cells. Arrows indicate mitotic cells and scale bar indicate 5 µm (Antosch et al. 2012). **(B)** Root cells of *A. thaliana* plants expressing 3xHMG-box1 fused to GFP under the control of 35S promoter were used for subsequent FISH with probes that stain 45S rDNA and an antibody directed against GFP. 3xHMG-box1 appear to colocalize with 45S rDNA. DAPI was used for counterstaining and scale bar indicates 5 µm (Pedersen et al. 2011).

1.5 Aim of the thesis

Until now, only a few studies have been performed that suggested functions of 3xHMG-box proteins in cell division processes. It could be shown that 3xHMG-box proteins associate with condensed chromosomes during mitosis and meiosis and that 3xHMG-box1 exhibits specificity for 45S rDNA regions. Furthermore, DNA binding properties were analyzed for full length 3xHMG-box2 as well as for its single domains. Still many questions regarding function, spatiotemporal distribution, specificity of 3xHMG-box proteins and the contribution of the single domains in this context, remain open.

One of the goals of this thesis was to further enlighten the spatiotemporal distribution of 3xHMG-box proteins. It was already shown by Immunocytochemistry that 3xHMG-box proteins are associated with condensed chromosomes at different stages during mitosis. In order to monitor the occurrence of 3xHMG-box proteins during cell cycle and specifically mitosis, life cell imaging with roots of *Arabidopsis* seedlings which express 3xHMG-box1/2-GFP under the control of the respective endogenous promoters, was the method of choice.

One of the major tasks of this work was to gain further insights into the possible function of 3xHMG-box proteins. Functional analyzes of unknown proteins is often the most interesting, but also most difficult aspect to approach. In order to do so, one of the main approaches is the reverse genetics. In this work a T-DNA insertion line containing an insertion in the *3xHMG-box1* gene was analyzed and transcription of the *3xHMG-box2* gene was tried to shut down by RNA interference (RNAi) approaches. The other way around, as overexpression of 3xHMG-box1/2-GFP leads to accumulation in the cytoplasm and causes no effects, 3xHMG-box proteins were fused to GFP-NLS in order to force the proteins into the nucleus. Plants were used for phenotypical studies and further molecular biological approaches.

Another project was to analyze the contribution of single domains of 3xHMG-box1 to specificity for 45S rDNA regions. For that, truncated versions of 3xHMG-box proteins were fused to GFP-NLS and analyzed by microscopy.

2. Material and Methods

2.1 Materials

2.1.1 Instruments

Blotting System	Semy-Dry-Blotting System, Carl Roth
Centrifuges	Evolution RC+SLA1500 and SS34 Sorvall
	5417R, 5427R, 5864R , Eppendorf
Digital Cameras	AxioCam MRm, Zeiss
	D90, Nikon
Hybridization oven	UV Stratalinker™ 1800, Stratagene
Imager	BioDocAnalyzer, Biometra
	Multiimage II FC2, Alpha Innotech
	Cyclone™, Packard Instrument Co.
Membranes	Hybond N membrane, GE Healthcare
	Immobilon™ PVDF Transfer Membrane, Millipore
Microscopes	Eclipse TE 2000-5, Nikon
	Primo Star, Zeiss
	C-PS stereoscope, Nikon
	LSM510 CLSM, Zeiss
	SP8 CLSM, Leica
Microtome	OmU2, C. Reichert
Objectives	2,8/100 Pro D Macro, Tokina
	Plan Fluor 4x/0.13, Nikon
	HC PL CS2 40x/1.3 Oil
Plant Incubator	CU-36L4/D, Percival Scientific
Phosphoscreen	Cyclone Storage Phospho Screen, Packard Instruments Co.
Spectrophotometer	NanoDrop 2000, Thermo Scientific
Sonicator	Sonopuls+MS73, Bandalin
Thermocycler	T3000 and T-Gradient, Biometra
Shaking Incubator	Multitron Standart, Infors HT
Quantum Meter	Quantum Flux ML-200, Apogee Instruments

2.1.2 Chemicals, Antibodies and Enzymes

Chemicals were purchased from Abcam (UK), Affymetrix (USA), Applichem (Germany), Braun (Germany), Bayer Crop Science (Germany), Biomol (Germany), Carl Roth (Germany), Duchefa (Netherlands), Fluka (Swizerland), Jena Biosciences (Germany), Life Technologies (USA), Merck (Germany), Qiagen (Netherlands), Sigma Aldrich (Germany), Thermo Fisher Scientific (Germany), Vector Laboratories (USA) and VWR (USA).

Phosphorhus-32 was obtained from Hartman Analytic (Germany).

2.1.3 Antibiotics

Antibiotics that were used in this work and respective suppliers, concentrations and solvents are listed in Table 1. All antibiotics were sterile-filtered prior to use.

Table 1. List of antibiotics.

Name	Concentration stock solution	Final concentration	Solvent	Provider
Ampicillin	100mg/ml	100µg/ml	H_2O	Roth
Carbinicillin	50mg/ml	500µg/ml	H_2O	Duchefa
Gentamycin	100mg/ml	100µg/ml	H_2O	Duchefa
Hygromycin B	502mg/ml	30µg/ml	H_2O	Duchefa
Kanamycin	50mg/ml	50µg/ml	H_2O	Roth
Tetracyclin	6mg/ml	12µg/ml	EtOH	Sigma-Aldrich
Vancomycin	50mg/ml	500µg/ml	H_2O	Duchefa

2.1.4 Oligonucleotides

Oligonucleotides used in this study (Table 2) were purchased from MWG (Germany).

Table 2. List of oligonucleotides. Restriction sites are highlighted in red.

Number (Lab-number)	Name	Sequence (5'-3')
P1 (2684)	X3_Prom_for_XbaI	GCTCTAGAAGCTAGAGTTTCTAATGAACCG
P2 (2685)	X3_Prom_rev_XbaI	GCTCTAGATGTGAGAGAGATTGAGCGAG
P3 (2480)	X4PromforHindIII	CCCAAGCTTTATTGATTCTTGGGAGCTAGC
P4 (2481)	X4PromrevXbaI	GCTCTAGATTCTAAAGTCGAAAATGAGAGA
P5 (2360)	HMGX3_for_XbaI	GCTCTAGAATGTCGACAGTTTCTTCAGATCC
P6 (2646)	X3osrevXmaI	CCCCCCGGGCGACGAAGTCTTGGTCTT
P7 (2362)	HMGX4_for_XbaI	GCTCTAGAATGGCGACCAACGCAGATC
P8 (2647)	X4os+1revBamHI	CGGGATCCTGCTACTGGTAGTAGCCG
P9 (2484)	GFP_rev+Stop_EcoRI	GGAATTCTTATTTGTATAGTTCATCCATGCCATGTG
P10 (750)	AthHMGA 5'forw BamHI	AATTGGATCCATGGCCTTCGATCTCCACCAT
P11 (751)	AthHMGA 3'rev SmaI	AATTCCCGGGTCAGCACCCAACCGGAGCAA
P12 (3465)	X4_degmut_for	AGTGCAAAGGCGGCGAAGCAGAAGAAT
P13 (3466)	X4_degmut_rev	ATTCTTCTGCTTCGCCGCCTTTGCACT
P14 (3046)	X3_for_RT	ATCTGATGGAGATGCAAGCG
P15 (3047)	X3_rev_RT	TTCTGCTTCTGCTCATCATC
P16 (3048)	X4_for_RT	GAGCAGGAGAAGCTCAAGG
P17 (3049)	X4_rev_RT	CCTGTTCAGCTTCCTGGAC
P18 (1354)	AtUBQ5_FW	GAAGGCGAAGATCCAAGACAAGGAA
P19 (1355)	AtUBQ5_RV	GGAGGACGAGATGAAGCGTCGA

P20 (2491)	HMGX4forAscIXbaI	GGCGCGCCTCTAGAAGCGACCATCGTCCTCATAC
P21 (2492)	HMGX4revSwaIBamHI	GGATTTAAATGGATCCAGGCTTCTTTGGTTTGTTAGG
P22 (1075)	pFGC5941_MCS1_fw	AGTTCATTTCATTTGGAGAGGACACG
P23 (1076)	pFGC5941_MCS1_rv	GAAGAGCCAATTAAGATAAAACGTTGAATGTA
P24 (1077)	pFGC5941_MCS2_fw	TTCTTCTTTTATTTATTGAGGGTTTTTGCA
P25 (1078)	pFGC5941_MCS2_rv	TCGCATATCTCATTAAAGCAGGACTCTAGG
P26 (1473)	realTimeAtActin8fw2	TGCTGGTCGTGACCTTACTGATTACC
P27 (1474)	realTimeAtActin8rv2	TCTCCATCTCTTGCTCGTAGTCGACA
P29 (3002)	X4_I_miRs	GATCTTCGCGTAAAGCCGCTCTTTCTCTCTTTTGTATTC
p30 (3003)	X4_II_miRa	GAAAGAGCGGCTTTACGCGAAGATCAAAGAGAATCAATGA
p31 (3004)	X4_III_miR*s	GAAAAAGCGGCTTTAGGCGAAGTTCACAGGTCGTGATATG
P32 (3005)	X4_IV_miR*a	GAACTTCGCCTAAAGCCGCTTTTTCTACATATATATTCCT
P33 (2998)	Hau62	CACCAAACACACGCTCGGACGCATATTAC
P34 (2999)	Hau63	CATGGCGATGCCTTAAATAAAGATAAA
p35 (1939)	pGreen sequencin rw primer after 35S MCS	ATTTGTAGAGAGAGACTGGTG
P36 (2752)	GS for+ATG SmaI	AATTCCCGGGATGGAGCAGAAGCTTATCTCC
P37 (2506)	GS-tag rv SacI	AATTGAGCTCCTATTCAGTGACAGTGAAAG
P38 (1937)	pGreen sequencin fw primer before 35S prom.	GTTGTAAAACGACGGCCAGTG
P39 (2980)	GFPa_revStoEcoRI	GGAATTCTTACTTGTACAGCTCGTCCATGCCGAGAG
P40 (2696)	18SrRNAfwd	CGGGTGACGGAGAATTAGGGTTC
P41 (2697)	18SrRNArev	GCCCTCCAATGGATCCTCGTTA
P42 (2772)	ITS1_fwd	GATACCTGTCCAAAACAGAACGACCCGCG
P43 (2767)	5,8S_rev	TGCGTTCAAAGACTCGATGG
P44 (2768)	5'ETS1_fwd	GAGTCTGGGCAGTCCGTGG
P45 (2860)	IGS_thaFISH_rev	CGATATCCGATACCATCCCT
P46 (2771)	5'ETS2_rev	AAGGACGGATGAGCTTTGGCGGG
P47 (2991)	5'ETS_north_fwd	CTCATCCGTCCGTCCTTCGGGCAA
P48 (2992)	5'ETS_north_rev	GCATTCATCGATCACGGCAA
P49 (2698)	25SrRNA_rev	ACGGACTTAGCCAACGACAC
P50 (2699)	25SrRNA_for	CTAGTACGAGAGGAACCGTTGATTC
P51 (2968)	X3prebox1revXmaI	CCCCCCGGGTTCTTCAGTTTGTGCCAAAGA
P52 (2967)	X3prebox1forXbaI	GCTCTAGAATGTCTTTGGCACAAACTGAAGAA
P53 (2970)	X3prebox2revXmaI	CCCCCCGGGTCTTGTTGTCATGTTCAGCTT
P54 (2969)	X3prebox2forXbaI	GCTCTAGAATGCAGGAAGCTGAACATGACAAC
P55 (2972)	X3prebox3revXmaI	CCCCCCGGGCTTGTTCTTCGCCGTCTC
P56 (2971)	X3prebox3forXbaI	GCTCTAGAATGGAGACGGCGAAGAACAAG
P57 (3404)	X3-N-ter_rev (+2360)	AAGCAAAAGTCATGTTAGG
P58 (3405)	X4ohneN-ter_for (+2363)	CCTAACATGACTTTTGCTT
P59 (3500)	Hyb2_Nter_rev	ACAATCCTTTTTCTTCTTCTTATTCGCCTTTTCT
P60 (3501)	Hyb2_Cter_for	AAGAAGAAGAAGAAGGATTGTGCTGAAACAAAG
P61 (2648)	45S rDNA_bp_for	CCCCAACTAGACCATGAA
P62 (2651)	45S rDNA2_revHindIII	CCCAAGCTTCAGTTTCACAGTCTGAATTCGT
P63 (2650)	45S rDNA2_forKpnI	GGGGTACCCGAATGGCTCATTAAATCAGTT
P64 (2653)	25S rDNA_revHindIII	CCCAAGCTTAGTCGTCTGCAAAGGATTC
P65 (2652)	25S rDNA_forKpnI	GGGGTACCCGACGGGGTATTGTAAGTG
P66 (2649)	45S rDNA_bp_rev	CTCCGTGGGCATATTTGA
P67 (3463)	X3_for_BamHI	CGGGATCCATGTCGACAGTTTCTTCAGAT
P68 (3464)	X3_revNt_HindIII	CCCAAGCTTCTTCTTCTTTCCCTTCTT
P69 (2973)	FISH_are_IGSifor	CATCAATAAAGAGTGTAGGATGTC
P70 (2862)	IGS_areFISH_rev	GCATTCATCGATCACAGCAA
P71 (3451)	eGFP(NLS)forXbaI	GCTCTAGAATGGTGAGCAAGGGCGAGGA
P72 (3452)	eGFP(NLS)revXhoI	CGGCTCGAGTCAGACCTTTCTCTTCTTTTTTG
P73 (2895)	H1.1 fw XbaI	GCTCTAGAATGTCAGAGGTGGAAATAGAG
P74 (2896)	H1.2 fw XbaI	GCTCTAGAATGTCTATAGAGGAAGAAAACG
P75 (2605)	RFP stop rv BamHI	AATTGAATTCTAAGGCGCCGGTGGAGTGG
P76 (1595)	GABI-KAT LB 8409	ATATTGACCATCATACTCATTGC

2.1.5 Plasmids

Plasmids that were already available in our lab are listed in Table 3. For this work constructed plasmids with description of the inserts, used primers and target plasmids are listed in Table 4.

Table 3. List of plasmids used in this study.

Name (Lab-number)	Description	Resistance
pL1(778)	pGreen0179+35S terminator: heterologous expression in *Arabidopsis*	kan/hyg
pL2 (408)	3xhmg-box2 cDNA+3'GFP in pGreen0179+35S cassette	kan/hyg
pL3 (415)	3xhmg-box1cDNA+3'GFP in pGreen0179+35S cassette	kan/hyg
pL4 (ori 39)	pFGC5941: RNAi approach to silence genes in *Arabidopsis*	amp/Basta
pL5 (782)	pGreen0229+35S terminator+Ubiquitin10 promotor	kan/Basta
pL6 (743)	pCAMBIA-2300 with 35S terminator	kan/kan
pL7 (712)	pCambia2300 3'GS-tag Elf7 CDS	kan/hyg
pL8 (781)	pGreen0229+ 35S cassette+GFP-NLS: heterologous expression of reporter constructs in *Arabidopsis*	kan/Basta
pL9 (381)	N-terminal region of 3xhmg-box2 (M1-K132) in pQE9	amp
pL10 (ori 72)	pWS3638: heterologous expression in yeast	amp
pL11(666)	654+H11endogeneous promoter+H11genomic sequence	kan/hyg
pL12 (664)	652+H11cDNA	kan/hyg
pL13 (665)	652+H12 cDNA	kan/hyg
pUC19 (ori 24)	cloning vector	amp
pRS300 (ori 66)	generation of microRNA for amiRNA approach	amp

Table 4. List of plasmids constructed in this study.

Name (Lab-number)	Description (insert, vector, primer)	Resistance	Restrictionsites
pM1(576)	3xHMG-box2 promoter+3xHMG-box2+3`GFP in pGreen0179, plasmid 780, primer 2362/2463	kan/hyg	SmaI/blunt
pM2 (586)	3xHMG-box1promoter+3xHMG-box1+3`GFP in pGreen0179, plasmid 779, primer 2360/2646	kan/hyg	SmaI/blunt
pM3 (748)	3xHMG-box2 promoter+3xHMG-box2 with mutation of R17 and R20 to Alanin+GFP in pGreen0179 plasmid 778, primer 2480/3465/3466/2484	kan/hyg	SmaI/blunt
pM4 (566)	RNAi construct for 3xHMG-box2 in pFGC5941, primer 2491/2492	kan/Basta	XbaI/BamHI+AscI/SwaI
pM5 (784)	3xHMG-box2 amiRNA construct in pGreen0229+Ubiquitin10 promotor+35S terminator plasmid 782, primer 3002/3003/3004/3005/2998/2999	kan/Basta	Sma/blunt
pM6 (668)	3xHMG-box2 promoter+GS in pCambia-2300, plasmid 660, primer 2752/2506	kan/kan	SmaI/SacI
pM7 (669)	3xHMG-box2 promoter+3xhmg-box1-GS in pCambia-2300, plasmid 668, primer 2360/2646	kan/kan	SmaI/blunt
pM8 (670)	3xHMG-box2 promoter+3xhmg-box2-GS in pCambia-2300, plasmid 660, primer 2362//2647	kan/kan	SmaI/blunt
pM9 (590)	35S cassette+3xHMG-box1+3'GFP-NLS in pGreen0229, plasmid 781, primer 2360/2646	kan/Basta	XbaI/XmaI
pM10 (591)	35S cassette+3xHMG-box2+3'GFP-NLS in pGreen0229, plasmid 781, primer 2362/2647	kan/Basta	XbaI/BamHI
pM11(716)	N-terminal region (M1-E115) of 3xhmg-box1in pGreen0229, plasmid 781, primer 2360/2968	kan/Basta	XbaI/XmaI
pM12 (717)	N-terminal region+HMG-box1(M1-K234) of 3xhmg-box1+GFP-NLS in pGreen0229, plasmid 781, primer 2360/2970	kan/Basta	XbaI/XmaI
pM13 (718)	N-terminal region+HMG-box1/2 (M1-K361) of 3xhmg-box1+GFP-NLS in pGreen0229, plasmid 781, primer 2360/2972	kan/Basta	XbaI/XmaI
pM14 (719)	HMG-box1/2/3 (S109-S446) of 3xhmg-box1+GFP-NLS in pGreen0229, plasmid 781, primer 2967/2646	kan/Basta	XbaI/XmaI
pM15 (720)	HMG-box 2/3 (Q227-S446) of 3xhmg-box1+GFP-NLS in pGreen0229, plasmid 781, primer 2969/2646	kan/Basta	XbaI/XmaI
pM16 (721)	HMG-box 3 (E356-S446) of 3xhmg-box1+GFP-NLS in pGreen0229, plasmid 781, primer 2971/2646	kan/Basta	XbaI/XmaI
pM17 (722)	HMG-box 1/2 (S109-K361) of 3xhmg-box1+GFP-NLS in pGreen0229, plasmid 781, primer 2967/2972	kan/Basta	XbaI/XmaI
pM18 (723)	HMG-box 2 (Q227-K361) of 3xhmg-box1+GFP-NLS in pGreen0229, plasmid 781, primer 2969/2972	kan/Basta	XbaI/XmaI
pM19 (724)	HMG-box 1(S109-K234) of 3xhmg-box1+GFP-NLS in pGreen0229, plasmid 781, primer 2967/2970	kan/Basta	XbaI/XmaI
pM20 (769)	3xHMG-box-hybrid1(N-terminal rgion of 3xHMG-box1+C-terminal rgion of 3xHMG-box2 in pGreen0229+ 35S cassette+GFP-NLS, plasmid 781, primer 2362/3404/3405/2647	kan/Basta	Xba/BamHI
pM21(770)	3xHMG-box-hybrid2 (N-terminal rgion of 3xHMG-box2+C-terminal rgion of 3xHMG-box1in pGreen0229+ 35S cassette+GFP-NLS, plasmid 781, primer 2360,3500,3501,2646	kan/Basta	Xba/Xma
pM22 (592)	45S rDNA bp-45 in pUC19, primer 2648/2651	amp	SmaI/blunt
pM23 (593)	45S rDNA 45-25 in pUC19, primer 2650/2653	amp	SmaI/bluntI
pM24 (594)	45S rDNA 25-bp in pUC19, primer 2652/2649	amp	SmaI/blunt
pM25 (747)	N-terminal region of 3xHMG-box1in pQE9, plasmid ori 64, primer 3463/3464	amp	BamHI/HindIII
pM26 (744)	GFP-NLS in pWS3638, plasmid 72, primer 3451/3452	amp	XbaI/XhoI
pM27 (745)	3xHMG-box1-GFP-NLS in pWS3638, plasmid 72, primer 2360/3452	amp	XbaI/XhoI
pM28 (746)	3xHMG-box2-GFP-NLS in pWS3638, plasmids 72, primer 2362/3452	amp	XbaI/XhoI

2.1.6 Seed stocks and plant cell culture

Arabidopsis thaliana (Col-0), *Arabidopsis arenosa (*Luca Comai/Care-1, N3901) and GABI-Kat-T-DNA insertion line GK-171F06.01 (Col, N302986) were provided by Nottingham Arabidopsis Stock Centre. Allotetraploid *Arabidopsis suecica* (Luca Comai/Sue3) was kindly donated by Ortrun Mittelsten Scheid from the Gregor Mendel Institute of Molecular Plant Biology (Vienna, Austria). *Arabidopsis thaliana* (Col-0) plant lines expressing linker histones (H1.1/H1.1) that are fused to RFP were produced in our group. Respective lines are described in the bachelor thesis of Philipp Holzinger (2012). *Arabidopsis* cell culture PBS-D (Ler) was obtained from Geert De Jaeger (VIB, Belgium)

2.1.7 Bacterial and yeast strains

Bacterial strains with respective genotype, antibiotic resistance marker and provider are listed in Table 5.

Table 5. List of bacterial and yeast strains.

Name	Genotype	Resistance	Provider
E. coli XL1-Blue	endA1 gyrA96(nal^R) thi-1 recA1 relA1 lac glnV44 F'[::Tn10 proAB$^+$ lacI^q Δ(lacZ)M15] hsdR17(r_K^- m_K^+)	tet	Stratagene
E. coli M15	F-, Φ80ΔlacM15, thi, lac-, mtl-, recA+, KmR	kan	Quiagen
A.tumefaciens GV3101	pSOUP	tet/gent/rif	DSMZ
C.cerevisiae NOY505	mata; ade2-1 ura3-1 his3-11 trp1-1 leu2-3,112 can1-100		H. Tschochner
C. cerevisiae yR44	mata; ade2-1; ura3-1; trp1-1; leu2-3,112; his3-11; can1-100; hmo1::TRP_KL; PHO5: ; RDN:		J. Griesenbeck

2.1.8 Software

Adobe ® Photoshop® CS5 Extended Version 12.0.4 x64 (Adobe Systems Incorporated)

Alpha view® Software Version 3.0.3.0 (Alpha Innotech Corporation)

AxioVision40 V4.8.0.0 (Zeiss)

BioDocAnalyze Software Vesion 2.1 (Biometra)

Clone Manager Professional Suite 6 (Sci Ed Central)

EndNote X6.0.1 (Thomson Reuters)

ImageJ 1.48c (ImageJ Jenkins server)

Microsoft Office 2010 (Microsoft)

OptiQuant Software Version 3.0 (Packard Instrument Co.)

Rx64 3.0.3 (The R Foundation for Statistical Computing)
SeaView Software Version 4.0 (Laboratoire de Biometrie et Biologie Evolutive)

2.2 Plant work and cell biological methods

2.2.1 Plant growth conditions

Plants were grown on soil [10 % perlite, 10 % sand, 80 % Profisubstrat (Einheitserde), 30 g osmocote start (Everris)] in a growth chamber under long day (LD) conditions (16 h light and 8 h dark at 22 °C). Pots containing soil were watered from the bottom with water containing 1.5 ml/l pervicur (Bayer CropScience) and 0.2 g/l confidor (Bayer CropScience) in order to prevent growth of fungi and flies. Light intensity was measured in PPFD and adjusted to 100 $\mu molm^{-2}s^{-1}$. Plants harbouring a construct with nos-bar cassette were selected by spraying young seedlings two to three times with a glufosinate solution (100 mg/l Basta®, 200 µl/l Silwet® in H_2O). Plants for FISH or IHS assays were grown on wet filter paper, which was placed in round petridishes and grown in a plant incubator under long day conditions.

For plant growth under sterile conditions, seeds were surface-sterilized by washing 20 min. with 70 % EtOH followed by incubation with chlorine solution (15.6 ml sterile MQ-water, 9.4 ml chlorine, 25 µl Tween 20) for 2 min and an additional washing-step with sterile MQ-water. Seeds were then sown out on solid MSO-media [4,4 g/l murashige and skoog media including vitamins (Duchefa), (Murashige and Skoog 1962)], 0,8 % phyto agar (w/v), diluted in deionized H_2O, pH 5,9, sterilized by autoclaving) and grown in a plant incubator under long day conditions. For selection of plant lines resistant to kanamycin or hygromycin, respective antibiotics were added to the media in concentrations of 50 µg/ml and 15 µg/ml (Harrison et al. 2006). For life cell imaging of roots, seedlings were grown in Lab-Tek® chamber slides ™ with two wells, which were sterilized with UV light prior filling with MSO-media.

After plants were sown out, plant lines in the Columbia background were stratified for 48h and *Arabidopsis suecica* or *Arabidopsis arenosa* were stratified for 5 days at 4°C in the dark.

2.2.2 Soil-based phenotypic analyzes

For soil based phenotyping, plants were sown out in 7x7 cm square pots, which were placed in trays with lid, in order to keep humidity high. After stratification, trays were

moved to the growth chamber and lid was removed after appearance of cotelydons. Growth stage-based phenotypic analyzes was performed accordingly (Boyes et al. 2001). Bolting- and flowering time were measured in days after stratification (DAS). For analyzes of the flower- and silique phenotype, the whole flower buds and siliques were placed on a 0.8 % phytoagar gel or dissected parts of the flower were taken. Pictures were taken with a digital camera and a macro objective.

2.2.3 Phenotypic analyzes of roots

For phenotypical analyzes of the roots, seedlings were grown on solid ½ MSO medium containing 1 % sucrose (w/v) in 13x13 cm square petri dishes. Plates were placed upright in the plant incubator. In order to count cells in the elongation zone, roots were placed on object slides and 20 µM propidiumiodide diluted in MQ-water was added before applying coverslip.

2.2.4 Crossing of *Arabidopsis thaliana*

Plants with varying genetic backgrounds were used for crossing to obtain double mutants. From one crossing partner, sepals, petals and stamen were gently removed with a tweezer and remaining carpel was brushed with two-day-old pollen from the other crossing partner. Developing siliques were harvested at maturation. Resulting plants were selected and confirmed by PCR.

2.2.5 Preparation of semi-thin sections from leaf tissue

In order to count numbers of leaf epidermal cells in different mutants plants, first leaf of the second leaf pair from 14 day old seedlings was taken for embedding in methacrylate according to (Paiva et al. 2011). Leafs were put into 2 ml microcentrifuge tubes and fixation solution (EtOH:HAc=3:1) was added. After two hours at 4 °C, leafs were washed 3 times with 70 % EtOH and incubated in 70EtOH+1mM DTT over night at 4 °C. Tissue was dehydrated by stepwise application of an ethanolseries (20min in 85 % EtOH+1 mM DTT, 20 min in 90 % EtOH+1 mM DTT, 20 min in 95 % EtOH+1 mM DTT, 2x30 min in 100 % EtOH+1 mM DTT) at 4 °C. After ethanol series, methacrylate was infiltrated by application of different dilutions of a methacrylate-mix (75 % v/v butylmethacrylate, 25 % v/v metylmethacrylate, 10mM DTT, 0,5 % bonzoinethylether) with Ethanol (4h in 100 %

EtOH+10mM DTT:methacrylate-mix=2:1, 4 h in 100 % EtOH+10 mM DTT:methacrylate-mix=1:1, 4 h in 100 % EtOH+10 mM DTT:methacrylate-mix=1:2 and 2x4 h in methacrylate-mix) at 4 °C. Incubation times can be prolonged up to 18 h. After infiltration of methacrylate, leafs are placed in 0.2 ml PCR-tubes with attached dome caps (VWR) in the desired orientation and filled with the methacrylate-mix till the margin. Lids were cut-off and placed in inverse orientation on the tubes, avoiding air bubbles. Polymerization of the methacrylate-mix was initiated by radiation with UV light for 15 h. Embedded leaf tissue was cut at its broadest area with a microtome. Sections were placed on an objective slide and dried on a hot plate. MQ-water was added to the sections and a coverslip was applied.

2.2.6 Alexander stain of pollen

Viability of pollen was tested according to (Alexander 1969). Anthers were collected and incubated for 2 h in fixative (EtOH:chloroform:AcOH=6:3:1). After placing anthers on a objective slide and drying, one drop of Alexander stain (10 %EtOH (v/v), 25 % glycerol (v/v), 0,01 % malachite green (w/v), 0,05 % acidfuchsin (w/v), 0,005 % orange G (w/v) and 4 % AcOH in MQ-water) was added and a coverslip applied.

2.2.7 Stable transformation of *Arabidopsis thaliana*

Arabidopsis was transformed by the floral-dip method described by (Clough and Bent 1998). Chemically competent *A. tumefaciens* were transformed with the desired constructs and grown over night in 5 ml liquid LB-media (10 g trypton, 5 g yeast extract and 5 g NaCl diluted in 1 l H_2O), containing tetracycline for selection of the pSOUP helper plasmid, gentamycin for selection of the *Agrobacteria*-strain and kanamycin for selection of plasmids with constructs, supposed to be integrated in *Arabidopsis*. 0.5 l liquid LB medium, containing the three above mentioned antibiotics, was inoculated with 0.5 ml of the overnight culture and incubated 18 h at 200 rpm and 30 °C. Bacteria were spun down at 6000xg and resuspended in infiltration medium (5 % sucrose w/v, 10mM $MgCl_2$, 10 µM acetosyringon and 200 µl Silwet L77/l). *Arabidopsis* plants were grown densely in 11x11 cm square pots till approximately one week to 10 days after the first flower occurred. Plants were dipped upside down for 1min in a 0.5 l beaker containing the infiltration media with the *Agrobacteria.* Dipped plants were covered with plastic foil for one day and grown two

more weeks in the plant chamber after stopping of watering. When the plants were completely dried out, seeds were harvested. Transformed plants were selected with Basta®, kanamycin or hygromycin as described in chapter 2.1.1.

2.2.8 Growth and *Agrobacterium*-mediated transformation of *Arabidospsis* cell suspension cultures

Arabidopsis cell suspension culture (PSB-D) were maintained one week in MSMO-media (4.4 g murashige and skoog salt mixture (USBiological), 30 g sucrose, 0.5 g NAA and 0.05 g kinetin diluted in 1 l MQ-water, pH 5.7 adjusted with 0.2 M KOH) at 25 °C in the dark by gentle agitation (130 rpm) before diluting 7 ml of culture in 43 ml of MSMO-medium in order to start a new growth cycle. Transformation of *Arabidopsis* cell suspension culture was performed with minor alterations according to (Van Leene et al. 2007). An overnight culture of transformed *Agrobacteria* was washed 2 times with MSMO medium and adjusted to an OD_{600} of 1.0. 300 µl of the washed *Agrobacteria* were added to 5 ml of a two-day old PSB-D cell suspension culture supplemented with 12 µl of 100 mM acetosyringone and incubated for two days at 25 °C in the dark by gentle agitation (130 rpm). After two days, transformation mixture was transferred into a 25 ml Erlenmeyer flask containing 8 ml MSMO-medium supplemented with kanamycin, vancomycin and carbenicillin and incubated 9 days at 25 °C in the dark by gentle agitation (130 rpm). Plant cell suspension culture was then transferred completely into a 100 ml Erlenmeyer flask containing 35 ml MSMO-medium supplemented with kanamycin, vancomycin and carbinicillin and incubated 7 days at 25 °C in the dark by gentle agitation (130 rpm). Transformed *Agrobacteria* cell suspension cultures were tested for presence of the desired construct by PCR and could be subcultured like the initial PSB-D culture by addition of kanamycin to the MSMO-media. For affinity purification of GS-tagged proteins, transformed *Arabidopsis* cell suspension cultures were upscaled by sequential dilution and incubation in higher volumes of MSMO-media till 10 l of two day old cultures per construct could be harvested. Sedimented cells were collected, frozen in liquid nitrogen and stored as 15 g aliquots at -80 °C.

2.2.9 Immunocytochemistry (ICC)

Arabidopsis seedlings, which were grown for 4-14 days were fixated in 3-4 % paraformaldehyd (w/v) diluted in 1xPBS-buffer (8 g/l NaCl, 1.78 g/l $Na_2HPO_4x2H_2O$, 0.2 g/l KCl, 0.27 g/l KH_2PO_4) at 4 °C for 20-30min, while applying a vacuum for the first five minutes. Seedlings were washed 3 times for 5 min in 1xPBS-buffer before adding a cocktail of digestion enzymes (0.7 % cellulase R-10, 0.7 % cellulase (w/v), 1 % pectolyase (w/v) and 1 % cytohelicase (w/v)) and incubating at 37 °C for 20-30 min. Enzyme mix was removed and 1xPBS was added to the seedlings. After stirring, root tips fell of and were transferred to an object slide. After application of a coverslip, roots were squashed using a toothpick to apply punctual pressure on the coverslip. Object slides were dipped in liquid nitrogen, coverslips were blasted away, using a razorblade and object slides, containing the squashed root tips, were then put into 1xPBS. Blocking solution (4 %BSA (w/v), 0.1 % Tween20, 0.1 % Triton X-100, diluted in 1xPBS) was applied to the samples, covered by a square piece of parafilm and incubated for 1h. Slides were washed one time in 1xPBS, primary antibody diluted in 100 µl 1xPBS per slide was added to the samples and covered with parafilm. After incubation with the first antibody over night at 4 °C, slides were washed three times in 1xPBS and samples were incubated with the fluorescently labelled secondary antibody, diluted in 1xPBS, for 2 h. Finally, samples were washed three times for 5min with 1xPBS before DAPI solution (VECTASHIELD® mounting media) and cover slip was added.

2.2.10 Flourescence *in situ* hybridization (FISH)

Fluorescent probes were generated using PCR labeling kits (Jena Bioscience) according to the manufacturer's instructions. Root cells were prepared as described in 2.2.9. For subsequent ICC and FISH, hybridization with fluorescent probes was carried out after incorporation of primary and secondary antibodies.

30 µl of hybridization solution (50 % formamid v/v), 10 % dextran sulfate (w/v), 0.3 mg/ml salmon testes DNA, 2xSSC, diluted in MQ-water) was supplemented with 40-60 ng labeled probe and heated to 99 °C for 5 min. After chilling, 30 µl of the hybridization solution containing fluorescent probe was added onto the objective slide and cover slip was applied. Objective slide was heated to 72 °C, or 67 °C when performing the subsequent ICC/FISH assay for 2 min. Samples were incubated at 37 °C overnight and washed 2 times for 5 min at RT in 2xSSC followed by a washing

step with 50 % formamid in 2xSSC for 10 min at RT. Finally, slides were washed two more times for 5 min at RT in 2xSSC before adding DAPI solution (VECTASHIELD® mounting media) and cover slip.

2.2.11 Microscopy

Pictures of semi-thin sections from *Arabidopsis* leafs were taken, using an inverse light microscope and an objective with a fourfold magnification. Single pictures were then merged with Photoshop®.

Confocal pictures were taken with a Zeiss LSM510 or a Leica SP8 using oil-objectives with 40 fold and 63 fold magnification. Pinhole was adjusted between 1µm and 1.6 µm and resolution was set between 512x512 ppi to 2048x2048 ppi. For life cell imaging, one picture was taken every 30 s or every minute with a pinhole adjusted to 1.6 µm. Excitation and filter wavelengths that were used are listed in Table 6

Table 6. Wavelengths for excitation and filters.

Dye	Excitation wavelengh	Filter wavelenghts
DAPI	405	410-450
GFP/A488	488	505-530 (LSM510)/500-550(SP8)
RFP/Cy3	561	570-627
Cy5	633	645-752

2.3. Microbiological work

2.3.1 Growth of bacteria

All bacterial strains used in this work, were grown using sterile LB-medium (5 g NaCl, 5 g yeast-extract and 10 g trypton, sterilized by autoclaving) by agitation of 200 rpm. For growth on solid media 1.5 % agar was added prior autoclaving. Antibiotics used for selection of strains and containing plasmid constructs were sterile-filtered and added to the sterile liquid LB-medium and to the autoclaved LB-medium containing agar, before pouring the still liquid LB-medium in petridishes. *E.coli* strains were incubated at 37 °C, while *A. tumefaciens* were incubated at 30 °C.

2.3.2 Growth of yeast

All yeast strains used in this work were grown in liquid YPAD-medium (10 g/l yeast extract, 20 g/l peptone, 20 g/l glucose and 40 mg/l adenine sulfate diluted in H_2O, sterilized by autoclaving) at 30 °C by agitation of 200 rpm. For growth on solid media

2 % agar was added prior autoclaving. For microscopy, an overnight culture was used to inoculate fresh YPAD-medium to an OD_{600} of 0.1. After the culture reached an OD_{600} of 0.5, 2.5 µg/ml DAPI was added and culture was grown for additional 30 min. Yeast cells were washed one time and resuspended in 1xPBS (8 g/l NaCl, 1.78 g/l $Na_2HPO_4x2H_2O$, 0,2 g/l KCl, 0,27 g/l KH_2PO_4, diluted in MQ-water, pH 7.4). Objective slides with well were used for microscopy.

2.3.3 Production of chemically competent *E.coli* and *A. tumefaciens*

5ml of liquid LB-medium containing antibiotics for selection (Table 1) was inoculated with *E.coli* or *A. tumefaciens* stocks and grown overnight at 37 °C and 30 °C respectively. The next morning 100 ml fresh LB-medium containing antibiotics for selection was inoculated with overnight cultures to achieve an OD_{600} of 0.1. Cultures were grown to an OD_{600} between 0.3-0.5, spun down, resuspended in 30 ml buffer TBF1 (100 mM RbCl, 10 mM $CaCl_2$, 50 mM $MnCl_2$, 30 mM NaOAc, 15 % (v/v) glycerol diluted in MQ-water and adjusted to pH 5,8 with 0,2 M AcOH, autoclaved prior to use and stored at 4 °C in the dark) and incubated for 90 min on ice. Cells were spun down, resuspended in 3 ml of buffer TFB2 (10 mM MOPS, 10 mM RbCl, 75 mM $CaCl_2$, 15 % (v/v) glycerol diluted in MQ water, autoclaved prior to use and stored at 4 °C in the dark) and aliquots of 150 µl were frozen in liquid nitrogen and stored at -80°C.

2.3.4 Production of chemically competent yeast cells

Yeast was grown overnight and used to inoculate 50 ml fresh medium to an OD_{600} of 0.1. Cell suspension was then grown to an OD_{600} between 0.8-1, spun down and washed once in 10 ml sterile MQ-water. Cells were spun down again and washed one times in 2.5 ml SORB (100 mM LiOAc, 10 mM Tris-HCl, 1 mM EDTA, 1 M sorbitol in MQ-water, pH8, filter-sterilized) and one time in 500 µl SORB. After washing yeast cells were sedimented and resuspended in 360 µl SORB. 40 µl ssDNA (10 mg/ml denatured at 100 °C and snap-cooled on ice) was added to the yeast cells and mixed gently. Competent cells were put in aliquots of 50 µl and stored at -80 °C.

2.3.5 Transformation of *E.coli*

Chemically competent *E.coli* cells were thawn on ice and plasmid (50-500 ng) or ligation was added. After mixing gently cells were incubated for 20 min on ice, before applying a heatshock of 42°C for 2 min and an additional incubation step on ice for 10 min. After the transformation process, 1 ml sterile LB-medium was added and cells were incubated at 37 °C for 1 h. Cells were then plated out on LB-plates with respective antibiotics and incubated at 37 °C over night in order to select for cells harboring the desired construct.

2.3.6 Transformation of *Agrobacterium tumefaciens*

Chemically competent *A.tumefasciens* cells were thawn on ice and plasmid (2-5 µg) was added. After mixing gently cells were incubated for 5 min in liquid nitrogen, before applying a heatshock of 37 °C for 5 min and an additional incubationstep on ice for 10 min. After the transformation process, 1 ml sterile LB-medium was added and cells were incubated at 30 °C for 3 h. Cells were then plated out on LB-plates with respective antibiotics and incubated at 30 °C for 48 h in the dark, in order to select for cells harboring the desired construct.

2.3.7 Transformation of yeast

Chemically competent yeast cells are thawn on ice, 10 µg of linearized plasmid and 6 volumes PEG (100 mM LiOAc, 10 mM Tris-HCl, 1 mM EDTA, 40% (w/v) PEG3350 diluted in MQ-water, pH8, filter-sterilized) were added and mixed gently. After incubation for 30 °C at RT, 1/9 of total volume, sterile DMSO was added and a heat shock of 42 °C was applied for 15 min. After heat shock yeast cells were streaked on selective plates and grown till colonies were visible.

2.4. Molecular biological methods

2.4.1 Extraction of genomic DNA from *Arabidopsis*

Extraction of genomic DNA from *Arabidopsis* was performed according to (Edwards et al. 1991). Leaf tissue was harvested in 1.5 ml reaction tubes and frozen at -80 °C. After grinding tissue to fine powder, 400 µl Edward buffer was added (200 mM Tris-HCl pH 7.5, 250 mM NaCl, 25 mM EDTA, 0,5 % SDS) and mixed thoroughly.

Debris was spun down in a table centrifuge at full speed for 1 min and 300 µl of supernatant was transferred to a new reaction tube before adding equal volume of 100 % isopropanol. Precipitated DNA was dissolved in 50 µl MQ water and stored at 4 °C

2.4.2 Extraction of total RNA from *Arabidopsis*

For extraction of RNA from *Arabidopsis,* 100-200 mg plant tissue was harvested in 1.5 ml reactiontubes and frozen in liquid nitrogen. Tissue was ground, 400-1000 µl Z6 buffer (8 M guanidinium-HCl, 20 mM MES, 20 mM EDTA, diluted in MQ-water, pH 7.0, add 350 µl 2-mercaptoethanol to 50 ml prior use) and 500 µl CIP (phenol:chloroforme:isoamylalcohol=25:24:1, pH 4.5-5.2) was added. After mixing thoroughly, mixture was centrifuged at 15000 rpm and 4 °C for 15 min. Supernatant was transferred to a new reaction tube and 1/20 volume of 1 N AcOH and 7/10 volume of 100% EtOH was added and mixed. After centrifugation at 15000 rpm for 10 min at 4 °C, the pellet was washed one time with 3 M Na-acetate and one time with 80% EtOH before drying. RNA was resolved in 30-70 µl ultrapure water (Millipak) at 60 °C for 10 min. RNA was stored at -20 °C.

2.4.3 First strand cDNA synthesis

Synthesis of cDNA from RNA was performed according to (Gerard and D'Alessio 1993) using RevertAid^{TM} H Minus M-MuLV Reverse Transcriptase (Thermo Fisher Scientific). 1-2 µg RNA and 0.2 µg random hexamer primer were filled up to 12.5 µl with ultrapure water and incubated for 5 min at 70 °C and chilled on ice. 4 µl of 5x reaction buffer, 2 µl 10 mM dNTP mix and 0.5 µl ribonuclease inhibitor (RNAsin$^{®}$) was added and incubated for 5min at 25 °C. After addition of 1µl reverse transcriptase, reaction mixture was incubated for 10 min at 25 °C followed by an incubation step of 60 min at 42 °C. Reaction was inhibited by heating to 70 °C for 10 min. cDNA was stored at -20 °C.

2.4.4 Polymerase chain reaction (PCR)

For semi-quantitative PCRs and to confirm T-DNA insertions in the *Arabidopsis*-genome as well as testing of bacterial colonies for possession of desired plasmids Dreamtaq^{TM}-DNA polymerase (Thermo Fisher Scientific) and Taq DNA polymerase (PEQLAB) were used. Elongation time was estimated about 1 kbp/min. Genomic

DNA, cDNA or bacterial colonies were used. For semiquantitative PCR, cell cyle number was set between 22 and 32 depending on template and primer. Aim was to stop the amplification in the exponential stage. For amplification of templates that were used for cloning, KAPAHiFi^{TM} DNA polymerase was chosen, due to its low failure rate. Reaction mixture was prepared and PCR program was set up according manufacturer's protocols. Elongation time of one min per kbp was used for both polymerases.

2.4.5 Agarose gel electrophoresis

In order to separate and visualize DNA and RNA fragments 0.8-2 % (w/v) Agarose gels were used. Agarose was mixed with TAE-buffer (40 mM Tris-HCl, 20 mM AcOH, 1 mm EDTA, diluted in MQ-water, pH 8.3) and heated in a microwave till boiling. 10 µl of a 10 mg/ml ethidium bromide solution was added to 150 ml of agarose solution during cooling process. Still liquid solution was poured into casting systems and combs were added to form wells for loading of DNA and RNA. DNA and RNA samples were supplemented with 10xDNA loading buffer (42 mM Tris-HCl pH 7.5, 50 % glycerol, 0.05 % (w/v) bromophenyl blue and 0.05 % (w/v) xylene cyanol) and loaded in the wells. Gels were put into chambers containing 1xTAE buffer and an electric field was applied with 120-150 V. When Agarose gels were used for gelshift assays and Southern blot, 1xTBE-buffer (10 g/l TrisHCl, 5.5 g/l boric acid, 5 mM EDTA, diluted in MQ-water, pH 8.3) was used instead of TAE-buffer and no ethidiumbromide was added to the agarose gel. Gels were run at 60-80 V. For Northern blot 1 % (w/v) Agarose was diluted in 1xMOPS-buffer (40 mM MOPS, 10 mM NaAc, 1 mM EDTA, diluted in MQ-water, pH 7.2)) and heated in a microwave till boiling. While cooling down 8.1ml of 37 % formaldehyde was added and gels were prepared as mentioned before. Agarose gels for gelshift assays, Southern blot and Northern blot were stained after separation of DNA/RNA by putting the gels in respective running buffer supplemented with 15 µl/100 ml of a 10 mg/ml ethidium bromide solution

2.4.6 Construction of plasmids

Cloning was performed according to (Sambrook et al. 1989). PCR templates used for cloning were generated from genomic DNA, cDNA or plasmids. For purification of

DNA fragments and isolation from agarose gels, the NucleoSpin® Gel and PCR Clean-up kit (Macherey-Nagel) was used. For restriction digest and ligation, enzymes and buffers from Thermo Fisher Scientifc were used according the manufacturer's protocol. For dephosphorylation of linearized vectors prior to ligation, antarctic phosphatase (NEB) was used as described in the manufacturer's protocol.

2.4.7 Small scale purification of plasmids

5 ml LB was inoculated with a positive selected clone from a ligation or retransformation and incubated overnight, keeping selection pressure by adding respective antibiotics. The next day, 1.5 ml of the cell culture was transferred to a 1.5 ml reaction tube and spun down. Supernatant was discarded and the resulting pellet resuspended in 150 µl resuspension buffer (50 mM Tris-HCl pH 8.0, 10 mM EDTA, 100 µg/ml RNase A) before adding 150 µl of lysis buffer (1 % SDS (w/v), 200 mM NaOH). Mixture was inverted and incubated for approximately 1 min. Then 200 µl neutralization buffer (3 M KAc pH 4.8 pH) was added and after inverting several times, insoluble precipitate was spun down in a table centrifuge at full speed for 10 min at 4 °C and 350 µl of the supernatant was transferred to a new tube. After addition of an equal volume of isopropanol, the reaction was spun down in a tablecentrifuge at full speed for 20 min at 4 °C and resulting pellet was washed once in 70 % ethanol before drying and resuspending in 50 µl of MQ-water.

2.4.8 Medium scale preparation of plasmids

For preparation of higher amounts of pure plasmid, 50 ml LB was inoculated with a positive selected clone from a ligation or retransformation and incubated overnight, keeping selection pressure by adding respective antibiotics. The NucleoBond® Xtra Midi kit (Macherey-Nagel) was used for purification according to the manufacturer's instructions.

2.4.9 Sequencing

Sequencing was done by GATC Biotech (Konstanz) or by Eurofins MWG Operon (Ebersberg). Plasmids were purified accoding to 2.4.8 and sent with primers in the recommended concentrations.

2.4.10 Bradford assay

In order to measure protein concentrations, Bradford assay (Bradford 1976) was used. 10 µl of samples or respective dilutions added to 90 µl of MQ-water were mixed with 1 ml of Bradford reagent (50mg Coomassie Blue G250 diluted in 5 % (v/v) EtOH, 8,5 % (v/v) H_3PO_4, add water MQ to 1 l and filter to remove precipitates) and incubated for 10 min at RT. After incubation, samples were transferred into cuvettes and extinction at 595 nm was measured. For blanking, MQ-water was used instead of sample. Values were interpolated using a straight calibration line that was made by measuring samples with known BSA-concentrations from 0-50 µg/ml.

2.4.11 Sodium dodecyl sulphate polyacrylamide gel electrophoresis (SDS-PAGE)

Depending on the size of the protein that was supposed to be analyzed, different separation gels were made in a Bio-RAD Mini-Protean® 3 Multicaster system (Bio-Rad) with either 9 % (w/v), 12 % (w/v) or 18 % (w/v) acrylamide:bisacrylamide (30:0.15), 0.75 M Tris-HCl pH 8.8, 0.2 % SDS (w/v), 0.1 % ammonium persulfate (APS) and 0.02 % N,N,N‘,N‘-tetramethylethylenediamine (TEMED (v/v)) diluted in MQ-water. Stacking gels were made of 10 % acrylamide:bisacrylamide (30:0.8) (w/v), 0.14 M Tris-HCl pH 6.8, 0.23 % SDS (w/v), 0.11 % APS (w/v) and 0.06 % TEMED (v/v) diluted in MQ-water. Prior to loading, proteins were denaturated by heating the sample to 95 °C for 5 min with 5xSDS loading dye (150 mM Tris-HCl pH 7.0, 150 mM DTT, 5 % SDS (w/v), 25 % glycerol (v/v), and 0.1 % bromophenol blue (w/v), diluted in MQ-water). Proteins were separated in a Bio-RAD Mini-Protean® 3 running chamber at 160-200 V using Laemmli running buffer (14.41 g/l glycine, 0.1 % SDS (w/v), 3.03 g/l Tris-HCl, diluted in MQ water, pH 8.3). Gels were used for Western blotting as described in 2.4.16 or either stained using silverstaining as described in 2.4.12, or with Coomassie blue (30 % EtOH (v/v), 10 % AcOH (v/v) and 5 g/l Coomassie Brilliant Blue R-250) for 1 h at RT before washing several times with destain solution (7.5 % (v/v) AcOH, 5 % (v/v) EtOH diluted in in H_2O_{deo}).

2.4.12 Silver staining

A mass spectrometry compatible silver staining method was choosen and was performed as described in (O'Connell and Stults 1997). After running the gel, it was placed in a plastic tray with 200 ml of fixation solution (30 % (v/v) EtOH, 10 % (v/v)

AcOH diluted in H_2O_{deo}) under gentle agitation. After fixation gel was rinsed for 15 min in rinsing solution (20 % EtOH (v/v) diluted in H_2O_{deo}) and 15 minutes with $H_2O_{deo.}$ Gel was sensitized with sensitize solution for 1.5 min and rinsed twice for 20 s with plenty of in H_2O_{deo} prior staining with silver nitrate (0.2 % in H_2O_{deo}) for 30 min under gentle agitation. Gel was then put into development solution under gentle agitation till protein bands become visible and have the desired intensity. Development is stopped by shaking the gel for 2 min in stop solution (2.5 % (v/v) AcOH, 50 g/l Tris-HCl in in H_2O_{deo}) and rinsing two times with H_2O_{deo} for 10 min.

2.4.13 Expression and purification of His-tagged proteins

For expression and purification of His-tagged proteins, the procedure described in the manufacturer instructions (The QIA*expressionist*™, fifth edition) was followed. *E.coli* M15 expression strain was transformed with plasmids containing the expression cassette for respective proteins. A positive selected colony was used to inoculate 50 ml LB-medium containing respective antibiotics to keep selection pressure. After growing bacteria overnight, 1 l LB-medium was inoculated with the overnight culture to reach an OD_{600} of 0.1 and grown untill an OD_{600} of approximately 0.75 was reached. Expression was induced by adding IPTG to an end concentration of 0.5 mM and cells were grown for 2 h before harvesting. Harvested cells were frozen in liquid nitrogen and stored at -80 °C until further use. In order to monitor overexpression, 1ml aliquots of cellculture were taken just before induction, 1 h after induction and 2 h after induction, spun down and resuspended with 1x SDS-loading dye to a theoretical OD_{600} of 0.1 and boiled for 30 min before loading on a SDS-gel. For purification bacteria pellets were washed one time with 40 ml wash buffer (20 mM Tris-HCl, 300 mM NaCl, 250 mM imidazole, diluted in MQ-water, pH 8.0), spun down and resuspended with 6ml of lysis buffer (20 mM Tris-HCl, 1 M NaCl, 20 mM imidazole, 1.5 % Triton X-100, 1 mM DTT, 1 mM EDTA, 0.5 mM PMSF, diluted in MQ-water, pH 8.0). Cells were lysed by sonification (Bandelin Sonoplus HD 2070 with MS 73 tip) on ice using 6 bursts of 20 s at 45 %. Cell debris were spun down and cleared lysate was added to 1 ml Ni-NTA slurry that was washed two times with 10 ml wash buffer using a column with bottom outlet. Cleared cell lysate was incubated with Ni-NTA slurry for 1 h at 4 °C under gentle agitation. Bottom cap was removed and flow-through was collected. Slurry was washed three times with 10ml wash buffer before eluting 4 times with 0.5 ml elution buffer (20 mM Tris-HCl, 50 mM NaCl, 250 mM

imidazol, 1 mM DTT, 1 mM EDTA, 0.5 mM PMSF diluted in MQ-water, pH 8.0). 10 µg of protein of each fraction was loaded on an SDS-gel in order to analyze the purification procedure.

2.4.14 Desalting of proteins

For changing the buffer of protein solutions, a PD-10 column (GE Healthcare) was used. After washing the column 5 times with storage buffer (10 mM Tris-HCl, 50 mM NaCl, 1 mM DTT, 1 mM EDTA diluted in MQ-water, pH 7.5), 2.5 ml of protein solution, e.g. elution fraction of Ni-NTA purification, was loaded. Flow-through was discarded and 3.5 ml of storage buffer was loaded on the column. Flow-through, containing the proteins, was collected.

2.4.15 Purification of plant nuclei and micrococcal nuclease (MNase) digestion

3 g of leaf tissue from 15 day old plants was harvested, frozen in liquid nitrogen and homogenized using a mortar. 30 ml of buffer H (25 mM HEPES, 10 mM NaCl, 5 mM EDTA, 250 mM sucrose, 0.15 mM spermine, 5 mM 2-mercaptoethanol, 0.1 % Nonidet P-40 (v/v), 0.2 mM PMSF, diluted in MQ-water, pH 7.0) was mixed with the leaf tissue and filtered through 2 layers of miracloth. Suspension was centrifuged at 2000 x g for 20 min at 4 °C and supernatant was discarded. Remaining pellet was resuspended in 15 ml of buffer H and centrifuged at 2000 x g for 10 min at 4 °C. This step was repeated untill supernatant was clear of chlorophyll. Nuclei were then washed two times with 2 ml of MNase buffer (300 mM sucrose, 3 mM $CaCl_2$, 20 mM Tris-HCl, diluted in MQ-water, pH 7.5) and finally resuspended with 120 µl of MNase buffer. 7 x 1.5 ml reactiontubes with 10 µl stop solution (50 mM EDTA, 1 % SDS (w/v)) were prepared, indicating 7 timepoints and negative control respectively. 15 µl of nuclei solution is transferred to a 1.5 ml eppendorfcup resembling the negative control (no MNase digestion). 100 µl of the nuclei suspension and negative control are preheated to 37 °C in a heating block with shaking function (250-400 rpm) for 5 min. 0.1 U of MNase (Roche) was added to the nuclei suspension and shortly mixed. After 30 s, 1 min, 2 min, 3 min, 4 min and 10 min, 10 µl samples and finally the negative control were transferred to the reaction tubes containing the stop solution and mixed well. DNA was extracted by adding one volume of phenol:chloroform:isoamyl alcohol (25:24:1), mixing and centrifuging in a table

centrifuge for 2 min at full speed. Top phase was isolated and substituted with 10x DNA loading buffer prior loading on an agarose gel (2.4.5).

2.4.16 Western blot (Immunoblot)

Proteins were separated by SDS PAGE (2.4.11) and then blotted on a Immobilon™-P Polyvinylidene Fluoride (PVDF) Transfer Membrane using a Semidry Mini Trans-Blot Blotter (Bio-Rad). Membrane was first soaked with methanol and then with blotting buffer (200 mM glycine, 20 mM Tris-HCl, 20 % methanol (v/v), 0.01 % SDS (w/v), diluted in MQ-water). Blot was set up by 3 layers of Whatman paper, membrane, gel and 3 layers of Whatman paper, all soaked in blotting buffer. Proteins were transferred using 0.2 A per gel for 3 h. After transfer, the membrane was put into basic buffer (20 mM Tris-HCl pH 7.5, 150 mM NaCl, 0.05 % Tween 20 (v/v), diluted in MQ-water) containing 5 % (w/v) skimmed milk powder, for 1 h with gentle agitation before adding primary antibody in a concentration of 1:5000 and incubating over night at 4 °C. The next day, the membrane was washed three times for 10 min with washing buffer (20 mM Tris-HCl pH 7.5, 150 mM NaCl, 0.05 % Tween 20 (v/v) and 1 % Triton X-100 (v/v), diluted in MQ-water) and was incubated with basic buffer containing 5 % skimmed milk powder and an IgG antibody (Anti-Rabbit IgG-Peroxidase, Sigma-Aldrich) in a concentration of 1:10000 for 2 h at RT with gentle agitation. Finally the membrane was washed as described before and signals were visualized using SuperSignal® West Pico Chemiluminescent Substrate (Thermo Fisher Scientific) and a Multiimage II FC2 (Alpha Innotech).

2.4.17 Northern Blot

10µg of total RNA was denatured for 3 min at 95 °C and loaded on a formaldehyde-containing agarose gel (2.4.5). Gel was run until bromphenol blue migrated three fourth of the gel. Gel was soaked 4 times in 5 volumes of H_2O_{deo}. and washed one time in 20 X SSC (3 M NaCl, 0.3 M sodium citrate dehydrate, diluted in MQ-water and autoclaved). Hybond-N membrane (GE Healthcare) was cut to the excact size of the agarose gel and soaked in 20 x SSC for 15-20 min. Capillary blot was set up as shown in Figure 12 and transfer was allowed to proceed overnight. After transfer, membrane was rinsed shortly in 2 x SSC and RNA was fixed by UV-crosslinking.

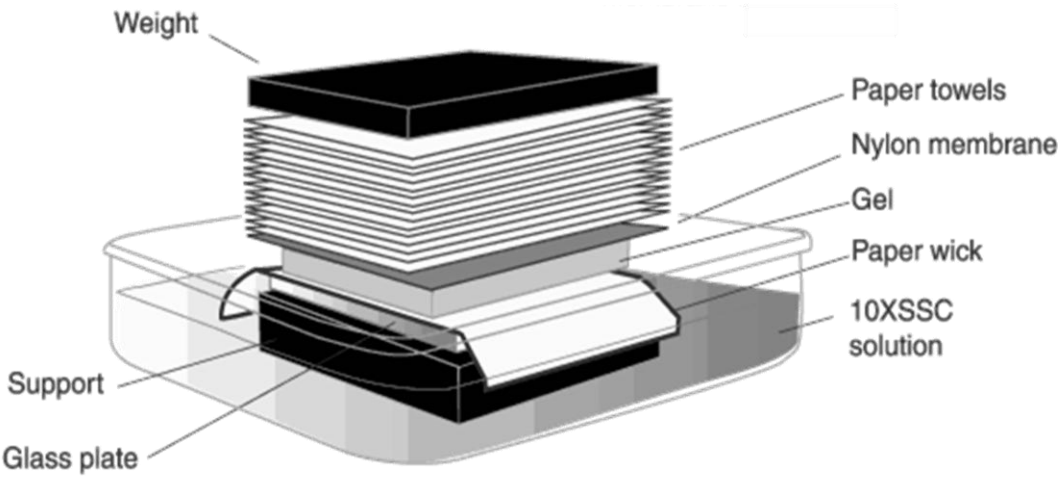

Figure 12. Capillary blot. Set-up of a capillary blot as used for Northern blot and Southern blot. (http://www.biochem.arizona.edu, Department of Biochemistry & Molecular Biophysics)

2.4.18 Southern blot

DNA 8was separated in a 0.8 % agarose gel (2.4.5). After separation, the agarose gel was stained with ethidium bromide, a picture was taken and the gel was incubated in 0.25 M HCl for 10 min at RT. Then the gel was soaked sequentially under gentle agitation in denaturation solution (0.5 M NaOH, 1.5 M NaCl) for 30 min followed by neutralisation solution (0.5 M Tris-HCl pH 7.2, 1.5 NaCl, 1 mM EDTA) for 30 min with a change of solution after 15 min. Hybond-N membrane (GE Healthcare) was cut to the excact size of the agarose gel, soaked in 20 x SSC for 15-20 min and blot was assembled as shown in Figure 12. Transfer was allowed to proceed overnight and after transfer, the membrane was rinsed shortly in 2 x SSC and RNA was fixed by UV-crosslinking.

2.4.19 Preparation of radioactive probes for Northern blot and Southern blot

A DNA template of 200-700 bp was generated according to 2.4.4. and purified. 25 ng of template was used to incorporate [α-32P]dATP (3000 Ci/mmol) using the Prime-It II Random Primer Labeling Kit (Stratagene) according manufacturer's description. G50 Sephadex Cloumn (Roche) was used to seperate the radioactive probe from non-incorporated radioactive dNTP's. 100 µg/ml salmon sperm was added to the probe and boiled for 3-5 min.

2.4.20 Hybridization and detection of radioactively labelled probes

Blot was placed in a hybridization tube and 20 ml QuikHyb® Hybridisation solution (Stratagene) was added and incubated under rotation in a hybridization oven for 30 min at 68 °C before adding radioactively labelled probe (2.4.19) and further incubation overnight at 68 °C. The next day the membrane was washed sequentially for approximately 30 min in 2xSSC containing 0.1 % SDS (w/v) and 0.1 x SSC containing 0.1 % SDS (w/v) using a water bath with temperature adjusted to 60 °C. The membrane was covered with wrapping film and put in a light excluding cassette, facing a phosphor storage screen, for 6-72 h. The screen was scanned using a Cyclone™ phosphor imager.

2.4.21 Coupling of rabbit-IgG to Epoxy-activated BcMag-beads

300 mg magnetic beads (Bioclone 1 µm BcMag Epoxy-activated Magnetic Beads No. Fc102, 1.7 x 10^8 beads/mg) were resuspended in 10 ml of 50 % acetone (v/v) and mixed vigorously. Tubes were then placed in a magnetic separator and supernatant was removed followed by washing the beads 4 times with 10 ml of coupling buffer (0.1 M $NaPO_4$, diluted in MQ-water, pH8.5). Beads were resuspended in 4 ml coupling buffer and incubated at RT for 10 min.

Antibody mix was prepared by resuspending 50 mg of rabbit IgG's in 3.5 ml MQ-water and centrifuging at 15000 g and 4 °C for 10 min. Supernatant was transferred to 50 ml falcon tube and 9.85 ml coupling buffer and 6.65 ml ammonium sulfate (diluted in coupling buffer) was slowly added while stirring the solution. Antibody mix was spun down at 4000 g for 3 min at RT, to remove impurities. Supernatant was added to the beads and incubated at 4 ° on a rotating wheel for 18-48 h.

After the coupling reaction beads were washed subsequently with 20 ml of 100 mM glycine (diluted in MQ-water, pH 2.5), 20 ml of 10 mM Tris-HCl (diluted in MQ-water, pH 8.8) and 20 ml of freshly prepared triethylamine solution (300 µl triethylamine in 20 ml MQ-water), followed by 4 washingsteps with 1 x PBS using 4000 x g to spin down beads. Beads were finally washed two times with 20ml of 1xPBS containing 0.5 % Triton X-100 before resuspending in 16 ml of 1 x PBS containing 0.02 % natrium azide (w/v) and storing at 4 °C.

2.4.22 Immunoprecipitation of GS-tagged proteins

15 g of frozen PBS-D cells (2.2.8.) or plant seedlings were diluted in 10 ml extraction buffer (25 mM HEPES, 100 mM NaCl, 0.05 % NP-40, 1 mM DTT, 2 mM $MgCl_2$, 5 mM EGTA, 10 % glycerol (v/v), proteinase inhibitor cocktail (2 µg/ml Antipain, 4 µg/ml Benzamidin, 2 µg/ml Leupeptin, 6 µg/ml N-α-Tosyl-L-phenylchlormethylketon, 0.25 µg/ml Aprotinin, 0.5 µg/ml Pepstatin A and 1.5 µg/ml Tosyl-L-phenylalanin-chlormethylketon), 1mM PMSF, diluted in MQ-water, pH 7.4) and disrupted by sonification (Bandeln Sonoplus HD 2070 with MS 73 tip) on ice, using 5 bursts at 30 % for 30 s. Celldebris were spun down at 40000 x g for 20 min and supernatant was filtered, using a 0.45 µm filter unit giving raise to the input fraction. 100 µl of IgG metal beads (2.4.19) were washed three times with extraction buffer and mixed with the protein solution for 1-2 h at 4 °C. Beads were spun down at 2000 g and after discarding the supernatant, transferred to a 2 ml reactiontube, washed three times with extraction buffer and finally IgG bound proteins were eluted using 300 µl elution buffer (0.1 M glycine, diluted in MQ-water, pH 2.8). In order to precipitate proteins, the eluate was mixed with 1.2 ml ice-cold acetone in incubated at -20 °C overnight. Next day, the precipitate was washed 3 times with ice-cold acetone before dissolving in 10 µl 1 x PBS. Samples were analyzed using SDS-PAGE as described in 2.4.11.

3. Results

3.1 Analyzes of the spatiotemporal distribution of 3xHMG-box proteins in roots of *A. thaliana*

3.1.1 Life cell imaging of 3xHMG-box-GFP fusion proteins in *Arabidopsis* roots

3xHMG-box GFP fusion proteins have already been studied in BY-2 protoplast and roots of *Arabidopsis* using the strong constitutive cauliflower mosaic virus 35S promoter to drive expression. In BY-2 protoplast and the majority of root cells, GFP signal could be observed in the cytoplasm (Pedersen et al. 2011). Only in very few cells, that appeared to be in mitosis, 3xHMG-box GFP fusion proteins were associated with chromatin. In order to monitor the occurrence of 3xHMG-box proteins, *Arabidopsis* plants were stably transformed with constructs, allowing expression of 3xHMG-box GFP fusion proteins under the control of the endogenous promoters. For construction of the expression cassette, *3xHMG-box1* and *3xHMG-box2* promoter sequences were first cloned in pGreen0179 containing a 35S terminator, followed by insertion of *3xHMG-box1* and *3xHMG-box2* coding sequences (CDS) that were amplified together with a GFP CDS from existing plasmids, giving rise to pM1 and pM2 (Figure 13A). Plants were transformed using *Agrobacterium* mediated transformation and integration of the construct in selected plants was tested by PCR-based genotyping (Supplemental Figure 1).

Roots were analyzed by Confocal Laser Scanning Microscopy (CLSM) and a weak cytosolic fluorescent signal could be detected in some of the cells, while a strong fluorescent signal associated with condensed chromosomes in cells undergoing mitosis could be observed. In general the 3xHMG-box1 derived signal was weaker compared to the 3xHMG-box2 derived signal (Figure 13B). In line with results obtained from immune staining experiments (Pedersen et al. 2011) 3xHMG-box2-GFP decorates generally condensed chromosomes, while 3xHMG-box1-GFP seems to be specifically associated with 2 foci in metaphase and 4 foci in anaphase and telophase likely representing 45S rDNA regions (Figure 13B). In order to get a better impression and temporal resolution of the occurrence of 3xHMG-box-GFP in root cells, life cell imaging was performed. In order to do so, seedlings were grown for approximately 5 days in Lab-Tek® chamber slides ™ till the roots reached the glass bottom. Chambers could be directly put on the inverse CLSM system and used for

microscopy, while roots were still growing. Pictures were taken every 30 seconds to 1min for about 1-1.5 hours. A sequence for each of the constructs is shown in (Figure 13C). Prior to mitosis, plants that express 3xHMG-box2 show a fluorescent signal in the cytoplasm (a'), while the signal for 3xHMG-box1-GFP, is on the limit of detection. Upon nuclear envelope breakdown (NEBD) during transition from prophase to metaphase, fluorescent signal can be immediately detected on condensing chromosomes and cytosolic GFP signal decreases (b,b'). At metaphase 3xHMG-box2-GFP seem to completely cover the aligned chromosomes (c'), while 3xHMG-box1-GFP derived signal concentrates on two distinct foci (c). During anaphase (d), until late telophase (e) these two 3xHMG-box1-GFP derived foci are still seen at each diploid chromosome set. 3xHMG-box2-GFP overall decorates the chromosomes during anaphase (d') and seems to detach from chromatin at telophase, when the chromosomes start to decondense (e').

A

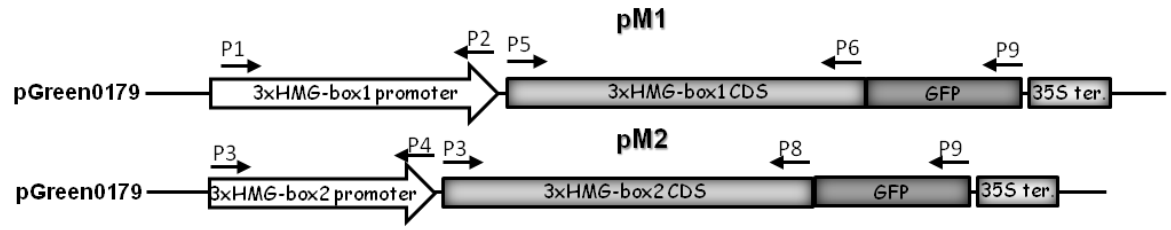

B

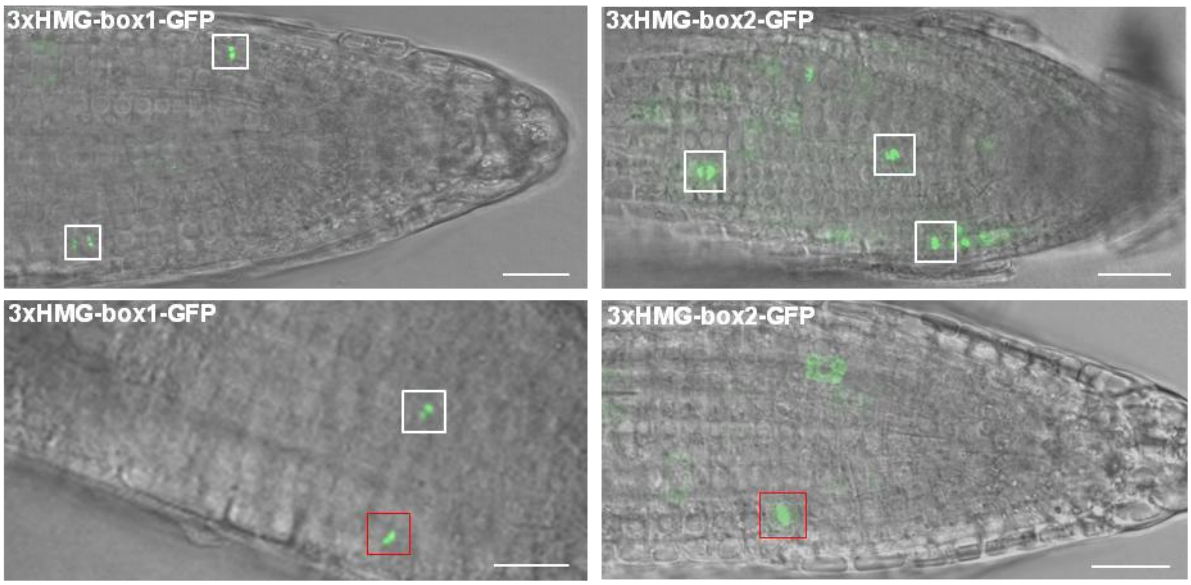

C

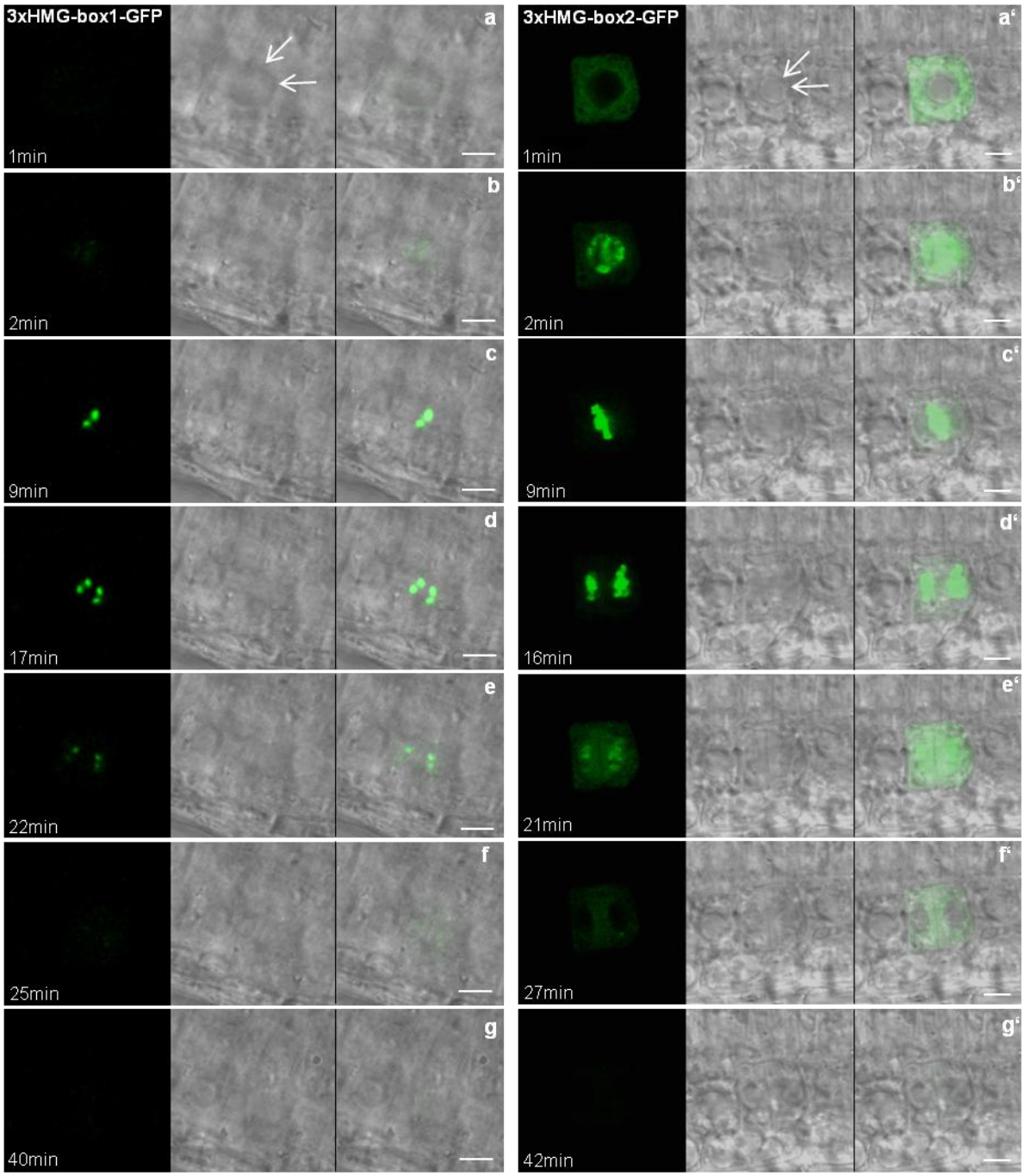

Figure 13. Live cell imaging of 3xHMG-box-GFP fusion proteins in root tips. (A) Shematic representation of plasmids pM1 and pM2 with primer used for cloning and genotyping. **(B)** Overview of roots from Arabidopsis plants harboring constructs that allow the expression of 3xHMG-box1-GFP and 3xHMG-box2-GFP fusion proteins under the control of its native promoters. Brightfield pictures and pictures of the GFP-derived fluorescent light were merged. Cells that reside in mitosis are framed by squares. Scale bar indicates 20µm. **(C)** A time sequence of the cells framed by red squares in Figure 13A. Arrows indicates the nuclear envelope before break down. Scale bar indicates 5µm.

Upon completion of cytokinesis, 3xHMG-box1-GFP and 3xHMG-box2-GFP derived signals can only be detected in the cytoplasm (f,f') and finally disintegrate shortly after mitosis(g,g'). Independent plant lines that express 3xHMG-box2-GFP under the control of the *3xHMG-box2* promoter were used to estimate time of mitosis starting

from NEBD until late telophase. Based on a total number of 29 analyzed root cells in the meristematic zone, duration of this phase was determined around 23.8 (+/-2.9) min. Live cell imaging with root cells of plants expressing 3xHMG-box2-GFP under the control of its endogeneous promoter was also performed over a long term of 8h. Based on a total number of 9 cells undergoing mitosis, span of time from appearance of the 3xHMG-box2-GFP-derived fluorescent signal to the nuclear envelope break down was estimated around 88.2 (+/-19.6) min (data not shown).

3.1.2 Investigation of a putative D-box like degradation domain in the N-terminal region of 3xHMG-box1

3xHMG-box proteins appear to vanish shortly after mitosis, leading to the assumption that they are actively degraded as often observed for proteins with mitotic functions. To confirm this hypothesis, amino acid sequences of 3xHMG-box proteins were screened for KEN-box and D-box sequence motifs representing recognition sites for specific degradation machineries, among them the M-phase specific E3 ligase APC/C. (Chapter 1.2.1).

As mentioned in chapter 1.4.4 both 3xHMG-box proteins share a high sequence identity of 77,3%. Conserved minimal D-box sequence motifs are found in the N-terminal region, second HMG-box of both 3xHMG-box proteins and in the third HMG-box of 3xHMG-box2. Additionally 3xHMG-box2 contains a KEN-box motif in the first HMG-box (Figure 14).

A

```
Length: 459 aa
Identity:       355/459 (77.3%)
Similarity:     394/459 (85.8%)
Gaps:            16/459 ( 3.5%)

3xHMG-box1         1 MSTVSSDPAHAKKSRNSRKALKQKNEIVES--SPVSDKGKETKSFEKDLM     48
                     |:| ::||||..||.|||||||||||:||:  ||||.|||..||||:|||
3xHMG-box2         1 MAT-NADPAPTKKPRNSRKALKQKNELVETPPSPVSVKGKSAKSFEQDLM     49

3xHMG-box1        49 EMQAMLEKMKIEKEKTEDLLKEKDEILRKKE-------VEQEKLKTELKK     91
                     |||.||||||||:|||:||||||||||||||       .|||||||||||
3xHMG-box2        50 EMQTMLEKMKIEKDKTEELLKEKDEILRKKEEELETRDAEQEKLKVELKK     99

3xHMG-box1        92 LQKMKEFKPNMTFAFSQ-SLAQTEEEKKGKKKKKDCAETKRPSTPYILWC    140
                     |||||||||||||..| ||.|.|:||..|||||||.||||||:.|:|||
3xHMG-box2       100 LQKMKEFKPNMTFACGQSSLTQAEQEKANKKKKKDCPETKRPSSSYVLWC    149

3xHMG-box1       141 KDNWNEVKKQNPEADFKETSNILGAKWKGISAEEKKPYEEKYQADKEAYL    190
                     ||.|.||||:||||||||||||||||.:|||:||||||:||.:|||||
3xHMG-box2       150 KDQWTEVKKENPEADFKETSNILGAKWKSLSAEDKKPYEERYQVEKEAYL    199
```

```
3xHMG-box1      191 QVITKEKREREAMKLLDDEQKQKTAMELLDQYLHFVQEAEHDNKKKAKKI    240
                    |||.|||||:||||||:|:|||:||||||||||:||||||.|||||.||.
3xHMG-box2      200 QVIAKEKREKEAMKLLEDDQKQRTAMELLDQYLNFVQEAEQDNKKKNKKE    249

3xHMG-box1      241 KDPLKPKQPISAYLIYANERRAALKGENKSVIEVAKMAGEEWKNLSEEKK    290
                    |||||||.|:||:|:||||||||||:.|||||:||||:.|||||||||::||
3xHMG-box2      250 KDPLKPKHPVSAFLVYANERRAALREENKSVVEVAKITGEEWKNLSDKKK    299

3xHMG-box1      291 APYDQMAKKNKEIYLQEMEGYKRTKEEEAMSQKKEEEEFMKLHKQEALQL    340
                    |||:::||||||.|||.||.|||||||||:||||||||.:|||||||||:
3xHMG-box2      300 APYEKVAKKNKETYLQAMEEYKRTKEEEALSQKKEEEELLKLHKQEALQM    349

3xHMG-box1      341 LKKKEKTDNIIKKTKETAKNKKKNENVDPNKPKKPTSSYFLFCKDARKSV    390
                    |||||||||:|||.|.|  .|||||||||||||.|||||||.||.||.:
3xHMG-box2      350 LKKKEKTDNLIKKEKAT--KKKKNENVDPNKPKKPASSYFLFSKDERKKL    397

3xHMG-box1      391 LEEHPGINNSTVTAHISLKWMELGEEEKQVYNSKAAELMEAYKKEVEEYN    440
                    .||.||.||:||||.|||||.||.|||||||||.|||:||||||||||.||
3xHMG-box2      398 TEERPGTNNATVTALISLKWKELSEEEKQVYNGKAAKLMEAYKKEVEAYN    447

3xHMG-box1      441 K---TKTSS    446
                    |   ..|||
3xHMG-box2      448 KKSAATTSS    456
```

Figure 14. Identification and site directed mutagenesis of a putative D-box degradation domain in 3xHMG-box2. Pairwise amino acid sequence alignment of 3xHMG-box1 and 3xHMG-box2 using EMBOSS needle (http://www.ebi.ac.uk). Global alignment was generated using Needleman-Wunsch algorithm. Sequences were analyzed for containment of KEN-box and D-box minimal consensus sequences. N-terminal regions are underlined in black and the three HMG-boxes are underlined in red, green and blue. Putative D-boxes and KEN-boxes are highlighted in yellow.

As motifs mediating APC/C-dependent destruction often occur in unstructured N-terminal regions of the substrates (Glotzer et al. 1991, Pfleger and Kirschner 2000), the RxxL motif in the N-terminal region of 3xHMG-box2 (Figure 14) was chosen for site directed mutagenesis. The arginin 17 and leucin 20 were replaced with an alanin each, using overlap extension PCR and plasmid pM2 as a template, giving rise to pM3 (Figure 15A). *A. thaliana* plants were stably transformed with pM3 by *Agrobacterium* mediated transformation. Independent plant lines were tested for integration of the construct (Supplemental Figure 2) and used for microscopy.

In order to test the effect of the mutated D-box sequence motif, verified plant lines were applied for live cell imaging as described in chapter 3.1.1 and compared with plant lines that express the non-mutated 3xHMG-box2-GFP fusion protein. Fluorescence signal in root cells of plants, that express non-mutated 3xHMG-box2-GFP under the control of the 3xHMG-box2 promoter vanishes relatively fast after mitosis (Figure 15B). The time interval from telophase, when 3xHMG-box2 detaches from chromosomes, until the extinction of the 3xHMG-box2-GFP derived signal was deduced from a total number of 22 root cells from three independent plant lines and

estimated around 21.8 (+/-) 8.9 min. In plant lines that express 3xHMG-box2-GFP with a mutation in the N-terminal D-box motif, no disintegration of the fluorescent signal could be observed (Figure15C). Even after more than 1h after telophase, 3xHMG-box2 derived signal didn't show any reduction. In total 8 root cells of three independent plant lines were monitored in average 68.8 min after telophase and in none of them, depletion of the 3xHMG-box2 derived signal could be observed. Evidently, the overall cytoplasmatic signal was stronger in plants that express the mutated 3xHMG-box2-GFP version.

A

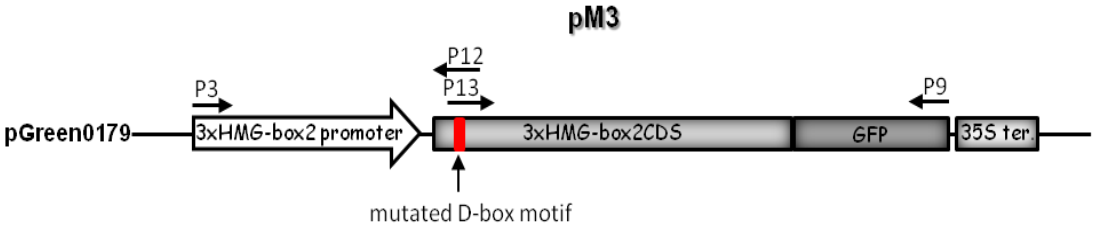

B

+N-terminal D-box motif

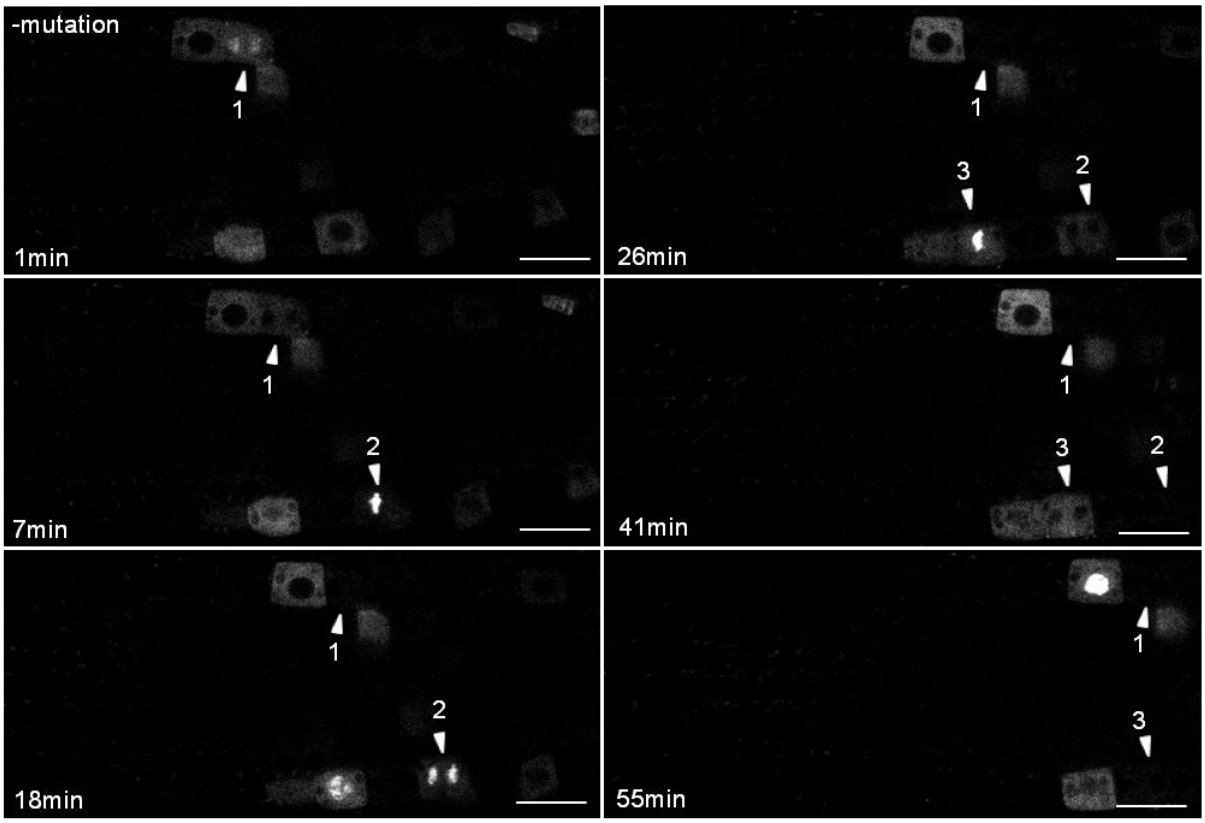

C

-N-terminal D-box motif

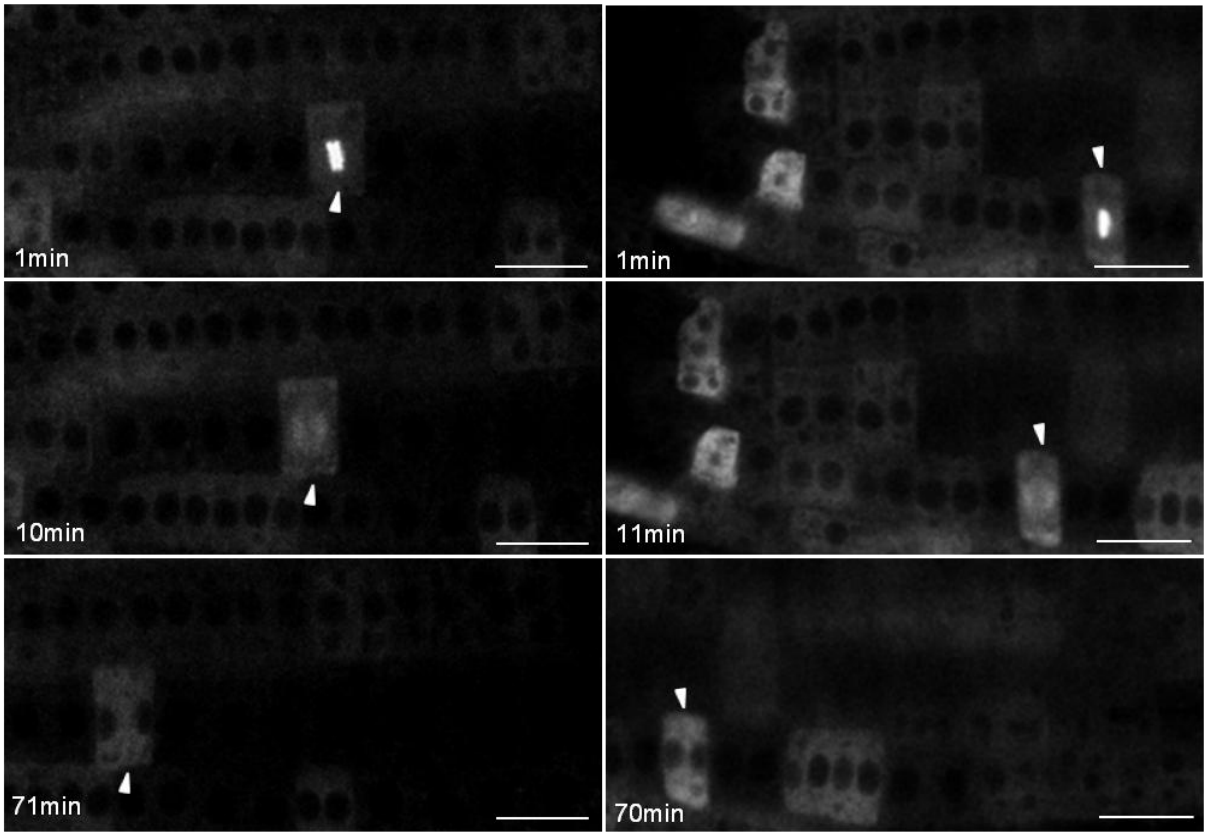

Figure 15. Contribution of N-terminal D-box motif to degradation of 3xHMG-box2 after mitosis. **(A)** Schematic representation of pM3 with indication of primers used to generate the construct and introduce a mutation in the putative D-box. Time lapse microscopy of roots from plant lines stably expressing 3xHMG-box2-GFP **(B)** or 3xHMG-box2-GFP with mutation of the N-terminal D-box motif **(C)** under the control of the 3xHMG-box2 promoter. Arrowheads indicate cells during and shortly after undergoing mitosis. Scale bar indicates 20µm.

The significant difference in depletion of the 3xHMG-box2-GFP signal, upon mutation of the D-box motif, suggests a function of this motif in protein degradation of 3xHMG-box2 proteins after mitosis.

3.2 Reverse genetic approach

3.2.1 Verification of the T-DNA insertion line GK-171F06-013466

In order to unveil functions of 3xHMG-box proteins The Arabidopsis Information Resource (TAIR) database was screened for T-DNA insertion lines, annotated to contain a T-DNA insertion in one of the *3xHMG-box* genes. As for *3xHMG-box2* no candidate was found, T-DNA insertion line GK-171F06-013466, annotated to harbor

the T-DNA insertion in the second exon of the *3xHMG-box1* coding sequence was chosen for further characterization (Figure 16A). T-DNA insertion lines were tested for the position of the insertion by PCR-based genotyping. One line was tested positive for the T-DNA insertion at the annotated position and appeared to contain the insertion in both alleles. Amplification of genomic DNA with primer pair P5/P76 leads to a PCR-fragment with the expected size of 1007 bp for the T-DNA insertion line, while no signal could be obtained for the wild type. Using primer pair P14/P15 for amplification of genomic DNA lead to generation of a PCR fragment around the expected size of 880 bp for the WT, which could not be detected in the T-DNA insertion line suggesting the DNA being integrated in both alleles (Figure 16B).

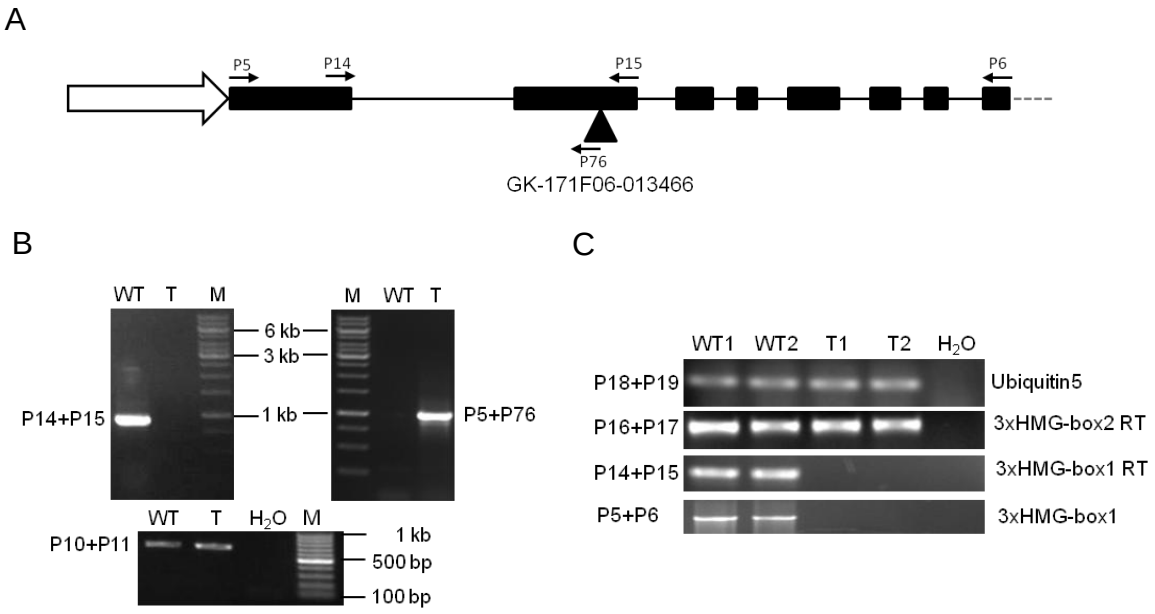

Figure 16. Molecular characterization of T-DNA insertion line GK-171F06-013466. (A) Schematic representation of the *3xHMG-box1* gene with the position of the T-DNA insertion and binding sites of primer (P) that were used for genotyping and semi quantitative PCR. **(B)** PCR based genotyping using indicated primer pairs and genomic DNA extracted from wild type (WT) and T-DNA insertion line GK-171F06-013466 (T). **(C)** Semi quantitative RT-PCR using indicated primer pairs to amplify cDNA from wild type (WT1, WT2) and T-DNA insertion line GK-171F06-013466 (T1, T2) 12 DAS.

Transcrip level of *3xHMG-box1* and *3xHMG-box2* was determined by semi quantitative RT-PCR (Figure 16C). RNA was extracted from wild type (Col-0) and T-DNA insertion line GK-171F06-013466 to generate cDNA. Amplification of cDNA with specific primers allows the estimation of the transcript level of certain regions. *Ubiquitin* was used as reference gene and amplification of the coding region of *3xHMG-box1* didn't generate a product, when cDNA of the T-DNA insertion line was

used. Besides, transcript level of *3xHMG-box2* gene doesn't seem to be affected in the mutant.

As T-DNA insertion line GK-171F06-013466 appear to be a knock-out mutant for 3xHMG-box1, phenotypic analyzes were done and mutant was referred to as *3xhmg-box1*. As can be seen in Figure 17A, *3xhmg-box1* does not shown any obvious growth defect, either at 22 days after stratification (DAS), nor 40 DAS. Flowers of the mutant do not show any alterations (Figure 17B) and siliques appear to have the same size compared to the wild type (Figure 17C). Furthermore siliques of *3xhmg* plants contain a complete seed set.

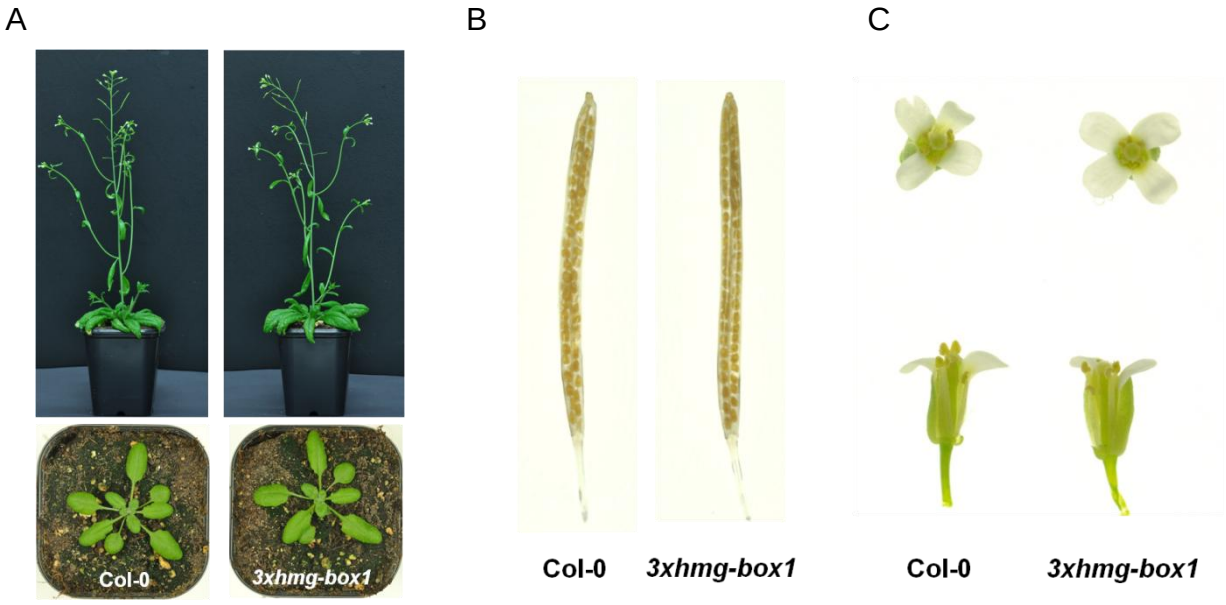

Figure 17. Phenotype of *3xhmg-box1* compared to Col-0. (A) Photograph of plants 22 DAS (lower panel) and plants 40DAS (upper panel). **(B)** Photograph of flowers from above and from a side view with two petals and sepals each dissected. **(C)** Photograph of bleached siliques

3.2.2 Knock-down approach using long hairpin RNA (lhRNA)

As no T-DNA insertion line, containing an insertion in the *3xHMG-box2* gene, could be identified, RNA interference (RNAi) approach based on lhRNAs was chosen to achieve a down regulation in *3xHMG-box2* expression. A 684 bp DNA fragment of the *3xHMG-box2* coding sequence was amplified using primer pair P20 and P21. The resulting PCR product was cloned in opposite orientations in pFGC5941 (pL4) giving rise to plasmid pM4 (Figure 18A). As both fragments have similar sequences and are interrupted by a linker, upon transcription driven by 35S promoter, they are able to form a hairpin loop that can be utilized by the RNA Induced Silencing Complex (RISC).

3xhmg-box1 plants were used for stable *Agrobacterium* mediated transformation in order to rule out possible redundant effects. Selected plants were screened for possession of the T-DNA insertion and the hairpin construct. Primers P10 and P11 binding at the coding sequence of *HMGA* were used to check the input gDNA. 14 independent plant lines containing both, the T-DNA insertion within the *3xHMG-box1* gene and the hairpin construct, were chosen to test the transcript level of *3xHMG-box2* by semi quantitative RT-PCR (Figure 18B). cDNA was generated from wild type and *3xhmg-box1* plants as control and *3xhmg-box1* lines harboring the lhRNA construct. cDNA was used for amplification with primer pair P16/P17 that binds in the coding region of *3xHMG-box2* gene but not in the area which was amplified with primer pair P20/P21 in order to construct the hairpin. Transcript level was deduced from intensity of the PCR band in an agarose gel. *Ubiquitin5* and *Actin8* were used as reference genes as their transcript level should not be affected by the lhRNA construct. PCR cycle number was adjusted specifically for each primer pair in order not to reach saturation of the reaction.

A

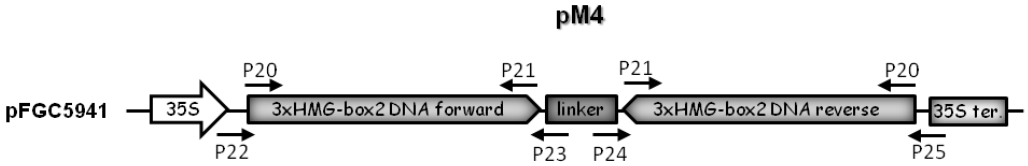

B

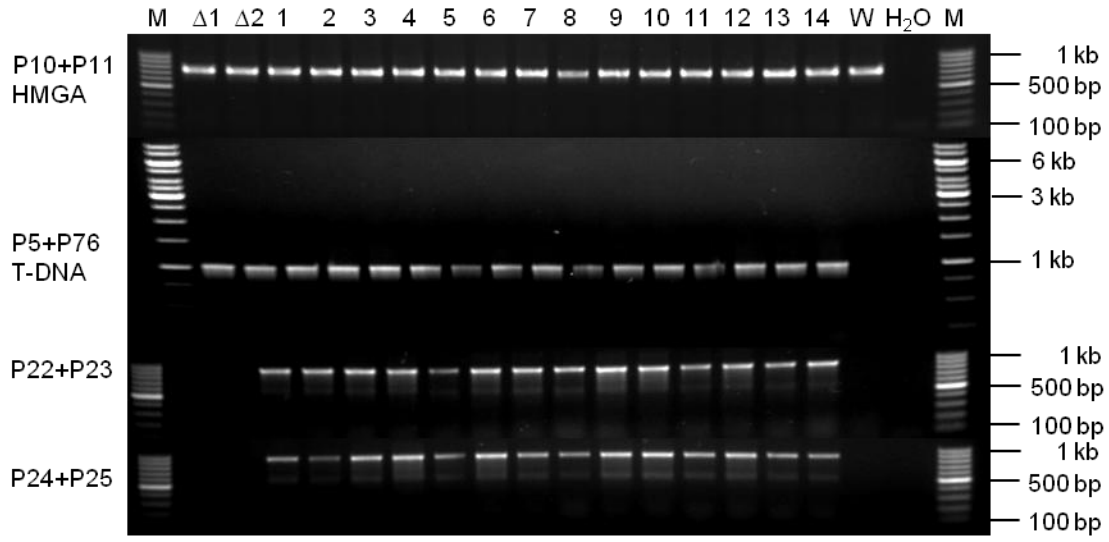

C

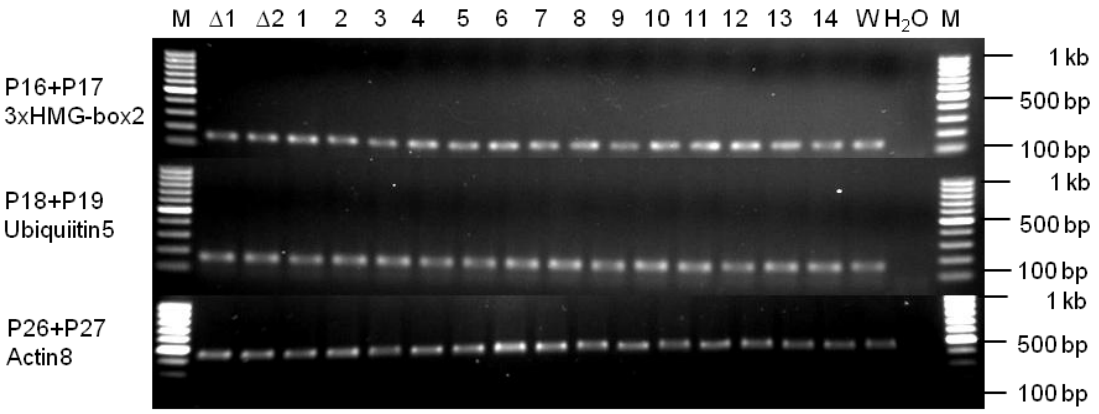

Figure 18. Construction of shRNA vector pM4 and introduction in *3xhmg-box1* lines. (A) Schematic representation of pM4 and respective primers used for cloning and PCR based genotyping. **(B)** PCR-based genotyping of *3xhmg-box1* plant lines, containing the shRNA construct (1-14). Untransformed *3xhmg-box1* (Δ) and wild type (W) were used as control. **(C)** Semi quantitative PCR with cDNA derived from the same lines that were genotyped. PCR fragments of control genes and *3xHMG-box2* were generated using indicated primer pairs.

As expected, PCR fragment signals show the same intensity in all tested lines for the reference genes, ensuring that equal amounts of cDNA were used for quantification. PCR signal strength for the *3xHMG-box2* DNA fragment also show the same intensity for all tested lines suggesting that *3xHMG-box2* gene transcript level is not reduced in plant lines.

3.2.3 Knock-down approach using artificial micro RNA (amiRNA)

An alternative to gene silencing by lhRNAs, amiRNA approach was used in order to reduce transcription of the *3xHMG-box2* gene (Parizotto et al. 2004). amiRNAs are 21mer small RNAs , which can be genetically engineered and function to specifically silence single or multible genes. The artificial microRNA designer WMD (http://wmd3.weigelworld.org) delivers four oligonucleotide sequences, which are used to engineer a specific amiRNA into the miR319a precursor by site-directed mutagenesis.

Primers P29-P34 were used to engineer *3xHMG-box2* specific amiRNA in miR319a precursor by using pRS300 vector as template. Modified miR319a was then cloned blunt end into pGreen0229 vector backbone containing an *Ubiquitin5* promoter in

front of the multiple cloning site of pGreen0229+Ubiquitin10 promoter+35S terminator (pL5) giving rise to vector pM5 (Figure 19A).

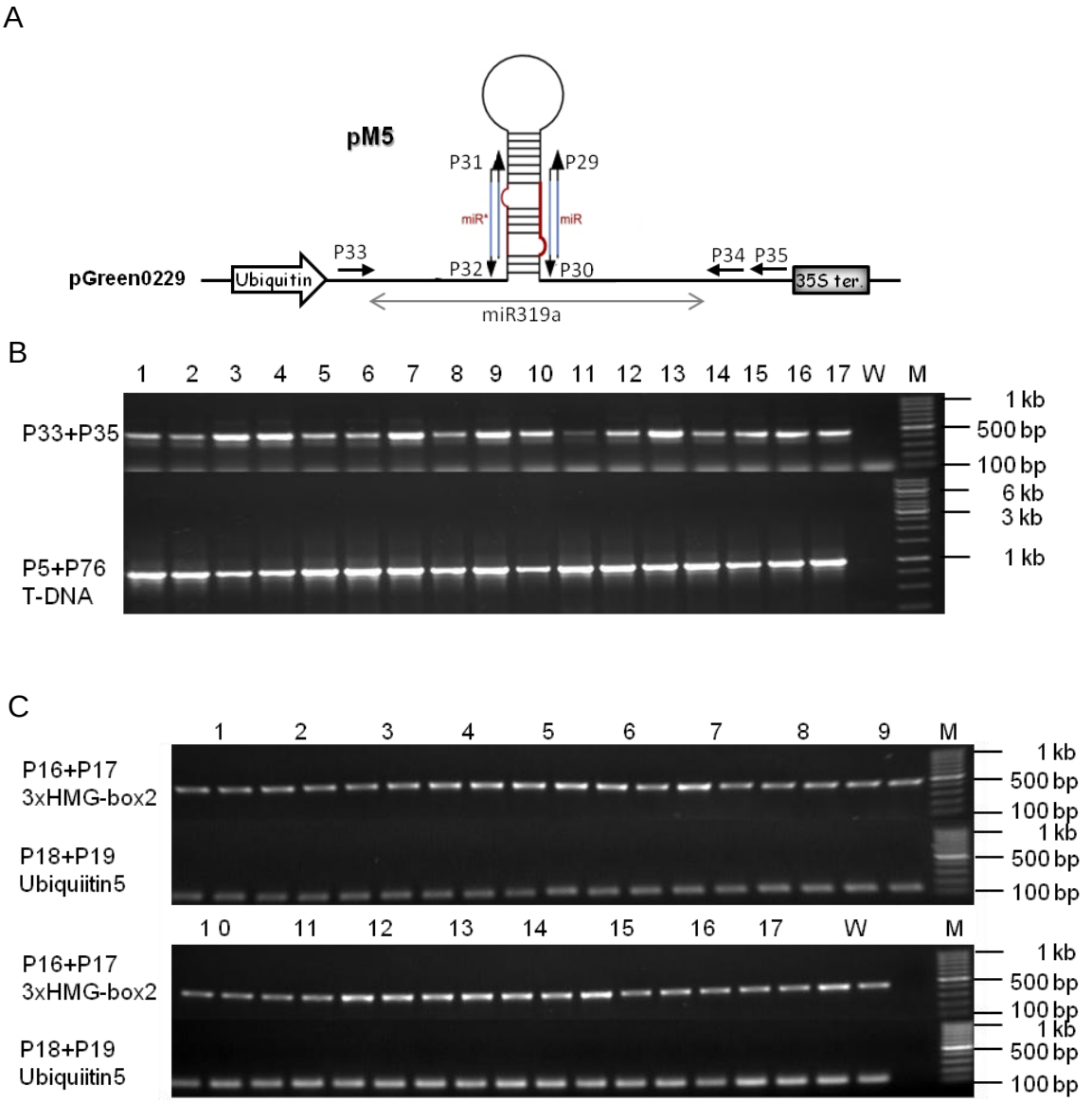

Figure 19. Construction of amiRNA construct pM5 and introduction in *3xhmg-box1* lines. (A) Schematic representation of pM5 and respective primers used for cloning and PCR based genotyping. **(B)** PCR-based genotyping of *3xhmg-box1* plant lines, containing the amiRNA construct (1-17) and wild type (W) as control. **(C)** Semi quantitative PCR with cDNA derived from the same lines that were genotyped. PCR fragments of control genes and *3xHMG-box2* were generated using indicated primer pairs.

3xhmg-box1 plants were used for *Agrobacterium* mediated stable transformation with pM5. Selected plants were analyzed by PCR-based genotyping and 17 positively tested independent plant lines containing the modified miR319a were used to examine transcript level of the *3xHMG-box2* gene (Figure 19B).

RNA was exctracted from positively tested plant lines and wild type as control, two times each for double determination. cDNA was generated from RNA and a part of

the coding sequence of *3xHMG-box2* and *Ubiquitin5* as reference were amplified using the indicated primer pairs (Figure 19C). As expected signal strength of the PCR fragments for *Ubiquitin5* are relatively equal in all tested plant lines, indicating that equal amounts of cDNA with comparable quality was used. The signal strength for PCR fragments of *3xHMG-box2* cDNA also shows no striking differences in the plant lines harboring the *3xHMG-box2* specific amiRNA construct, when compared to the wild type. This indicates that the transcription level of the *3xHMG-box2* gene was not decreased in analyzed plants.

3.3 Immunoprecipitation with GS tagged 3xHMG-box proteins

Identification of putative interaction partners is an attractive path to unveil potential functions for newly described proteins. One way to do so is the Co-IP using a tag for affinity purification, which is coupled to the protein of interest. For the plant system the GS tag, which combines two IgG-binding domains of protein G with a streptavidin binding peptide, has been proven to be highly efficient regarding specificity and yield (Van Leene et al. 2011).

As 3xHMG-box proteins are specifically expressed around M-phase, *3xHMG-box2* promoter was used to drive expression of the GS tagged 3xHMG-box proteins. For that purpose, the *3xHMG-box2* promoter was first cloned into a pCAMBIA2300 backbone with 35S terminator (pL6) and in the second step, GS coding DNA sequence was cloned in front of the terminator sequence, giving rise to plasmid pM6. Coding sequences of *3xHMG-box1* and *3xHMG-box2* were then cloned into pM6 between *3xHMG-box2* promoter and GS tag giving rise to plasmids pM7 and pM8 (Figure 20A). *Arabidopsis* cell suspension cultures (PBS-D) as well as plants were transformed with the constructs by using *Agrobacterium* mediated transformation and verified by PCR-based genotyping (Supplemental Figure 3).

Confirmed cell cultures were further grown to obtain a total volume of 10 l for each construct and frozen in liquid nitrogen after harvesting.15 g of frozen PBS-D cells per construct were used for Co-IP procedure as described in 2.4.20. When cells that express GS under the control of the *3xHMG-box2* promoter were used for Co-IP, a protein of approximately 21 kDa corresponding to the expected size of the GS protein could be detected in a Coomassie stained gel after SDS-PAGE (Figure 20B), thus indicating that the *3xHMG-box2* promoter is able to drive enough expression to generate sufficient amounts of GS protein for Co-IP. When PBS-D cells that were

transformed with pM7 and pM8 were applied to Co-IP, no protein could be detected around the expected size of ~73 kDa for 3xHMG-box1-GS and ~74 kDa for 3xHMG-box2-GS fusion proteins. Co-IP precipitates and input fractions were also tested by immunoblot assay. Antibodies raised against the N-terminal region of 3xHMG-box2

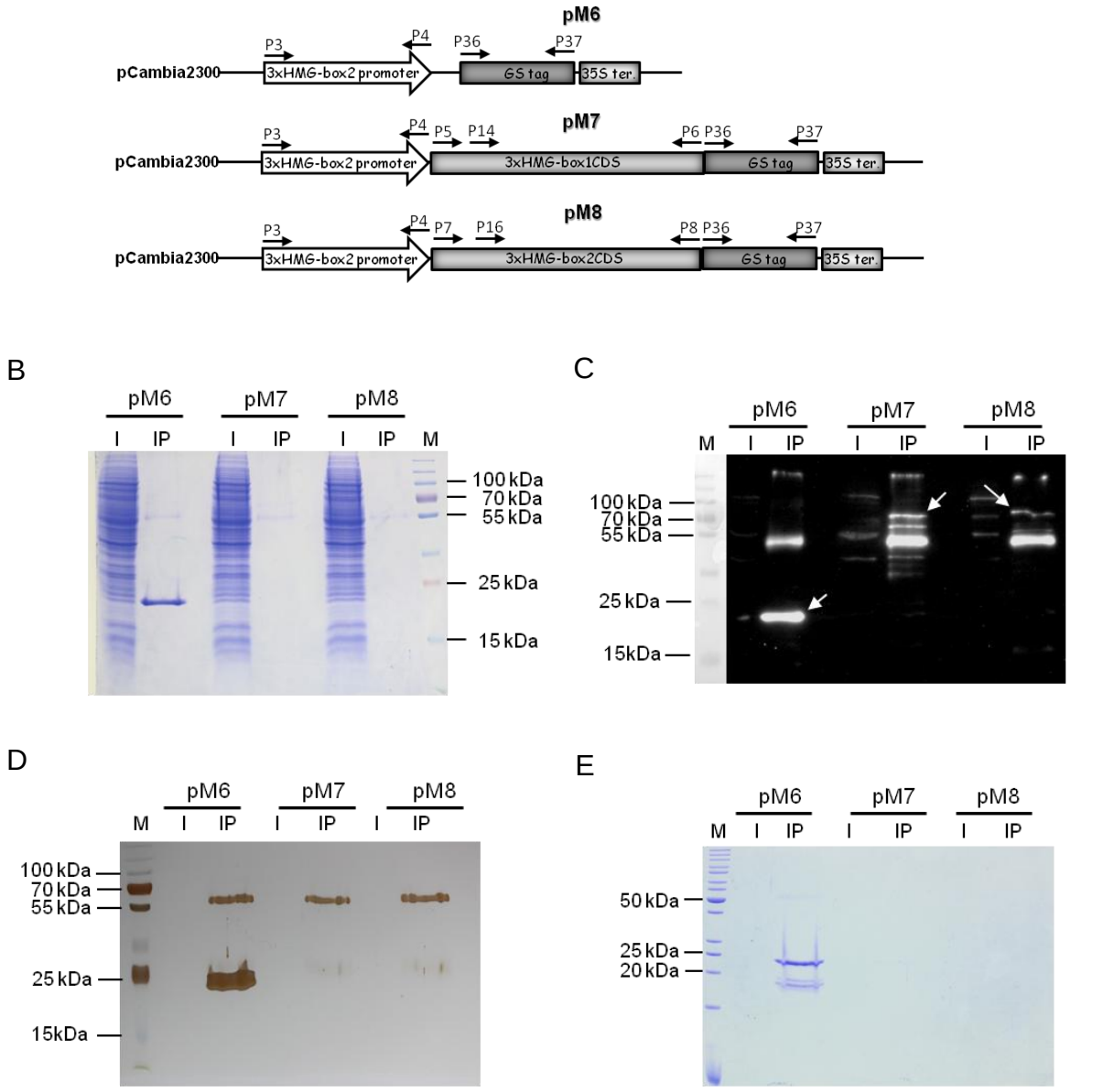

Figure 20. Co-IP with GS-tagged 3xHMG-box proteins using *Arabidopsis* cell suspension cultures and seedlings. (A) Schematic representation of vector constructs used for expression of GS tagged 3xHMG-box proteins. Primers that were used for cloning and PCR based genotyping are indicated. **(B)** Coomassie stained gel after SDS-PAGE. Cell free extracts of cultured cells transformed with indicated constructs were used as input (I) for Co-IP. Complete eluate fraction of one Co-IP was precipitated and loaded (IP). **(C)** Immunoblot of a gel after SDS-PAGE, using a 3xHMG-box protein specific antibody. Arrows indicate signals that correspond to the expected sizes of the GS-tagged proteins and control respectively. Lanes were loaded as in A. **(D)** Silver staining of a gel after SDS-PAGE. Lanes are loaded as described in A. **(E)** Coomassie stained gel after SDS-PAGE. Cell free extracts of 10 DAS old seedlings transformed with indicated constructs were used as input (I) for Co-IP. Complete eluate fraction of one Co-IP was precipitated and loaded (IP)

that were shown to bind 3xHMG-box1 protein as well (Pedersen et al. 2011) were used for detection. In the Co-IP elution fraction of PBS-D cells that were transformed with pM6, a signal around 21 kDa corresponding to the GS protein could be detected (Figure 20C), because the secondary antibody is likely to bind protein G epitopes. Additionally in all elution fractions a signal around 50 kDa could be observed, which can be assigned to the heavy chain derived from IgG antibodies that were used for Co-IP. In the precipitated elution fractions of PBS-D cells that were transformed with pM7 and pM8 additional faint signals could be detected above 70 kDa that might be derived from 3xHMG-box-GS fusion proteins. In order to verify 3xHMG-box-GS fusion proteins and to be able to identify interaction partners by mass spectrometry a minimal protein concentration has to be exceeded. Silver staining method, as the most sensitive staining method for proteins in a polyacrylamide gel, was used to test if sufficient protein amounts can be detected. As can be seen in Figure 20D, only the GS protein in the control and proteins likely to be the heavy and light chains of the IgG could be detected by silver staining. Therefore IP fractions were not used for further analyzes. Alternatively, heterozygous plants of the T_1 generation of six independent lines which were transformed with pM6, pM7 or pM8 (Supplemental Figure 3B) were used as starting material for immunoprecipitation. Seedlings were harvested 10 DAS as it was shown that transcript level of *3xHMG-box* genes is higher in younger plants than in older plants, probably due to higher cell division rates. However, also by using young seedlings, no 3xHMG-box-GS fusion proteins could be obtained by immunoprecipitation (Figure 20E).

3.4 Artificial targeting of 3xHMG-box proteins to the nucleus during interphase

3.4.1 35S promoter driven expression of 3xHMG-box-GFP in *Arabidopsis thaliana*

Stable plant lines, which express 3xHMG-box-GFP fusion proteins under the control of the 35S promoter were already generated and tested in previous works (Pedersen et al. 2011). In the majority of the root cells, 3xHMG-box-GFP derived signal can be detected in the cytoplasm, while in very few cells that appear to reside in mitosis, GFP signal is associated with chromatin (Figure 21A). Phenotype of respective plants

was analyzed and compared to wild type plants, but no defect could be assigned to overexpression of 3xHMG-box proteins (Figure 21B/C).

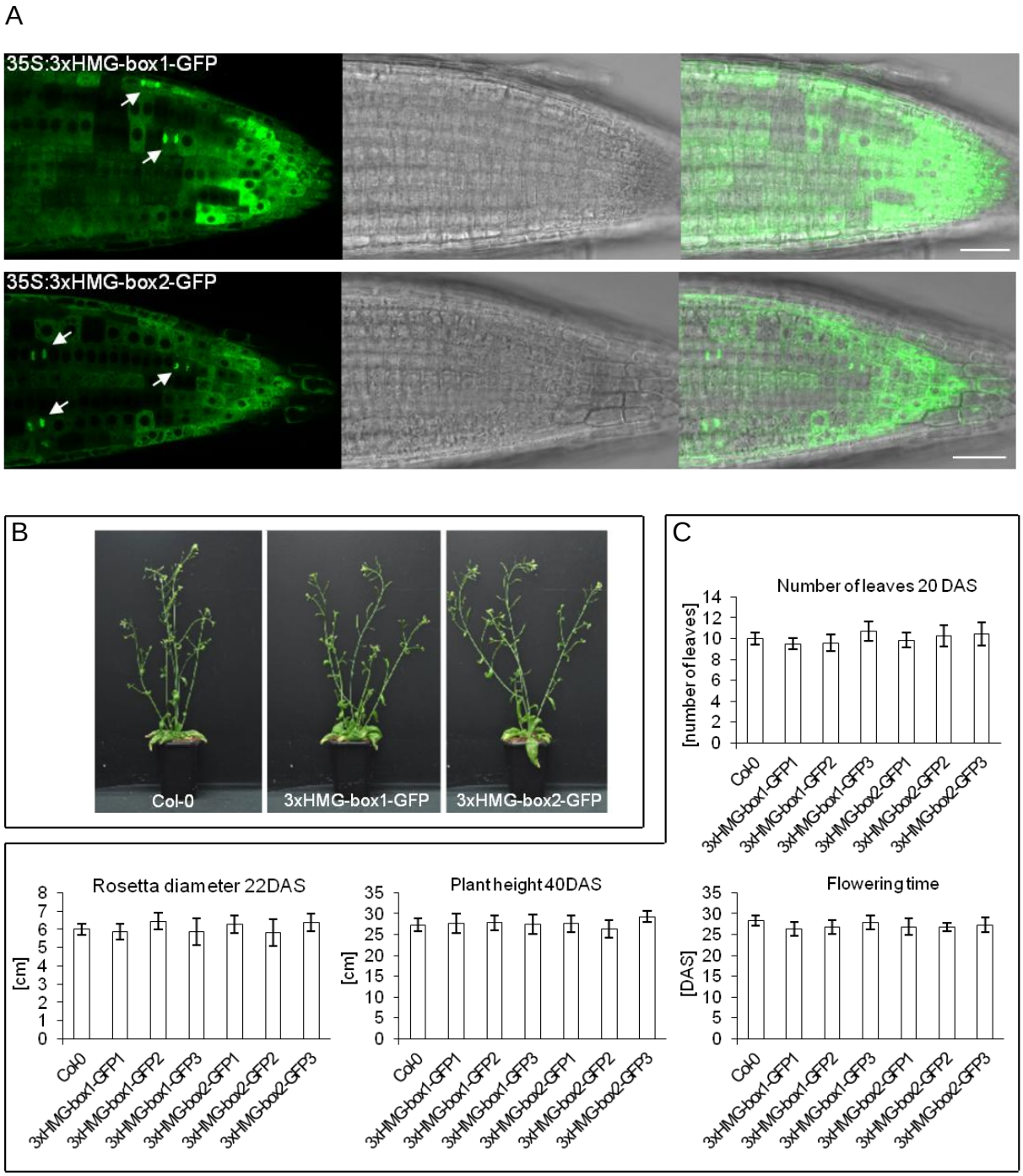

Figure 21. Phenotypcial analyzes of stably transformed *Arabidopsis* plants which express 3xHMG-box-GFP under the control of the 35S promoter. (A)Seedlings of stable transformed plant lines which express 3xHMG-box-GFP fusion proteins were grown sterile on MSO-medium until approximately 5DAS before applying to CLSM. Left panel shows GFP-derived signal, middle panel bright field picture und right panel the overlay of both chanels. Arrows indicate mitotic cells and scale bar correlates with 30µm **(B)** Photographs of plants 43DAS. **(C)** Quantification of basic growth parameter with data derived from 7-12 individual plants per line. Error bars indicate standard deviation. No significant difference between the parameters was obtained using one-way ANOVA ($p<0.05$).

3.4.2 35S promoter driven expression of 3xHMG-box-GFP-NLS in *Arabidopsis thaliana*

In order to investigate the consequences of constitutive expression and targeting of 3xHMG-box proteins to the nuclei during interphase, coding DNA sequences of both proteins were translationally fused to a GFP coding DNA sequence with attached nuclear localization signal (NLS), which expression is driven by the 35S promoter. *3xHMG-box1* and *3xHMG-box2* CDS were amplified and cloned into pGreen0229+35S cassette+GFP-NLS (pL8) giving rise to plasmids pM9 and pM10 (Figure 22A). Col-0 plants were transformed with respective constructs using *Agrobacterium* mediated transformation and independent lines were verified by PCR-based genotyping (Supplemental Figure 4). In addition, nuclear proteins of respective plant lines were extracted and tested by immmunoblot assays using an anti-GFP antibody (Figure 22B). A protein between 25 kDa and 35 kDa could be detected in nuclei of plant lines that were transformed with pL8. In nuclei of plants that were transformed with pM9 and pM10 signals were obtained between 70 and 100 kDa. This is in line with expected protein masses of 28.1 kDa for GFP-NLS 80.5 kDa for 3xHMG-box1-GFP-NLS and 81.7 kDa for 3xHMG-box2-GFP-NLS. Furthermore, it seems that the majority of fusion proteins are not degraded within the nucleus.

Plants were further analyzed by CLSM. Control lines that express GFP-NLS under the control of the 35S promoter show, as expected, a GFP-derived signal in the nuclei of root cells and leaf cells (Figure 22C, upper row) and the signal within the nucleus is relatively equally distributed. In root tip and leaf epidermal cells of plant lines which express 3xHMG-box1-GFP-NLS under the control of the 35S promoter, a GFP derived signal can indeed be observed in interphase nuclei (Figure 22C, middle row), unlike in plants that express 3xHMG-box1-GFP under the control of the 35S

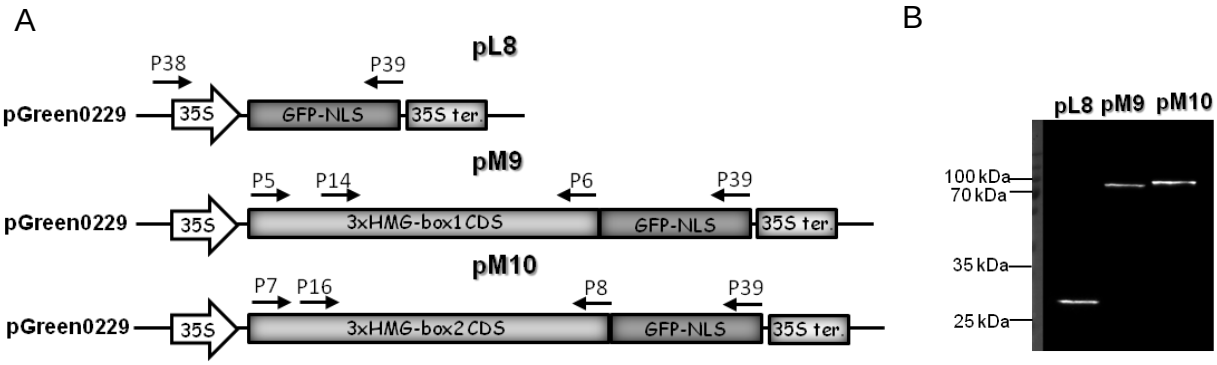

C

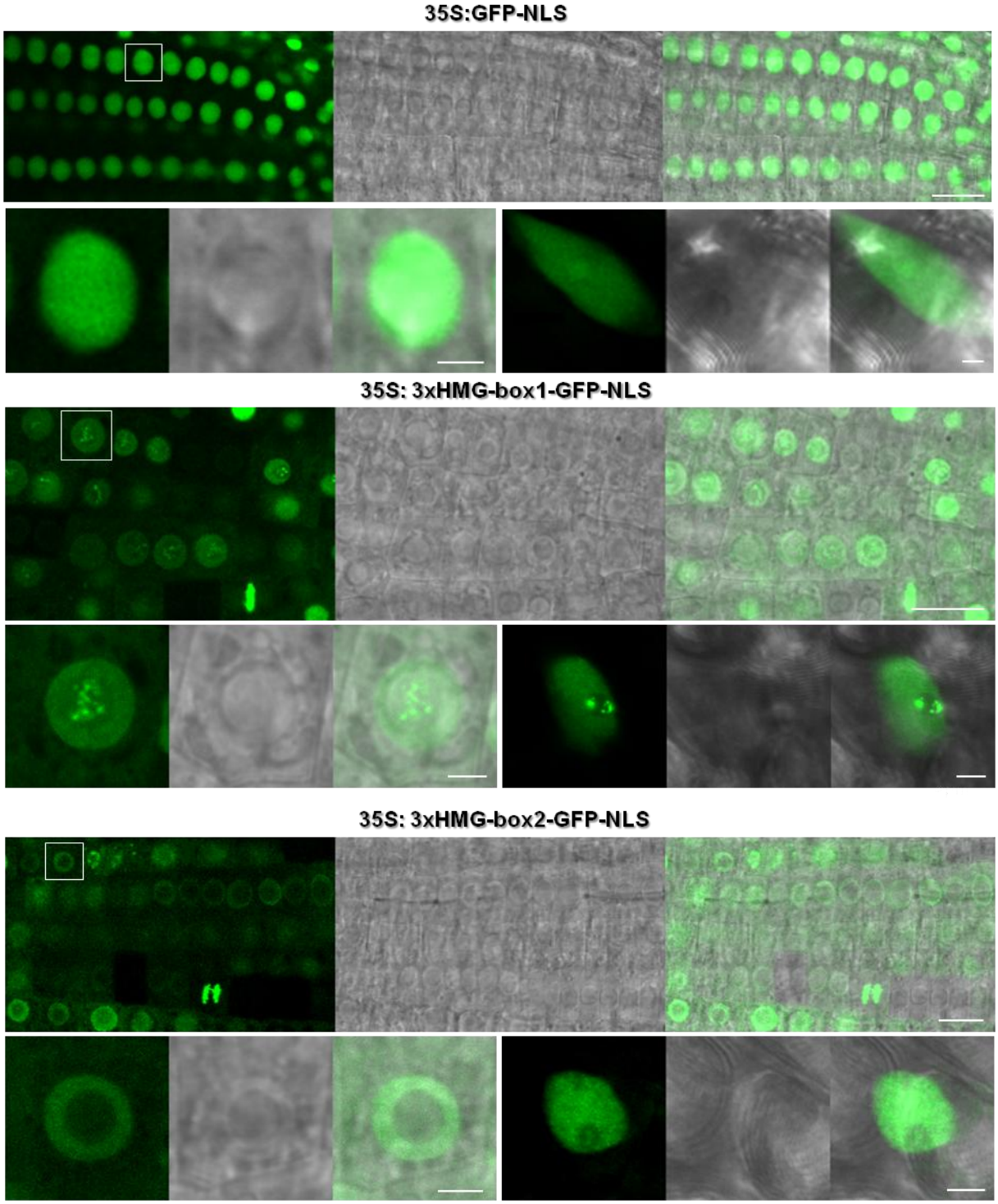

Figure 22. CLSM and Immunostaining analyses of stably transformed *Arabidopsis thaliana* plant lines, which express GFP-NLS and 3xHMG-box-GFP-NLS fusion proteins. (A) Schematic representation of vector constructs used for expression of 3xHMG-box-GFP-NLS fusion proteins under the control of the 35S promoter. Primers that were used for cloning and PCR based genotyping are indicated. **(B)** Nuclei of plant lines which harbor the constructs pL8, pM9 or pM10 were extracted and subjected to SDS PAGE followed by immunoblot assay using an anti-GFP antibody. **(C)** Top panel shows a section of a root tip of stably transformed *Arabidopsis thaliana* plant lines either expressing GFP-NLS, 3xHMG-box1-GFP-NLS or 3xHMG-box2-GFP-NLS under the control of the 35S promoter. Scale bar indicates 15µm. Lower left panel shows a magnification of one root cell that is marked by a white square in the upper panel. Lower right panel shows a leaf epidermal cell. Scale bar in the lower panels indicates 3 µm. The GFP-derived signal, a bright field picture and an overlay are shown for each picture.

promoter (Figure 21A). Within the nuclei, 3xHMG-box1-GFP-NLS accumulates in form of foci in the area of the nucleolus in both root and epidermal leaf cells. While the signal in root cell nucleoli is rather dispersed, foci within the nucleoli of epidermal leaf cells seem to be rather compact. Subnuclear distribution of 3xHMG-box1-GFP-NLS fits with the results obtained from immunostaining experiments in which it was shown that 3xHMG-box1-GFP associates with 45S rDNA in *Arabidopsis thaliana* root tip cells during mitotis (Pedersen et al. 2011). During mitosis, 3xHMG-box-GFP1-NLS fusion proteins associate with condensed chromosomes (Figure 22C, middle row, upper panel). Possibly due to the strong expression, 3xHMG-box1-GFP-NLS generally decorates mitotic chromosomes instead of specifically associating with NORs.

In plant lines expressing 3xHMG-box2-GFP-NLS, fluorescent signal can be detected in interphase nuclei of root cells and epidermal leaf cells as well (Figure 22C, lower row). In contrast to 3xHMG-box1-GFP-NLS, 3xHMG-box2-GFP-NLS is rather excluded from the nucleolar area of root nuclei. In leaf epidermal cells faint speckles of GFP-derived signals can be observed in the nucleolar area, but much weaker than compared to 3xHMG-box1-GFP-NLS. In mitotic cells, 3xHMG-box2-GFP-NLS associates with condensed chromosomes in a general fashion as well (Figure 22C, middle row, upper panel). Interestingly, in some root tip cells of plant lines that express 3xHMG-box2-GFP-NLS fusion proteins, no GFP-derived signal can be observed. These cells have small nuclei that are likely to be formed shortly after mitosis, underpinning an active degradation process at the end of cytokinesis.

3.4.3 Phenotypical consequences of 3xHMG-box-GFP-NLS expression during interphase

Three independent plant lines each, which are homozygous for the constructs that drive the constitutive expression of 3xHMG-box1-GFP-NLS, 3xHMG-box2-GFP-NLS and GFP-NLS were tested for growth defects. Different growth parameters under long day conditions, flowers, siliques and pollen were analyzed as well as the root division zone and number of leaf palisade parenchyma cells.

When growth parameters of plants that overexpress 3xHMG-box1-GFP-NLS, 3xHMG-box2-GFP-NLS and GFP-NLS are compared with wild type (Col-0), only the lines overexpressing 3xHMG-box1 show clear alterations in the habitus (Figure 23A). Multiple alterations in growth like reduced plant height, smaller rosetta diameter and

leaf number can be measured reproducibly in these lines (Figure 23C). Furthermore these three lines show a slightly earlier bolting time and two of the three lines an earlier flowering time compared to wild type.

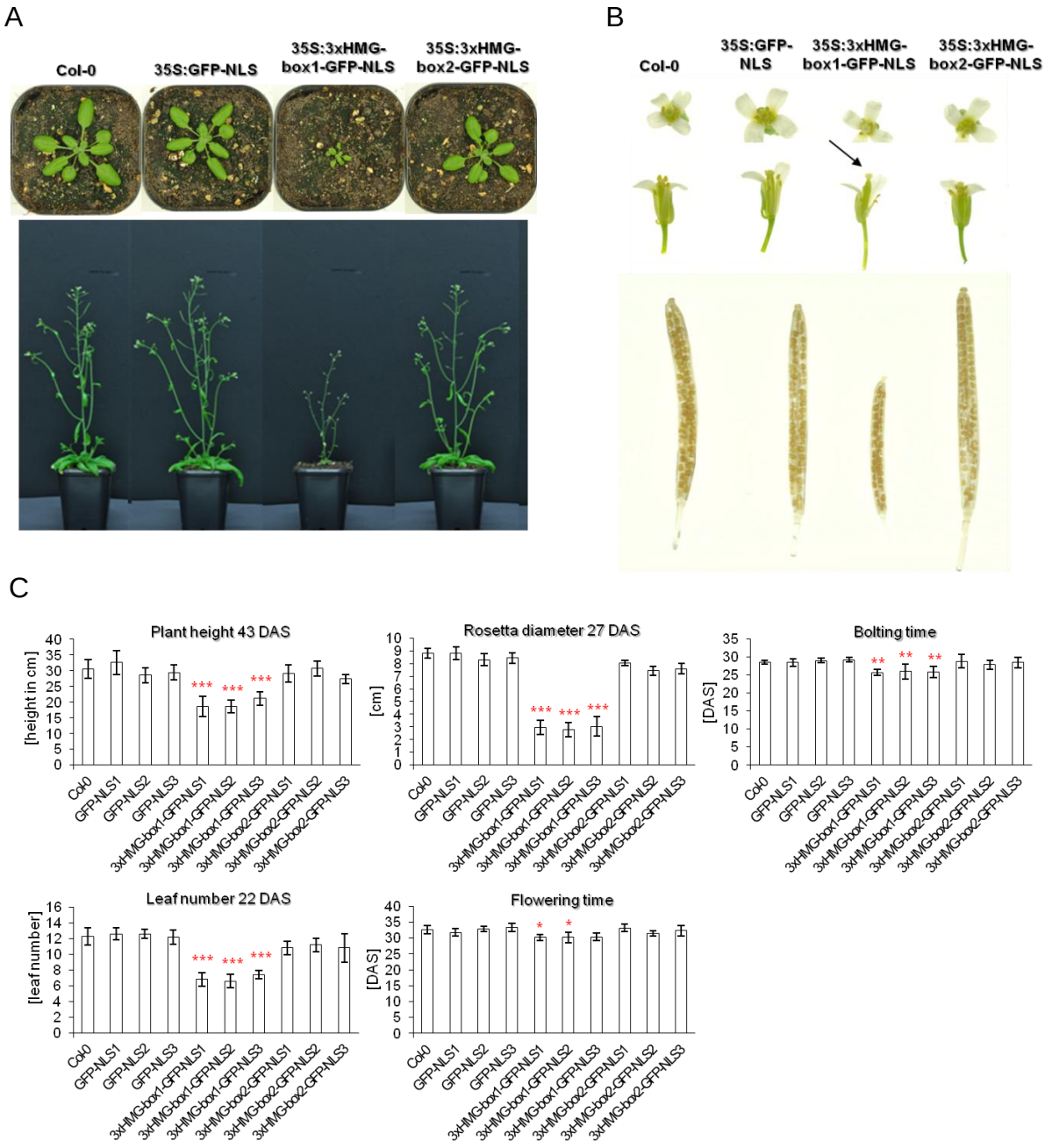

Figure 23. Phenotype of *Arabidopsis thaliana* plant lines overexpressing 3xHMG-box1-GFP-NLS, 3xHMG-box2-GFP-NLS and GFP-NLS compared to wild type (Col-0). (A) Upper panel shows photographs of *Arabidopsis thaliana* Col-0 and plant lines homozygous for the vector constructs pL8, pM9 and pM10 at 22DAS grown under long day conditions. Lower panel shows same plants at 40DAS **(B)** Flowers and siliques of Col-0 and plants homozygous for constructs pL8, pM9 and pM10 **(C)** Comparison of growth parameters from at least 7 plants per independent line and 10 plants of Col-0 using one-way Anova statistical analyses (*p<0.05, **p<0.01, ***p<0.001).

Flowers and siliques of all tested plants show a normal appearance, except plants that express 3xHMG-box1-GFP-NLS (Figure 23B). Constitutive expression of 3xHMG-box1-GFP-NLS leads to a reduced size of siliques. Regardless of their size, siliques of this mutant apparently do not contain an elevated number of non developing ovules. Flowers of plants overexpressing 3xHMG-box1-GFP-NLS look relatively normal except the pistils, which are slightly elongated relative to the rest of the flowers (Figure 23B, arrow). Additionally less pollen are attached to the stigmata of these plants. Stigmata of independent plants lines that overexpress 3xHMG-box1-GFP-NLS were pollinated with pollen derived from the anthers of the same flower.

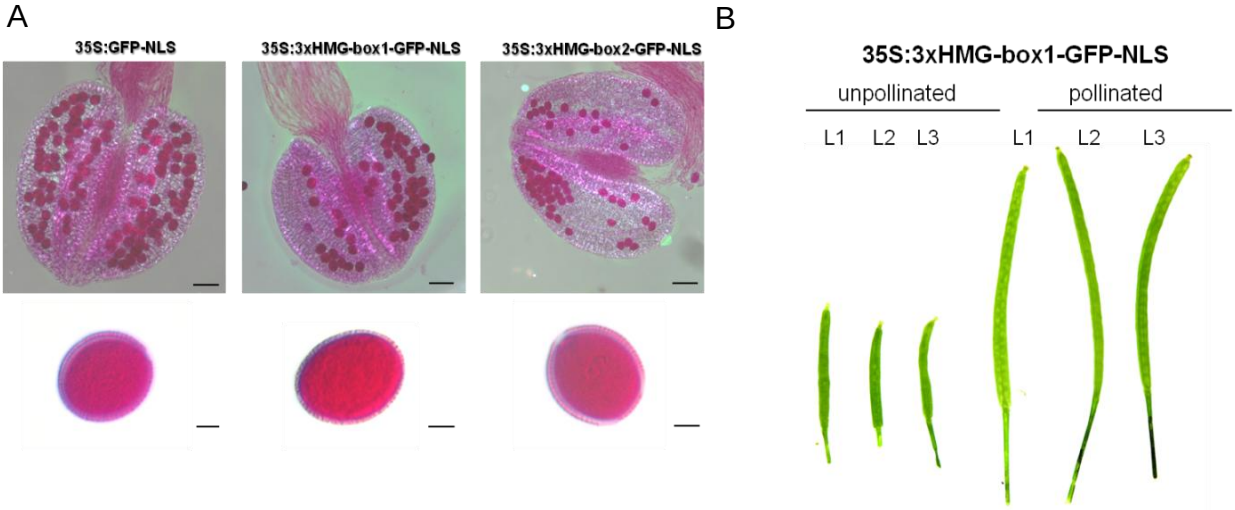

Figure 24. Pollen viability in *Arabidopsis thaliana* plant lines homozygous for pL8, pM9 and pM10 and self pollination of plants that overexpress 3xHMG-box1-GFP-NLS. (A) Alexander stain of anthers and pollen respectively**.** Viable pollen show a red staining. **(B)** Pistils of plants that are homomzygous for pM9 (overexpressing 3xHMG-box1-GFP-NLS) were pollinated with pollen derived from anthers of the same flower. Siliques of three independent lines (L1-3) that emerged of unpollinated or self pollinated pistils are shown.

Hand-pollinated pistils of these plants develop into siliques with a normal size (Figure 24B). Furthermore pollen of 3xHMG-box1-GFP-NLS, 3xHMG-box2-GFP-NLS and GFP-NLS overexpression plants were tested for viability using Alexander staining indicating that pollen viability in these plants is not affected (Figure 24A). Taken together the results of Alexander staining and hand-pollination suggest that reduced silique size in plants that overexpress 3xHMG-box1-GFP-NLS is due to steric hindrance of pistils to become pollinated by the anthers of the same flower. Plants that constitutively express 3xHMG-box-GFP-NLS fusion proteins were also analyzed

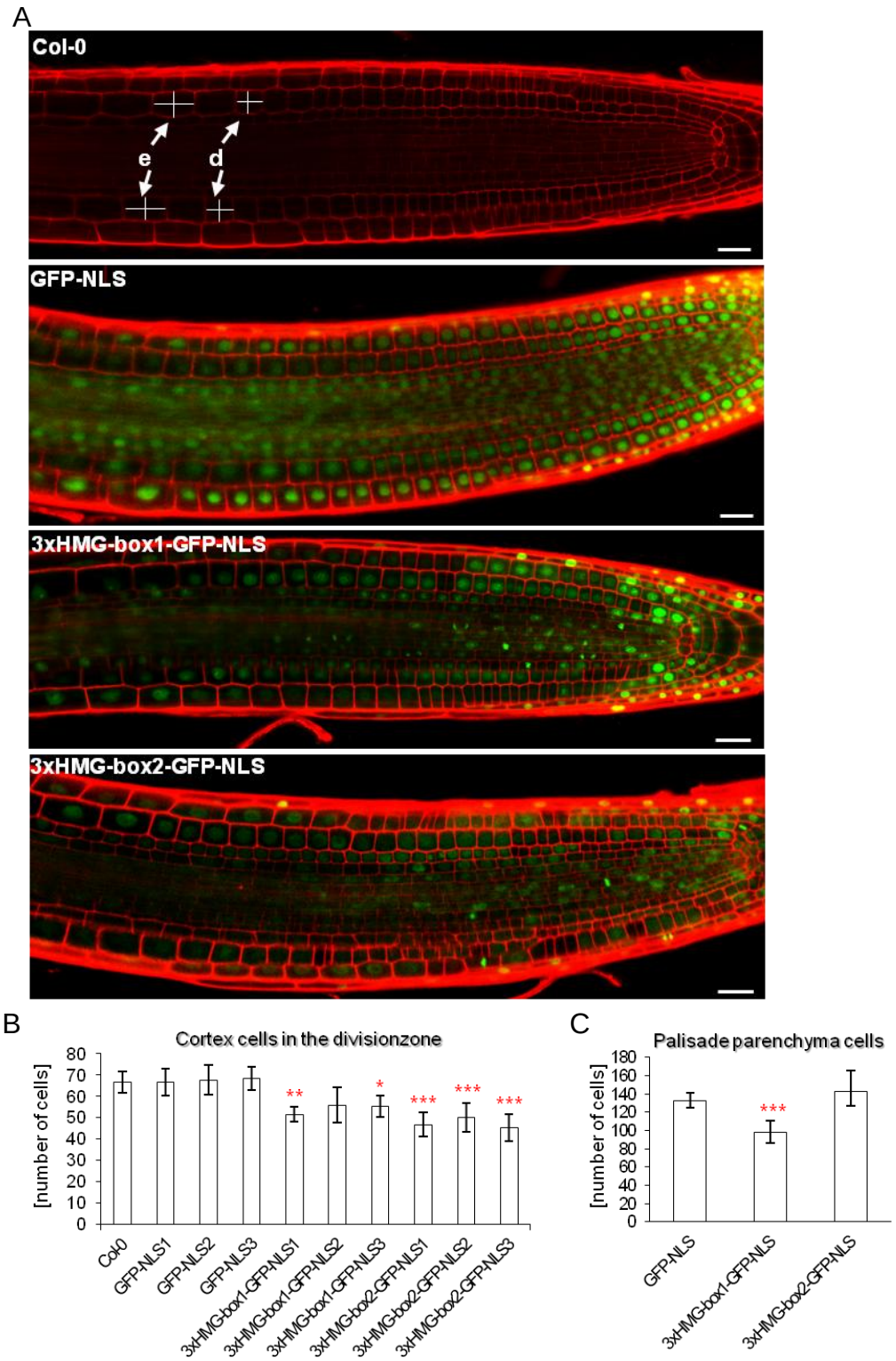

Figure 25. Cell number in the division zone of roots and palisade parenchyma of leaves from *Arabidopsis thaliana* plants lines homozygous for pL8, pM9 and pM10 and Col-0. (A) Roots of plants 5 DAS were stained with propidium iodide (red) and applied to CLSM. Cortex cells that emerge from the quiescent center which are broader than long were assigned to cells in the zone of active cell division (d) and cortex cells which are longer than broad are assigned to cells of the zone of cell elongation (e). GFP-derived fluorescent signal is shown in green. Scale bar indicates 20 µm.
Statistical comparison of **(B)** outer cortex cells in root tips assigned to the division zone (both sides) and **(C)** palisade parenchyma cells in one leaf section (as shown in Supplemental Figure 5), using one-way Anova. At least 6 roots per plant line and 10 roots for Col-0 as well as three leaves of each line, which were pooled according to the construct used for transformation, were used for evaluation. (*p<0.05, **p<0.01, ***p<0.001).

for number of cortex cells in the division zone of the root tip and the palisade parenchyma cells in leaves (Figure 25A, Supplemental Figure 5). Indeed, for two independent plant lines which constitutively express 3xHMG-box1-GFP-NLS and three independent plant lines which constitutively express 3xHMG-box2-GFP-NLS a significantly reduced number of outer endodermal cortex cells in the division zone was determined (Figure 25B). This difference can't be the reason for, or directly connected to the growth defect of 3xHMG-box1-GFP-NLS overexpressing plants as 3xHMG-box2-GFP-NLS plants show a normal development. Palisade parenchyma cells across the leaf blade of the first leaf of the second emerging leaf pair from independent plant lines that are homozygous for pL8, pM9 and pM10 were counted and compared. Only in plants overexpressing 3xHMG-box1-GFP-NLS, the number of palisade parenchyma cells is reduced compared to the control (35S:GFP-NLS). In line with that, leaves of these mutants are obviously smaller.

3.4.4 Analysis of nucleoli, 45S rDNA regions and 45S rDNA transcript level in overexpression lines

As only overexpression of 3xHMG-box1-GFP-NLS leads to severe phenotypical alterations and 3xHMG-box1 was shown to exhibit specificity for 45S rDNA regions, effects may be correlated to 45S rDNA were further investigated.

The different overexpression lines were subjected to immunostaining and FISH to check appearance of nucleoli using fibrillarin antibodies and rDNA regions using *A. thaliana* specific 45S rDNA probes. Fibrillarin is a protein taking part in multiple aspects of RNA biogenesis and represents a major component of the fibrillar regions of the nucleolus (Eichler and Craig 1994). Therefore, an antibody was used to monitor a change in nucleolar appearance that could be assigned to 3xHMG-box1-GFP-NLS overexpression. As can be seen in Figure 26A, nucleolar shape in root tip cells of 3xHMG-box1-GFP-NLS and 3xHMG-box2-GFP-NLS overexpression lines doesn't show any diversification in size, number or form when compared to GFP-NLS overexpression lines. Also no obvious change in rDNA organization like strong compaction or dispersion could be observed in 3xHMG-box-GFP-NLS overexpression lines (Figure 26B).

To test if growth defects in plant lines that constitutively express 3xHMG-box1-GFP-NLS are due to a change in 45S rDNA transcription or processing, 45S rDNA

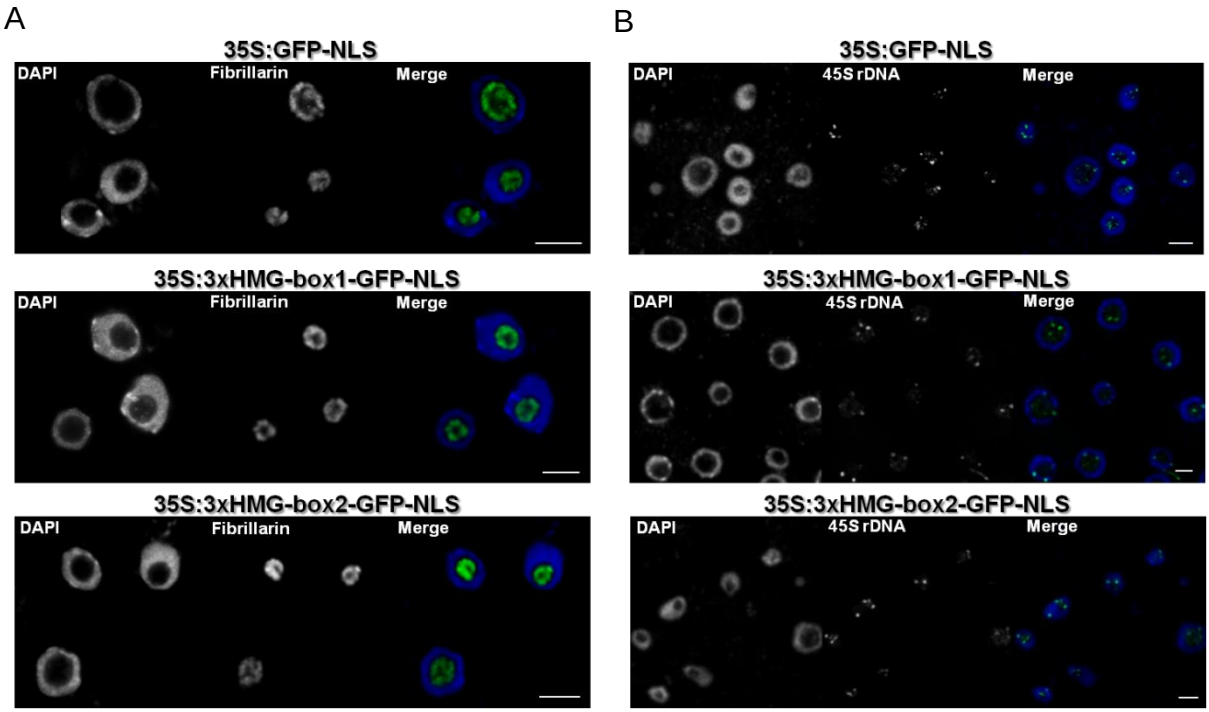

Figure 26. Immunostaining and FISH with root tip cells of overexpression lines. (A) Roots of plants 4 DAS were subjected to immunostaining using antibodies raised against fibrillarin (green). DAPI (blue) was used to stain DNA. Scale bar indicates 5 µm **(B)** Roots of plants 4DAS were subjected to FISH using specific DNA probes generated from a part of the intergenic spacer (IGS) of the *A. thaliana* 45S region (green). DAPI (blue) was used to stain DNA. Scale bar indicates 5 µm.

transcript levels in the different overexpression lines and in the *3xhmg-box1* plants 11DAS were analyzed by semi quantitative RT PCR and Northern blot. Different areas of the 45S rDNA transcribed region and reference genes from Col-0, *3xhmg-box1* and two independent that constitutively express either GFP-NLS, 3xHMG-box1-GFP-NLS or 3xHMG-box2-GFP-NLS were analyzed by semi quantitative RT PCR (Figure 27B). PCR cycles were optimized to not reach saturation of the reaction. No differences in the signal strength of PCR fragments amplified from 45S rDNA regions could be detected. This is to expect because RNA used for cDNA synthesis has to be normalized and as the majority of RNA is composed of rRNA, 45S rRNA amounts should be relatively equal in all samples. Nonetheless, when parts of the coding regions of *Actin8* and *Ubiquitin5* were amplified from cDNA derived from the analyzed plant lines, also no difference in intensity of the PCR fragments could be observed. This leads to the conclusion, that the rDNA transcript level is not affected in 3xHMG-box1-GFP-NLS overexpressing plants. Northern blot was chosen as an additional approach to compare transcript level in different plant lines. Furthermore as a probe binding to the 5' external transcribed spacer was used, possible alterations in the

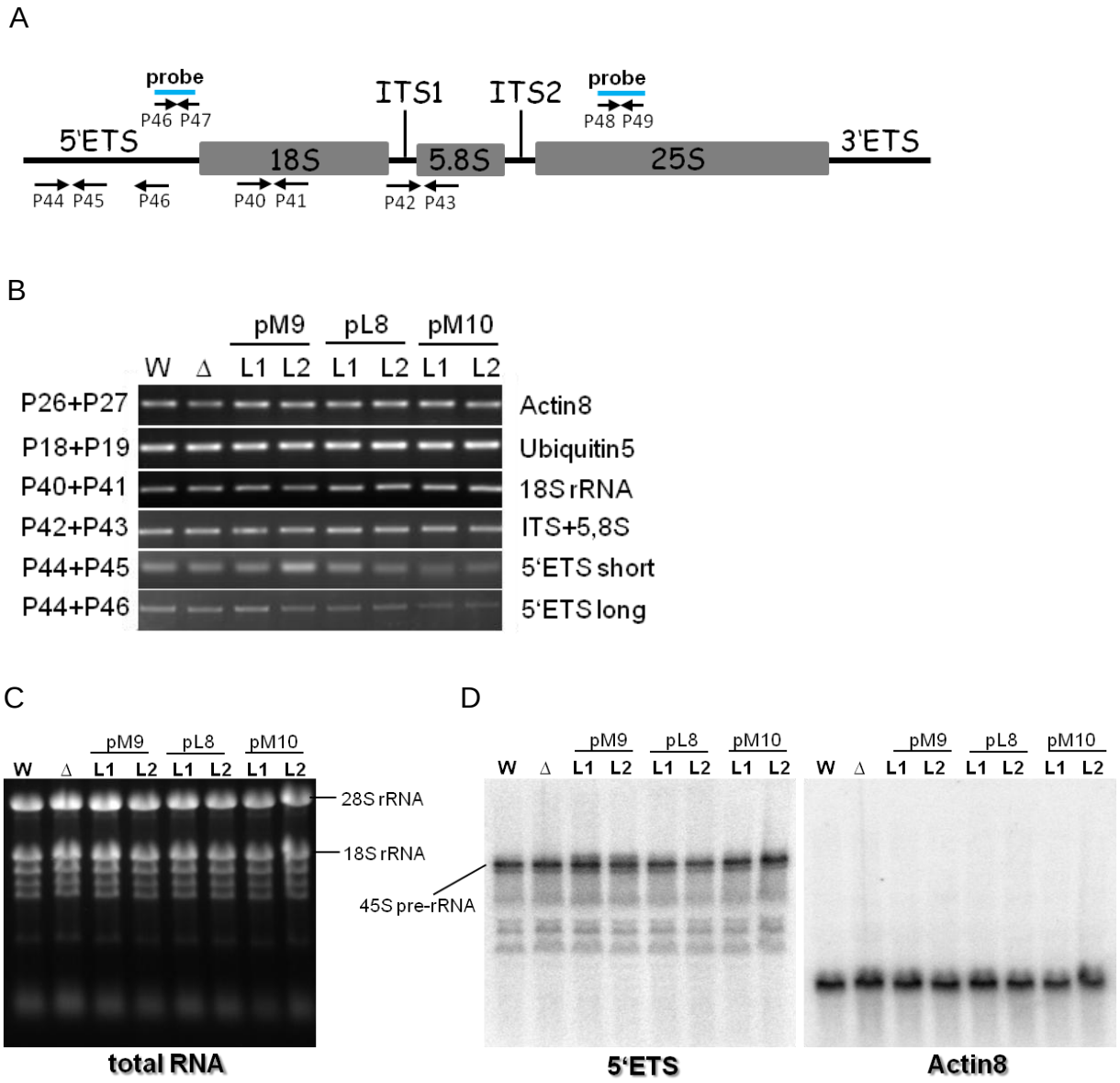

Figure 27. Transcript level and processing of 45S rDNA in knock-out and overexpression lines. **(A)** Schematic representation of *A. thaliana* 45S rDNA region with 5' and 3' external transcribed spacer (ETS) and internal transcribed spacer (ITS). Primer (P) and probes that were used for PCR or Northern and Southern blot analysis respectively are indicated. **(B)** Semi quantitative RT PCR of different 45 rDNA regions and reference genes. cDNA was extracted from wild type (W), *3xhmg-box1*(Δ), and two independent lines (L) homozygous for constructs pL8 (35S:GFP-NLS), pM9 (35S:3xHMG-box1-GFP-NLS) and pM10 (35S:3xHMG-box2-GFP-NLS and used for amplification with designated primer pairs. **(C)** RNA extracted from wild type (Col-0), *3xhmg-box1,* and independent plant lines (L) homomzygous for the constructs pL8 (35S:GFP-NLS), pM9 (35S:3xHMG-box1-GFP-NLS) or pM10 (35S:3xHMG-box2-GFP-NLS) was separated in a TBE agarose gel and stained with EtBr. **(D)** Separated RNA was transferred on a nitro cellulose membrane and labeled with radioactive DNA probes that hybridize specifically with the 5'ETS region of 45S rDNA or actin8.

pattern of processed 45S rDNA can be surveyed. Here as well, RNA used for blotting was measured by Nanodrop and total amounts were adjusted. As rRNA makes the biggest portion of RNA in growing cells, it is not surprising that 18S and 28S rRNA amounts appear to be relatively equal in all tested samples (Figure 27C). Also the

signal intensities of 45S are comparable in all tested lines (Figure 27D). Besides, the pattern of processed 45S rDNA fractions doesn't show any alterations. As the signal intensity for Actin8 is also relatively equal in all tested samples, it can be deduced that rDNA transcript level is not impaired in any of the analyzed plants lines.

3.4.5 Investigation of the 45S rDNA compaction state in 3xHMG-box-GFP-NLS overexpression lines

To test if 45S rDNA regions in the 3xHMG-box1-GFP-NLS overexpression lines are altered in compaction state, a MNase digestion combined with Southern blot assay was performed. First, nuclei were extracted from leaf tissue of plant lines constitutively expressing GFP-NLS, 3xHMG-box-GFP-NLS1 or 3xHMG-box2-GFP-NLS respectively and MNase was added to the nuclei solutions and incubated for different time intervals. MNase cuts DNA preferentially at linker DNA between nucleosomes and depending on time and enzyme concentration chromatin is degraded to varying fractions of mononucleosomes, dinucleosomes, trinucleosomes and so forth (Hewish and Burgoyne 1973). Compaction state of chromatin should influence the accessibility for MNase enzyme and thus lead to alterations in degradation kinetics. Overexpression of 3xHMG-box-GFP-NLS proteins seems not to alter the general compaction grade of nuclear chromatin as degradation kinetics are comparable between the different overexpression lines (Figure 28A). After 30 s, nuclear chromatin has already started to be degraded and after 10 min most of the chromatin is composed of mononucleosomes. Separated MNase digests were subjected to southern blot to be able to specifically monitor degradation kinetics in 45S rDNA chromatin regions (Figure 28B). Resulting 45S rDNA nucleosome fractions were then quantified to be able to directly compare degradation of chromatin in nuclei of respective overexpression lines at given time points (Figure 28C). 3xHMG-box1-GFP-NLS overexpression does not lead to an altered degradation of nuclear chromatin as formation of smaller nucleosome fractions happens as fast as with chromatin of 3xHMG-box2-GFP-NLS overexpression lines and GFP-NLS overexpression lines. Only the portion of non-degraded chromatin seems to be stable for a slightly longer time in control lines that overexpress GFP-NLS. MNase approach doesn't proof any alteration in compaction state of chromatin in 3xHMG-box1-GFP-NLS or 3xHMG-box2-GFP-NLS overexpressing plants. However, minor changes in chromatin structure are presumably not detectable by using this method.

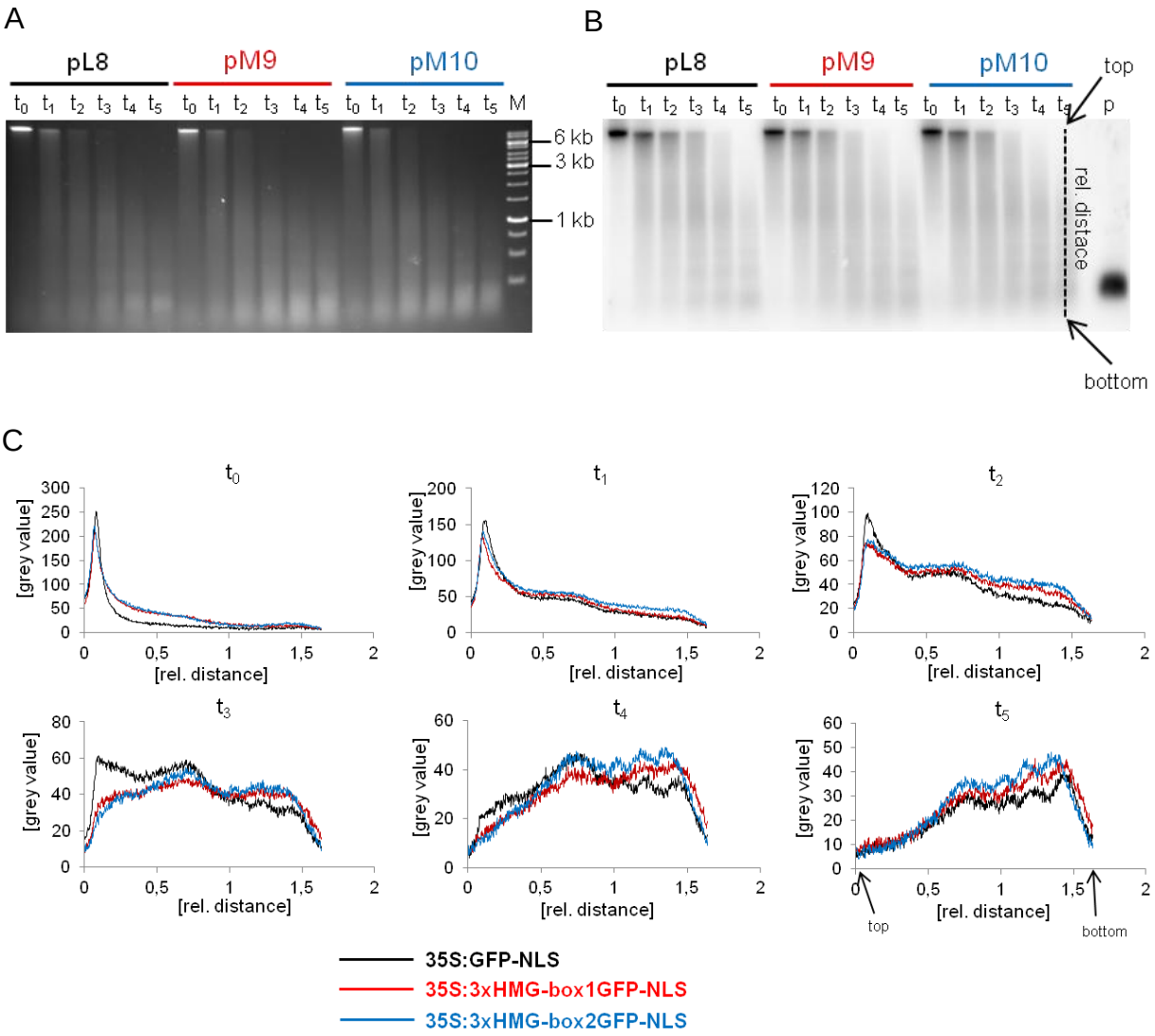

Figure 28. MNase accessibility of leaf nuclei chromatin combined with southern blot in order to test compaction state of rDNA in different overexpression mutants. (A) Nuclei were extracted from plants homomzygous for the constructs pL8 (35S:GFP-NLS), pM9 (35S:3xHMG-box1-GFP-NLS) or pM10 (35S:3xHMG-box2-GFP-NLS) 15 DAS and digested at 37°C with 0.1 U MNase for 30 s (t_1), 1 min (t_2), 2 min (t_3), 4min (t_4) and 10min (t_5) or incubated without MNase for 11min (t_0). After digest, DNA was extracted and subjected to agarose gel electrophoresis and stained with EtBr after seperation. **(B)** Separated DNA was transferred on a nitro cellulose membrane and hybridized with a radioactive probe (p) specific for 25S rDNA (Figure 27A). Radioactive signals were detected using a phosphor storage screen and a phosphor imager. Resulting 8 bit picture was used for lane scan based quantification. **(C)** Quantification of signal intensities using Image J. At each time point (t) grey values were measured along a lane as exemplified in B and blotted against the relative distance of the scanned lane using the indicated colors for the respective overexpression line.

3.5 Contribution of different domains of 3xHMG-box1 to rDNA specificity

3.5.1 Construction of reporter constructs for different truncated versions of 3xHMG-box1-GFP-NLS

To test if a certain part of 3xHMG-box1 mediates specificity for NOR association, truncated versions of 3xHMG-box1-GFP-NLS (Figure 29A) were expressed under the control of the 35S promoter in *A. thaliana*. Coding sequences of the N-terminal basic region, every single HMG-box and possible combinations of these domains when adjacent were amplified and cloned into pGreen0229 containing a 35S expression cassette and the coding sequence for a GFP with nuclear localisation sequence (pL8) giving rise to plasmids pM11-pM19 (Figure 29A). *A. thaliana* was transformed with these plasmids by Agrobacterium mediated transformation and positive selected plant lines were confirmed by PCR-based genotyping (Supplemental Figure 6). Three independent plant lines for each construct were chosen for further analysis. All tested lines show a GFP-derived signal in interphase nuclei (Figure 29B). Strikingly, in most of the tested lines GFP derived signal is higher in the nucleolus, when compared to the nucleoplasm. The higher intensity of GFP-derived signal in the nucleolus is unlikely due to the GFP-NLS component of the fusion proteins as GFP-NLS alone is relatively equal distributed within the nucleus. Evidently, all truncated versions which contain the N-terminal basic region show a very strong fluorescent signal in the nucleolus relative to the nucleoplasm. T3-GFP-NLS even shows a subnuclear distribution that is not very different from the distribution of the full length protein. When life cell imaging was performed with root tips of transformed plant lines, an association of T3-GFP-NLS with mitotic chromosomes could be observed throughout all mitotic phases (Figure 29C).

A

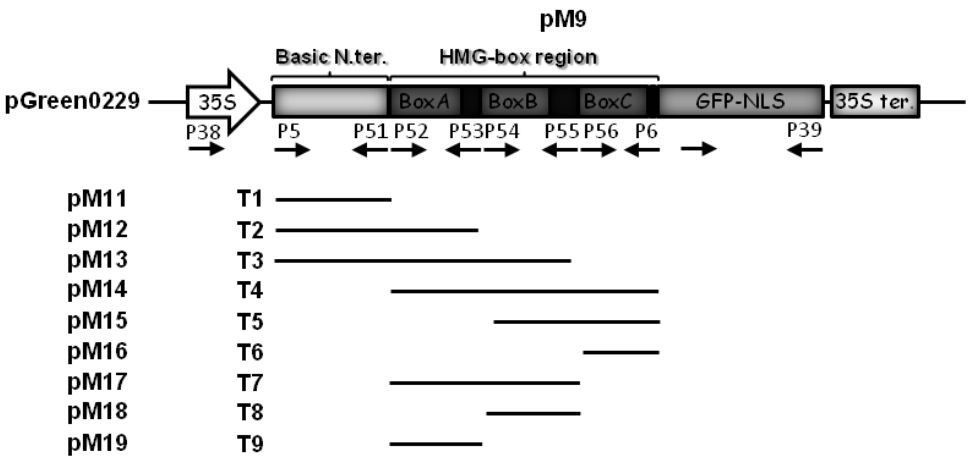

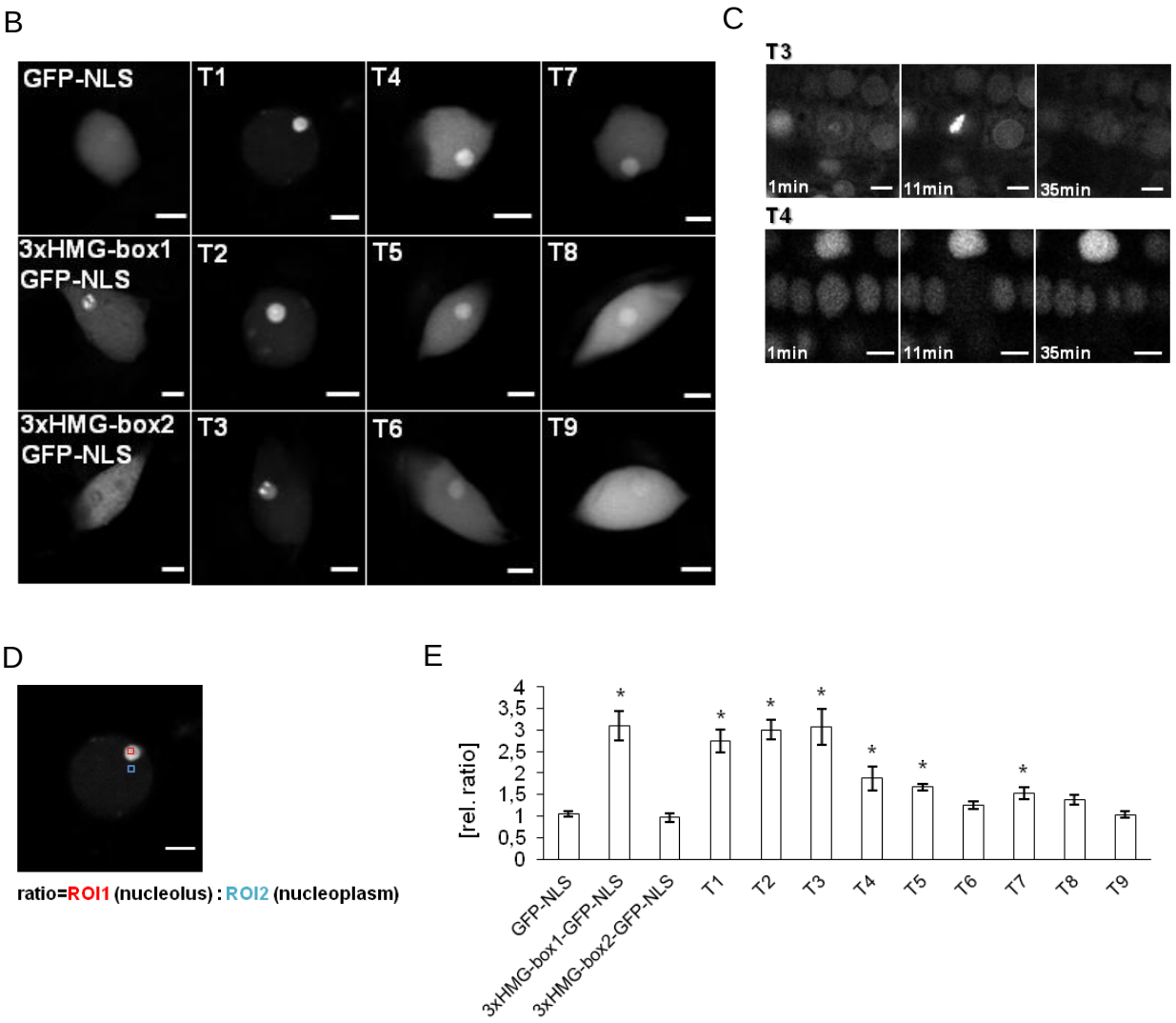

Figure 29. Subnuclear localisation of 3xHMG-box1-GFP-NLS truncated version. (A) Schematic representation of 3xHMG-box1-GFP-NLS in pL8 and truncated protein versions (T1-T9). Single protein domains and primers that were used for cloning and genotyping are indicated. **(B)** Leaves of plants that overexpress GFP-NLS, 3xHMG-box1-GFP-NLS, 3xHMG-box2-GFP-NLS or truncated versions of 3xHMG-box1-GFP-NLS were subjected to CLSM. GFP-derived signal in leaf nuclei is shown. Scale bar indicates 3 µm. **(C)** Sequence of CLSM life cell imaging with mitotic root nuclei of plants that express T3-GFP-NLS or T4-GFP-NLS. Pictures show the GFP-derived signals. Scale bar indicates 5 µm **(D)** Example for the quantification of the relative ratio between nucleolar GFP-derived signal strength and nucleoplasmic GFP-derived signal strength by dividing average gray values in region of interest1 (ROI1) and ROI2 **(E)** Statistical analyses of relative ratios of nucleolar and nucleoplasmic GFP-derived signals in leaf nuclei. Three independent plant lines were analyzed for each construct and at least 5 nuclei per independent plant line were quantified. Datasets were analyzed using one way Anova. Datasets that are marked with asterisk are significantly different from GFP-NLS derived datasets as assessed by Dunnett's multiple comparison test: *P<0,001

This was not the case for T4-GFP-NLS, which is absent during all mitotic phases and reoccurs in the new forming daughter nuclei. The obtained data suggest an important role of the N-terminal region for association of 3xHMG-box proteins with condensed chromosomes during M-phase but also that this domain might facilitate the specificity

of 3xHMG-box1 to 45S rDNA regions. Datasets were quantified by measuring the intensity of GFP-derived signals in the nucleolus and in the nucleoplasm (Figure 29D). The resulting ratios were tested for statistical significant differences when compared to GFP-NLS and illustrated in a graph (Figure 29E). Indeed, all truncated versions that contain the N-terminal domain have ratios that are comparable to the full length protein. Furthermore, all truncated versions that contain at least two adjacent HMG box domains also show a significantly higher accumulation in the nucleolus, when compared to GFP-NLS. Still, accumulation in the nucleolus in all truncated versions that lack the N-terminal domain is less pronounced than compared to the truncated versions that contain the N-terminal region.

3.5.2 Expression of 3xHMG-box chimera with exchanged N-terminal domains

N-terminal domains were exchanged between 3xHMG-box1 and 3xHMG-box2 in order to test a potential function of the N-terminal region for specificity of 3xHMG-box1 to 45S rDNA regions (Figure 30). Therefore, overlapping PCR was used. CDS of the N-terminal region of *3xHMG-box1* and the HMG-box region of *3xHMG-box2* were amplified. In a second step, both PCR fragments were used as template for an overlapping PCR and the resulting DNA fragment was then cloned into pL8 (pGreen0229+35S cassette+GFP-NLS) giving rise to pM20. Vice versa, CDS of the N-terminal region of *3xHMG-box2* and the HMG-box region of *3xHMG-box1* were amplified and used as template for an overlapping PCR. Resulting DNA fragment was then cloned in pL8 giving rise to pM21.

Col-0 plants were transformed with pM20 or pM21 by *Agrobacterium*-mediated transformation and three independent plant lines that were confirmed by PCR-based genotyping to carry respective constructs (Supplemental Figure 7), were chosen for further analyses.

Leaves of plants that express either Hybrid1-GFP-NLS or Hybrid2-GFP-NLS were subjected to CLSM. Hybrid1-GFP-NLS which contains the N-terminal region of 3xHMG-box1 seems to accumulate, in contrast to 3xHMG-box2-GFP-NLS, in form of distinct foci in the nucleolus. Nevertheless, Hybrid2-GFP-NLS, which contains the N-terminal domain of 3xHMG-box2, also can be found enriched in distinct foci within the nucleolus. Nuclei of plants that express chimeric 3xHMG-box-GFP-NLS proteins were analyzed with respect to their nucleolar und nucleoplasmatic GFP-derived signal. Both, Hybrid1-GFP-NLS and Hybrid2-GFP-NLS derived signals are

significantly higher in the nucleolus compared to the nucleoplasm when related to GFP-NLS. Hybrid2-GFP-NLS derived nucleolus to nucleoplasma signal ratio is even a bit higher in average compared to Hybrid1-GFP-NLS.

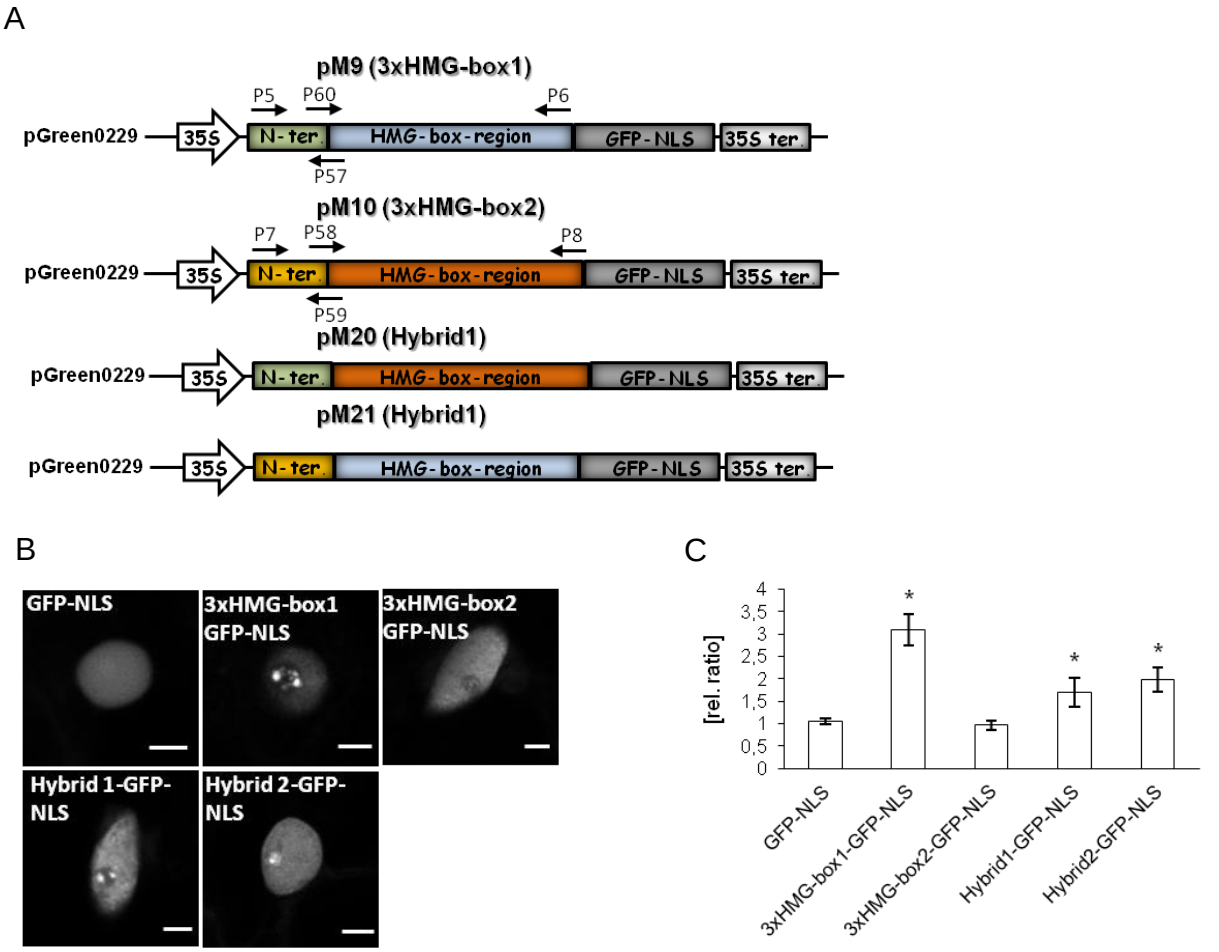

Figure 30. Subnuclear localisation of chimeric 3xHMG-box proteins. (A) Schematic representation of constructs that facilitate expression of chimeric 3xHMG-box proteins. N-terminal region (N-ter.) was exchanged for both 3xHMG-box proteins. Primers that were used for cloning and PCR-based genotyping are indicated **(B)** Leaves of plants that overexpress GFP-NLS, 3xHMG-box1-GFP-NLS, 3xHMG-box2-GFP-NLS, Hybrid1 and Hybrid2 were subjected to CLSM. GFP-derived signal in leaf nuclei is shown. Scale bar indicates 3 µm **(C)** Statistical analysis of relative ratios of nucleolar and nucleoplasmic GFP-derived signals in leaf nuclei. Three independent plant lines were analyzed for each construct and at least 5 nuclei per independent plant line were quantified. Datasets were analyzed using one-way Anova. Datasets that are marked with asterisk are significantly different from GFP-NLS derived datasets as assessed by Dunnett's multiple comparison test: *P<0,001

Taken together, the data partially supports the hypothesis, that the N-terminal region is important for specificity of 3xHMG-box1 to 45S rDNA preference. Still, N-terminal region is apparently not sufficient to completely mediate specificity for 45S rDNA. Thus, the N-terminal domain together with the HMG-box region seems to provide features that facilitate affinity for the 45S rDNA region in a synergistic manner.

3.5.3 Affinity of N-terminal domains to 45S rDNA gene fragments

Gel shift experiments were performed to test affinity of N-terminal domains of 3xHMG-box1 and 3xHMG-box2 to 45S rDNA fragments in order to test a possible sequence specific binding mode. *A.thaliana* 45S rDNA was amplified in three portions by using primer pairs P61/P62, P63/P64, P65/P66 (Figure 31A) and resulting fragments with expected sizes of 2149 bp, 5638 bp and 2743 bp were cloned into pUC19 vector. Fragment 3 doesn't correspond to the expected size, which is due to problems with amplification of this highly repetitive region. For gel shift assay 45S rDNA fragments were cut out of the vector by using flanking restriction sites giving rise to fragments 1, 2 and 3 (Figure 31A). pUC19 vector backbone was used

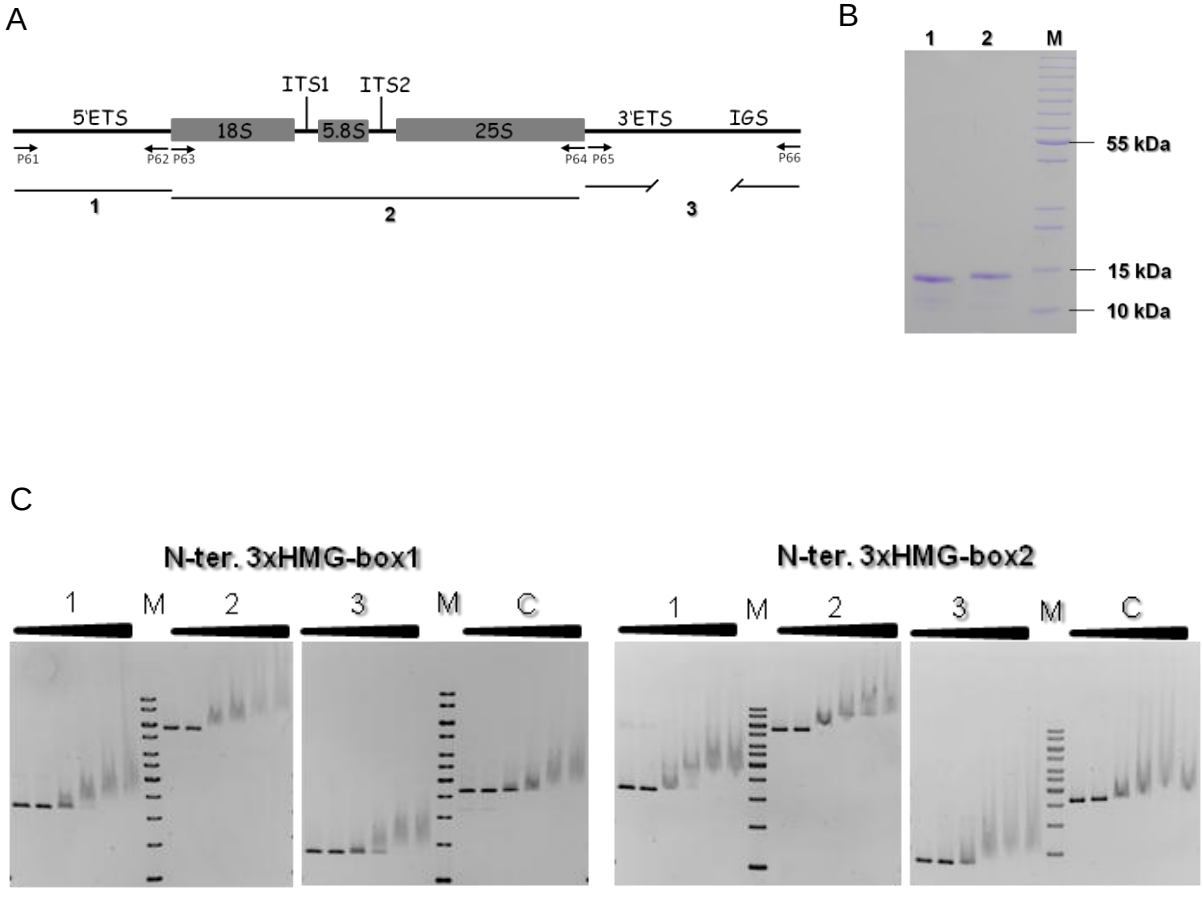

Figure 31. Affinity of the N-terminal regions of 3xHMG-box proteins for 45S rDNA. (A) Schematic representation of *A.thaliana* 45S rDNA region with intergenic spacer (IGS). Primers that were used for cloning are indicated. **(B)** Approximately 500ng of purified 3xHMG-box1 N-terminal peptide (1) and 3xHMG-box2 N-terminal peptide (2) were subjected to SDS PAGE followed by Coomassie staining. **(C)** Agarose gel shift assay with purified N-terminal domains and 45S rDNA fragments (1, 2, 3). 50ng DNA was incubated with increasing concentrations of respective proteins starting from 0 mM, 600mM, 800mM, 1000 mM, 1200 mM. DNA was stained by using EtBr

as control for non-sequence specific DNA binding. N-terminal domains of 3xHMG-box1 and 3xHMG-box2 were recombinantly produced in *E. Coli* M13 with a hexahistidin tag and purified by affinity chromatography. To avoid contaminating proteins, high salt and detergent concentrations of 1 M NaCl and 1.5% (v/v) Triton X-100 were used in the lysis buffer. After elution of His-tagged proteins from Ni-NTA agarose, elution fractions were desalted and applied to SDS-PAGE to check purity and adjust concentrations (Figure 31B).

It was already shown that the N-terminal domain of 3xHMG-box2 is sufficient to bind small linear P^{32}-labeled DNA fragments beginning at concentrations of 400 nM (Pedersen et al. 2011). In this gel shift assay both peptides start to bind DNA at a concentration of 800 nM. The N-terminal region of 3xHMG-box1 as well as the N-terminal region of 3xHMG-box2 binds all fragments with similar affinity. In addition 3xHMG-box1 N-terminal peptide has no higher affinity for 45S rDNA fragments compared to the 3xHMG-box2 N-terminal region. No sequence specific binding of 3xHMG-box1 N-terminal region to 45S rDNA or a specific 45S rDNA region respectively could be demonstrated.

3.6 Association of 3xHMG-box1 with silenced NORs in allotetraploid *Arabidopsis suecica*

As mentioned in 1.3.3 allotetraploid *A. suecica* contains the diploid karyotypes of each, *A. thaliana* and *A. arenosa*. Therefore *A. suecica* possesses NORs of both progenitor species, in which the *A. thaliana* derived NORs are transcriptionally silenced. The *A. suecica* strain (Luca Comai/Sue3) that was used in this study was shown to contain 6 *A. arenosa* derived NORs and 2 A. *thaliana* derived NORs as 2 *A. thaliana* NORs got lost during phylogenesis (Pontes et al. 2003). An interesting question is whether 3xHMG-box1 or rather 3xHMG-box proteins in general preferentially associate with species specific NOR fractions and if a possible association with NORs of a certain species might be explained by its activity state or condensation grade respectively. It could already be shown by structured illumination microscopy (SIM), that chromocenters of mitotic chromosomes of *A. thaliana*, which represent transcriptionally inactive and highly condensed regions, contain less 3xHMG-box proteins (Figure 32, pictures are kindly provided by Dr. Veit Schubert). Therefore, together with anti-3xHMG-box antibodies, antibodies raised against

H3S10ph were used to specifically mark centromeric regions of condensed chromosomes (Houben et al. 2007).

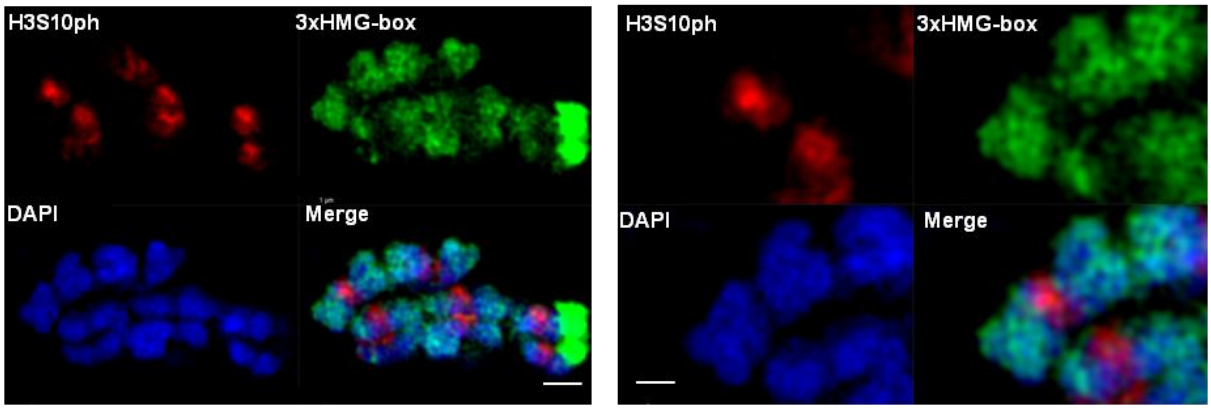

Figure 32. Immunostaining of mitotic chromosomes with chromocenter specific anti H3S10ph antibody and anti 3xHMG-box antibody. Immunostaining of mitotic cells in root tips of *A. thaliana* DAS with an anti H3S10ph antibody (red) and an anti 3xHMG-box antibody (green). DNA was counterstained with DAPI (blue). Pictures were taken by using SIM. Scale bar indicates 1 µm or 0.5 µm for the higher magnification.

Immunocytochemistry (ICC) was combined with FISH assay in order to test if 3xHMG-box proteins are associated with silenced 45S rDNA regions in *Arabidopsis suecica.* The anti 3xHMG- box antibody that was used is able to bind epitopes of both 3xHMG-box proteins, which doesn't allow specific labeling of 3xHMG-box1 in ICC experiments. Several attempts were made to transform *A. suecica* with pM1 (3.1.1) to be able to specifically mark 3xHMG-box1 with anti-GFP antibodies, but no positive selected plants could be obtained. Nonetheless, some chromosome areas that are likely to represent 45S rDNA regions are stained more intense in ICC experiments using anti-3xHMG-box antibody (Pedersen et al. 2011). Indeed, when *A. suecica* seedlings 14 DAS were applied to ICC using anti-3xHMG-box antibody, certain chromosome sectors are labeled more intensely (Figure 33A). To test if these regions first represent NORs and second can be assigned to a species specific NOR fraction, root cells were labeled additionally with probes which hybridize with *A.thaliana* or *A. arenosa* 45S rDNA IGS regions. Probes were generated using Primer pairs P61/P45 and P69/P70. ICC with an anti-3xHMG-box antibody was combined with labeling of *A. thaliana* 45S rDNA IGS (Figure 33B). IGS signals correspond to the by anti 3xHMG-box antibody brighter stained regions. Thus it is very likely that these more intense stained regions are indeed 45S rDNA regions. Additionally to the two *A.thaliana* NORs, also other chromosome areas appear to bind more anti-3xHMG-box antibodies. ICC with an anti 3xHMG-box antibody was also combined with FISH,

using probes that should hybridize either with *A. thaliana* NORs or with *A. arenosa* NORs. As it can be seen in Figure 33C, the probe that was supposed to specifically bind *A. arenosa* NORs, also stains *A. thaliana* NORs. This is probably due to high sequence homologies between the IGS regions of both species. Several attempts were made to establish a specific probe, but without success. Regardless, when mitotic chromosomes were stained with an anti 3xHMG-box antibody and both IGS probes, again chromosome regions that are stained more intense by the antibody

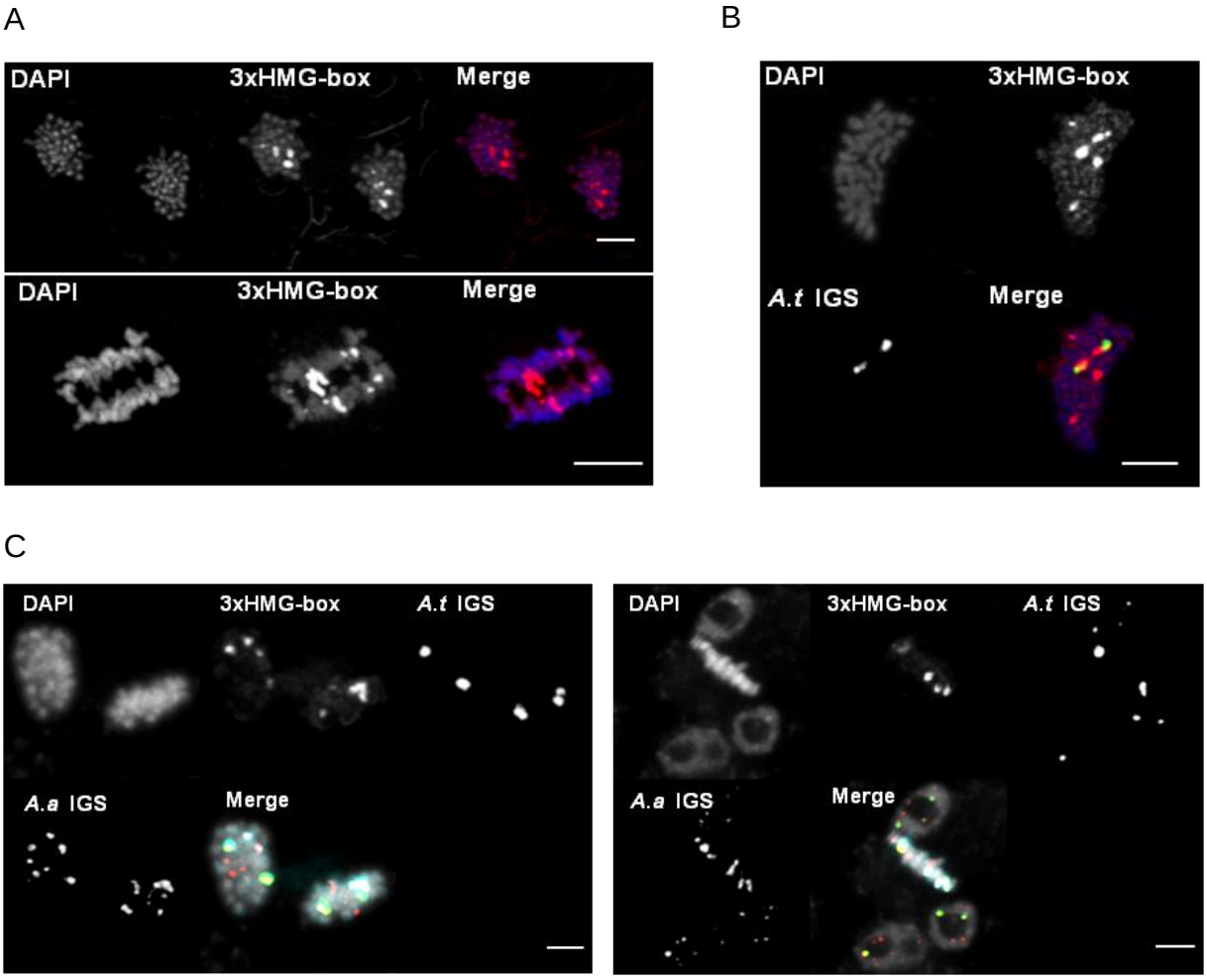

Figure 33. Association of 3xHMG-box proteins with 45S rDNA regions in allotetraploid A. suecica.(A) Immunostaining of mitotic cells in root tips of *A. suecica* 14 DAS with an anti 3xHMG-box antibody. In the merged picture, DAPI is shown in blue and anti-3xHMG-box in red. Scale bar indicates 5 µm. In the upper panel a telophase and in the lower panel an anaphase is shown **(B)** Immunostainig of a mitotic prophase cell in root tips of *A. suecica* 14 DAS with an anti 3xHMG-box antibody was combined with subsequent FISH with probes that hybridize with *A. thaliana* 45S rDNA IGS. Scale bar indicates 5µm. In the merged picture, DAPI is shown in blue and anti-3xHMG-box in red and *A. thaliana* 45S rDNA FISH signals in green. **(C)** Immunostainig of mitotic cells in root tips of *A. suecica* 14 DAS with an anti 3xHMG-box antibody (cyan) was combined with subsequent FISH with probes that hybridize with *A. thaliana* 45S rDNA IGS (green) or *A. arenosa* 45S rDNA IGS (red). In the left panel a telophase and in the right panel a metaphase is shown. Scale bar indicates 5µm

show a colocalization with *A. thaliana* NORs (Figure 33C). Additionally some of the *A. arenosa* NORs are stained more intense with the anti 3xHMG-box antibody.
Data obtained from ICC and subsequent ICC combined with FISH suggest that 3xHMG-box1 or 3xHMG-box proteins respectively are associated with the more condensed transcriptionally silenced *A. thaliana* NORs in *A. suecica*. Additionally anti-3xHMG-box stains more than two NORs more intense. These also more intensed stained regions could be shown to colocalize with some of the *A.arenosa* NORs.

3.7 Subcellular localisation of 3xHMG-box proteins in yeast.

In yeast it was shown that UBF can partially substitute HMO1. Both factors were mentioned in chapter 1.3.3. HMO1 contains one HMG-box, belongs to the rRNA transcription apparatus of yeast and was shown to be localized in the nucleolus (Gadal et al. 2002). UBF contains 6 HMG-boxes and is a component of the rDNA transcription complex in vertebrates. Especially the high number of HMG-boxes, DNA binding properties and association with rDNA suggest possible UBF-like functions of 3xHMG-box1 during mitosis. To test if 3xHMG-box1 shows specificity for rDNA in yeast, yeast strains NOY505 and yR44 which lacks HMO1 were transformed with constructs that mediate expression of GFP-NLS, 3xHMG-box1-GFP-NLS and 3xHMG-box2-GFP-NLS. Constructs were generated by amplifying GFP-NLS CDS, 3xHMG-box1-GFP-NLS CDS and 3xHMG-box2-GFP-NLS CDS with primer pair followed by cloning resulting DNA fragments in pL10 (pWS3638+TEF2 promoter+Cy1 terminator) giving rise to pM26, pM27 and pM28 (Figure 34A).
All *S. cerivisiae* NOY505 that were transformed with either one of the constructs show a GFP-derived fluorescent signal (Figure 34B). Fluorescent signal in cells that express GFP-NLS is absent from the vacuole and distributed relatively equally within the rest of the yeast cell. NOY505 cells that express 3xHMG-box1-GFP-NLS and 3xHMG-box2-NLS show the same distribution but additionally both proteins seem to accumulate in form of one or more dots or cluster respectively. These brighter foci do not necessarily colocalize with DAPI stained DNA regions. Between 3xHMG-box1 and 3xHMG-box2, no clear difference in distribution could be observed.

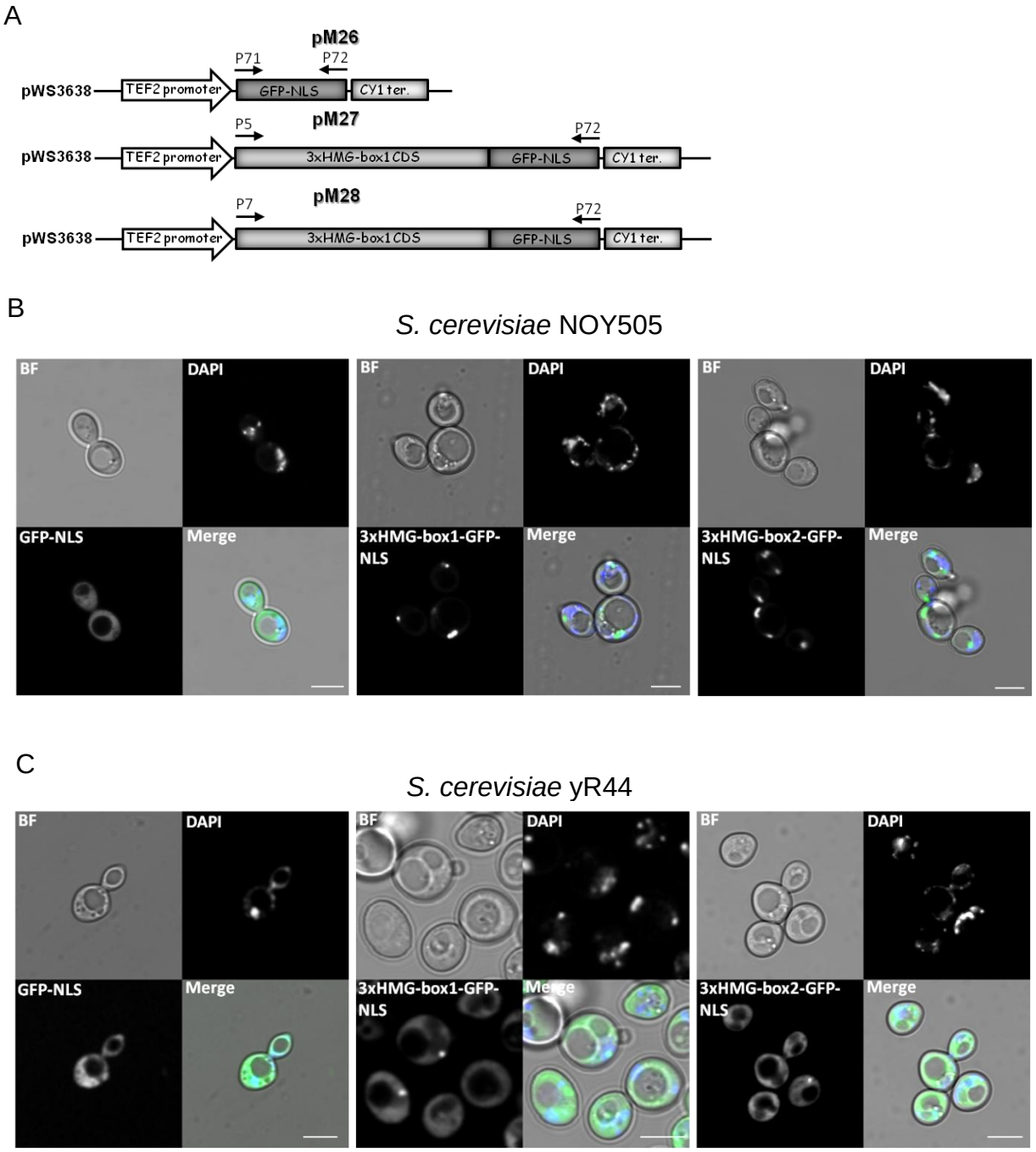

Figure 34. Subcellular localization of 3xHMG-box proteins with 45S in yeast. (A) Schematic representation of vector constructs pM26, pM27 and pM28 which facilitate expression of GFP-NLS, 3xHMG-box1-GFP-NLS and 3xHMG-box2-GFP-NLS in yeast. Plasmids contain the TEF2 promoter and a CYC1 terminator. Primers that were used for cloning are indicated. *S. cerevisiae* strains NOY505 **(B)** or yR44 (Δ*hmo1*) **(C)** which were either transformed with pM26, pM27 or pM28, were subjected to CLSM. In the merged picture, bright-field (BF) picture is shown in grey, DAPI in blue and GFP-derived signals in green. Scale bar indicates 5µm.

When yR44 cells that express GFP-NLS were subjected to CLSM, distribution of GFP-NLS derived signal is indistinguishable from that of NOY505 cells that were transformed with the same construct (Figure 34B). Distribution of 3xHMG-box1-GFP-NLS and 3xHMG-box2-GFP-NLS derived signals differs slightly in yR44. In some of

the cells, the signal is stronger in a small dot-like structure but apart from that relatively equally distributed around the vacuole.

As in none of the yeast strains 3xHMG-box1-GFP-NLS appears to accumulate in nucleolus like structures and as no difference in distribution between 3xHMG-box1-GFP-NLS and 3xHMG-box2-GFP-NLS could be observed, it is unlikely that 3xHMG-box1 displays specificity for rDNA in yeast. Thus no further attempts were made to test if 3xHMG-box1-GFP-NLS can compensate growth defects in yeast strain yR44 that are attributed to the absence of HMO1.

3.8 Effects of overexpression of linker histones with respect to the distribution of 3xHMG-box proteins on mitotic and interphase chromosomes and vice versa.

For several HMG-box containing proteins it could be shown that they share same binding sites with linker histones (1.4.2). Furthermore plant linker histones where suspected to facilitate microtubule nucleation during prophase (1.2.2). It might be possible that 3xHMG-box proteins bind DNA at the same binding sites like linker histones during mitosis. This could lead to a release of a certain fraction of linker histones which then might provide functions in microtubule nucleation (Jerzmanowski and Kotlinski 2011).

To study if 3xHMG-box proteins and linker histones bind chromatin in a correlative manner and if any displacement effects due to overexpression of one of the members of either 3xHMG-box proteins or linker histones occur, several lines that harbour 3xHMG-box-GFP(NLS) and linker histone-RFP reporter constructs or overexpression constructs respectively, were crossed with each other and examined by CLSM. Plant lines that were transformed with constructs, which mediate the expression of linker histone-GFP fusion proteins (Figure 35A) were generated in collaboration with a bachelor student (Holzinger 2012).

First, plants that express 3xHMG-box-GFP fusion proteins under the control of its endogenous promoters were crossed with plants that express H1.1-RFP fusion proteins under the control of its endogenous promoter or H1.1-RFP and H1.2-RFP fusion proteins under the control of the 35S promoter. Crossed plants were verified by PCR based genotyping (Supplemental Figure 8) and subjected to CLSM. 3xHMG-box1-GFP is only associated with chromatin during mitosis and is concentrated at two distinct foci per diploid chromosome set (Figure 35B, left lane). H1.1-RFP and

H1.2 RFP is also associated with chromosomes during mitoses and rather equally distributed among them (Figure 35B, middle lane). To analyze if there is any correlation between 3xHMG-box1-GFP derived signal and H1.1/H1.2-RFP derived signal, grey values of both channels were measured along a lane and profiles were plotted in a graph (Figure 35B).

In mitotic root cells of plants that express 3xHMG-box1-GFP and H1.1-RFP under the control of the endogenous promoters, both fusion proteins seem not to be exclusive. In contrary both profiles rather peak in the same area (Figure 35B, upper graphs). In plants that express H1.1-RFP and H1.2 RFP under the control of the 35S promoter together with 3xHMG-box1-GFP under the control of the endogenous promoter the correlation of the fluorescent signals derived from both fluorophores varies. On some mitotic chromosomes, RFP-and GFP-derived signals seem to be distributed in an antagonistic manner, whereas on others peaks of signal intensities overlap partially or even completely (Figure 35B, middle/lower graphs). In crossed plant lines that express 3xHMG-box2-GFP under the control of the endogeneous promoter together with H1.1-RFP and H1.2-RFP fusion proteins, correlation of signal intensities derived from the different fluorophores shows a variable behaviour as well (Figure 36). For example in the two representative mitotic root cells of a crossed plant line that expresses 3xHMG-box2-GFP under the control of its endogenous promoter and H1.1 under the control of the 35S promoter, signals derived of RFP and GFP show a correlative distribution in one cell, while they show an anti-correlative distribution in the other (Figure 36, middle graphs).

Taken together, 3xHMG-box proteins and linker histones appear not to be exclusive on mitotic chromosomes as in plants that express H1.1-RFP and 3xHMG-box1/2-GFP under the control of its endogeneous promoters, both proteins show a rather overlapping distribution. Also no displacement of 3xHMG-box proteins on mitotic chromosomes due to overexpression of linker histones could be observed.

A

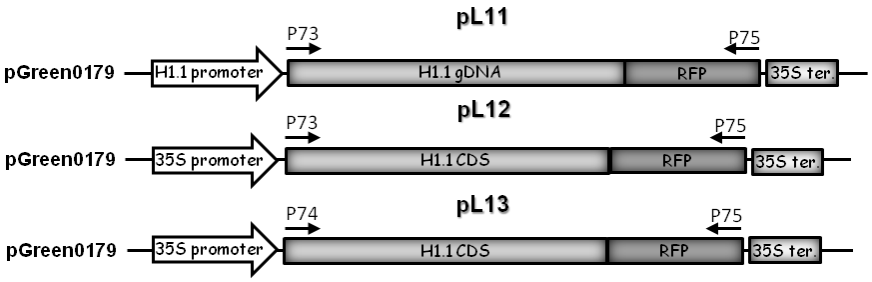

B

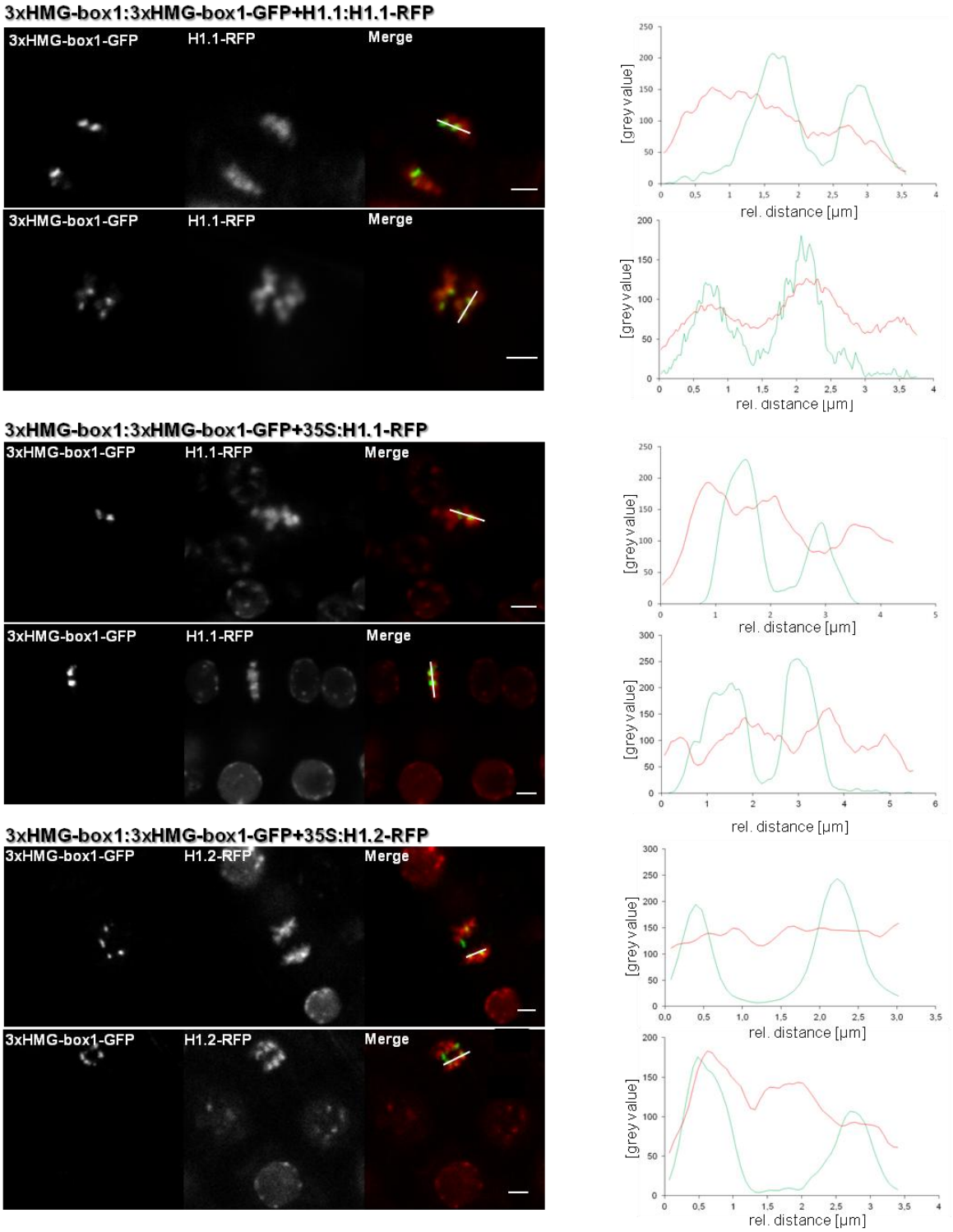

Figure 35. CLSM analysis of mitotic chromosomes in root tips of plants that express 3xHMG-box1-GFP fusion proteins together with either H1.1-RFP or H1.2-RFP fusion proteins. (A) Schematic representation of vector constructs pL11, pL12 and pL13 which facilitate expression of H1.1-RFP under the control of its own promoter or H1.1 and H1.2 respectively under the control of the 35S promoter. Primers that were used for cloning are indicated. (B) Left lane shows CLSM pictures of root tip cells including one cell undergoing mitosis. Left panel shows GFP-derived signal, middle panel shows RFP-derived signal and right panel shows the merged picture of both channels. Grey values (16 bit) of the red and the green channel were measured along a lane and blotted relative to the distance (right lane). Green profile corresponds to intensity of the GFP-derived signal and red profile to the RFP-derived signal.

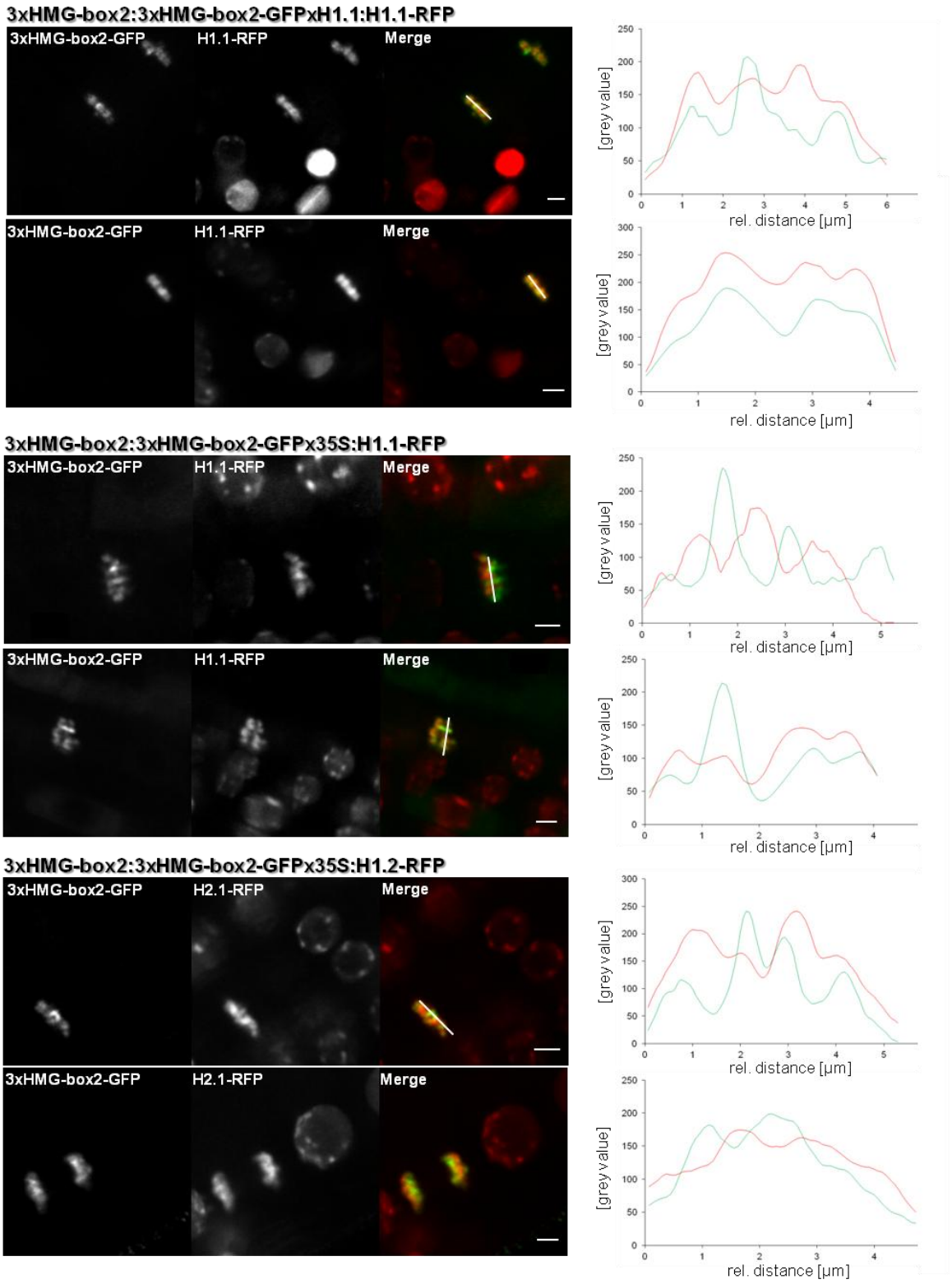

Figure 36. CLSM analysis of mitotic chromosomes in root tips of plants that express either 3xHMG-box1-GFP. Left lane shows CLSM pictures of root tip cells including one cell undergoing mitosis. Left panel shows GFP-derived signal, middle panel shows RFP-derived signal and right panel shows the merged picture of both channels. Grey values (16 bit) of the red and the green channel were measured along a lane and blotted relative to the distance (right lane). Green profile corresponds to intensity of the GFP-derived signal and red profile to the RFP-derived signal.

In plant lines that overexpress 3xHMG-box1-GFP-NLS or 3xHMG-box2-GFP-NLS, no displacement of either H.1.1-RFP or H1.2-RFP on mitotic chromosomes could be observed (Figure 37). Rather, 3xHMG-box1-GFP-NLS and 3xHMG-box2-GFP-NLS derived signals show broad overlapping areas with H1.1-RFP or H1.2-RFP derived signals. Respective crossed lines were also used to study possible displacement processes of linker histones due to overexpression of 3xHMG-box proteins during interphase. In root as well as in leaf cells, no exclusion of linker histones and 3xHMG-box proteins could be observed in the nucleoplasm. 3xHMG-box1-GFP-NLS derived signals concentrate in form of dispersed speckles in nucleoli of interphase root cells.

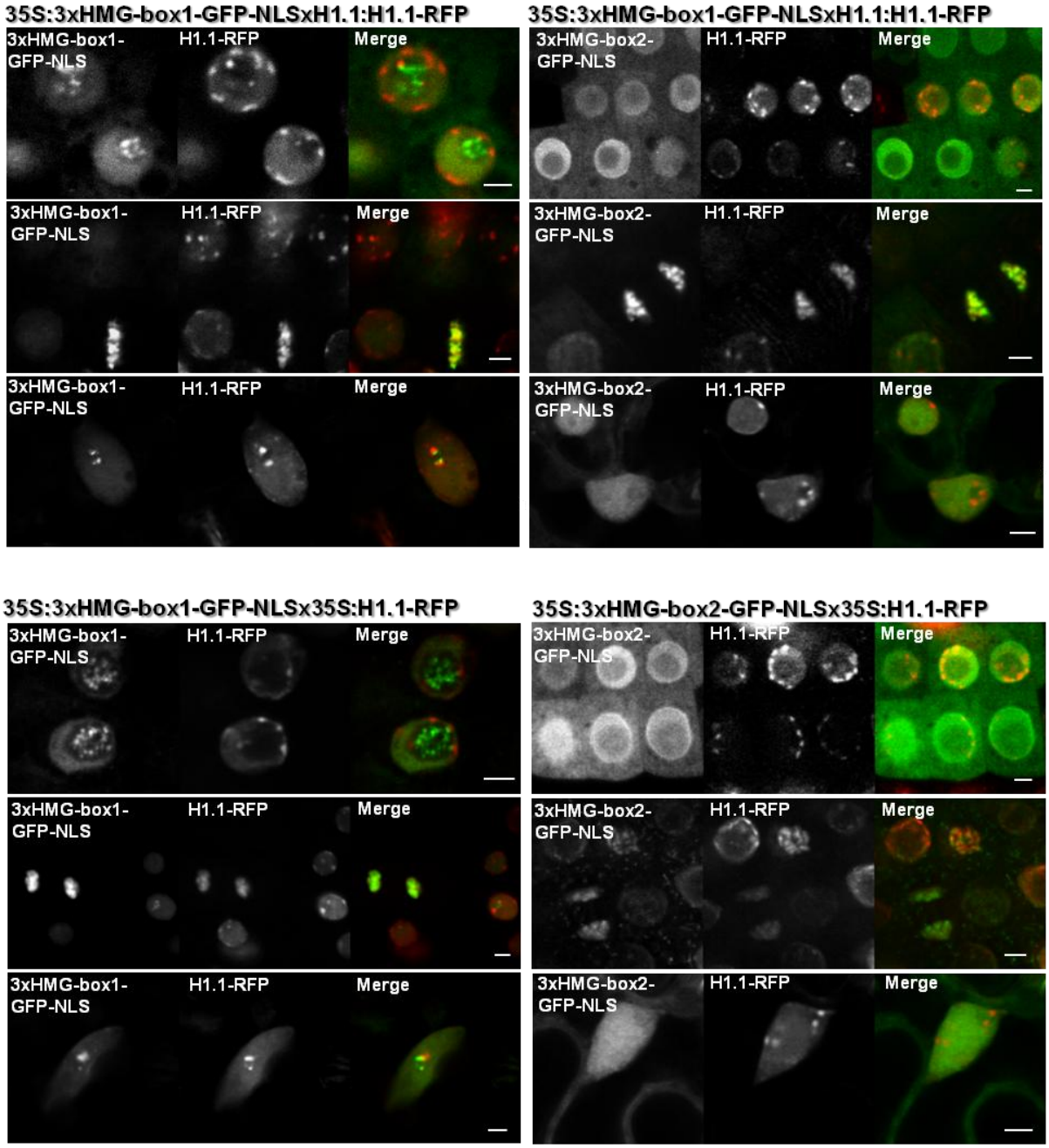

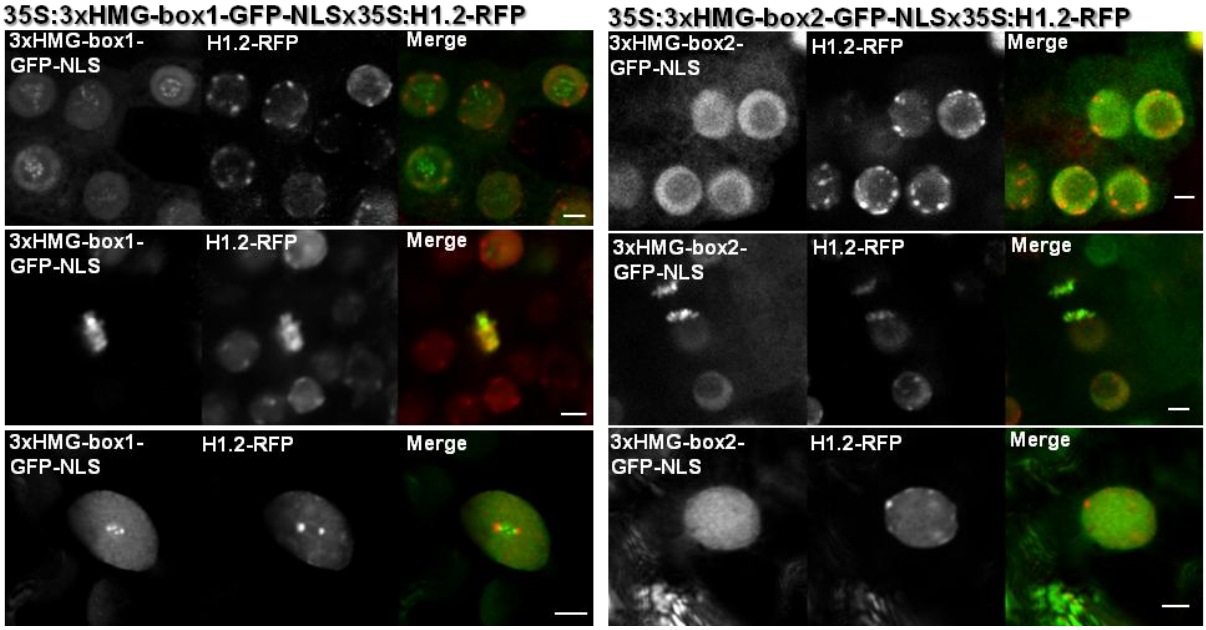

Figure 37. Distribution of 3xHMG-box-GFP-NLS and linker histone-RFP fusion proteins during interphase and mitosis. Plants that overexpress either 3xHMG-box1-GFP-NLS or 3xHMG-box2-GFP-NLS together with H1.1-RFP or H1.2-RFP fusion proteins were subjected to CLSM. For each crossed line, root cells that reside in interphase (upper panel) or mitosis (middle panel) and a leaf cell during interphase (lower panel) are illustrated. GFP-NLS derived signals are depicted in green and RFP derived signals in red. Scale bar indicates 3 µm.

Both, H1.1-RFP, irrespectively if expressed under the control of the 35S or the endogenous promoter, and H1.2-RFP derived signals are less dense in the nucleoli and concentrate in heterochromatic regions (Signals correspond to DAPI staining, Data not shown). Some of the heterochromatic regions can be found at the periphery of the nucleolus. Interestingly, foci of 3xHMG-box1-GFP-NLS derived signal in the nucleolus and H1.1 and H1.2-RFP derived signals at the nucleolar periphery appear to be in close proximity and partially overlapping. This phenomenon can be seen clearest in interphase cells of leaves (Figure 37, left row). 3xHMG-box2-GFP-NLS-derived signal is lower in the nucleus and is equally distributed within the nucleoplasm. No anti correlation of the GFP-NLS and RFP derived signal could be seen at the heterochromatic regions.

Also during interphase, no anti-correlation of 3xHMG-box1/2-GFP-NLS derived signal and H1.1/2-RFP-derived signal could be witnessed. Members of either one of the two protein families show the same distribution regardless if one of the members of the other protein family is overrepresented.

4. Discussion

Major attempt of this work was to assign a molecular function of 3xHMG-box proteins or to indicate an implication in certain cellular processes. In order to narrow down possible roles in cellular processes, functions or features that have been shown for other classes of HMG-box containing proteins were tested for 3xHMG-box proteins. Although no conclusive answer regarding the biological functions of 3xHMG-box proteins was obtained, new interesting features of 3xHMG-box proteins could be revealed *in vitro* and *in vivo* which may contribute to the unveiling of the role of this plant specific group of proteins.

Members of various classes of HMG-box containing proteins were shown to coordinate and facilitate various DNA-dependent nuclear processes like transcription, replication and DNA repair etc. (Malarkey and Churchill 2012). For mammalian HMGB1, functions in extracellular processes like cell migration, tumor invasiveness, neuronal innervations, inflammation and immunity were described as well (Andersson et al. 2002, Lotze and Tracey 2005, Yang et al. 2010).

In plants, no evidence for an extacellular or cytoplasmatic function of HMG-box containing proteins has been provided yet, besides the fact that by photo activation experiments HMGB2 and HMGB4 were shown to be able to shuttle between nucleus and cytoplasm (Pedersen et al. 2010). In their nuclear function as architectural factors involved in modulating nucleosome and chromatin structure as well as influencing participation of other proteins in vital nuclear processes, their specificity can rather be regarded as broad ranged. Nonetheless, implications in certain cellular processes like stress responses (Lildballe et al. 2008), differentiation and proliferation (Hu et al. 2011) as well as maintenance of chromosome ends (Schrumpfova et al. 2011) could be demonstrated for members of the HMGB family.

4.1 Reverse genetic approach to study effects of down regulation of *3xHMG-box* gene expression

One straight-forward approach which was also used to unveil the above mentioned roles of HMGB proteins in plants is the reverse genetics, by which possible functions are deduced from phenotypic and molecular effects resulting from altered gene expression. In model plants sequence-indexed insertion collection provides a large source of potential loss-of-function alleles. For 3xHMG-box1, GK-171F06-013466 line

that contains a T-DNA insertion in the second exon of the coding sequence of the *3xHMG-box1* gene was analyzed. The annotated position of the T-DNA was verified by PCR based genotyping and transcript level was determined by semi quantitative RT-PCR. No transcript for *3xHMG-box1* could be detected in young seedlings of the GK-171F06-013466 T-DNA insertion line and transcript level of *3xHMG-box2* doesn't seem to be affected in these plants. No obvious developmental effects due to the lack of *3xHMG-box1* transcript could be observed. Also examined null alleles for members of the plant HMGB family like *A. thaliana* HMGB1 (Lildballe et al. 2008) or HMGB4, HMGB5 and HMGB6 (Pedersen 2010) show rather minor developmental effects under standard growth conditions, despite their ubiquitous expression pattern (Launholt et al. 2007). Possibly, functional redundancy of 3xHMG-box1 and 3xHMG-box2 might mask phenotypical consequences due to the absence of 3xHMG-box1 in the GK-171F06-013466 T-DNA insertion line. Hence, efforts were made to achieve a knock-out or down regulation of the *3xHMG-box2* gene in the *hmg-box1* background. Therefore hairpin RNA interference (hpRNAi) and artificial micro RNA (amiRNA), two of the most popular methods to reduce gene activity in plants, were chosen. Appropriate vectors were constructed and used for stable transformation of the GK-171F06-013466 T-DNA insertion line. Stable transformants were screened for down-regulation of *3xHMG-box2* expression levels but no reduction in transcript level could be obtained. As micro-RNAs were shown to impair gene expression on the translational level (Pontes et al. 2003) it could not be ruled out, that 3xHMG-box2 protein levels are lower in the tested plant lines. Due to the lack of obvious phenotypical defects and problems with detection of 3xHMG-box protein levels by immunoblot, no further efforts were taken to achieve down-regulation in 3xHMG-box2 expression. Alternatively, other approaches which are based on designer transcription activator-like effector nucleases (TALENs) or clustered regularly interspaced palindromic repeats (CRISPRs) (Mahfouz et al. 2014) could be used in the future in order to study effects of the absence of 3xHMG-box proteins in plant cells.

4.2 Constitutive expression of 3xHMG-box proteins that are fused to GFP or GFP-NLS

Besides the disruption of a gene, induction of constitutive and elevated gene expression is another important tool in the reverse geneticts. Constructs that allow

constitutive expression of 3xHMG-box1-GFP and 3xHMG-box2-GFP fusion proteins in the tobacco cell suspension culture (BY-2) system as well as in stably transformed *A. thaliana,* have already been generated and tested in a previous work (Pedersen et al. 2011). Although, 3xHMG-box2 was shown to have typical HMG-box protein like DNA binding and bending properties, 3xHMG-box1-GFP and 3xHMG-box2 GFP were found to be located in the cytoplasm in the majority of BY-2 and *A. thaliana* root cells when expressed under the control of the strong constitutive 35S promoter. The finding that both fusion proteins appear to associate with chromatin in some of the *A. thaliana* root tip cells was the first evidence that 3xHMG-box proteins might have mitotic functions. In this work, independent plant lines that overexpress 3xHMG-box1-GFP and 3xHMG-box2-GFP were analyzed with regard to developmental defects. Main growth parameters like plant height, rosette diameter, leaf number and flowering time doesn't alter significantly from that of wild type plants. Thus cytoplasmatic appearance and overrepresentation of 3xHMG-box proteins during mitosis don't seem to affect plant development or cell division. In order to import 3xHMG-box proteins into the cell nuclei during interphase, vectors that facilitate the constitutive expression of 3xHMG-box proteins which are fused to GFP with attached nuclear localization signal were constructed and used to generate stably transformed plant lines. Indeed, besides association of 3xHMG-box-GFP-NLS fusion proteins with condensed chromosomes during mitosis, they could be also found in nuclei of cells that resided in interphase. Still, large amounts of 3xHMG-box-GFP-NLS derived fluorescent signals remained in the cytoplasm when compared to the control (only GFP-NLS). This might be due to active export of 3xHMG-box proteins out of the nuclei or slow nuclear import rates relative to synthesis of the proteins. The phenomenon that 3xHMG-box proteins, when fused to GFP, couldn't be detected in nuclei just shortly after mitosis supports the first hypothesis. Expression of 3xHMG-box proteins fused to photoactivatable GFP (Patterson and Lippincott-Schwartz 2002) or photoconvertible fluorescent proteins (Mathur 2007) with attached NLS could be used to test if 3xHMG-box proteins are actively exported from the nucleus. Immunoblot with an anti GFP antibody and extracts of isolated leaf nuclei from plants that express GFP-NLS, 3xHMG-box1-GFP-NLS or 3xHMG-box2-GFP-NLS provides no evidence for degradation. Interestingly, 3xHMG-box proteins that are fused to GFP or GFP-NLS seem to disintegrate shortly after mitosis as no GFP-derived signal could be obtained in post mitotic root cells in respective plant lines. This is not the

case for plants that possess overexpression cassettes for GFP-NLS, ruling out that 35S driven transcription is shut off after mitosis.

Furthermore, subnuclear distribution of 3xHMG-box1-GFP-NLS and 3xHMG-box2-GFP-NLS during interphase differs. Whereas 3xHMG-box2-GFP-NLS appears to be equally distributed in the nucleoplasm apart from the nucleolar region where it is less pronounced, 3xHMG-box1-GFP-NLS derived signal accumulates in form of distinct foci within the nucleolus besides its equally dispersed distribution within the nucleoplasm. It is worth to mention that 3xHMG-box1-GFP-NLS derived foci within the nucleoli are more diffused in nuclei of root cells when compared to the rather compact shape in cotyledons or leaves of young seedlings. Taken together with findings that 3xHMG-box1-GFP fusion proteins associate specifically with NOR regions during mitosis, these results suggest a sustainment of this spatial specificity during interphase. Unfortunately, it could not be proven that 3xHMG-box1-GFP-NLS derived foci resemble 45S rDNA regions. Attempts to show a colocalisation by ICC combined with FISH were not successful. Abrogation of interaction of HMGB proteins with chromatin by cross-linking fixatives in HeLa cells has already been observed before, albeit in context with mitotic chromosomes (Pontes et al. 2003).

Strikingly, *Arabidopsis* histone variant H3.3/HTR4 was shown to display a comparable distribution pattern to 3xHMG-box1-GFP-NLS in epidermal leaf nuclei (Figure 38). This protein is thought to associate with rDNA arrays, as upon inhibition of PolI-directed nucleolar transcription, H3.3/HTR4-GFP derived nucleolar foci

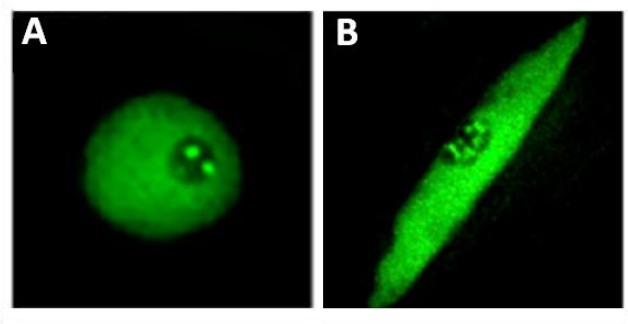

Figure 38. Distinct localization pattern of plant histone H3.3/HTR4. H3/HTR4-GFP in the nucleus of a leaf epidermal cell of stably transformed *A. thaliana* (**A**) or transiently transformed *Nicotiana benthamiana* (**B**). (Shi et al. 2011)

disappear (Shi et al. 2011). Furthermore, it was demonstrated that two amino acid residues in the N-terminal region of H3.3/HTR4 mediate nucleolar distribution of this histone variant. No comparable consensus sequence could be found in 3xHMG-box1.

4.3 Effects of nuclear targeting of 3xHMG-box proteins during interphase

Main growth parameters of plants that constitutively express 3xHMG-box1-GFP-NLS, 3xHMG-box2-GFP-NLS and GFP-NLS as control, were analyzed. 3xHMG-box2-GFP-NLS showed no significant differences in growth parameters, when compared to wild type (Col-0) or plants that overexpress GFP-NLS respectively. In contrast, plants that overexpress 3xHMG-box1-GFP-NLS showed significant alterations in main growth parameters like plant height, rosette diameter, leaf number and bolting time when compared to wild type or plants that overexpress 3xHMG-box2-GFP-NLS. Additionally, siliques of these plants were evidently smaller when compared to the controls, which can be assigned to a steric hindrance of anthers and stigma contact. Pollen viability appeared to be not affected in the tested plant lines. Obviously, pleiotropic effects in plants that constitutively express 3xHMG-box1-GFP-NLS could not be connected to mitotic defects, as plants that constitutively express 3xHMG-box1-GFP did not display these phenotypical peculiarities.

Palisade parenchyma cells and cells in the root division zone were determined to gain information about possible defects in cytokinesis or cell cycle progression. Number of palisade parenchyma cells was significantly lower in 3xHMG-box1-GFP-NLS overexpressing mutants when compared to plants that overexpress GFP-NLS or 3xHMG-box2-GFP-NLS which is in agreement with the finding that leaves are markedly smaller in these mutants. Regarding the number of cells in the zone of active division within root tips, for all three independent lines that overexpress 3xHMG-box2-GFP-NLS, significantly reduced numbers were measured, whereas only in two of the three analyzed lines that constitutively express 3xHMG-box1-GFP-NLS reduced numbers were obtained. Thus, reduced numbers of active dividing cells in root tips do not explain the pleiotropic effect in plant lines that consitutively express 3xHMG-box1-GFP-NLS.

As 3xHMG-box1-GFP-NLS in contrast to 3xHMG-box2-GFP-NLS accumulated in nucleolar foci, cellular and molecular phenotypes were investigated that can be assigned to structural alteration of rDNA regions or defects in rDNA transcription or procession, respectively. An anti-fibrillarin antibody was used in an ICC assay to monitor shape and number of nucleoli in the overexpression lines. No difference could be observed in plants that constitutively express 3xHMG-box1-GFP-NLS. Also number and distribution of rDNA regions in these mutants did not greatly differ in number and extend of dispersion within the nucleolus, when determined by FISH

assays. In the next step, transcript level of 45S rRNA genes was investigated by semi quantitative PCR and northern blot. Both assays did not emphasize any change in 45S rRNA transcript levels in the 3xHMG-box1-GFP-NLS overexpression mutant. Additionally, Northern blot assays could deliver information about effects in 45S rRNA processing. As there was no alteration in the pattern of 5'ETS containing rRNA fragments in independent 3xHMG-box1-GFP-NLS compared to 3xHMG-box2-GFP-NLS overexpressing lines and the controls, processing defects due to over representation of 3xHMG-box1 during interphase seem to be unlikely.

The ability to bend DNA and thus alter functional characteristics of chromatin is a well studied feature of several HMG-box containing proteins. For 3xHMG-box2 it was shown that all three boxes in combination as well as the N-terminal region alone display DNA bending activity (Pedersen et al. 2011). Additionally, the fact that 3xHMG-box proteins are exclusively associated with mitotic chromosomes under normal circumstances, suggests a putative function in condensation processes or maintenance of compacting chromatin structures during mitosis.

MNase accessibility assays were combined with southern blot in order to test the possibility that overexpression of 3xHMG-box-NLS fusion proteins might lead to compaction of chromatin and furthermore compaction of chromatin in the 45S rDNA regions during interphase, which might be a reason for the strong growth defects that can be observed in 3xHMG-box1-GFP-NLS overexpression lines. A similar assay was successfully applied to show implications of mammalian protein Suv4-20h in compaction of chromatin that involves heterochromatic regions (Hahn et al. 2013). Leaf nuclei were isolated from plants that overexpress either GFP-NLS, 3xHMG-box1-GFP-NLS or 3xHMG-box2-GFP-NLS and supplemented with MNase. Depending on the incubation time and constitution of the chromatin, catalytic activity of MNase leads to generation of variable amounts of chromatin fragments of different sizes. For neither 3xHMG-box1-GFP-NLS nor 3xHMG-box2-GFP-NLS derived nuclear chromatin, altered fragmentation kinetics could be observed. Also fragmentation pattern of chromatin which contains 45S rDNA genes in leaf nuclei of 3xHMG-box1-GFP-NLS overexpressing plants was comparable to that of the control. Hence, accessibility of chromatin or chromatin regions which contains 45S rDNA respectively to MNase seems not to be affected in plants that overexpress 3xHMG-box1-GFP-NLS or 3xHMG-box2-GFP-NLS. In regard to the obtained results, compaction of chromatin mediated by the binding of 3xHMG-box proteins during

interphase seems to be rather unlikely. Still it could be worthwhile to study effects of binding of recombinant 3xHMG-box proteins to isolated chromatin *in vitro* in order to gain information about possible 3xHMG-box protein functions in restructuration of chromatin.

4.4 Spatiotemporal distribution of 3xHMG-box proteins and possible functions in mitotic processes

In previous studies it could be shown that expression of *3xHMG-box* genes is highest in tissues with high amounts of actively dividing cells and peaks during M-phase in synchronized *Arabidopsis* suspension-cultured cells (Pedersen et al. 2011). Furthermore, ICC with an antibody that marks both 3xHMG-box proteins and studies with 3xHMG-box proteins that are translationally fused to GFP and expressed under the control of the strong constitutive 35S promoter demonstrated that both proteins are associated with chromosomes only during mitosis and that 3xHMG-box1-GFP can be specifically found within 45S rDNA regions.

In order to monitor the appearance and distribution of 3xHMG-box proteins during M-phase *in vivo*, 3xHMG-box proteins that are fused to GFP were expressed under the control of their endogenous promoters. In root tips, condensed chromosomes of cells that undergo mitosis are decorated by 3xHMG-box proteins and weak signals could be observed in the cytoplasm of a small fraction of cells. 3xHMG-box1-GFP appeared as two distinct foci during metaphase and 4 distinct foci at anaphase and telophase, which are very likely to represent NORs. Time lapse imaging was applied to obtain a higher temporal resolution of 3xHMG-box occurrence during M-phase. Hereby, appearance of 3xHMG-box2 was estimated approximately 88 min prior nuclear envelope break down, which supports the assumption of a cell cycle dependent activity of *3xHMG-box* promoters. 3xHMG-box proteins gain access to chromosomes immediately after nuclear envelope break down (NEBD), which in plants happens in late prophase (Rose 2008). Thus, binding of 3xHMG-box proteins to chromatin might be a rather passive process mediated by their affinity to either DNA, specific DNA structures or certain proteins. Both proteins are associated with chromosomes until telophase, when the sister chromatids reach opposite poles around which the new daughter cells start to form. Coinciding with the event of decondensation, chromatin associated 3xHMG-box proteins can not be detected any more. Immediately after mitosis, during the final steps of cytokinesis when the

nuclear envelopes of and a new cell wall between the daughter cells are generated, 3xHMG-box proteins vanish.

In view of the spatiotemporal distribution of 3xHMG-box proteins during cell cycle, functions of these proteins that can be linked to condensation processes, e.g. sister chromatid segregation or maintenance and protection of compact chromatin structures seem not unlikely. Even though the condensation process is postulated to initiate in mammals at the end of S-phase and culminates in mitosis (Rao and Adlakha 1984), different levels of condensation can be distinguished and known factors that were shown to be implied in condensation processes gain access to chromosomes in later stages of M-phase. hCAP-G for example, a subunit of the vertebrate condensing I complex was also shown to bind chromosomes immediately after NEBD and stays attached until cytokinesis, while it is localized in the cytoplasm of interphase cells (Ono et al. 2004). An analog pattern could be observed for AtCAP-H, a non-SMC subunit of the *Arabidopsis* condensin I complex (Fujimoto et al. 2005). Albeit, 3xHMG-box proteins don't have any catalytic domains that point on functions in condensation or segregation processes, spatiotemporal distribution of 3xHMG-box coincide with this important mitotic events. With regard to its DNA bending properties and the containment of multiple DNA-binding domains, a function of 3xHMG-box proteins in one of these processes is an attractive hypothesis.

Ostensibly, localisation of 3xHMG-box2 has certain characteristics in common with the perichromosomal region (PR). As mentioned in the introduction, the PR layer is of irregular thickness and decorates condensed mitotic chromosomes except the centromeric regions. Interestingly SIM analyses of mitotic chromosomes, marked with anti 3xHMG-box antibodies and anti H3S10ph antibody reveal an exclusion of 3xHMG-box proteins from centromers. Until now, very little is known about the function of this compartment. It is speculated that the PR (1) provides a binding site for proteins necessary in early nuclear assembly, (2) is forming a barrier around chromosomes in mitosis to provide protection from cytoplasmic constituents or (3) organizes chromosomes by providing external chromosome scaffolding. Furthermore, it contains proteins implicated in a variety of cellular processes, including the synthesis of messenger RNA, assembly of ribosomes, repair of DNA double strand brakes and telomere maintenance (Van Hooser et al. 2005). Remarkably, cytologists in the late 1800s already concluded that a matrix of nucleolar material accumulates on the surface of late prophase chromosomes (Montgomery

1898). Indeed, the PR was shown to include pre-RNA, U3 snoRNAs and over 20 ribosomal proteins (Gautier et al. 1992) and is suggested to serve as a platform during nucleolar reassembly (Booth et al. 2014). Implications of the PR in nucleolar disassembly and reassembly appear to be especially interesting in context of the specific association of 3xHMG-box1 with NORs.

As a side aspect, plants which express 3xHMG-box-GFP fusion proteins under the control of their endogenous promoters could be used as marker lines to study mitosis in *Arabidopsis.* 3xHMG-box-GFP reporter constructs seem not to cause any phenotypic effects and exhibit some advantages compared to other markers that can be applied to study chromosome dynamics during mitosis. As 3xHMG-box2-GFP derived signals can be detected approximately 1.5 h before NEBD, it could be used as marker for late G_2/M phase as well. Until now, GUS- or GFP-fused to B1-type cyclins (CYCB1;1 and CYB1;2) or B2-type cyclin dependent kinase (CDKB2) are typically used as G_2/M specific marker genes in plants (Colon-Carmona et al. 1999, Adachi et al. 2006, Iwata et al. 2011). To visualize chromatin structures and to study morphology of somatic and meiotic chromosomes, H2B-mCherry was successfully used as a marker in maize (Howe et al. 2012). H2B-CFP was also used to monitor cell division in HeLa cells (Mackay et al. 2009). Here, 3xHMG-GFP constructs could be used to specifically stain and monitor chromosomes after NEBD in late prophase until telophase. This allows *in vivo* studies of late condensation and decondensation processes during these well defined steps of M-phase. Another example for a mitotic chromosome marker is CenH3-RFP that was used to study kinetochore dynamics during cell division (Kurihara et al. 2008) and specifically marks centromeric regions. 3xHMG-box2-GFP, in contrast, can be used to mark chromosome parts excluding centromeric regions. In addition, 3xHMG-box1 can be used to mark NORs during mitosis which is especially interesting because these regions have distinct properties compared to other regions, namely they are decondensed, form secondary constrictions and were shown in yeast to be among the last regions that segregate (Fuchs and Loidl 2004).

Reports about duration of mitosis in plants are limited. In the early 1960, time of different cell phases in meristematic tissues of higher plants were estimated by using the Quastler-Sherman method which utilizes ^{3}H-thymidine and autoradiography (Van't Hof 1974). According to these studies, M-phase ranges between 1-4 h while the mitotic cell cycle takes between 9.8-23 h. By time lapse microscopy of BY-2 cells

that express the CenH3-RFP constructs, time after NEBD in which cells reside in mitosis was estimated about 63.4 min (Kurihara et al. 2008) while the whole mitotic cycle in the meristematic zone of *A. thaliana* roots was recently shown to take 17h as measured by 5-ethynyl-2'-deoxy-uridine (EdU) incorporation. Time lapse microscopy of meristematic root cells of *A. thaliana* seedlings that express 3xHMG-box2-GFP constructs deliverd data which suggest that the duration of mitosis measured after NEBD until late telophase ranges around 24 min. When compared to the duration of this phase in BY-2 cultured suspension cells or other reports of duration of M-phase in higher plants as well as cytokinesis in HeLa cells, mitosis of cells in the meristematic zone of roots of *A. thaliana* seedlings appear to be remarkably short.

4.5 Identification of putative 3xHMG-box interaction partners

Attempt was made to identify putative protein interaction partners by co-immunoprecipitation to unveil possible functions of 3xHMG-box proteins in mitotic processes. An optimized tag for plant expression, consisting of protein G and streptavidin, was fused to either 3xHMG-box1 or 3xHMG-box2 and expressed under the control of the *3xHMG-box2* promoter in *Arabdidopsis* suspension cell cultures. The *3xHMG-box2* promoter was chosen to restrict expression of *3xHMG-box* genes to the late G_2/M phase and thus reduce precipitation of artificial binding partners. Indeed*, 3xHMG-box2* promoter was sufficient to drive enough expression of the sole GS-tag control construct in order to be able to isolate the protein from a cell extract by affinity purification via metal beads coated with rabbit IgG. In contrast, the attempt to isolate sufficient amounts of 3xHMG-box1-GS or 3xHMG-box2-GS fusion proteins for detection after polyacrylamide gel electrophoresis by Coomassie staining or silver staining was not successful. Only by immunoblot analyses, proteins with expected sizes of 3xHMG-box proteins which contain a GS tag could be detected. However, as protein amounts in elution fractions of the immunoprecipitation preparations were so low, detection of putative binding partners by mass spectrometry wasn't taken into consideration. Problems with low protein amounts might be due to lower transcription as well as lower translation rates of fusion proteins in comparison to the sole GS tag. Another likely factor might be fast degradation of 3xHMG-box proteins in *Arabidopsis* suspension cell cultures and seedlings after mitosis. This problem was tried to be overcome by application of known proteasome inhibitors MG132 and MG115 but without improvement. Both inhibitors were also tested by time laps microscopy with

plants that express 3xHMG-box2-GFP reporter constructs under the control of the endogenous promoter, but without any retention of degradation of the fusion proteins (Data not shown). In future attempts, it might proof reasonable to synchronize cell cultures and harvest cells during M-phase. Synchronization of *Arabidopsis* cultured cells appears to be not trivial. Two methods have been proven to be applicable namely sucrose starvation-induced synchronization and blocking cells in late G_1/early S phase by aphidicolin. Highest synchronization rates that were described for rapidly dividing cell suspensions MM1 and MM2d ranged around 13% and were achieved by application of aphidicolin (Menges and Murray 2002). A replication stress-induced approach utilizing hydroxyurea treatment was successfully applied for synchronization of root cells in *Arabidopsis thaliana* (Kurihara et al. 2008). To obtain sufficient amounts of synchronized root cells for Co-IP assay is a technical challenge, but displays a considerable approach to identify putative interaction partners for 3xHMG-box proteins.

4.6 Investigation of possible roles of the 3xHMG-box N-terminal domain in 45S rDNA specificity and identification of a D-box motif

Proteins that are fast degraded often possess domains or sequence motifs that allow its identification as substrates for the respective degradation machineries. Especially proteins that are assigned to mitotic functions often underlie a degradation dependent temporal regulation. The multisubunit E3 ligase APC/C complex is one of the most prominent key players in this cell cycle regulatory degradation processes and was originally identified as a ubiquitin ligase for cyclin B in *Xenopus* egg extracts (King et al. 1995). In addition to the mitotic cyclins, the APC/C targets also numerous other proteins that are involved in important mitotic processes, like for example securin, which is essential for sister chromatid separation (Zur and Brandeis 2001) or *Saccharomyces cerevisiae* anaphase inhibitor Cut2p (Cohen-Fix et al. 1996). The APC/C complex was shown to either recognize KEN-box (K-E-N) or D-box (R-x-x-L) amino acid motifs in their target substrates. Therefore 3xHMG-box amino-acid sequences were screened for containment of these APC/C specific degradation motifs. Two conserved R-x-x-L motifs were found, one in the very N-terminal region and one in the second HMG-box. Due to its position, the D-box domain in the N-terminal region was chosen as promising candidate for further studies. Indeed, site directed mutagenesis of this sequence leaded to a significantly prolonged time span

of degradation of 3xHMG-box2 after mitosis when compared to the 3xHMG-box2 with the native amino acid sequence. This supports the theory that 3xHMG-box proteins are efficiently degraded by the APC/C complex shortly after completion of mitosis and that the D-box motif in the N-terminal region is crucial for this process. Here, it can't be ruled out that also other putative D-box or KEN-box domains that were identified might play roles in degradation processes of 3xHMG-box proteins in *A. thaliana.* Taken together, results obtained during this work suggest a function of the N-terminal domain in protein degradation.

In previous works it could be demonstrated that the N-terminal region of 3xHMG-box2 contributes to the DNA binding of the entire protein and possesses DNA bending properties (Pedersen et al. 2011). By using the Basic Local Search Tool (BLAST) algorithm no homologues of the basic N-terminal domain of 3xHMG-box proteins could be identified in other eukaryotes besides the embryophyta. In this work, by overexpressing truncated versions of 3xHMG-box1 that are fused to GFP-NLS in stably transformed plants, a possible outstanding function of the N-terminal domain could be demonstrated. 3xHMG-box1-GFP-NLS proteins that are lacking the N-terminal region did not associate with mitotic chromosomes anymore and were only weakly accumulated in the nucleolus in leaf and root cells than compared to the complete 3xHMG-box1-GFP-NLS, which accumulated at distinct foci within nucleoli which are likely to represent 45S rDNA regions. In contrast, a truncated 3xHMG-box1-GFP-NLS version that only lacks the C-terminal domain displayed features that are comparable to that of the full length version. It accumulated as distinct foci within the nucleolus and is associated with condensed chromosomes during mitosis. Plants that overexpressed 3xHMG-box1-GFP-NLS fusion proteins lacking the C-terminal domain did show growth defects, which is not the case for plants that overexpressed 3xHMG-box1-GFP-NLS fusion proteins lacking the N-terminal domain (data not shown). Furthermore only the N-terminal region of 3xHMG-box1 when fused to GFP-NLS and overexpressed in stably transformed plant lines was able to weakly associate with condensed mitotic chromosomes (data not shown) and was highly enriched in nucleoli of interphase cells. A possible implication of the N-terminal region of 3xHMG-box proteins in specificity for 45S rDNA could be further emphasised by the generation of chimeric 3xHMG-box protein versions consisting of either the N-terminal region of 3xHMG-box1 and the HMG-box region of 3xHMG-box2 and vice versa. Here both chimeric proteins displayed features that where somewhat between

these of the native 3xHMG-box proteins GFP-NLS fusions. Hence the N-terminal region of 3xHMG-box1 seems not to be sufficient to completely mediate an affinity for nucleolar chromatin, when fused to the HMG-box region of 3xHMG-box2 but appears to definitely enhance this affinity.

Attempts to generate plants that express truncated versions of 3xHMG-box1-GFP fusion proteins under the control of the *3xHMG-box1* promoter have not been successful so far. These constructs might add further information about the importance of the N-terminal region in protein degradation processes and for the specific association with 45S rDNA regions during M-phase. Additionally, expression of chimeric versions of 3xHMG-box-GFP fusion proteins under the control of the endogenous *3xHMG-box2* promoter might be helpful with respect to the 45S rDNA specificity as well. Recombinant N-terminal domain of 3xHMG-box2 was also applied to crystallisation approaches in order to get structural information about this unique domain but no crystals could be obtained so far. Chances here are probably little, as XtalPred-RF, an algorithm for prediction of protein crystallizability (fas.burnham.org/XtalPred-cgi/xtal.pl) gave only very poor scores due to long unstructured stretches.

Basic regions in HMG-box containing proteins have been shown before to exhibit important functions. In several architectural proteins of various species that are assigned to the HMGB family, basic regions can be found adjacent to the HMG-box.

In vertebrate HMG1 and HMG2 for example, the linker region between the two HMG-box domains as well as the C-terminal adjacent region of the second HMG-box are comprised of basic stretches (Thomas and Travers 2001), while yeast Nhp6A and NHP6B as well as plant HMGB proteins contain highly basic N-terminal regions (Stemmer et al. 1997, Allain et al. 1999). The *Drosophila melangolaster* HMG-D and mouse LEF, a typical sequence specific HMG-box transcription factor, contain basic C-terminal extensions of the HMG-box. Basic regions of the latter two examples were shown to bind in the compressed major groove on the face of the helix opposite to the widened minor groove and thus stabilizing the HMG-box induced bend by charge neutralization (Love et al. 1995, Lnenicek-Allen et al. 1996, Dow et al. 2000). The 16 amino acid N-terminal basic segment of NHP6A has been demonstrated to be essential for high affinity DNA binding and the formation of monomeric DNA complexes (Yen et al. 1998) and also the basic N-termial domain of the maize HMGB1 has the ability to enhance the affinity of the protein for linear DNA, whereas it

has little effect on the structure-specific binding to DNA minicircles (Ritt et al. 1998). Additionally, the basic N-terminal domains of plant HMGB proteins are implicated in intra and intermolecular interplay. Here, the basic N-terminal region of the maize HMGB1 as well as the *Arabidopsis* HMGB1 and HMGB4 has been shown to interact with the C-terminal acidic tails of the same proteins, thus modulating their function (Thomsen et al. 2004, Stott et al. 2014), while a negative effect on binding of the transcription factor Dof2 to DNA has been demonstrated for the basic N-terminal domains of maize HMGB1 and HMGB5 (Grasser et al. 2007). Bioinformatic analyses by using PONDR-FIT, a meta-predictor of intrinsically disordered amino acids (Xue et al. 2010) suggest that the N-terminal region of 3xHMG-box proteins contains intrinsic disordered regions (Data not shown), which is especially interesting in context of possible protein functions. Structural disorder might serve additionally to specific sequence motifs as signal for intracellular protein degradation (Tompa et al. 2008). Conformational flexibility in disordered regions is also assumed to allow transcription factors of the Basic Leucine Zipper (bZIP) family to interact with a large number of diverse molecular partners and to accomplish their manifold cellular tasks (Miller 2009). A concrete example is the *Arabidopsis* HY5. Its N-terminal region is intrinsically unstructured under physiological conditions. It is speculated that this region might constitute into stable tertiary structures upon binding to its interaction partner(s) (Yoon et al. 2006).

In order to investigate if the N-terminal domain of 3xHMG-box1 is able to mediate sequence specific association with 45S rDNA, gel-shift assays were performed. Recombinantly produced N-terminal domains of 3xHMG-box1 and 3xHMG-box2 were incubated with different 45S rDNA gene fragments and separated in an agarose gel. Neither preferential binding of the N-terminal domain of 3xHMG-box1 to any of the 45S rDNA gene regions could be observed, nor a higher affinity to 45S rDNA when compared to the N-terminal region of 3xHMG-box2. A similar EMSA assay was performed before by using recombinant full length 3xHMG-box proteins instead of N-terminal domains. Also between full length 3xHMG-box1 and 3xHMG-box2, no differences in affinity for 45S rDNA gene fragments or preferential binding to any of the tested fragments could be observed (Holzinger 2012). The hypothesis that the three HMG-boxes of the full length proteins mask an elevated affinity of the 3xHMG-box1 N-terminal domain for 45S rDNA gene sequences could not be confirmed.

Depending on the plant species one to two copies of genes that code for 3xHMG-box proteins can be found in the respective genomes. Strikingly, all monocot members of plants that were used to create a phylogenetic tree possess only one gene copy that encodes for a 3xHMG-box protein. As it could be shown in *Arabidopsis thaliana* that one member of 3xHMG-box proteins associates specifically with 45S rDNA regions while the other is associates with all 5 chromosomes, the theory that 3xHMG-box proteins might group in two clades and that monocots only possess a 3xHMG-box protein that can be assigned to one clade, appeared as an attractive working hypothesis. However, amino acid sequence alignment of 3xHMG-box proteins from different species doesn't support this assumption (Figure 39A). While 3xHMG-box proteins of monocot plants used for the alignment are grouped together, the rest of the 3xHMG-box proteins are grouped according the species they belong to. Because CLSM studies of the truncated 3xHMG-box1-GFP-NLS proteins and chimeric 3xHMG-box proteins with exchanged N-terminal regions suggest a possible implication of this domain in specific association of 3xHMG-box1 with 45S rDNA, a

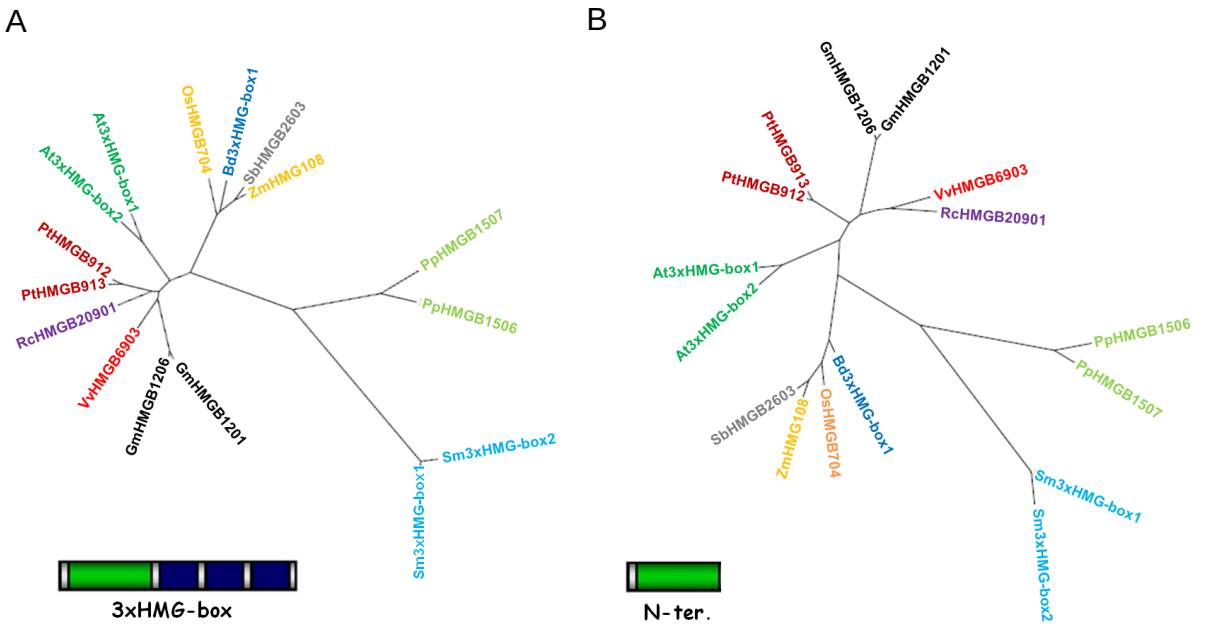

Figure 39. Sequence alignment of 3xHMG-box plant proteins and their N-terminal domains. Amino acid sequences of **(A)** plant 3xHMG-box proteins or their **(B)** N-terminal domains were aligned to create a neighbor-joining tree using SeaView software. Sequences are derived from *Brachipodium distachyon* (Bd), *Oryza sativa* (Os), *Zea mays* (Zm), *Arabidopsis thaliana* (At), *Populus trichocarpa* (Pt), *Vitis vinifera* (Vv), *Selaginella moellendorffii* (Sm), *Physcomitrella patens (*Pp), *Chlamydomonas reinhardtii* (Cr), *Ricinus communis* (Rc), *Glycine max* (Gm). Overall structure of 3xHMG-box proteins that were identified in plants are represented schematically: HMG-box domain (blue), basic region (green).

phylogenetic tree based on the amino acid sequences of the N-terminal regions of 3xHMG-box proteins from several plant species was also generated. Here as well, N-terminal regions are clustered according to the different species and not in two distinct groups that could be assigned to possible differences in chromatin association specificity (Figure 39B).

4.7 Analogies of 3xHMG-box proteins with UBF or HMO1 respectively

The finding that 3xHMG-box proteins are only encoded in plant genomes raises the question if other organisms contain functional equivalents. This approach might help to uncover possible functions of this protein family. Examples of HMG-box containing proteins that have mitotic functions or are associated with mitotic chromosomes a relatively rare. A *Schizosaccharomyces pombe* strain that is only able to express a truncated version of the HMGB protein Cmb1 exhibits elevated mitotic mutation rates that can be related to defects in nucleotide excision repair (Kunz et al. 2003). Implication of 3xHMG-box proteins in certain repair pathways is surely an interesting working hypothesis which might be worth to be tested experimentally. Human HMG20b was reported to decorate condensing chromosomes and injection of an anti-HMG20b antibody was found to delay the transition from G_2 into mitosis (Marmorstein et al. 2001). However, later studies rather suggested an association of HMG20b with mitotic microtubules then with condensed chromatin (Lee and Kim 2003). In line with that, the mammalian SSRP1 protein, besides its functions during interphase, is able to facilitate growth and bundling of microtubules during mitosis (Zeng et al. 2010). A function of 3xHMG-box proteins in microtubule organization or attachment to condensed chromosomes seems unlikely though, as they clearly decorate chromosomes and are rather absent from kinetochore regions. *A. thaliana* HMGB1 and HMGB2 as well as SSRP1 were shown in immunostaining experiments to be absent from mitotic chromosomes (Duroux et al. 2004, Launholt et al. 2006, Pedersen et al. 2010). For the vertebrate HMGB1 and HMGB2 a clear association with condensed chromosomes throughout all mitotic phases could be visualized by using fluorescent protein tags (Pallier et al. 2003). Fluorescence Loss in Photobleaching (FLIP) experiments that were performed in this study indicate that soluble and chromatin-bound forms do rapidly exchange.

One of the most striking candidates sharing the several common features with 3xHMG-box1 is represented by the Pol I transcription factor UBF, which is absent in

plants. Depending on the species, UBF contains five HMG boxes as in *Xenopus laevis* (Bachvarov and Moss 1991) or six HMG boxes as in *homo sapiens* (Jantzen et al. 1990). In vertebrates, UBF facilitates the initial step in formation of the Pol I initiation complex by induction of the ribosomal enhanceosome. DNA looping of the enhanceosome is probably the result of six in-phase bends induced by the HMG boxes of a UBF dimer (Stefanovsky et al. 2001). Studies in *Xenopus laevis* demonstrated that a dimer of Nbox13, a truncated version of the xUBF that only contains the three N-terminal HMG-boxes, is sufficient to generate a 350° loop which is required for generation of the enhanceosome (Stefanovsky et al. 1996). Interestingly, the human UBF binds to the ribosomal promoter with only relaxed specificity and no discernible recognition sites have been defined. In the yeast genome no gene that encodes for UBF exists, but instead another *bona fide* Pol I transcription factor named HMO1 can be found that bears one canonical HMG-box and a additional HMG-box like domain (Kamau et al. 2004). HMO1 is also able to induce DNA bends and preferentially binds to distorted DNA. In both, UBF and HMO1 the N-terminal domain functions as dimerization modules. Recently, it could be demonstrated that UBF localizes to the nucleolus and is able to functionally substitute for HMO1 in rDNA transcription (Albert et al. 2013).

It appears that functional homologies between 3xHMG-box proteins and UBF or HMO1 respectively are very unlikely as 3xHMG-box association with chromatin is restricted to mitosis, while the main function of UBF and HMO1 is Pol I transcription initiation and control. Still, an evolutionary link between these protein families and possible mechanistically commonalities in e.g. rDNA association or dimerization could not be ruled out. Therefore *S. cerevisiae* strain NOY 505 and HMO1 deficient strain yR44 were transformed with plasmids that allow the expression of 3xHMG-box1-GFP-NLS, 3xHMG-box2-GFP-NLS and GFP-NLS. When compared to the sole GFP-NLS, both 3xHMG-box-GFP-NLS fusion proteins accumulate as aggregates or single small foci within the yeast cells. Rather than accumulating in specific cellular structures, proteins seemed to fail to fold correctly in yeast cells or/and become targets of degradation due to overexpression. As 3xHMG-box1 was not found to localize to the nucleolus, no further tests for functional complementation of rDNA transcription in HMO1 deficient yR44 strains were made. In conclusion, it seems to be unlikely that 3xHMG-box1 can substitute UBF or HMO1 in their function as PolI transcription factors.

Still, as UBF has also functional implications in mitotic processes like de novo biogenesis of nucleoli and maintenance of NOR competency and remains associated with M-phase chromosomes (Grob et al. 2014), comparative analyzes of both proteins might deliver information about possible functions for 3xHMG-box proteins.

4.8 Association of 3xHMG-box1 with NORs during mitosis

When mitotic chromosomes of *A. thaliana* root cells were labeled with anti-3xHMG-box antibodies, the constitutive heterochromatic and transcriptionally silent centromere regions appear to be recessed from antibody binding (Pedersen et al. 2011). Further evidence for that could be provided by high resolution microscopy of mitotic chromosomes in *A. thaliana* root cells that were, additionally to the anti-3xHMG-box antibodies, labeled with anti H3S10ph antibodies. In plants, H3S10ph antibodies specifically mark centromeric regions (Gernand et al. 2003).

A specific labeling of 3xHMG-box1-GFP on mitotic chromosomes in *A. thaliana* root cells revealed an association with 3xHMG-box1 with 45S rDNA regions. In eukaryotes, the rDNA genes that encode for the large ribosome subunit are organized as repeated arrays in so called NORs. Not all NORs are actively transcribed during interphase. Only the competent NORs from which nucleoli emanate, are assumed to be transcriptionally active, while the non-competent NORs remain transcriptionally inactive throughout interphase (Savino et al. 2001). During mitosis when transcription is inactivated, some NORs are undercondensed and visible as secondary constrictions (McClintock 1934). Studies with *Crepis* hybrids suggested that only competent NORs are able to form secondary constrictions, while non-competent NORs fail to exhibit this feature. (Navashin 1934, Wallace and Langridge 1971). The phenomenon that in hybrids NORs which are derived from one parental progenitor are silenced while NORs which are derived from the other parental progenitor are active was later on termed as nucleolar dominance (Honjo and Reeder 1973).

One of the goals of this work was to test, if 3xHMG-box1 association with rDNA can be assigned to the transcriptional competency of NORs and thus the condensation grade of this region. To address this question, 3xHMG-box1 occupancy on mitotic NORs in *A. suecica*, the allotetraploid hybrid of *A. thaliana* and *A. arenosa*, should be monitored. In these hybrids *A. thaliana* derived NORs are transcriptionally silent during interphase, while *A. arenosa* derived NORs are active (Chen et al. 1998). To

be able to specifically label 3xHMG-box1, attempts were made to transform *A. suecica* with a construct that allows the expression of a 3xHMG-box1-GFP fusion protein. As no transgenic lines were obtained, an alternative approach was used. Mitotic chromosomes in *A. suecica* root cells were marked with anti 3xHMG-box antibodies that were shown to bind both 3xHMG-box proteins. When this antibody was used in an ICC approach with *A. thaliana* root cells, the distal region of two mitotic chromosome pairs, which were likely to represent NORs, exhibited a very strong immunofluorescence signal, (Pedersen et al. 2011). In *A suecica,* brighter stained regions could be also detected on certain chromosome regions that are likely to represent NORs. Number of foci with higher signal intensity definitely extended the expected number of the two *A. thaliana* derived NORs. Both, the two *A. thaliana* NORs as well as some of the *A. arenosa* derived NORs colocalized with these regions of elevated immunofluourescence signal. Therefore, inactive *A. thaliana* NORs as well as some of the *A. arenosa* NORs were occupied by 3xHMG-box proteins.

Despite some technical problems in detection of A. thaliana and A. arenosa NORs together with 3xHMG-box proteins by subsequent ICC and FISH and the lack of a 3xHMG-box1 specific marker, some valuable information could be obtained from these experiments. 3xHMG-box proteins were also present on the transcriptionally silent *A. thaliana* NORs that represent the rather condensed and compacted form of rDNA. Some of the *A. arenosa* derived NORs appeared to be also bound by 3xHMG-box proteins. If all of the *A. arenosa* NORs were transcriptionally active or if the NOR regions that were occupied by 3xHMG-box proteins are entirely decondensed could not be said. In general, the finding that 3xHMG-box proteins were rather excluded from centromeric regions and colocalize with *A. arenosa* NORs in *A. suecica* argues against a role of 3xHMG-box proteins in maintaining heterochromatic chromatin structures or transcriptional silencing.

4.9 Investigation of possible competitive DNA binding of 3xHMG-box proteins and linker histones

Direct and indirect Interactions of linker histones and HMG-box containing proteins could be demonstrated in several studies. Members of both families are considered to act as chromatin architectural factors and thus constantly modulating nucleosome accessibility and the local structure of the chromatin fiber. An important feature with

regard to dynamic modulation of chromatin structure is the transient binding to chromatin with short residence times, which was shown for members of the HMGB family and linker histones (Lever et al. 2000, Phair et al. 2004, Grasser et al. 2007). Linker histones and HMG-box containing proteins like UBF and members of the HMGB family are postulated to have opposite effects on chromatin stability. H1 stabilizes both, the nucleosome and chromatin higher order structure (Thoma et al. 1979), thereby restricting the ability of regulatory factors, nucleosome remodeling complexes and histone modifiers to access their chromatin binding sites (Laybourn and Kadonaga 1991) (Herrera et al. 2000, Hill and Imbalzano 2000, Cheung et al. 2002), whereas HMG-box containing proteins decompact the higher-order chromatin structure and promote the binding of nuclear regulatory factors (Thomas and Travers 2001, Agresti and Bianchi 2003, Sanij et al. 2014). Different HMG-box containing proteins could be demonstrated to compete with linker histones for the same binding sites. Data from foot printing assays indicate that *X. laevis* UBF is sufficient to displace linker histone H1 from its binding site on a preassembled nucleosome (Kermekchiev et al. 1997) and by Fluorescence Recovery After Bleaching (FRAP) assays it could be proven that HMGB proteins weaken the binding of H1 to nucleosomes by dynamically competing for distinct chromatin binding sites (Catez et al. 2004).

One attractive hypothesis was that 3xHMG-box protein binding might lead to displacement of linker histones, which therefore become available for their function in microtubule nucleation (Jerzmanowski and Kotlinski 2011). To test if 3xHMG-box proteins and linker histones associate with chromatin in a competitive or even exclusive manner, distribution patterns of fluorescently labeled linker histones and 3xHMG-box proteins in leaf and root cells were compared. Linker histones in *A. thaliana* are bound to condensed chromosomes during mitosis, as observed before in BY-2 suspension cell cultures (Juranic et al. 2012). Here, 3xHMG-box2 and linker histones show a largely overlapping distribution pattern and also for 3xHMG-box1 and linker histones no clear anticorrelation of their binding sites could be observed. Neither overexpression of 3xHMG-box proteins seems to have an effect on linker histone binding to mitotic chromosomes, nor overexpression of linker histones for the distribution of 3xHMG-box proteins on mitotic chromosomes. Also during interphase, overexpression and artificial targeting of 3xHMG-box proteins did not result in apparent dissociation or displacement of linker histones. Signals that were derived

from fluorescently labeled linker histones still showed the strongest intensity within chromocenters (Ascenzi and Gantt 1999). Distribution of 3xHMG-box1-GFP-NLS or 3xHMG-box2-GFP-NLS fusion proteins was not altered in the H1.1-RFP and H1.2-RFP overexpression background and also no weaker signals in chromocenters could be observed. Taken together, there is no indication for competitive binding of linker histones and 3xHMG-box proteins.

One problem might lay in the spatial resolution of the applied microscopy technology. Enhanced resolution by using SIM technology might give further information about possible antagonistic binding of these two protein families. Additionally, FRAP could be used as an alternative approach to test if overexpression of either a member of one of the protein families lead to alleviated binding of a member of the other protein family.

4.10 Perspective

So far, 3xHMG-box proteins have been investigated in a rather descriptive manner and according to their biochemical properties. To uncover the biological relevance of this protein family, the generation of a double knock-out mutant for 3xHMG-box1 and 3xHMG-box2 might give an important tool in hand. Possible defects during mitosis or at reentry in the interphase could deliver valuable information about implications of 3xHMG-box proteins. Still, a complete knock-out of both genes doesn't necessarily result in phenotypical effects, as experienced for many other factors that are involved in important cellular functions. Maybe, lack of 3xHMG-box proteins only leads to particular effects under certain environmental conditions.

Further investigation of 3xHMG-box1/2-GFP-NLS overexpression lines could also proof as a reasonable approach to gain information about properties of this class of proteins. A main aspect would be to clarify why 3xHMG-box1-GFP-NLS abundance in interphase nuclei causes drastic developmental defects, while this is not the case for 3xHMG-box2-GFP-NLS.

Besides the forward genetics, identification of putative protein interaction partners is certainly a useful approach in order to identify implications of 3xHMG-box proteins in certain cellular, probably mitotic processes. In this work, isolation of sufficient amounts of 3xHMG-box proteins from cell extracts was not successful, likely due to little protein amounts and fast degradation. Establishment of synchronization of

Arabidopsis cultured cells and roots might be an opportunity to overcome this obstacle.

As DNA binding and bending properties as well as possible functions in specificity for rDNA regions and degradation recognition could be demonstrated for the N-terminal region of 3xHMG-box proteins, further investigation of this unique domain might lead to interesting findings.

5. Summary

The plant specific family of 3xHMG-box proteins contains three HMG-box domains and an N-terminal basic domain that synergistically contribute to its DNA binding and bending properties. So far, they resemble the first group of HMG-box containing proteins which association with chromatin is restricted to mitosis and meiosis.

In this work, a reporter system that allows *in vivo* studies of 3xHMG-box proteins was successfully developed and tested. Through the usage of the endogenous promoters of *3xHMG-box1* and *3xHMG-box2*, expression of the reporter constructs should correspond to the expression of the endogenous genes with respect to transcript level and cell cycle dependency. The reporter system was used to monitor occurance and distribution of 3xHMG-box proteins during G_2/M phase in root cells and to test the effect of a putative D-box motif in degradation of 3xHMG-box2.

In contrast to overexpression of 3xHMG-box1-GFP-fusion proteins, overexpression of fusion proteins that consist of 3xHMG-box1 and a GFP with an attached nuclear localization signal leads to strong developmental defects in *A. thaliana* plants. The 3xHMG-box1-GFP-NLS derived signal was observed to be accumulated as distinct speckles within in the nucleolus, in which rDNA is transcribed and processed. Growth defects in 3xHMG-box1-GFP-NLS overexpression lines could not be connected to decreased transcript levels of 45 rDNA or altered compaction state of 45S rDNA gene regions.

Construction of truncated and chimeric proteins in which the N-terminal domains of 3xHMG-box1 and 3xHMG-box2 were exchanged, suggested a function of the N-terminal domain for the specificity of 3xHMG-box1 for certain rDNA regions. EMSA experiments with 45S rDNA fragments and recombinant N-terminal domains of 3xHMG-box1 and 3xHMG-box2 did not support a sequence specific binding of 3xHMG-box1 N-terminal domain for 45S rDNA.

Association of 3xHMG-box proteins with NORs in allotetraploid *A. suecica* was tested in subsequent Immunostain and FISH experiments. 3xHMG-box proteins were found to associate with silenced *A. thaliana* NORs but also with some of the *A. arenosa* NORs.

Furthermore, plants that simultaneously express 3xHMG-box proteins fused to GFP and linker histones fused to RFP were analyzed. No evidences for antagonistic binding could be obtained.

6. References

(2000). "Analysis of the genome sequence of the flowering plant Arabidopsis thaliana." Nature **408**(6814): 796-815.
Adachi, S., H. Uchimiya and M. Umeda (2006). "Expression of B2-type cyclin-dependent kinase is controlled by protein degradation in Arabidopsis thaliana." Plant Cell Physiol **47**(12): 1683-1686.
Agresti, A. and M. E. Bianchi (2003). "HMGB proteins and gene expression." Curr Opin Genet Dev **13**(2): 170-178.
Alam, T. I., T. Kanki, T. Muta, K. Ukaji, Y. Abe, H. Nakayama, K. Takio, N. Hamasaki and D. Kang (2003). "Human mitochondrial DNA is packaged with TFAM." Nucleic Acids Res **31**(6): 1640-1645.
Albert, B., C. Colleran, I. Leger-Silvestre, A. B. Berger, C. Dez, C. Normand, J. Perez-Fernandez, B. McStay and O. Gadal (2013). "Structure-function analysis of Hmo1 unveils an ancestral organization of HMG-Box factors involved in ribosomal DNA transcription from yeast to human." Nucleic Acids Res **41**(22): 10135-10149.
Alberts, B., A. Johnson, J. Lewis, R. Martin, K. Roberts and P. Walter (2002). "Molecular Biology of the Cell." Garland Science(4).
Alexander, M. P. (1969). "Differential staining of aborted and nonaborted pollen." Stain Technol **44**(3): 117-122.
Allain, F. H., Y. M. Yen, J. E. Masse, P. Schultze, T. Dieckmann, R. C. Johnson and J. Feigon (1999). "Solution structure of the HMG protein NHP6A and its interaction with DNA reveals the structural determinants for non-sequence-specific binding." EMBO J **18**(9): 2563-2579.
Andersson, U., H. Erlandsson-Harris, H. Yang and K. J. Tracey (2002). "HMGB1 as a DNA-binding cytokine." J Leukoc Biol **72**(6): 1084-1091.
Antosch, M., S. A. Mortensen and K. D. Grasser (2012). "Plant proteins containing high mobility group box DNA-binding domains modulate different nuclear processes." Plant Physiol **159**(3): 875-883.
Arce, L., N. N. Yokoyama and M. L. Waterman (2006). "Diversity of LEF/TCF action in development and disease." Oncogene **25**(57): 7492-7504.
Armstrong, W. P. (1988). "Biology 100 Laboratory Manual & Workbook." Burgess Publishing **5**.
Ascenzi, R. and J. S. Gantt (1999). "Subnuclear distribution of the entire complement of linker histone variants in Arabidopsis thaliana." Chromosoma **108**(6): 345-355.
Bachvarov, D. and T. Moss (1991). "The RNA polymerase I transcription factor xUBF contains 5 tandemly repeated HMG homology boxes." Nucleic Acids Res **19**(9): 2331-2335.
Badis, G., M. F. Berger, A. A. Philippakis, S. Talukder, A. R. Gehrke, S. A. Jaeger, E. T. Chan, G. Metzler, A. Vedenko, X. Chen, H. Kuznetsov, C. F. Wang, *et al.* (2009). "Diversity and complexity in DNA recognition by transcription factors." Science **324**(5935): 1720-1723.
Baxevanis, A. D., S. H. Bryant and D. Landsman (1995). "Homology model building of the HMG-1 box structural domain." Nucleic Acids Res **23**(6): 1019-1029.
Bazett-Jones, D. P., B. Leblanc, M. Herfort and T. Moss (1994). "Short-range DNA looping by the Xenopus HMG-box transcription factor, xUBF." Science **264**(5162): 1134-1137.
Benham, C. J. and S. P. Mielke (2005). "DNA mechanics." Annu Rev Biomed Eng **7**: 21-53.

Bhasin, M., E. L. Reinherz and P. A. Reche (2006). "Recognition and Classification of Histones Using Support Vector Machine." JOURNAL OF COMPUTATIONAL BIOLOGY **13**(1): 102–112.
Bianchi, M. E. and A. Agresti (2005). "HMG proteins: dynamic players in gene regulation and differentiation." Curr Opin Genet Dev **15**(5): 496-506.
Boisvert, F. M., S. van Koningsbruggen, J. Navascues and A. I. Lamond (2007). "The multifunctional nucleolus." Nat Rev Mol Cell Biol **8**(7): 574-585.
Bonawitz, N. D., D. A. Clayton and G. S. Shadel (2006). "Initiation and beyond: multiple functions of the human mitochondrial transcription machinery." Mol Cell **24**(6): 813-825.
Booth, D. G., M. Takagi, L. Sanchez-Pulido, E. Petfalski, G. Vargiu, K. Samejima, N. Imamoto, C. P. Ponting, D. Tollervey, W. C. Earnshaw and P. Vagnarelli (2014). "Ki-67 is a PP1-interacting protein that organises the mitotic chromosome periphery." Elife **3**: e01641.
Boyes, D. C., A. M. Zayed, R. Ascenzi, A. J. McCaskill, N. E. Hoffman, K. R. Davis and J. Gorlach (2001). "Growth stage-based phenotypic analysis of Arabidopsis: a model for high throughput functional genomics in plants." Plant Cell **13**(7): 1499-1510.
Bradford, M. M. (1976). "A rapid and sensitive method for the quantitation of microgram quantities of protein utilizing the principle of protein-dye binding." Anal Biochem **72**: 248-254.
Brown, J. W. and P. J. Shaw (1998). "Small nucleolar RNAs and pre-rRNA processing in plants." Plant Cell **10**(5): 649-657.
Bruhn, S. L., P. M. Pil, J. M. Essigmann, D. E. Housman and S. J. Lippard (1992). "Isolation and characterization of human cDNA clones encoding a high mobility group box protein that recognizes structural distortions to DNA caused by binding of the anticancer agent cisplatin." Proc Natl Acad Sci U S A **89**(6): 2307-2311.
Buck, S. W., J. J. Sandmeier and J. S. Smith (2002). "RNA polymerase I propagates unidirectional spreading of rDNA silent chromatin." Cell **111**(7): 1003-1014.
Bustin, M. (2001). "Revised nomenclature for high mobility group (HMG) chromosomal proteins." Trends Biochem Sci **26**(3): 152-153.
Bustin, M., F. Catez and J. H. Lim (2005). "The dynamics of histone H1 function in chromatin." Mol Cell **17**(5): 617-620.
Cairns, J. (1963). "The bacterial chromosome and its manner of replication as seen by autoradiography." J Mol Biol **6**: 208-213.
Campell, B. R., Y. Song, T. E. Posch, C. A. Cullis and C. D. Town (1992). "Sequence and organization of 5S ribosomal RNA-encoding genes of Arabidopsis thaliana." Gene **112**(2): 225-228.
Caperta, A. D., N. Neves, L. Morais-Cecilio, R. Malho and W. Viegas (2002). "Genome restructuring in rye affects the expression, organization and disposition of homologous rDNA loci." J Cell Sci **115**(Pt 14): 2839-2846.
Catez, F., H. Yang, K. J. Tracey, R. Reeves, T. Misteli and M. Bustin (2004). "Network of dynamic interactions between histone H1 and high-mobility-group proteins in chromatin." Mol Cell Biol **24**(10): 4321-4328.
Cato, L., K. Stott, M. Watson and J. O. Thomas (2008). "The interaction of HMGB1 and linker histones occurs through their acidic and basic tails." J Mol Biol **384**(5): 1262-1272.
Cavalier-Smith, T. (2000). "Membrane heredity and early chloroplast evolution." Trends Plant Sci **5**(4): 174-182.

Chen, Z. J., L. Comai and C. S. Pikaard (1998). "Gene dosage and stochastic effects determine the severity and direction of uniparental ribosomal RNA gene silencing (nucleolar dominance) in Arabidopsis allopolyploids." Proc Natl Acad Sci U S A **95**(25): 14891-14896.
Chen, Z. J. and C. S. Pikaard (1997). "Epigenetic silencing of RNA polymerase I transcription: a role for DNA methylation and histone modification in nucleolar dominance." Genes Dev **11**(16): 2124-2136.
Cheung, E., A. S. Zarifyan and W. L. Kraus (2002). "Histone H1 represses estrogen receptor alpha transcriptional activity by selectively inhibiting receptor-mediated transcription initiation." Mol Cell Biol **22**(8): 2463-2471.
Choi, E., J. M. Dial, D. E. Jeong and M. C. Hall (2008). "Unique D box and KEN box sequences limit ubiquitination of Acm1 and promote pseudosubstrate inhibition of the anaphase-promoting complex." J Biol Chem **283**(35): 23701-23710.
Churchill, M. E., J. Klass and D. L. Zoetewey (2010). "Structural analysis of HMGD-DNA complexes reveals influence of intercalation on sequence selectivity and DNA bending." J Mol Biol **403**(1): 88-102.
Ciechanover, A., A. Orian and A. L. Schwartz (2000). "Ubiquitin-mediated proteolysis: biological regulation via destruction." Bioessays **22**(5): 442-451.
Clough, S. J. and A. F. Bent (1998). "Floral dip: a simplified method for Agrobacterium-mediated transformation of Arabidopsis thaliana." Plant J **16**(6): 735-743.
Cohen-Fix, O., J. M. Peters, M. W. Kirschner and D. Koshland (1996). "Anaphase initiation in Saccharomyces cerevisiae is controlled by the APC-dependent degradation of the anaphase inhibitor Pds1p." Genes Dev **10**(24): 3081-3093.
Colon-Carmona, A., R. You, T. Haimovitch-Gal and P. Doerner (1999). "Technical advance: spatio-temporal analysis of mitotic activity with a labile cyclin-GUS fusion protein." Plant J **20**(4): 503-508.
Copenhaver, G. P., C. D. Putnam, M. L. Denton and C. S. Pikaard (1994). "The RNA polymerase I transcription factor UBF is a sequence-tolerant HMG-box protein that can recognize structured nucleic acids." Nucleic Acids Res **22**(13): 2651-2657.
De Veylder, L., T. Beeckman, G. T. S. Beemster, L. Krols, F. Terras, I. Landrieu, E. Van Der Schueren, S. Maes, M. Naudts and D. Inzé (2001). "Functional Analysis of Cyclin-Dependent Kinase Inhibitors of Arabidopsis." The Plant Cell Online **13**(7): 1653-1668.
Delgado, M., L. Morais-Cecilio, N. Neves, R. N. Jones and W. Viegas (1995). "The influence of B chromosomes on rDNA organization in rye interphase nuclei." Chromosome Res **3**(8): 487-491.
Desvoyes, B., M. Fernandez-Marcos, J. Sequeira-Mendes, S. Otero, Z. Vergara and C. Gutierrez (2014). "Looking at plant cell cycle from the chromatin window." Front Plant Sci **5**: 369.
Dow, L. K., D. N. Jones, S. A. Wolfe, G. L. Verdine and M. E. Churchill (2000). "Structural studies of the high mobility group globular domain and basic tail of HMG-D bound to disulfide cross-linked DNA." Biochemistry **39**(32): 9725-9736.
Dundr, M., T. Misteli and M. O. Olson (2000). "The dynamics of postmitotic reassembly of the nucleolus." J Cell Biol **150**(3): 433-446.
Duroux, M., A. Houben, K. Ruzicka, J. Friml and K. D. Grasser (2004). "The chromatin remodelling complex FACT associates with actively transcribed regions of the Arabidopsis genome." Plant J **40**(5): 660-671.
Edgar, B. A. and T. L. Orr-Weaver (2001). "Endoreplication cell cycles: more for less." Cell **105**(3): 297-306.

Edwards, K., C. Johnstone and C. Thompson (1991). "A simple and rapid method for the preparation of plant genomic DNA for PCR analysis." Nucleic Acids Res **19**(6): 1349.
Eichler, D. C. and N. Craig (1994). "Processing of eukaryotic ribosomal RNA." Prog Nucleic Acid Res Mol Biol **49**: 197-239.
Engel, C., S. Sainsbury, A. C. Cheung, D. Kostrewa and P. Cramer (2013). "RNA polymerase I structure and transcription regulation." Nature **502**(7473): 650-655.
Fang, Y. and D. L. Spector (2005). "Centromere positioning and dynamics in living Arabidopsis plants." Mol Biol Cell **16**(12): 5710-5718.
Franklin, R. E. and R. G. Gosling (1953). "Molecular configuration in sodium thymonucleate." Nature **171**(4356): 740-741.
Fransz, P., S. Armstrong, C. Alonso-blanco, T. C. Fischer, R. A. Torres-ruiz and G. Jones (1998). "Cytogenetics for the model system Arabidopsis thaliana." The Plant Journal **13**(6): 867-876.
Fuchs, J. and J. Loidl (2004). "Behaviour of nucleolus organizing regions (NORs) and nucleoli during mitotic and meiotic divisions in budding yeast." Chromosome Res **12**(5): 427-438.
Fujimoto, S., M. Yonemura, S. Matsunaga, T. Nakagawa, S. Uchiyama and K. Fukui (2005). "Characterization and dynamic analysis of Arabidopsis condensin subunits, AtCAP-H and AtCAP-H2." Planta **222**(2): 293-300.
Gadal, O., S. Labarre, C. Boschiero and P. Thuriaux (2002). "Hmo1, an HMG-box protein, belongs to the yeast ribosomal DNA transcription system." EMBO J **21**(20): 5498-5507.
Gautier, T., C. Dauphin-Villemant, C. Andre, C. Masson, J. Arnoult and D. Hernandez-Verdun (1992). "Identification and characterization of a new set of nucleolar ribonucleoproteins which line the chromosomes during mitosis." Exp Cell Res **200**(1): 5-15.
Gautier, T., M. Robert-Nicoud, M. N. Guilly and D. Hernandez-Verdun (1992). "Relocation of nucleolar proteins around chromosomes at mitosis. A study by confocal laser scanning microscopy." J Cell Sci **102 (Pt 4)**: 729-737.
Gavet, O. and J. Pines (2010). "Progressive activation of CyclinB1-Cdk1 coordinates entry to mitosis." Dev Cell **18**(4): 533-543.
Gebrane-Younes, J., N. Fomproix and D. Hernandez-Verdun (1997). "When rDNA transcription is arrested during mitosis, UBF is still associated with non-condensed rDNA." J Cell Sci **110 (Pt 19)**: 2429-2440.
Genschik, P., K. Marrocco, L. Bach, S. Noir and M. C. Criqui (2014). "Selective protein degradation: a rheostat to modulate cell-cycle phase transitions." J Exp Bot **65**(10): 2603-2615.
Gerard, G. F. and J. M. D'Alessio (1993). "Reverse transcriptase (EC 2.7.7.49): the use of cloned maloney murine leukemia virus reverse transcriptase to synthesize DNA from RNA." Methods Mol Biol **16**: 73-93.
Gerbi SA and B. AV (2000). "Processing in Multicellular Organisms." Madame Curie Bioscience Database.
Gernand, D., D. Demidov and A. Houben (2003). "The temporal and spatial pattern of histone H3 phosphorylation at serine 28 and serine 10 is similar in plants but differs between mono- and polycentric chromosomes." Cytogenet Genome Res **101**(2): 172-176.
Glotzer, M., A. W. Murray and M. W. Kirschner (1991). "Cyclin is degraded by the ubiquitin pathway." Nature **349**(6305): 132-138.

Gonzalez-Melendi, P., B. Wells, A. F. Beven and P. J. Shaw (2001). "Single ribosomal transcription units are linear, compacted Christmas trees in plant nucleoli." Plant J **27**(3): 223-233.
Goodwin, G. H., C. Sanders and E. W. Johns (1973). "A new group of chromatin-associated proteins with a high content of acidic and basic amino acids." Eur J Biochem **38**(1): 14-19.
Grafi, G., R. J. Burnett, T. Helentjaris, B. A. Larkins, J. A. DeCaprio, W. R. Sellers and W. G. Kaelin (1996). "A maize cDNA encoding a member of the retinoblastoma protein family: involvement in endoreduplication." Proceedings of the National Academy of Sciences **93**(17): 8962-8967.
Grasser, K. D., D. Launholt and M. Grasser (2007). "High mobility group proteins of the plant HMGB family: dynamic chromatin modulators." Biochim Biophys Acta **1769**(5-6): 346-357.
Grasser, M., J. M. Christensen, C. Peterhansel and K. D. Grasser (2007). "Basic and acidic regions flanking the HMG-box domain of maize HMGB1 and HMGB5 modulate the stimulatory effect on the DNA binding of transcription factor Dof2." Biochemistry **46**(21): 6375-6382.
Grasser, M., A. Lentz, J. Lichota, T. Merkle and K. D. Grasser (2006). "The Arabidopsis genome encodes structurally and functionally diverse HMGB-type proteins." J Mol Biol **358**(3): 654-664.
Grob, A., C. Colleran and B. McStay (2014). "Construction of synthetic nucleoli in human cells reveals how a major functional nuclear domain is formed and propagated through cell division." Genes Dev **28**(3): 220-230.
Gunning, B. E. and S. M. Wick (1985). "Preprophase bands, phragmoplasts, and spatial control of cytokinesis." J Cell Sci Suppl **2**: 157-179.
Hahn, M., S. Dambacher, S. Dulev, A. Y. Kuznetsova, S. Eck, S. Worz, D. Sadic, M. Schulte, J. P. Mallm, A. Maiser, P. Debs, H. von Melchner*, et al.* (2013). "Suv4-20h2 mediates chromatin compaction and is important for cohesin recruitment to heterochromatin." Genes Dev **27**(8): 859-872.
Hansen, F. T., C. K. Madsen, A. M. Nordland, M. Grasser, T. Merkle and K. D. Grasser (2008). "A novel family of plant DNA-binding proteins containing both HMG-box and AT-rich interaction domains." Biochemistry **47**(50): 13207-13214.
Hardman, C. H., R. W. Broadhurst, A. R. Raine, K. D. Grasser, J. O. Thomas and E. D. Laue (1995). "Structure of the A-domain of HMG1 and its interaction with DNA as studied by heteronuclear three- and four-dimensional NMR spectroscopy." Biochemistry **34**(51): 16596-16607.
Harrison, S. J., E. K. Mott, K. Parsley, S. Aspinall, J. C. Gray and A. Cottage (2006). "A rapid and robust method of identifying transformed Arabidopsis thaliana seedlings following floral dip transformation." Plant Methods **2**: 19.
Hartman, A. L., C. Norais, J. H. Badger, S. Delmas, S. Haldenby, R. Madupu, J. Robinson, H. Khouri, Q. Ren, T. M. Lowe, J. Maupin-Furlow, M. Pohlschroder*, et al.* (2010). "The complete genome sequence of Haloferax volcanii DS2, a model archaeon." PLoS One **5**(3): e9605.
Hernandez-Verdun, D. (2011). "Assembly and disassembly of the nucleolus during the cell cycle." Nucleus **2**(3): 189-194.
Herrera, J. E., K. L. West, R. L. Schiltz, Y. Nakatani and M. Bustin (2000). "Histone H1 is a specific repressor of core histone acetylation in chromatin." Mol Cell Biol **20**(2): 523-529.
Hewish, D. R. and L. A. Burgoyne (1973). "Chromatin sub-structure. The digestion of chromatin DNA at regularly spaced sites by a nuclear deoxyribonuclease." Biochem Biophys Res Commun **52**(2): 504-510.

Hill, D. A. and A. N. Imbalzano (2000). "Human SWI/SNF nucleosome remodeling activity is partially inhibited by linker histone H1." Biochemistry **39**(38): 11649-11656.
Holzinger, P. (2012). "Molecular Analysis of 3xHMG-box proteins in Arabidopsis thaliana." Bachelor thesis.
Honjo, T. and R. H. Reeder (1973). "Preferential transcription of Xenopus laevis ribosomal RNA in interspecies hybrids between Xenopus laevis and Xenopus mulleri." J Mol Biol **80**(2): 217-228.
Houben, A., D. Demidov, A. D. Caperta, R. Karimi, F. Agueci and L. Vlasenko (2007). "Phosphorylation of histone H3 in plants--a dynamic affair." Biochim Biophys Acta **1769**(5-6): 308-315.
Houben, A., T. Wako, R. Furushima-Shimogawara, G. Presting, G. Kunzel, I. I. Schubert and K. Fukui (1999). "Short communication: the cell cycle dependent phosphorylation of histone H3 is correlated with the condensation of plant mitotic chromosomes." Plant J **18**(6): 675-679.
Howe, E. S., T. E. Clemente and H. W. Bass (2012). "Maize histone H2B-mCherry: a new fluorescent chromatin marker for somatic and meiotic chromosome research." DNA Cell Biol **31**(6): 925-938.
Hu, L., X. Yang, D. Yuan, F. Zeng and X. Zhang (2011). "GhHmgB3 deficiency deregulates proliferation and differentiation of cells during somatic embryogenesis in cotton." Plant Biotechnol J **9**(9): 1038-1048.
Hudson, D. F., K. M. Marshall and W. C. Earnshaw (2009). "Condensin: Architect of mitotic chromosomes." Chromosome Res **17**(2): 131-144.
Ikeda, Y., Y. Kinoshita, D. Susaki, Y. Ikeda, M. Iwano, S. Takayama, T. Higashiyama, T. Kakutani and T. Kinoshita (2011). "HMG domain containing SSRP1 is required for DNA demethylation and genomic imprinting in Arabidopsis." Dev Cell **21**(3): 589-596.
Ito, M., S. Araki, S. Matsunaga, T. Itoh, R. Nishihama, Y. Machida, J. H. Doonan and A. Watanabe (2001). "G2/M-phase-specific transcription during the plant cell cycle is mediated by c-Myb-like transcription factors." Plant Cell **13**(8): 1891-1905.
Iwata, E., S. Ikeda, S. Matsunaga, M. Kurata, Y. Yoshioka, M. C. Criqui, P. Genschik and M. Ito (2011). "GIGAS CELL1, a novel negative regulator of the anaphase-promoting complex/cyclosome, is required for proper mitotic progression and cell fate determination in Arabidopsis." Plant Cell **23**(12): 4382-4393.
Jantzen, H. M., A. Admon, S. P. Bell and R. Tjian (1990). "Nucleolar transcription factor hUBF contains a DNA-binding motif with homology to HMG proteins." Nature **344**(6269): 830-836.
Jauch, R., C. K. Ng, K. Narasimhan and P. R. Kolatkar (2012). "The crystal structure of the Sox4 HMG domain-DNA complex suggests a mechanism for positional interdependence in DNA recognition." Biochem J **443**(1): 39-47.
Jerzmanowski, A. and M. Kotlinski (2011). "Conserved chromatin structural proteins – a source of variation enabling plant-specific adaptations?" New Phytologist **192**(3): 563-566.
Jimenez-Garcia, L. F., M. L. Segura-Valdez, R. L. Ochs, L. I. Rothblum, R. Hannan and D. L. Spector (1994). "Nucleologenesis: U3 snRNA-containing prenucleolar bodies move to sites of active pre-rRNA transcription after mitosis." Mol Biol Cell **5**(9): 955-966.
Juranic, M., K. O. Srilunchang, N. G. Krohn, D. Leljak-Levanic, S. Sprunck and T. Dresselhaus (2012). "Germline-specific MATH-BTB substrate adaptor MAB1 regulates spindle length and nuclei identity in maize." Plant Cell **24**(12): 4974-4991.

Kamau, E., K. T. Bauerle and A. Grove (2004). "The Saccharomyces cerevisiae high mobility group box protein HMO1 contains two functional DNA binding domains." J Biol Chem **279**(53): 55234-55240.
Kermekchiev, M., J. L. Workman and C. S. Pikaard (1997). "Nucleosome binding by the polymerase I transactivator upstream binding factor displaces linker histone H1." Mol Cell Biol **17**(10): 5833-5842.
Keys, D. A., B. S. Lee, J. A. Dodd, T. T. Nguyen, L. Vu, E. Fantino, L. M. Burson, Y. Nogi and M. Nomura (1996). "Multiprotein transcription factor UAF interacts with the upstream element of the yeast RNA polymerase I promoter and forms a stable preinitiation complex." Genes Dev **10**(7): 887-903.
Khorana, H. G., R. W. Holley and M. W. Nirenberg (1968). "The Nobel Prize in Physiology or Medicine ".
King, R. W., M. Glotzer and M. W. Kirschner (1996). "Mutagenic analysis of the destruction signal of mitotic cyclins and structural characterization of ubiquitinated intermediates." Mol Biol Cell **7**(9): 1343-1357.
King, R. W., J. M. Peters, S. Tugendreich, M. Rolfe, P. Hieter and M. W. Kirschner (1995). "A 20S complex containing CDC27 and CDC16 catalyzes the mitosis-specific conjugation of ubiquitin to cyclin B." Cell **81**(2): 279-288.
Kucej, M. and R. A. Butow (2007). "Evolutionary tinkering with mitochondrial nucleoids." Trends Cell Biol **17**(12): 586-592.
Kunz, C., K. Zurbriggen and O. Fleck (2003). "Mutagenesis of the HMGB (high-mobility group B) protein Cmb1 (cytosine-mismatch binding 1) of Schizosaccharomyces pombe: effects on recognition of DNA mismatches and damage." Biochem J **372**(Pt 2): 651-660.
Kurihara, D., S. Matsunaga, S. Uchiyama and K. Fukui (2008). "Live cell imaging reveals plant aurora kinase has dual roles during mitosis." Plant Cell Physiol **49**(8): 1256-1261.
Kurihara, D., S. Matsunaga, S. Uchiyama and K. Fukui (2008). "Live Cell Imaging Reveals Plant Aurora Kinase Has Dual Roles During Mitosis." Plant and Cell Physiology **49**(8): 1256-1261.
Kwak, K. J., J. Y. Kim, Y. O. Kim and H. Kang (2007). "Characterization of transgenic Arabidopsis plants overexpressing high mobility group B proteins under high salinity, drought or cold stress." Plant Cell Physiol **48**(2): 221-231.
Landsman, D. and M. Bustin (1993). "A signature for the HMG-1 box DNA-binding proteins." Bioessays **15**(8): 539-546.
Launholt, D., J. T. Gronlund, H. K. Nielsen and K. D. Grasser (2007). "Overlapping expression patterns among the genes encoding Arabidopsis chromosomal high mobility group (HMG) proteins." FEBS Lett **581**(6): 1114-1118.
Launholt, D., T. Merkle, A. Houben, A. Schulz and K. D. Grasser (2006). "Arabidopsis chromatin-associated HMGA and HMGB use different nuclear targeting signals and display highly dynamic localization within the nucleus." Plant Cell **18**(11): 2904-2918.
Lawrence, R. J., K. Earley, O. Pontes, M. Silva, Z. J. Chen, N. Neves, W. Viegas and C. S. Pikaard (2004). "A concerted DNA methylation/histone methylation switch regulates rRNA gene dosage control and nucleolar dominance." Mol Cell **13**(4): 599-609.
Laybourn, P. J. and J. T. Kadonaga (1991). "Role of nucleosomal cores and histone H1 in regulation of transcription by RNA polymerase II." Science **254**(5029): 238-245.
Lee, Y. M. and W. Kim (2003). "Association of human kinesin superfamily protein member 4 with BRCA2-associated factor 35." Biochem J **374**(Pt 2): 497-503.

Leitch, A. R., W. Mosgoller, M. Shi and J. S. Heslop-Harrison (1992). "Different patterns of rDNA organization at interphase in nuclei of wheat and rye." J Cell Sci **101 (Pt 4)**: 751-757.
Lermontova, I., J. Fuchs, V. Schubert and I. Schubert (2007). "Loading time of the centromeric histone H3 variant differs between plants and animals." Chromosoma **116**(6): 507-510.
Lever, M. A., J. P. Th'ng, X. Sun and M. J. Hendzel (2000). "Rapid exchange of histone H1.1 on chromatin in living human cells." Nature **408**(6814): 873-876.
Lildballe, D. L., D. S. Pedersen, R. Kalamajka, J. Emmersen, A. Houben and K. D. Grasser (2008). "The expression level of the chromatin-associated HMGB1 protein influences growth, stress tolerance, and transcriptome in Arabidopsis." J Mol Biol **384**(1): 9-21.
Lin, C. W., B. Moorefield, J. Payne, P. Aprikian, K. Mitomo and R. H. Reeder (1996). "A novel 66-kilodalton protein complexes with Rrn6, Rrn7, and TATA-binding protein to promote polymerase I transcription initiation in Saccharomyces cerevisiae." Mol Cell Biol **16**(11): 6436-6443.
Lnenicek-Allen, M., C. M. Read and C. Crane-Robinson (1996). "The DNA bend angle and binding affinity of an HMG box increased by the presence of short terminal arms." Nucleic Acids Res **24**(6): 1047-1051.
Lolas, I. B., K. Himanen, J. T. Gronlund, C. Lynggaard, A. Houben, M. Melzer, M. Van Lijsebettens and K. D. Grasser (2010). "The transcript elongation factor FACT affects Arabidopsis vegetative and reproductive development and genetically interacts with HUB1/2." Plant J **61**(4): 686-697.
Lotze, M. T. and K. J. Tracey (2005). "High-mobility group box 1 protein (HMGB1): nuclear weapon in the immune arsenal." Nat Rev Immunol **5**(4): 331-342.
Love, J. J., X. Li, D. A. Case, K. Giese, R. Grosschedl and P. E. Wright (1995). "Structural basis for DNA bending by the architectural transcription factor LEF-1." Nature **376**(6543): 791-795.
Luger, K., A. W. Mader, R. K. Richmond, D. F. Sargent and T. J. Richmond (1997). "Crystal structure of the nucleosome core particle at 2.8 A resolution." Nature **389**(6648): 251-260.
Mackay, D. R., S. W. Elgort and K. S. Ullman (2009). "The nucleoporin Nup153 has separable roles in both early mitotic progression and the resolution of mitosis." Mol Biol Cell **20**(6): 1652-1660.
Mahfouz, M. M., A. Piatek and C. N. Stewart, Jr. (2014). "Genome engineering via TALENs and CRISPR/Cas9 systems: challenges and perspectives." Plant Biotechnol J **12**(8): 1006-1014.
Malarkey, C. S. and M. E. Churchill (2012). "The high mobility group box: the ultimate utility player of a cell." Trends Biochem Sci **37**(12): 553-562.
Mariconti, L., B. Pellegrini, R. Cantoni, R. Stevens, C. Bergounioux, R. Cella and D. Albani (2002). "The E2F family of transcription factors from Arabidopsis thaliana. Novel and conserved components of the retinoblastoma/E2F pathway in plants." J Biol Chem **277**(12): 9911-9919.
Marmorstein, L. Y., A. V. Kinev, G. K. Chan, D. A. Bochar, H. Beniya, J. A. Epstein, T. J. Yen and R. Shiekhattar (2001). "A human BRCA2 complex containing a structural DNA binding component influences cell cycle progression." Cell **104**(2): 247-257.
Mathur, J. (2007). "The illuminated plant cell." Trends Plant Sci **12**(11): 506-513.
McClintock, B. (1934). "The relation of a particular chromosomal element to the development of the nucleoli in Zea mays." Zeitschrift für Zellforschung und Mikroskopische Anatomie **21**(2): 294-326.

McStay, B. (2006). "Nucleolar dominance: a model for rRNA gene silencing." Genes Dev **20**(10): 1207-1214.
McStay, B., M. W. Frazier and R. H. Reeder (1991). "xUBF contains a novel dimerization domain essential for RNA polymerase I transcription." Genes Dev **5**(11): 1957-1968.
Menges, M., S. M. de Jager, W. Gruissem and J. A. Murray (2005). "Global analysis of the core cell cycle regulators of Arabidopsis identifies novel genes, reveals multiple and highly specific profiles of expression and provides a coherent model for plant cell cycle control." Plant J **41**(4): 546-566.
Menges, M. and J. A. Murray (2002). "Synchronous Arabidopsis suspension cultures for analysis of cell-cycle gene activity." Plant J **30**(2): 203-212.
Miller, M. (2009). "The importance of being flexible: the case of basic region leucine zipper transcriptional regulators." Curr Protein Pept Sci **10**(3): 244-269.
Miller, O. J., D. A. Miller, V. G. Dev, R. Tantravahi and C. M. Croce (1976). "Expression of human and suppression of mouse nucleolus organizer activity in mouse-human somatic cell hybrids." Proc Natl Acad Sci U S A **73**(12): 4531-4535.
Montgomery, T. S. H. (1898). "Comparative cytological studies, with especial regard to the morphology of the nucleolus." Journal of Morphology **15**(2): 265-582.
Murashige, T. and F. Skoog (1962). "A Revised Medium for Rapid Growth and Bio Assays with Tobacco Cell Culture Systems." Physiologia Plantarum **15**.
Murphy, E. C., V. B. Zhurkin, J. M. Louis, G. Cornilescu and G. M. Clore (2001). "Structural basis for SRY-dependent 46-X,Y sex reversal: modulation of DNA bending by a naturally occurring point mutation." J Mol Biol **312**(3): 481-499.
Murphy, F. V. t. and M. E. Churchill (2000). "Nonsequence-specific DNA recognition: a structural perspective." Structure **8**(4): R83-89.
Murphy, F. V. t., R. M. Sweet and M. E. Churchill (1999). "The structure of a chromosomal high mobility group protein-DNA complex reveals sequence-neutral mechanisms important for non-sequence-specific DNA recognition." EMBO J **18**(23): 6610-6618.
Musacchio, A. and A. Ciliberto (2012). "The spindle-assembly checkpoint and the beauty of self-destruction." Nat Struct Mol Biol **19**(11): 1059-1061.
Navashin, M. (1934). "Chromosome Alterations Caused by Hybridization and Their Bearing upon Certain General Genetic Problems." CYTOLOGIA **5**(2): 169-203.
Neves, N., M. Delgado, M. Silva, A. Caperta, L. Morais-Cecilio and W. Viegas (2005). "Ribosomal DNA heterochromatin in plants." Cytogenet Genome Res **109**(1-3): 104-111.
Nigg, E. A. (1995). "Cyclin-dependent protein kinases: key regulators of the eukaryotic cell cycle." Bioessays **17**(6): 471-480.
Nosek, J., L. Tomaska, H. Fukuhara, Y. Suyama and L. Kovac (1998). "Linear mitochondrial genomes: 30 years down the line." Trends Genet **14**(5): 184-188.
O'Connell, K. L. and J. T. Stults (1997). "Identification of mouse liver proteins on two-dimensional electrophoresis gels by matrix-assisted laser desorption/ionization mass spectrometry of in situ enzymatic digests." ELECTROPHORESIS **18**(3-4): 349-359.
Ono, T., Y. Fang, D. L. Spector and T. Hirano (2004). "Spatial and temporal regulation of Condensins I and II in mitotic chromosome assembly in human cells." Mol Biol Cell **15**(7): 3296-3308.
Orphanides, G., W. H. Wu, W. S. Lane, M. Hampsey and D. Reinberg (1999). "The chromatin-specific transcription elongation factor FACT comprises human SPT16 and SSRP1 proteins." Nature **400**(6741): 284-288.

Oudet, P., M. Gross-Bellard and P. Chambon (1975). "Electron microscopic and biochemical evidence that chromatin structure is a repeating unit." Cell **4**(4): 281-300.
Paiva, E. A., S. Z. Pinho and D. M. Oliveira (2011). "Large plant samples: how to process for GMA embedding?" Methods Mol Biol **689**: 37-49.
Pallier, C., P. Scaffidi, S. Chopineau-Proust, A. Agresti, P. Nordmann, M. E. Bianchi and V. Marechal (2003). "Association of chromatin proteins high mobility group box (HMGB) 1 and HMGB2 with mitotic chromosomes." Mol Biol Cell **14**(8): 3414-3426.
Parizotto, E. A., P. Dunoyer, N. Rahm, C. Himber and O. Voinnet (2004). "In vivo investigation of the transcription, processing, endonucleolytic activity, and functional relevance of the spatial distribution of a plant miRNA." Genes Dev **18**(18): 2237-2242.
Parmacek, M. S. and J. A. Epstein (2009). "Cardiomyocyte renewal." N Engl J Med **361**(1): 86-88.
Patterson, G. H. and J. Lippincott-Schwartz (2002). "A photoactivatable GFP for selective photolabeling of proteins and cells." Science **297**(5588): 1873-1877.
Pedersen, D. S. (2010). "Molecular and functional analysis of Arabidopsis thaliana proteins containing the high mobility group (HMG) box motif." Ph.D. thesis.
Pedersen, D. S., F. Coppens, L. Ma, M. Antosch, B. Marktl, T. Merkle, G. T. Beemster, A. Houben and K. D. Grasser (2011). "The plant-specific family of DNA-binding proteins containing three HMG-box domains interacts with mitotic and meiotic chromosomes." New Phytol **192**(3): 577-589.
Pedersen, D. S. and K. D. Grasser (2010). "The role of chromosomal HMGB proteins in plants." Biochimica et Biophysica Acta (BBA) - Gene Regulatory Mechanisms **1799**(1–2): 171-174.
Pedersen, D. S., T. Merkle, B. Marktl, D. L. Lildballe, M. Antosch, T. Bergmann, K. Tonsing, D. Anselmetti and K. D. Grasser (2010). "Nucleocytoplasmic distribution of the Arabidopsis chromatin-associated HMGB2/3 and HMGB4 proteins." Plant Physiol **154**(4): 1831-1841.
Pesin, J. A. and T. L. Orr-Weaver (2008). "Regulation of APC/C activators in mitosis and meiosis." Annu Rev Cell Dev Biol **24**: 475-499.
Peters, J. M. (2006). "The anaphase promoting complex/cyclosome: a machine designed to destroy." Nat Rev Mol Cell Biol **7**(9): 644-656.
Pfleger, C. M. and M. W. Kirschner (2000). "The KEN box: an APC recognition signal distinct from the D box targeted by Cdh1." Genes Dev **14**(6): 655-665.
Phair, R. D., P. Scaffidi, C. Elbi, J. Vecerova, A. Dey, K. Ozato, D. T. Brown, G. Hager, M. Bustin and T. Misteli (2004). "Global nature of dynamic protein-chromatin interactions in vivo: three-dimensional genome scanning and dynamic interaction networks of chromatin proteins." Mol Cell Biol **24**(14): 6393-6402.
Pikaard, C. S. (2002). "Transcription and tyranny in the nucleolus: the organization, activation, dominance and repression of ribosomal RNA genes." Arabidopsis Book **1**: e0083.
Pontes, O., R. J. Lawrence, N. Neves, M. Silva, J. H. Lee, Z. J. Chen, W. Viegas and C. S. Pikaard (2003). "Natural variation in nucleolar dominance reveals the relationship between nucleolus organizer chromatin topology and rRNA gene transcription in Arabidopsis." Proc Natl Acad Sci U S A **100**(20): 11418-11423.
Pontes, O., C. F. Li, P. Costa Nunes, J. Haag, T. Ream, A. Vitins, S. E. Jacobsen and C. S. Pikaard (2006). "The Arabidopsis chromatin-modifying nuclear siRNA pathway involves a nucleolar RNA processing center." Cell **126**(1): 79-92.
Pontvianne, F., M. Abou-Ellail, J. Douet, P. Comella, I. Matia, C. Chandrasekhara, A. Debures, T. Blevins, R. Cooke, F. J. Medina, S. Tourmente,

C. S. Pikaard*, et al.* (2010). "Nucleolin is required for DNA methylation state and the expression of rRNA gene variants in Arabidopsis thaliana." PLoS Genet **6**(11): e1001225.

Pontvianne, F., T. Blevins, C. Chandrasekhara, W. Feng, H. Stroud, S. E. Jacobsen, S. D. Michaels and C. S. Pikaard (2012). "Histone methyltransferases regulating rRNA gene dose and dosage control in Arabidopsis." Genes Dev **26**(9): 945-957.

Pontvianne, F., T. Blevins, C. Chandrasekhara, I. Mozgova, C. Hassel, O. M. Pontes, S. Tucker, P. Mokros, V. Muchova, J. Fajkus and C. S. Pikaard (2013). "Subnuclear partitioning of rRNA genes between the nucleolus and nucleoplasm reflects alternative epiallelic states." Genes Dev **27**(14): 1545-1550.

Preuss, S. and C. S. Pikaard (2007). "rRNA gene silencing and nucleolar dominance: insights into a chromosome-scale epigenetic on/off switch." Biochim Biophys Acta **1769**(5-6): 383-392.

Pruitt, R. E. and E. M. Meyerowitz (1986). "Characterization of the genome of Arabidopsis thaliana." J Mol Biol **187**(2): 169-183.

Rao, P. N. and R. C. Adlakha (1984). "Chromosome condensation and decondensation factors in the life cycle of eukaryotic cells." Symp Fundam Cancer Res **37**: 45-69.

Riechmann, J. L., J. Heard, G. Martin, L. Reuber, C. Jiang, J. Keddie, L. Adam, O. Pineda, O. J. Ratcliffe, R. R. Samaha, R. Creelman, M. Pilgrim*, et al.* (2000). "Arabidopsis transcription factors: genome-wide comparative analysis among eukaryotes." Science **290**(5499): 2105-2110.

Ritt, C., R. Grimm, S. Fernandez, J. C. Alonso and K. D. Grasser (1998). "Basic and acidic regions flanking the HMG domain of maize HMGa modulate the interactions with DNA and the self-association of the protein." Biochemistry **37**(8): 2673-2681.

Rogers, S. and A. Bendich (1987). "Ribosomal RNA genes in plants: variability in copy number and in the intergenic spacer." Plant Molecular Biology **9**(5): 509-520.

Rogers, S. O. and A. J. Bendich (1987). "Ribosomal RNA genes in plants: variability in copy number and in the intergenic spacer." Plant Mol Biol **9**(5): 509-520.

Rose, A. (2008). Open Mitosis: Nuclear Envelope Dynamics. Cell Division Control in Plants. D. Verma and Z. Hong, Springer Berlin Heidelberg. **9:** 207-230.

Roussel, P., C. Andre, L. Comai and D. Hernandez-Verdun (1996). "The rDNA transcription machinery is assembled during mitosis in active NORs and absent in inactive NORs." J Cell Biol **133**(2): 235-246.

Russell, J. and J. C. Zomerdijk (2006). "The RNA polymerase I transcription machinery." Biochem Soc Symp(73): 203-216.

Sagan, L. (1967). "On the origin of mitosing cells." J Theor Biol **14**(3): 255-274.

Sajan, S. A. and R. D. Hawkins (2012). "Methods for identifying higher-order chromatin structure." Annu Rev Genomics Hum Genet **13**: 59-82.

Sambrook, J., E. F. Fritsch and T. Maniatis (1989). "Molecular cloning : a laboratory manual." Cold Spring Harbor: Cold Spring Harbor Laboratory Press.

Sanij, E., J. Diesch, A. Lesmana, G. Poortinga, G. Lidgerwood, N. Hein, D. P. Cameron, J. Ellul, G. J. Goodall, L. H. Wong, A. S. Dhillon, N. Hamdane*, et al.* (2014). "A novel role for the Pol I transcription factor UBTF in maintaining genome stability through the regulation of highly transcribed Pol II genes." Genome Res.

Savino, T. M., J. Gebrane-Younes, J. De Mey, J. B. Sibarita and D. Hernandez-Verdun (2001). "Nucleolar assembly of the rRNA processing machinery in living cells." J Cell Biol **153**(5): 1097-1110.

Scheer, U. and D. Weisenberger (1994). "The nucleolus." Curr. Opin. Cell Biol. **6**.

Schrumpfova, P. P., M. Fojtova, P. Mokros, K. D. Grasser and J. Fajkus (2011). "Role of HMGB proteins in chromatin dynamics and telomere maintenance in Arabidopsis thaliana." Curr Protein Pept Sci **12**(2): 105-111.
Scofield, S., A. Jones and J. A. Murray (2014). "The plant cell cycle in context." J Exp Bot **65**(10): 2557-2562.
Shaw, P. J. and E. G. Jordan (1995). "The nucleolus." Annu Rev Cell Dev Biol **11**: 93-121.
Shi, L., J. Wang, F. Hong, D. L. Spector and Y. Fang (2011). "Four amino acids guide the assembly or disassembly of Arabidopsis histone H3.3-containing nucleosomes." Proc Natl Acad Sci U S A **108**(26): 10574-10578.
Smetana K and B. H (1974). "The Nucleolus and Nucleolar DNA." New York: Academic press **1**.
Smith, L. G. (2001). "Plant cell division: building walls in the right places." Nat Rev Mol Cell Biol **2**(1): 33-39.
Stefanovsky, V. Y., D. P. Bazett-Jones, G. Pelletier and T. Moss (1996). "The DNA supercoiling architecture induced by the transcription factor xUBF requires three of its five HMG-boxes." Nucleic Acids Res **24**(16): 3208-3215.
Stefanovsky, V. Y., G. Pelletier, D. P. Bazett-Jones, C. Crane-Robinson and T. Moss (2001). "DNA looping in the RNA polymerase I enhancesome is the result of non-cooperative in-phase bending by two UBF molecules." Nucleic Acids Res **29**(15): 3241-3247.
Stemmer, C., S. Fernandez, G. Lopez, J. C. Alonso and K. D. Grasser (2002). "Plant chromosomal HMGB proteins efficiently promote the bacterial site-specific beta-mediated recombination in vitro and in vivo." Biochemistry **41**(24): 7763-7770.
Stemmer, C., C. Ritt, G. L. Igloi, R. Grimm and K. D. Grasser (1997). "Variability in Arabidopsis thaliana chromosomal high-mobility-group-1-like proteins." Eur J Biochem **250**(3): 646-652.
Stott, K., M. Watson, M. J. Bostock, S. A. Mortensen, A. Travers, K. D. Grasser and J. O. Thomas (2014). "Structural insights into the mechanism of negative regulation of single-box high mobility group proteins by the acidic tail domain." J Biol Chem **289**(43): 29817-29826.
Strambio-De-Castillia, C., M. Niepel and M. P. Rout (2010). "The nuclear pore complex: bridging nuclear transport and gene regulation." Nat Rev Mol Cell Biol **11**(7): 490-501.
Stros, M., D. Launholt and K. D. Grasser (2007). "The HMG-box: a versatile protein domain occurring in a wide variety of DNA-binding proteins." Cell Mol Life Sci **64**(19-20): 2590-2606.
Thoma, F., T. Koller and A. Klug (1979). "Involvement of histone H1 in the organization of the nucleosome and of the salt-dependent superstructures of chromatin." J Cell Biol **83**(2 Pt 1): 403-427.
Thomas, J. O. and K. Stott (2012). "H1 and HMGB1: modulators of chromatin structure." Biochem Soc Trans **40**(2): 341-346.
Thomas, J. O. and A. A. Travers (2001). "HMG1 and 2, and related 'architectural' DNA-binding proteins." Trends Biochem Sci **26**(3): 167-174.
Thomsen, M. S., L. Franssen, D. Launholt, P. Fojan and K. D. Grasser (2004). "Interactions of the basic N-terminal and the acidic C-terminal domains of the maize chromosomal HMGB1 protein." Biochemistry **43**(25): 8029-8037.
Thornton, B. R. and D. P. Toczyski (2006). "Precise destruction: an emerging picture of the APC." Genes Dev **20**(22): 3069-3078.
Tomb, J. F., O. White, A. R. Kerlavage, R. A. Clayton, G. G. Sutton, R. D. Fleischmann, K. A. Ketchum, H. P. Klenk, S. Gill, B. A. Dougherty, K. Nelson, J.

Quackenbush*, et al.* (1997). "The complete genome sequence of the gastric pathogen Helicobacter pylori." Nature **388**(6642): 539-547.
Tompa, P., J. Prilusky, I. Silman and J. L. Sussman (2008). "Structural disorder serves as a weak signal for intracellular protein degradation." Proteins **71**(2): 903-909.
Towbin, B. D., P. Meister and S. M. Gasser (2009). "The nuclear envelope--a scaffold for silencing?" Curr Opin Genet Dev **19**(2): 180-186.
Treiber, D. K., X. Zhai, H. M. Jantzen and J. M. Essigmann (1994). "Cisplatin-DNA adducts are molecular decoys for the ribosomal RNA transcription factor hUBF (human upstream binding factor)." Proc Natl Acad Sci U S A **91**(12): 5672-5676.
Van Hooser, A., P. Yuh and R. Heald (2005). "The perichromosomal layer." Chromosoma **114**(6): 377-388.
Van Leene, J., D. Eeckhout, G. Persiau, E. Van De Slijke, J. Geerinck, G. Van Isterdael, E. Witters and G. De Jaeger (2011). "Isolation of transcription factor complexes from Arabidopsis cell suspension cultures by tandem affinity purification." Methods Mol Biol **754**: 195-218.
Van Leene, J., H. Stals, D. Eeckhout, G. Persiau, E. Van De Slijke, G. Van Isterdael, A. De Clercq, E. Bonnet, K. Laukens, N. Remmerie, K. Henderickx, T. De Vijlder*, et al.* (2007). "A tandem affinity purification-based technology platform to study the cell cycle interactome in Arabidopsis thaliana." Mol Cell Proteomics **6**(7): 1226-1238.
van Leuken, R., L. Clijsters and R. Wolthuis (2008). "To cell cycle, swing the APC/C." Biochim Biophys Acta **1786**(1): 49-59.
Van't Hof, J. (1974). The Duration of Chromosomal DNA Synthesis, of the Mitotic Cycle, and of Meiosis of Higher Plants. Handbook of Genetics. R. King, Springer US**:** 363-377.
Venter, J. C., M. D. Adams, E. W. Myers, P. W. Li, R. J. Mural, G. G. Sutton, H. O. Smith, M. Yandell, C. A. Evans, R. A. Holt, J. D. Gocayne, P. Amanatides*, et al.* (2001). "The sequence of the human genome." Science **291**(5507): 1304-1351.
Veylder, L. D., J. Joubès and D. Inzé (2003). "Plant cell cycle transitions." Current Opinion in Plant Biology **6**(6): 536-543.
Vinogradov, A. E. (2005). "Genome size and chromatin condensation in vertebrates." Chromosoma **113**(7): 362-369.
Wallace, H. and W. H. R. Langridge (1971). "Differential amphiplasty and the control of ribosomal RNA synthesis1." Heredity **27**(1): 1-13.
Watson, J. D. and F. H. Crick (1953). "Molecular structure of nucleic acids; a structure for deoxyribose nucleic acid." Nature **171**(4356): 737-738.
Weingartner, M., H. R. Pelayo, P. Binarova, K. Zwerger, B. Melikant, C. de la Torre, E. Heberle-Bors and L. Bogre (2003). "A plant cyclin B2 is degraded early in mitosis and its ectopic expression shortens G2-phase and alleviates the DNA-damage checkpoint." J Cell Sci **116**(Pt 3): 487-498.
Wick, S. M. (1991). "The cytoskeletal basis of plant growth and form." Academic Press. London: 231-244.
Woese, C. R. and G. E. Fox (1977). "Phylogenetic structure of the prokaryotic domain: the primary kingdoms." Proc Natl Acad Sci U S A **74**(11): 5088-5090.
Wolters, H. and G. Jurgens (2009). "Survival of the flexible: hormonal growth control and adaptation in plant development." Nat Rev Genet **10**(5): 305-317.
Wu, Q., W. Zhang, K. H. Pwee and P. P. Kumar (2003). "Rice HMGB1 protein recognizes DNA structures and bends DNA efficiently." Arch Biochem Biophys **411**(1): 105-111.

Xie, Q., A. P. Sanz-Burgos, G. J. Hannon and C. Gutierrez (1996). "Plant cells contain a novel member of the retinoblastoma family of growth regulatory proteins." EMBO J **15**(18): 4900-4908.
Xue, B., R. L. Dunbrack, R. W. Williams, A. K. Dunker and V. N. Uversky (2010). "PONDR-FIT: a meta-predictor of intrinsically disordered amino acids." Biochim Biophys Acta **1804**(4): 996-1010.
Yang, D., P. Tewary, G. de la Rosa, F. Wei and J. J. Oppenheim (2010). "The alarmin functions of high-mobility group proteins." Biochim Biophys Acta **1799**(1-2): 157-163.
Yen, Y. M., B. Wong and R. C. Johnson (1998). "Determinants of DNA binding and bending by the Saccharomyces cerevisiae high mobility group protein NHP6A that are important for its biological activities. Role of the unique N terminus and putative intercalating methionine." J Biol Chem **273**(8): 4424-4435.
Yoon, M. K., J. Shin, G. Choi and B. S. Choi (2006). "Intrinsically unstructured N-terminal domain of bZIP transcription factor HY5." Proteins **65**(4): 856-866.
Zeng, S. X., Y. Li, Y. Jin, Q. Zhang, D. M. Keller, C. M. McQuaw, E. Barklis, S. Stone, M. Hoatlin, Y. Zhao and H. Lu (2010). "Structure-specific recognition protein 1 facilitates microtubule growth and bundling required for mitosis." Mol Cell Biol **30**(4): 935-947.
Zhang, H. and R. K. Dawe (2011). "Mechanisms of plant spindle formation." Chromosome Res **19**(3): 335-344.
Zhang, W., Q. Wu, K. H. Pwee and R. Manjunatha Kini (2003). "Interaction of wheat high-mobility-group proteins with four-way-junction DNA and characterization of the structure and expression of HMGA gene." Arch Biochem Biophys **409**(2): 357-366.
Zhao, K., E. Kas, E. Gonzalez and U. K. Laemmli (1993). "SAR-dependent mobilization of histone H1 by HMG-I/Y in vitro: HMG-I/Y is enriched in H1-depleted chromatin." EMBO J **12**(8): 3237-3247.
Zur, A. and M. Brandeis (2001). "Securin degradation is mediated by fzy and fzr, and is required for complete chromatid separation but not for cytokinesis." EMBO J **20**(4): 792-801.

7. Appendix

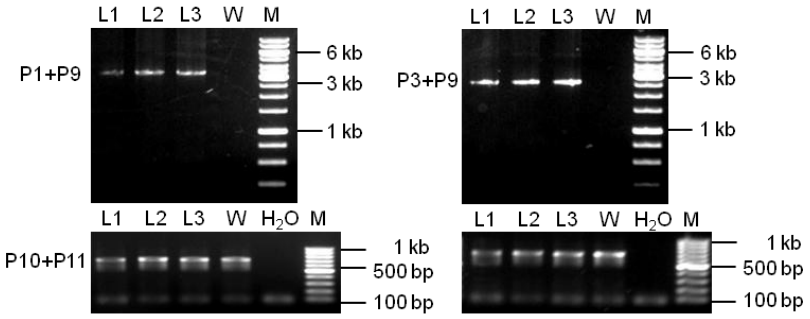

Supplemental Figure 1. Confirmation of 3xHMG-box reporter lines.
PCR based genotyping of independent transformed plants lines (L) and wild type (W) using the indicated primers (P). Resulting DNA fragments match the expected sizes of 3322 bps for pM1 mediated integration (left panel) and 2542 bp for pM2 mediated insertion (right panel). In order to test the input DNA, the coding sequence of HMGA was amplified using primer P10 and P11 resulting in a PCR fragment of 690 bp.

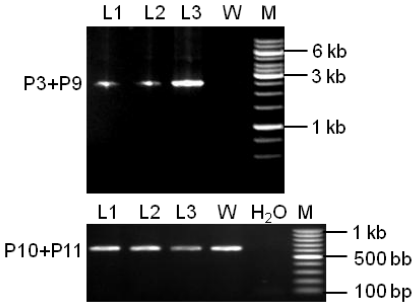

Supplemental Figure 2. Site directed mutagenesis of a putative D-box degradation domain in 3xHMG-box2. PCR based genotyping of three independent plant lines containing pM3, which facilitates the expression of 3xHMG-box2-GFP with the mutated D-box sequence motif. Amplification of genomic DNA from independent plant lines (L) using Primer P3/P9 lead to a PCR fragment with the expected size of 2542 bp. Input DNA was tested using Primer P10/P11

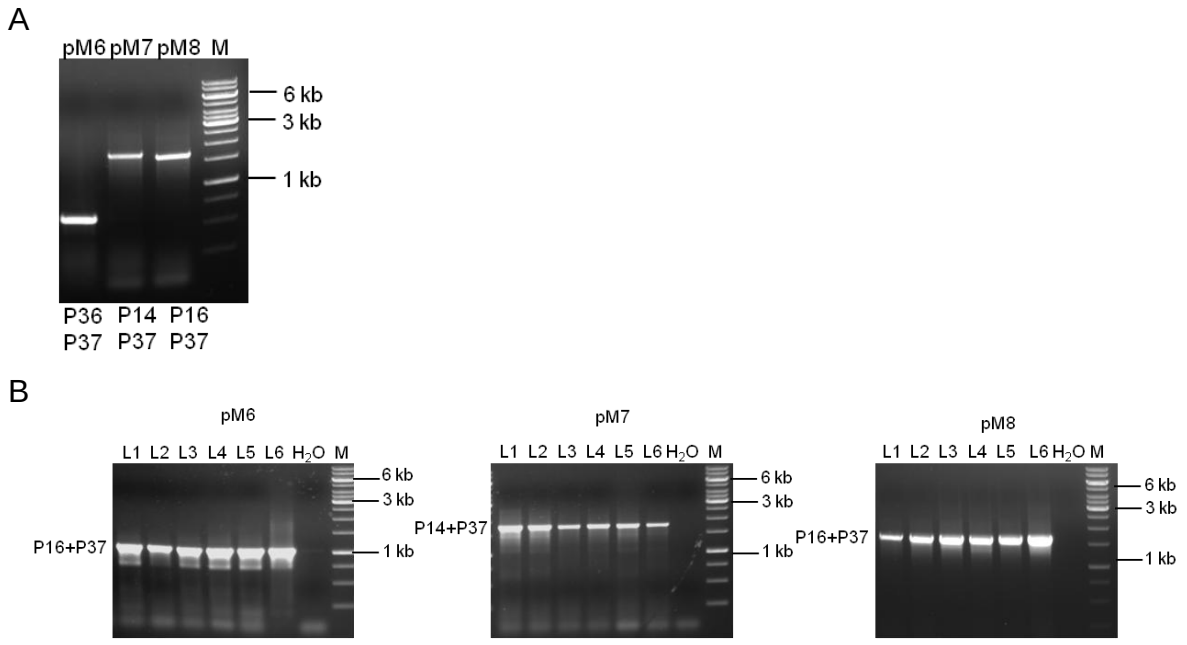

Supplemental Figure 3. Verification of stably transformed Arabidopsis cell suspension cultures and plants that contain plasmids which mediate expression of GS-tagged 3xHMG-box proteins or the sole GS tag. (A) PCR-based genotyping of *Arabidopsis* cell suspension cultures harboring constructs that enable plants to produce GS tagged 3xHMG-box proteins or only the GS tag under the control of the *3xHMG-box2* promoter. Plasmids used for transformation and primer pairs used for genotyping are indicated. **(B)** PCR-based genotyping of independent plant lines (L) harboring expression cassettes that allow the expression of GS tagged 3xHMG-box proteins as well as the GS tag under the control of the *3xHMG-box2* promoter. Constructs that were used for transformation and primer pairs are indicated.

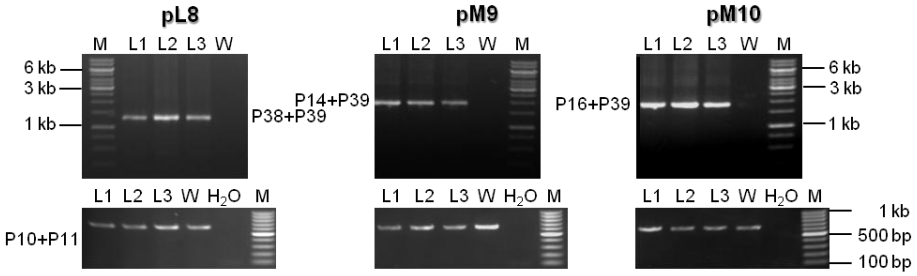

Supplemental Figure 4. Verification of stably transformed plant lines that contain plasmids which mediate overexpression of 3xHMG-box-GFP-NLS fusion proteins during interphase. PCR-based genotyping of Col-0 (W) and stable transformed independent *Arabidopsis thaliana* lines (L) harboring pL8, pM9 and pM10 derived expression cassettes. Primers (P) used for PCR are indicated.

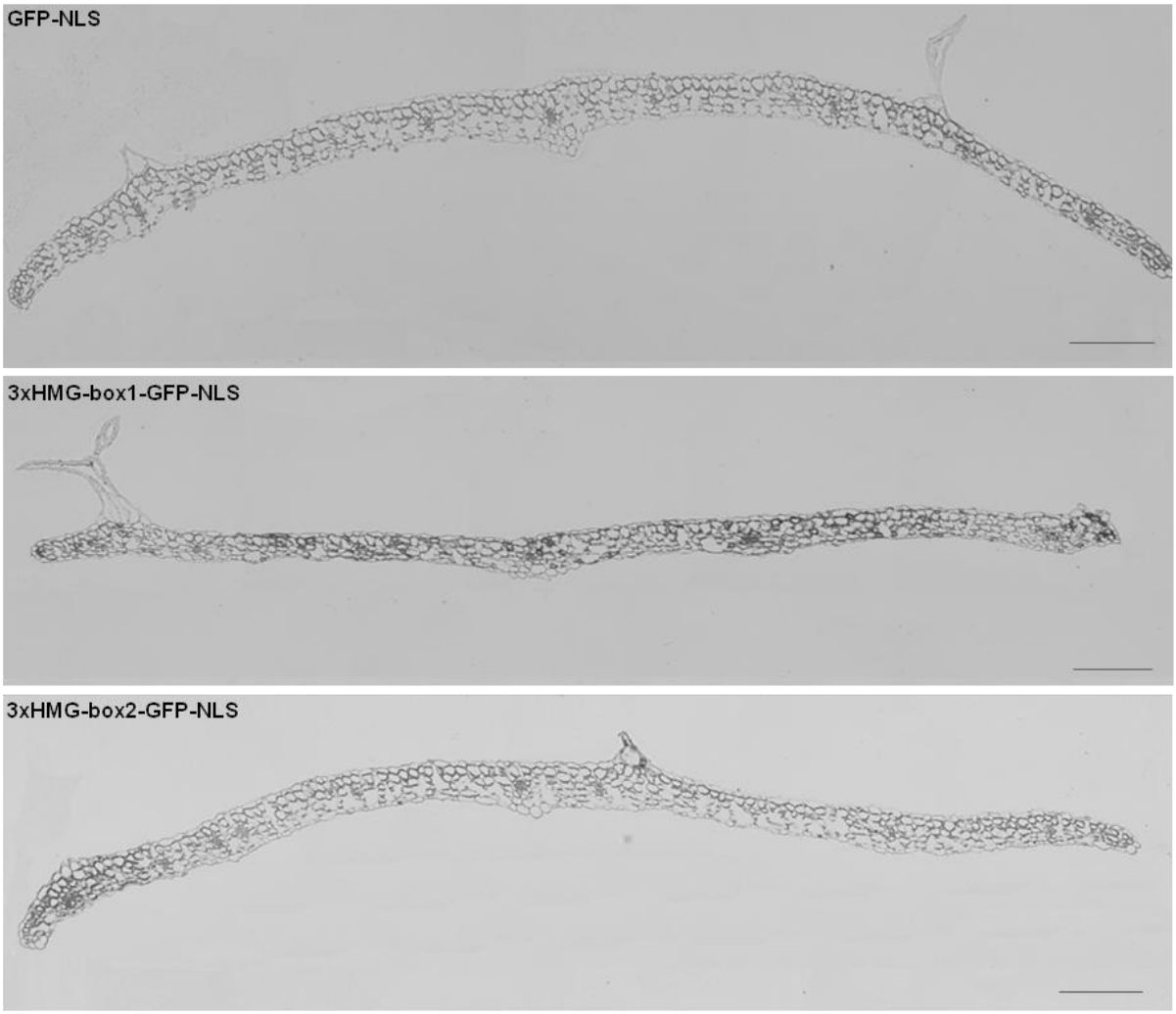

Supplemental figure 5. Number of palisade parenchyma cells of leaves from Arabidopsis thaliana plants lines homozygous for pL8, pM9 and pM10. Semi thin sections of the first leaf from the second leaf pair 14DAS. One representative leaf is shown for each construct. Scale bar indicates 100 µm.

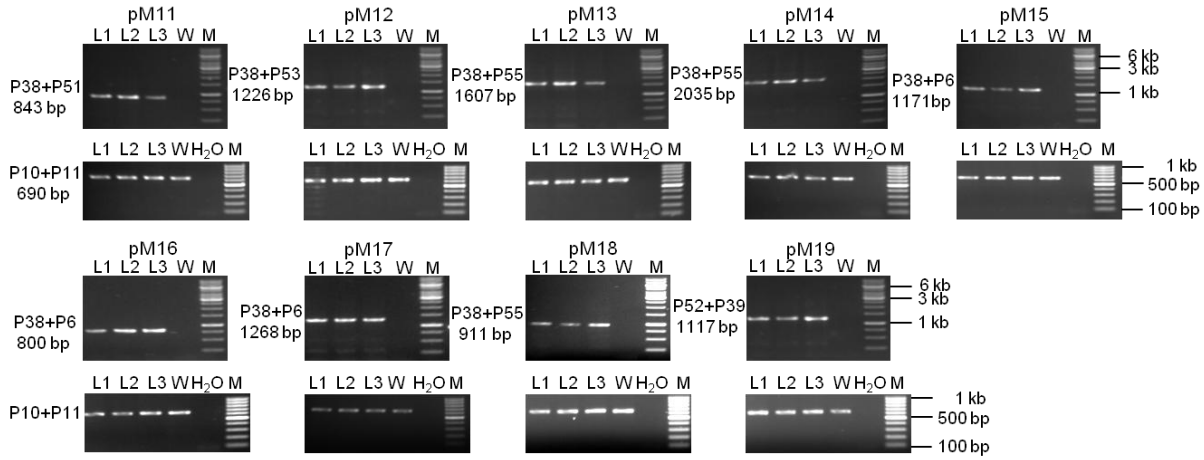

Supplemental figure 6. Confirmation of stably transformed *A.thaliana* plant lines that contain plasmids which facilitate expression of 3xHMG-box1-GFP-NLS truncated versions. PCR based genotyping of independent plant lines harboring T-DNA insertions which allow expression of truncated 3xHMG-box1-GFP-NLS versions. Plasmids (p) that were used for transformation and primers (P) that were used for PCR as well as the expected fragment size in bp are indicated.

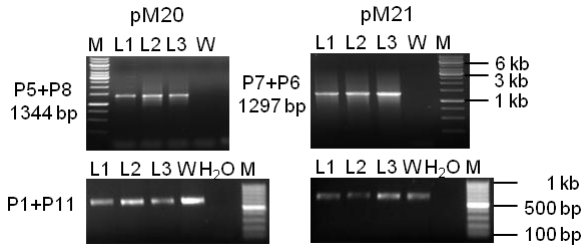

Supplemental figure 7. Confirmation of stably transformed *A.thaliana* plant lines that contain plasmids which facilitate expression of chimeric 3xHMG-box proteins. PCR-based genotyping of three independent plant lines that were transformed with either pM20 or pM21. Primers used for amplification and expected sizes are indicated.

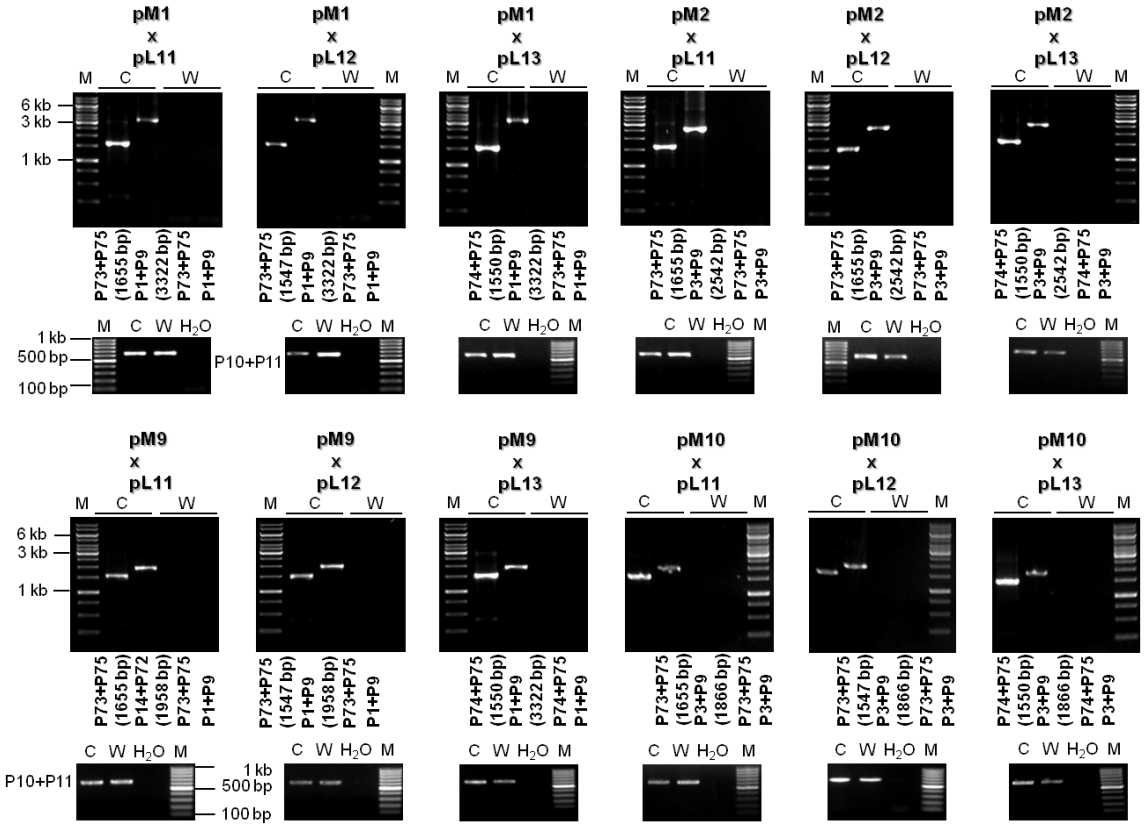

Supplemental Figure 8. Verification of crossed plant lines that harbor constructs which allow simultaneous expression of fluorescently labeled 3xHMG-box proteins and linker histones. PCR based genotyping of plant lines which result from crossing of plant lines that were transformed with the indicated plasmids. Genomic DNA was extracted from crossed lines (C) and Col-0 wild type (W) and used as template for PCR with indicated primers (P). Expected sizes are indicated.

Danksagung

Mein herzlicher Dank gilt all den vielen Leuten, die mich während der Doktorarbeit unterstützt haben.

Insbesondere natürlich Prof. Dr. Klaus Grasser, meinem Doktorvater und Betreuer, der mir ermöglicht hat diese Doktorarbeit in seiner Arbeitsgruppe durchzuführen und mir bei der Planung, Verfassung und Korrektur der Arbeit geholfen hat.

Des Weiteren ein großes Dankeschön an PD. Dr. Ortrun Mittelsten Scheid, meine Zweit-Mentorin, für die nette Zusammenarbeit und Zusammenkünfte in Gatersleben, Wien und Regensburg sowie die zusätzliche Arbeit die du dir als Mentorin und Gutachterin aufgebürdet hast. Ich weiß das sehr zu schätzen.

Vielen lieben Dank auch an PD Dr. Joachim Griesenbeck, für die Unterstützung beim HMO1 Projekt und die Bereitschaft als Gutachter und Prüfer zu fungieren. Dabei auch noch mal ein extra Dankeschön an Virginia Babel die mir tatkräftig beim Klonieren und Transformieren der Hefen geholfen hat.

Ein dickes Dankeschön an den ganzen Arbeitskreis für die gute Zusammenarbeit, die vielen schönen Stunden und die Unterstützung auch in den für mich nicht so schönen Stunden, in denen Experimente nicht so geklappt haben wie ich mir das gewünscht habe. Insbesondere möchte ich hier meine drei dänischen Kollegen und Freunde Dorthe Pedersen, Simon Mortensen und Brian Sørensen erwähnen mit denen ich viele feucht fröhliche, teils skurrile Abende erlebt und ebenso denkwürdige Diskussionen über Gott und die Welt geführt habe.

Ein großes Dankeschön auch an das ganze Institut und speziell an Prof. Dr. Thomas Dresselhaus, für die Hilfsbereitschaft, tollen Skiausflüge und gute Stimmung untereinander.

Ein ganz besonderer Dank gilt meiner Familie und meinen Freunden, die immer für mich da sind und mich so akzeptieren wie ich bin.

Und zum guten Schluss ein riesen Dankeschön an meine liebe Lena, die immer an mich geglaubt hat und mir in jeglicher Hinsicht eine unschätzbare Hilfe war.